Modeling and Evaluation of Cyclist Fall Prevention Interventions

A Proactive Cycling Safety Approach

Reijne, M.M.

DOI
10.4233/uuid:ada397a7-0c55-4284-9133-3c5ea515ea67

Publication date
2025

Document Version
Final published version

Citation (APA)
Reijne, M. M. (2025). *Modeling and Evaluation of Cyclist Fall Prevention Interventions: A Proactive Cycling Safety Approach*. [Dissertation (TU Delft), Delft University of Technology].
https://doi.org/10.4233/uuid:ada397a7-0c55-4284-9133-3c5ea515ea67

Important note
To cite this publication, please use the final published version (if applicable).
Please check the document version above.

Modeling and Evaluation of Cyclist Fall Prevention Interventions:

A Proactive Cycling Safety Approach

Marco Reijne

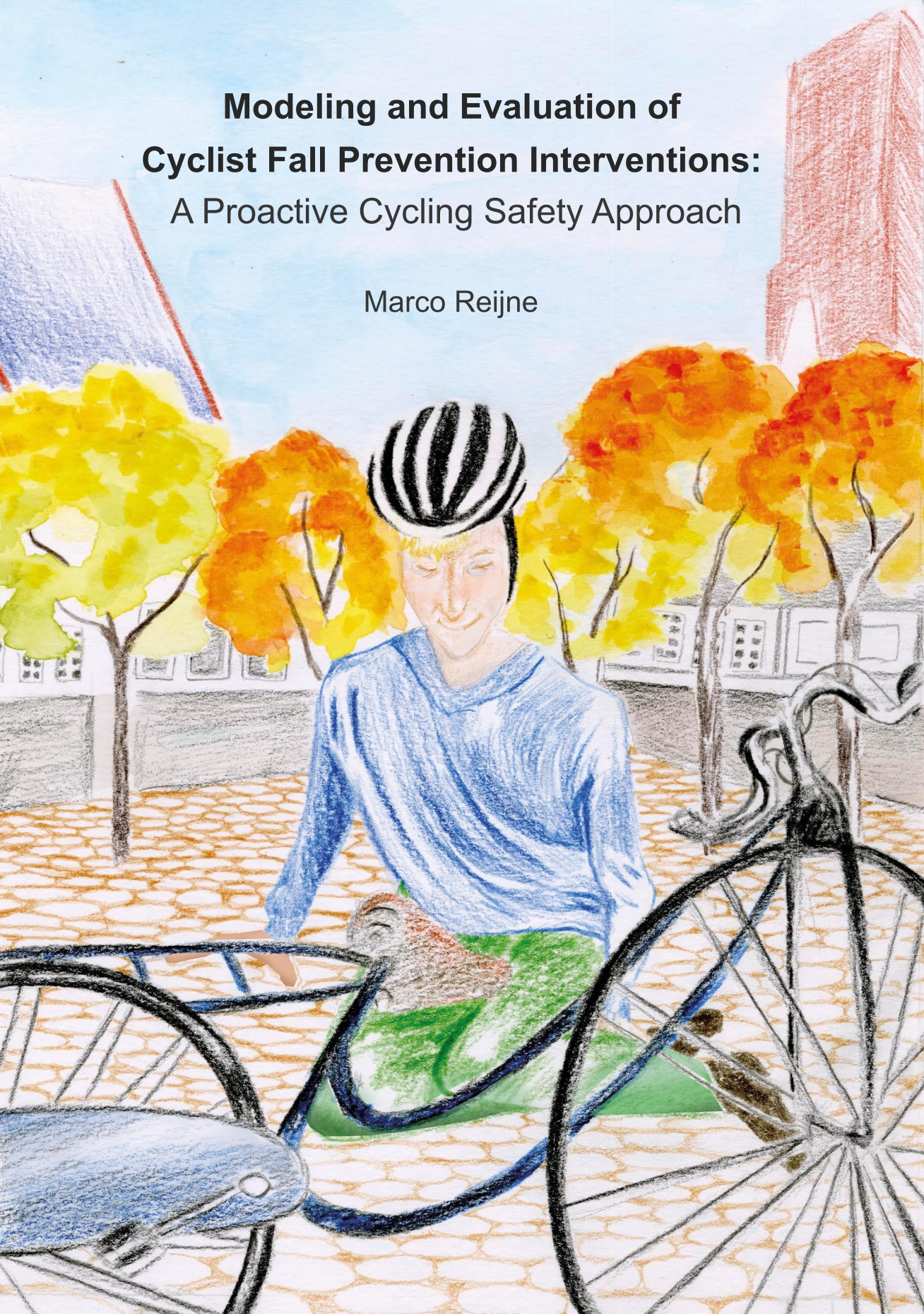

Modeling and Evaluation of Cyclist Fall Prevention Interventions: A Proactive Cycling Safety Approach

Modeling and Evaluation of Cyclist Fall Prevention Interventions: A Proactive Cycling Safety Approach

Proefschrift

ter verkrijging van de graad van doctor
aan de Technische Universiteit Delft,
op gezag van de Rector Magnificus Prof. dr. ir. T.H.J.J. van der Hagen,
voorzitter van het College voor Promoties,
in het openbaar te verdedigen op donderdag 27 februari 2025 om 15.00 uur

door

Marco Michiel Reijne

Master of Science in Aerospace Engineering,
Technische Universiteit Delft, Delft, Nederland,
geboren te Reimerswaal, Nederland.

Dit proefschrift is goedgekeurd door de

promotor: Prof. dr. F.C.T. van der Helm
copromotor: Dr. ir. A.L. Schwab

Samenstelling promotiecommissie:

Rector Magnificus,	voorzitter
Prof. dr. F.C.T. van der Helm,	Technische Universiteit Delft
Dr. ir. A.L. Schwab,	Technische Universiteit Delft
Onafhankelijke leden:	
Prof. dr. M. Dozza,	Chalmers University of Technology
Prof. dr. M. Pijnappels,	Vrije Universiteit Amsterdam
Prof. dr. ir. R. Happee,	Technische Universiteit Delft
Dr. ir. J.P. Meijaard,	Technische Universiteit Delft
Dr. ir. P. Schepers,	Rijkswaterstaat
Prof. dr. ir. A.C. Schouten,	Technische Universiteit Delft, reservelid

Keywords: bicycle dynamics, cyclist control, cycling safety

Printed by: Gildeprint

Front & Back: illustration by Julia Siddle

An electronic version of this dissertation is available at
http://repository.tudelft.nl/.

CONTENTS

SUMMARY

The goal of this dissertation was to develop an approach to safely and proactively evaluate cyclist fall prevention interventions, addressing a significant gap in cycling safety research. While bicycle dynamics and cyclist control models present a promising solution, they have yet to be applied in the context of cycling safety.

Chapter 1 outlines the potential of existing bicycle dynamics and cyclist control models for simulating eight commonly reported crash types. These are falls due to slipping on a slippery road surface, falls after a collision with an obstacle, falls following an evasive manoeuvre, falls involving (tram) rails, falls resulting from hard braking, falling over while cornering, falls due to loss of balance, and falls after a collision with another road user. Chapter 1 also discusses how various interventions — such as changes in bicycle design, cyclist control, and infrastructure — can be incorporated into these models for evaluation.

Additionally, **Chapter 1** highlights the necessary improvements required to advance the practical application of these models. These limitations include the need for bicycle tyre models, the incorporation of more intuitive human characteristics in cyclist control models, and the validation of these models in real-world crash scenarios. The subsequent chapters of this dissertation address most of these challenges.

Chapter 2 introduces the Maximum Allowable Handlebar Disturbance (MAHD) as a novel indicator for safely and proactively evaluating cyclist fall prevention interventions. Unlike the binary outcome of fall or recovery, the MAHD provides a detailed quantification of intervention effectiveness, allowing for a more detailed comparison between different interventions. Moreover, we demonstrate that this indicator can be applied to various crash scenarios that involve impulse-like disturbances and can systematically evaluate interventions targeting bicycle design, cyclist control, and infrastructure.

Chapter 3 presents the first-ever experiments that include actual cyclist falls, with 24 participants from younger and older age groups. These experiments generated a valuable dataset that can be used to validate the predictive performance of bicycle dynamics and cyclist control models.

In addition, important cyclist characteristics predictive of fall outcomes were identified in **Chapter 3** through Bayesian Model Averaging. These important predictors were forward speed — where it was less likely to fall at lower speeds — and skill performance, which was defined as the ability to maintain balance and follow a centreline while cycling undisturbed. Surprisingly, age was not an important predictor of fall outcomes.

In **Chapter 3**, we also developed a Bayesian multilevel logistic regression model to estimate the MAHD for individual participants. This was required because of human variations. There often was no clear-cut boundary for a participant in the disturbance magnitude between falling and being able to recover balance.

In **Chapter 4**, we introduced a cyclist control model for the bicycle balancing task with the perspective of safely and proactively studying what changes to cyclist control can reduce the risk of falling. The presented model incorporates human sensors with partial state feedback, multisensory integration for bicycle state estimation, human steer torque control and muscular dynamics. It simulates realistic cyclist behaviour by using lean rate and steering angle as sensory inputs without incorporating any delay. When tested, the model achieved an average Variance Accounted For (VAF) score of 65.6% (with a standard deviation of 25.8%) for experimental trials on a narrow treadmill setup and an average VAF score of 55.6% (with a standard deviation of 27.7%) for experimental trials in a pavilion setup. These results demonstrate the model's robustness in simulating cyclist balance control actions, reflecting the responses of different cyclists across varying forward speeds.

The presented model in **Chapter 4** requires calibration of only a single input value, which is the weight factor on the lean angle in the Linear Quadratic Regulator (LQR) state weighting matrix. The other input values are straightforward to measure. Importantly, this weight factor is independent of forward speed, allowing for calibration at just one speed, in contrast to existing models that require multiple calibrations for different speeds. This feature significantly improves the practical application of our cyclist control model.

In **Chapter 5**, we evaluated the reliability and practicality of a candidate bicycle dynamics and cyclist control model. This evaluation involved comparing the model's MAHD predictions with experimental data, where cyclists were exposed to handlebar disturbances resulting in falls and recoveries. Additionally, we demonstrated the model's practicality through three case studies that examined interventions targeting cyclist control, bicycle design, and infrastructure design.

The results of **Chapter 5** demonstrated the candidate model's effectiveness in accurately predicting MAHD for cyclists with varying skill levels and its ability to capture key aspects of cyclist responses to significant disturbances. Additionally, the model proved successful in evaluating the impact of modifications to bicycle design, cyclist control, and infrastructure on the MAHD. These findings highlight the model's reliability and potential as a valuable tool for safely and proactively evaluating various fall prevention interventions.

In conclusion, this dissertation's research contributed to the development of an approach that utilizes bicycle dynamics and cyclist control models to safely and proactively evaluate cyclist fall prevention interventions. By improving the practical application of these models and establishing a systematic framework for comparing intervention effectiveness, this work contributes to a valuable tool that can be used by designers, engineers, and policymakers to safely and proactively evaluate cyclist fall prevention interventions. Ultimately, this will improve the designs of bicycles, infrastructure, and training programs and allocate resources to the most effective interventions.

SAMENVATTING

Het doel van dit proefschrift was om een methode te ontwikkelen voor het veilig en proactief evalueren van interventies die valpartijen bij fietsers proberen te voorkomen. Hiermee wordt een belangrijke leemte in het onderzoek naar fietsveiligheid aangepakt. Hoewel modellen die de fietsdynamica en stuuracties van de fietser beschrijven een veelbelovende oplossing bieden, zijn ze nog niet toegepast in de context van fietsveiligheid.

Hoofdstuk 1 schetst het potentieel van bestaande modellen voor fietsdynamica en stuuracties van de fietser om acht vaak gerapporteerde ongevalstypen te simuleren. De vaak gerapporteerde valpartijen zijn: vallen door uitglijden op een glad wegdek, vallen na een botsing met een obstakel, vallen na een uitwijkmanoeuvre, valpartijen waarbij een (tram)rail een rol speelde, vallen als gevolg van hard remmen, omvallen tijdens het nemen van een bocht, valpartijen door verlies van evenwicht, en vallen na een botsing met een andere weggebruiker. **Hoofdstuk 1** bespreekt ook hoe verschillende interventies — zoals veranderingen in fietsontwerp, stuuracties van de fietser en infrastructuur — in deze modellen kunnen worden opgenomen zodat hun effectiviteit om de fietsveiligheid te verbeteren geëvalueerd kan worden.

Daarnaast benadrukt **Hoofdstuk 1** de noodzakelijke verbeteringen die nodig zijn om de praktische toepassing van deze modellen te vergroten. Deze verbeteringen omvatten de ontwikkeling van een fietsbandmodel, het opnemen van intuïtievere menselijke kenmerken in modellen die de stuuracties van de fietser simuleren en de validatie van deze modellen in ongevalsscenario's. De volgende hoofdstukken van dit proefschrift behandelen de meeste van deze uitdagingen.

Hoofdstuk 2 introduceert de Maximaal Toegestane Stuurverstoring (Maximum Allowable Handlebar Disturbance - MAHD) als een nieuwe indicator voor het veilig en proactief evalueren van interventies ter voorkoming van valpartijen bij fietsers. In tegenstelling tot de binaire uitkomst van vallen of herstellen, biedt de MAHD een gedetailleerde kwantificering van de effectiviteit van interventies, wat een gedetailleerdere vergelijking tussen verschillende interventies mogelijk maakt. Bovendien tonen we aan dat deze indicator kan worden toegepast op verschillende ongevalsscenario's die impulsachtige verstoringen omvatten en systematisch interventies kan evalueren gericht op fietsontwerp, fietserscontrole en infrastructuur zodat deze met elkaar vergeleken kunnen worden.

Hoofdstuk 3 presenteert de allereerste experimenten ooit waarin daadwerkelijke valpartijen van fietsers worden gesimuleerd. De experimenten zijn uitgevoerd met 24 deelnemers uit jongere en oudere leeftijdsgroepen. Deze experimenten leverden een waardevolle dataset op die kan worden gebruikt om de voorspellende prestaties van modellen voor fietsdynamica en stuuracties van de fietser te valideren.

Daarnaast werden in **Hoofdstuk 3** eigenschappen en vaardigheden van de fietser geïdentificeerd die belangrijk zijn voor het voorspellen van een val. Deze zijn

geïdentificeerd door middel van Bayesian Model Averaging. Belangrijke voorspellers waren voorwaartse snelheid — waarbij de kans op vallen kleiner was bij lagere snelheden — en balansvaardigheid, gedefinieerd als de vaardigheid om een middenlijn te volgen tijdens ongestoord fietsen. Verrassend genoeg was leeftijd geen belangrijke voorspeller of een fietser wel of niet valt.

In **Hoofdstuk 3** ontwikkelden we ook een Bayesiaans multilevel logistisch regressiemodel om de MAHD voor individuele deelnemers te schatten. Dit was nodig vanwege de menselijke variaties, waarbij er vaak geen duidelijke grens was voor een deelnemer in de specifieke grootte van de verstoring waarbij degene viel of overeind bleef.

In **Hoofdstuk 4** introduceerden we een model dat de stuuracties van de fietser voor de evenwichtstaak simuleert. Met dit model beogen we om veilig en proactief te bestuderen welke wijzigingen in stuuracties of stragieën het risico op vallen kunnen verminderen. Het gepresenteerde model omvat menselijke zintuigen, een gedeeltelijke terugkoppeling van de oriëntatie en bewegingen van de fiets, integratie van meerdere zintuigen om de complete oriëntatie en bewegingen van de fietsen te schatten, stuuracties van de fietser en spierdynamica. Dit model simuleert realistisch fietsgedrag waarbij alleen de leunhoeksnelheid en stuurhoek, zonder vertraging, worden teruggekoppeld. Bij tests behaalde dit model een gemiddelde Variance Accounted For (VAF) score van 65,6% (met een standaarddeviatie van 25,8%) in het voorspellen van de stuuracties in experimenten op een smalle loopbandopstelling en een gemiddelde VAF-score van 55,6% (met een standaarddeviatie van 27,7%) voor experimenten in een paviljoenopstelling. Deze resultaten tonen de robuustheid van het model aan bij het simuleren van stuuracties van de fietser voor de balanstaak. Het model weerspiegelt namelijk de reacties van verschillende fietsers bij verschillende snelheden.

Het gepresenteerde model in **Hoofdstuk 4** vereist slechts de kalibratie van één invoerwaarde — de weegfactor voor de leunhoek in de LQR-toestandsweegmatrix. De andere invoerwaarden zijn eenvoudig te meten. Belangrijk is dat deze weegfactor onafhankelijk is van de voorwaartse snelheid, waardoor kalibratie bij slechts één snelheid nodig is, in tegenstelling tot bestaande modellen die kalibraties vereisen van meerdere invoerwaardes bij verschillende snelheden. Deze eigenschap verbetert de praktische toepassing van ons model aanzienlijk.

In **Hoofdstuk 5** hebben we de betrouwbaarheid en praktische bruikbaarheid van een mogelijk model voor fietsdynamica en stuuracties van de fietser geëvalueerd. Deze evaluatie betrof het vergelijken van de MAHD-voorspellingen van het model met experimentele gegevens, waarbij fietsers werden blootgesteld aan stuurverstoringen die leidden tot zowel valpartijen als herstel van evenwicht. Bovendien demonstreerden we de bruikbaarheid van het model door middel van drie casestudies waarin interventies werden onderzocht die gericht waren op stuuracties om balans te houden, fietsontwerp en infrastructuurontwerp.

De resultaten van **Hoofdstuk 5** toonden de effectiviteit van dit bestaande model aan bij het betrouwbaar voorspellen van de MAHD voor fietsers met verschillende vaardigheidsniveaus. Bovendien heeft dit model het vermogen om belangrijke aspecten van stuuracties van de fietser op grote verstoringen te voorspellen. Bovendien bleek het model succesvol te zijn in het evalueren van het gevolg van aanpassingen

aan fietsontwerp, fietserscontrole en infrastructuur op de MAHD. Deze bevindingen onderstrepen de betrouwbaarheid en bruikbaarheid van het model en zijn potentieel als een waardevol instrument voor het veilig en proactief evalueren van verschillende interventies ter voorkoming van valpartijen.

Concluderend heeft het onderzoek in dit proefschrift bijgedragen aan de ontwikkeling van een aanpak die gebruik maakt van modellen voor fietsdynamica en stuuracties van de fietser om veilig en proactief interventies ter voorkoming van valpartijen bij fietsers te evalueren. Door de praktische toepassing van deze modellen te verbeteren en een systematisch kader voor vergelijking van interventies te creëren, draagt dit werk bij aan een waardevol instrument dat kan worden gebruikt door ontwerpers, ingenieurs en beleidsmakers om veilig en proactief interventies ter voorkoming van valpartijen bij fietsers te evalueren. Uiteindelijk zal dit bijdragen aan verbeterde ontwerpen van fietsen, infrastructuur en trainingsprogramma's, en de toewijzing van middelen aan de meest effectieve interventies.

PREFACE

You are about to read my dissertation on cyclist fall prevention interventions, a project that has spanned six years of dedication and growth. The first four years were spent as a PhD candidate at Delft University of Technology, followed by two years working as a road safety policy advisor at the Ministry of Infrastructure and Water Management. During these latter two years, I completed this dissertation while balancing my work as an advisor.

The motivation for this research stems from my firm belief in the transformative potential of replacing motorised vehicle trips, including public transport, with cycling (preferably non-pedal-assisted) or walking. Such a shift offers a powerful solution to some of society's most pressing challenges. Cycling instead of using motorised transport can reduce CO2 emissions while simultaneously increasing the number of people meeting physical activity guidelines, thus benefiting both the environment and public health. Moreover, expanding the availability of services and jobs within cycling distance can improve mobility for vulnerable groups, such as the elderly and low-income individuals, contributing to self-sufficiency, mental health and equality of opportunity. Furthermore, replacing car trips with cycling could free up substantial public space currently occupied by car infrastructure, allowing city centres to reallocate space for green areas, water storage, or biodiversity restoration — helping mitigate heat stress and environmental degradation.

However, with an increase in cycling kilometres comes a significant concern: the likely rise in crashes resulting in deaths and serious injuries. As a balancing vehicle, the bicycle inherently poses a higher risk of injury per kilometre travelled than most other modes of transport. Even today, with motorised trips still dominant, most serious cyclist injuries result from falls, not collisions with other road users.

While promoting the use of tricycles or helmets might mitigate the expected rise in crashes, I believe the unique characteristics of the bicycle — its instability and lack of user requirements — make it so efficient and appealing. The bicycle's inherent instability facilitates manoeuvrability — cornering itself is a controlled fall — where leaning helps riders to manage centrifugal forces. Additionally, the ease and spontaneity of cycling without needing a helmet encourages its use for even the shortest trips.

Therefore, I was motivated and inspired to contribute to research on preventing cyclist falls, which looked at a promising alternative. In collaboration with colleagues, I worked on a project to develop a bicycle balance-assistance system for cyclists, similar to the lane-keeping assistance systems found in modern cars, but specifically designed to help cyclists maintain balance.

However, during the early stages of my research, I encountered a major challenge. There was no established method for estimating the effectiveness of such a new intervention before its implementation. This limitation posed a significant hurdle: without a reliable predictive approach, it was impossible to evaluate whether the

steer-assist bicycle would effectively prevent cyclist falls or to determine which design elements would be critical to its success. This challenge shifted the scope and focus of my dissertation.

In this dissertation, I present the development of a novel approach to estimating the effectiveness of cyclist fall prevention interventions prior to their implementation. This undertaking required integrating two distinct fields of research: the engineering fields of bicycle dynamics and cyclist control with traffic safety research. This bridging process was both complex and intellectually demanding. However, I hope this work will bridge the gap between these fields, stimulating further research and innovation.

In addition, I also gained some valuable insights while working as a policy advisor. I realised that engineers, designers, and policymakers must adopt this approach to have a real-world impact. While a scientific dissertation is not the ideal format for communicating practical applications to these professionals, I still hope that my experience in policy has shaped the content of this work to be more accessible and applicable.

Though the approach still requires further development, I could provide a preliminary estimate of the potential effectiveness of the balance-assistance system. This estimate, in turn, allowed me to (partially) address one of the key research questions posed at the outset of this project. While this may seem like a modest step, I believe that accurately diagnosing the problem is crucial to ensuring that the solution we pursue is right.

Therefore, I am proud of the outcomes we have achieved and the approach we have developed. I believe that advancing this approach will significantly enhance our ability to evaluate and prioritise safety interventions for cyclists, helping us focus on the strategies that will most effectively protect cyclists in the future.

Marco Michiel Reijne
The Hague, February 2025

INTRODUCTION

The rising number of cyclist deaths and serious injuries underscores the need for better cycling safety interventions. These interventions are essential to reduce the human and economic impact of such crashes and meet the goals set by the United Nations [1, 2]. While historically, the impact and costs of cyclist crashes were considered lower than those involving car occupants, recent data indicate that in countries with a high volume of cyclists, the consequences of cycling crashes have become comparable to those of motor vehicle crashes [3–7]. For these countries, it is crucial to prioritise the efficient allocation of resources towards cycling safety to achieve the goal set by the United Nations — and adopted by many countries — to eliminate road deaths by 2050 and halving the number of road deaths and serious injuries between 2020 and 2030 [1]. Efficiently allocating the available resources requires identifying and implementing cost-effective safety interventions for cyclists. This identification is crucial, as existing and proposed cycling safety interventions vary widely in their objectives, strategies, target populations, and outcomes.

Although interventions are often categorised based on the road system component or crash phase they target [8], it is important to acknowledge the complexity of crashes, which typically is a multifaceted interplay of factors [9]. Despite this complexity, categorising interventions offers a useful framework to analyse their objectives, strategies, target populations, and outcomes.

For instance, an intervention targeting the infrastructure component and pre-crash phase are separated bicycle paths. This intervention aims to prevent high-risk crash situations by physically separating cyclists from motor vehicles [10]. Innovations in bicycle design, such as automatic saddle lowering, steer-assistance systems, and a tilting tricycle, focus on improving stability and reducing fall risk in situations in which there is already a higher risk of a crash [11–13]. Additionally, equipping bicycles with warning systems and improving visibility aims to prevent these high-risk situations [14–17]. Educational programs, tailored to various age groups, aim to equip cyclists with the knowledge and skills to avoid dangerous situations as well [18], while awareness campaigns promoting safety measures like helmet use aim to lessen injury severity in case of a crash [19].

The cost-effectiveness of these illustrative examples vary, because of their diverse objectives and methods. Knowing which interventions are most cost-effective would be valuable. While studies have identified the effectiveness of several interventions, some promising ones still need evaluation.

One particularly promising intervention is one designed to prevent cyclist falls because evidence shows that many cycling-related crashes and injuries are related to falls. Commonly reported crash types are, for instance, loss of balance and skidding [20]. Moreover, there is evidence indicating that even severe injuries resulting from collisions with other road users or obstacles are also primarily due to loss of balance and the

impact with the ground following a fall [21–23]. This evidence suggests that preventing a fall still reduces the risk of serious injury, even when the initial collision is unavoidable. By focusing on fall prevention, potential interventions can thus address a common cause of crashes and significantly reduce the number of serious injuries among cyclists.

Evaluating the effectiveness of these fall-prevention interventions is crucial for making informed design decisions and allocating resources to the most beneficial cycling safety interventions. However, existing evaluation approaches struggle to evaluate a wide range of cyclist fall prevention interventions.

EXISTING APPROACHES TO EVALUATE CYCLING SAFETY INTERVENTIONS

Various approaches have been developed to evaluate cycling safety interventions. These approaches are based on historical crash data, video observations, field studies, experimental studies, and computer models that simulate traffic scenarios. This section provides a review of these approaches, examining their applications, strengths, and limitations, with a specific focus on their suitability for evaluating cyclist fall prevention interventions

Reduction in crash rates determined from statistical analysis of historical crash data

The most common and direct approach to evaluate the effectiveness of cycling safety interventions is through statistical analysis of historical bicycle crash data. By comparing crash rates before and after safety interventions are implemented, researchers can isolate and quantify the impact of these interventions. The effectiveness is typically quantified by the reduction in fatal crashes or crashes resulting in serious injuries, which are objective safety indicators.

This approach has been used to evaluate interventions such as traffic calming measures like street closure and speed bumps [24], mandatory helmet laws [25], cars equipped with Advanced Driver Assistance Systems (ADAS) that detect and warn drivers about vulnerable road users [26], and safe speed limits for roads shared by motorists and cyclists [27].

A key strength of this approach is that it is capable of systematically evaluating the impact of diverse interventions, including infrastructure improvements, vehicle design modifications, and behavioural changes. Moreover, researchers can determine the impact of an intervention not only at a specific site but also across larger geographic areas, such as entire countries or regions.

Another significant strength of this approach is the use of real-world data and objective safety indicators, which increases confidence in the reliability and validity of the findings.

However, a considerable limitation of this approach is its inherent dependence on the availability of reliable and representative historical crash data. If such data is unavailable, the statistical analysis becomes infeasible or unreliable. In the case of cyclist fall prevention interventions, this dependency poses a challenge because single bicycle crashes, which are predominantly falls, are significantly underreported in police records [28]. The only alternative sources of data that provide a large enough sample size for reliable statistical analysis are hospital records or retrospective surveys, occasionally supplemented by site inspections, involving cyclists who have sought emergency care

[29–33]. While these sources likely offer a more accurate count of single bicycle crashes, the limited number and scope of variables collected often restrict the ability to isolate the effects of specific interventions. For example, it remains uncertain whether electric pedal-assisted bicycles (e-bikes) have a greater crash risk than traditional bicycles [34].

This limitation also creates challenging when wishing to proactively evaluate new interventions which have not yet been implemented. For instance, novel bicycle types or road designs for which historical data does not yet exist. Although indirect predictions can sometimes be made by drawing comparisons with similar interventions for which crash data is available, the reliability of the prediction diminishes if significant differences exist between the new and existing conditions.

When historical crash data is available, this approach can be conducted relatively quickly and at a low cost. However, if such data is unavailable — for instance, for single bicycle crashes or new interventions — collecting sufficient crash data is often time-consuming and expensive. It will often require multiple years of crash data before enough crashes have been registered for a robust and reliable statistical analysis [35]. In addition, it may require additional administrative effort during this period, further increasing costs. Ethical concerns about implementing untested interventions on a large scale and privacy legislation may further complicate the data collection and analysis process.

Surrogate safety indicators determined from video observation

Another approach to evaluate cycling safety interventions involves using surrogate safety indicators derived from observational video data collected at specific sites. Surrogate safety indicators are indicators that estimate the likelihood and severity of potential traffic conflicts or crashes without relying on actual crash data. These indicators are often determined from observable traffic behaviour in video data, such as vehicle trajectories, speeds, and interactions. This allows researchers to proactively evaluate safety, especially for interventions for which crash data is unavailable, incomplete, or insufficient for robust statistical analysis. By comparing surrogate safety indicators before and after interventions, researchers can isolate and quantify the effects of these interventions.

Surrogate safety indicators can be broadly categorised into two types [36]. The first type measures the presence of evasive manoeuvres, such as sudden stops or sharp turns, indicating an attempt to avoid a collision. The second type measures the proximity of road users in time and space, using indicators like Time-To-Collision (TTC) and Post-Encroachment Time (PET). TTC measures the time until a collision if no changes are made, while PET measures how closely two road users pass or follow one another.

This approach has been effectively used to evaluate interventions like improved signage and road markings, which clearly define yield requirements [37], and increased bicycle path widths, which reduce potential conflicts [38].

The key strengths of this approach are that it measures real-world behaviour and interactions, ensuring environmental validity, and it can systematically evaluate a wide variety of road safety interventions. While the focus of existing studies has been on infrastructural changes, this approach is equally suitable for evaluating the impact of vehicle design modifications and behavioural interventions on surrogate safety

indicators.

Additionally, this method allows for the proactive evaluation of new interventions before severe crashes occur, making it a valuable alternative to crash data analysis. Moreover, the required video-based data collection for a reliable and robust analysis typically spans days or months rather than years. Recent advancements in automated video analysis software further improve the speed, ease, and cost-effectiveness of this approach by enabling the automatic extraction of variables needed to compute surrogate safety indicators [39].

Despite these strengths, there are limitations to the use of surrogate safety indicators. Surrogate safety indicators provide an indirect measure of crash risk, as opposed to the direct measurement offered by crash data analysis. Although studies have validated their correlation with crash risk motor vehicle collisions [36], including the relationship between minor incidents and more severe crashes [40], their validity for cyclist-related crashes requires further investigation [36].

Another key limitation is the restricted applicability of surrogate safety indicators for evaluating cyclist fall prevention interventions. Indicators such as TTC and PET primarily address interactions between road users and have been most extensively validated for such scenarios. As a result, they are not well-suited to interventions targeting single bicycle crashes, which make up the majority of cycling falls [20]. These falls, caused by events like skidding, hitting a kerb, or riding over a pothole, typically do not involve interactions with other road users. Consequently, surrogate safety indicators currently have limited applicability for evaluating interventions aimed at preventing these types of falls.

Performance indicators determined from field studies

Cycling safety interventions can also be evaluated through field studies, which involve experiments conducted in real-world settings. Field studies range from naturalistic cycling studies to operational field cycling experiments.

Naturalistic cycling studies involve observing and recording cyclists' behaviour in their everyday environments without intervention or manipulation by researchers. This approach is similar to video observation at specific locations but differs in its emphasis on following individual cyclists rather than monitoring a fixed site.

In contrast, operational field cycling experiments involve controlled tests in real-world settings. Here, researchers actively design and implement experimental conditions through specific instructions, prescribed routes, or controlled interactions.

Data collection in field studies often involves equipping the cyclist, bicycle, or environment with sensors, along with administering questionnaires before, during, or after the experiment. This allows researchers to collect a broader range of variables than video observation alone, and often with greater accuracy.

Performance indicators used in combination with field studies to evaluate the effect of cycling safety interventions include surrogate safety indicators, as well as indicators such as subjective or perceived safety, workload, and bicycle dynamics (e.g., lean angle, steer rate). By comparing these indicators before and after an intervention, researchers can evaluate its effectiveness.

Past studies have used this approach to evaluate interventions such as bicycle lane

buffers and traffic calming measures on perceived safety [41], the effect of visual speed-reducing nudges at intersections [42], the impact of mobile phone use on cycling workload [43, 44], and the influence of dismounting techniques on bicycle stability [45].

Field studies offer several key strengths. They can evaluate a diverse range of interventions, including infrastructure improvements, vehicle design modifications, and behavioural changes. Unlike video observation approaches using surrogate safety indicators, field studies can also compute other performance indicators that can evaluate interventions that aim to prevent single bicycle crashes. Furthermore, this approach allows for proactive evaluation of new interventions before serious crashes occur, offering an advantage over crash data analysis approaches.

Another key strength of field studies, particularly operational field cycling experiments, is the level of control researchers can exert over experimental conditions and collected variables. This control enables faster and potentially more reliable analyses of the cause-effect relationships of interventions.

However, there are limitations to this approach. As with surrogate safety indicators, the performance indicators used in field studies are indirect measures of fall risk, as they are typically derived under normal cycling conditions or situations with increased crash risk but rarely during actual crash scenarios. While the link between these indicators and fall risk appears logical, their reliability in predicting falls requires further validation.

Validating these indicators presents challenges. Naturalistic cycling studies occasionally capture real crashes, but such events are too infrequent for robust analysis. Collecting sufficient data on serious crashes would require prolonged observation periods, perhaps even longer than the statistical analysis of crash records approach. Additionally, recording real crashes cancels the proactive nature of the approach. Operational field experiments, meanwhile, cannot yet ethically or safely replicate crash scenarios, further limiting opportunities to validate the performance indicators.

Furthermore, although cyclists in field studies are observed in real-world settings, their awareness of being monitored may lead them to alter their behaviour, reducing the environmental validity of the findings. This concern is less pronounced in naturalistic cycling studies than in operational field cycling experiments.

Finally, operational field cycling experiments often require complex preparation, specialised equipment, and instrumentation of the cyclist, bicycle, or environment, making them resource-intensive. However, the evaluation time for new interventions is typically shorter than that required for video observation or crash record analysis.

Performance indicators determined from cycling experiments in an isolated controlled environment

Cycling safety interventions can also be evaluated through experiments conducted in isolated, controlled environments such as closed test tracks, indoor halls, treadmills, or bicycle simulators. These experiments share similarities with field studies but provide greater control over testing conditions, enabling researchers to isolate specific factors and efficiently establish cause-effect relationships.

Similar performance indicators as those used in field studies – such as perceived safety, workload and lean angle – can be used in these experiments to evaluate cycling safety interventions. Through controlled test-control experiments, researchers can

evaluate the effects of interventions on these indicators.

This approach has been applied in various studies, such as evaluating the effect of infrastructure interventions on cyclist speed using a test track [46], examining the impact of alcohol intoxication on bicycle stability while cycling on a treadmill [47, 48], and evaluating the effect of road design on perceived safety using bicycle simulators [49, 50].

Cycling experiments in controlled environments offer several advantages. Like field studies, they can proactively evaluate a wide range of interventions, including infrastructure improvements, vehicle design modifications, and behavioural changes. They are also suitable for studying single bicycle crashes without the involvement of other road users.

The key strength of this approach is the high degree of control over experimental conditions, which allows researchers to reliably replicate specific scenarios and collect variables with greater accuracy. This control allows for systematic evaluations of cause-effect relationships, often faster than field studies.

However, this approach has several limitations. A significant concern remains the reliability of performance indicators, which are indirect measures of fall risk. Since actual falls have not yet been included in existing experiments, these indicators, although intuitively linked to fall prevention, remain unvalidated.

Controlled environments theoretically allow for safer replication of dangerous conditions compared with field studies, as additional safety measures can be implemented. While this has not yet been applied to cycling experiments, similar experiments have been conducted safely in other contexts, such as walking [51]. Such experiments could help validate the predictive reliability of performance indicators for fall prevention — at least in an experimental setting.

Another limitation is the potential lack of environmental validity — the extent to which findings from controlled environments translate to real-world behaviour. This is particularly relevant for simulators, where sensory inputs and bicycle dynamics differ from real-world conditions, potentially influencing cyclist behaviour. Similarly, while treadmill cycling preserves the bicycle dynamics, mismatched sensory feedback may affect experimental outcomes. In all types of experiments, the awareness of being monitored may lead participants to alter their behaviour.

Finally, while controlled settings simplify some aspects of data collection and analysis, these experiments often require complex preparation, specialised equipment, and significant resources, making them as time-consuming and expensive as field studies.

Performance indicators determined from crash experiments

Crash experiments provide an approach for evaluating cycling safety interventions by focusing on objective, direct safety indicators such as impact forces and energy absorption. These indicators are typically measured through controlled physical tests involving crash dummies [52, 53] or isolated testing of specific bicycle components and accessories [54–56]. This approach has been used to evaluate interventions such as helmet designs [54, 55] and vehicle crash zones designed to protect cyclists [56].

The key strength of crash experiments lies in their ability to provide detailed, objective evaluations of safety equipment under controlled conditions. By eliminating

confounding factors present in real-world studies, this approach enables researchers to isolate the effectiveness of specific interventions with great detail. For instance, studies have distinguished the safety performance of different helmet designs through controlled crash testing [55].

Despite this strength, crash experiments have notable limitations. This approach is primarily suited to interventions aimed at reducing injury severity after a fall or collision, such as helmets, airbags, or vehicle safety features. It is not applicable to evaluating interventions focused on preventing cyclist falls or crashes altogether, such as road design improvements, vehicle design modifications, or behavioural measures.

Performance indicators determined from models that simulate traffic scenarios
Cycling safety interventions can also be evaluated using models that simulate traffic scenarios, even replicating specific crash types or phases. These models allow researchers to incorporate various interventions and compute different performance indicators. Existing models can be categorised as traffic microsimulation models, behavioural or crash avoidance models, crash simulation models and Finite-Element-Modeling (FEM).

Traffic microsimulation models use mathematical equations to simulate the movements and interactions of individual road users, such as cyclists and motorists, within a road network. Each road user is modelled as an independent agent with unique behaviours based on predefined rules, enabling the replication of real-world traffic flow and interactions. These models are commonly used to evaluate motor vehicle safety interventions, such as road infrastructure designs and traffic management policies, before their implementation in the real world [57, 58].

Behavioural and crash avoidance models simulate the decision-making processes and actions of road users, focusing on their responses to potential hazards and crash scenarios. Behavioural models focus on human decision-making under various conditions [59, 60], while crash avoidance models focus on the decisions required to avoid collisions, often focussing on the execution of physical manoeuvres [61]. These models are often integrated with traffic microsimulation models to describe the behaviour of individual agents.

Crash simulation models and FEM models simulate the physical forces and deformation experienced by cyclists and their equipment during crashes, providing insights into biomechanics and injury risk [62, 63]. FEM models, in particular, allow for highly detailed simulations by dividing objects, such as helmets, bicycles, or human anatomy, into smaller elements to analyse how forces propagate through materials.

The key strength of these models is their ability to provide safe, fast, cost-effective, and proactive evaluations of cycling safety interventions. Compared with other approaches described earlier, the models offer significant advantages in testing new interventions without requiring real-world implementation.

However, there are limitations concerning the types of interventions that can be evaluated and the predictive validity and reliability of certain models. Crash simulation and FEM models, for instance, are well-validated but are primarily suited for evaluating injury mitigation interventions, such as helmets or other safety equipment, rather than cyclist fall prevention measures.

Traffic microsimulation, behavioural, and crash avoidance models also face limitations when applied to cyclist fall prevention interventions. These models are primarily designed to simulate interactions and conflicts involving multiple road users and are not well-suited for simulating single bicycle crashes, which account for the majority of cycling falls [20]. Moreover, while behavioural models have made progress in simulating cyclist behaviour, their validation for accurately predicting falls and incorporating bicycle dynamics and cyclist control related to balance — an essential component for accurately simulating cyclist falls — remains in its early stages [60].

PROBLEM STATEMENTS OF EXISTING INTERVENTION EVALUATION APPROACHES

Interventions aimed at preventing cyclist falls hold significant potential to improve cycling safety, given the prevalence of such crashes. While existing approaches for evaluating cycling safety interventions are diverse and complementary, a critical gap remains in the proactive evaluation of interventions specifically designed to reduce fall risk once in a critical situation.

Critical situations are situations in which there is a higher risk of a fall and include events such as riding over a pothole, colliding with a kerb, or briefly touching handlebars with another cyclist. These scenarios increase the likelihood of a fall but do not always lead to one, as balance can sometimes be recovered. Improving cyclists' reactions, bicycle design, or infrastructure can increase the likelihood of recovering balance in such situations.

Several intervention types target balance recovery and fall prevention. For example, balance training programs. These aim to improve cyclists' balancing skills, as seen in the multi-component cycling training program from the Safer Cycling in Older Age (SiFAr) initiative [64]. This program included exercises to improve balance, strength, and motor skills.

Another example is vehicle design modifications such as a steer-assist system [12]. This system uses sensors to measure the bicycle's lean rate and steering angle, an electric motor embedded in the headtube to provide a steering torque, and a speed-adaptive feedback controller to apply targeted control corrections. This system conceptually parallels ADAS in automotive engineering, which assists drivers in maintaining control during challenging scenarios. Empirical evidence also suggests that bicycle frame geometry adjustments, such as changes to wheelbase, trail, head tube angle, or bottom bracket height, can improve bicycle stability and balance recovery in critical situations.

Also, infrastructure design interventions could improve balance recovery in critical situations. Sloped kerbs and ridable road shoulders are examples of such interventions [65, 66]. These interventions provide a safer transition for cyclists who inadvertently leave the designated path — either because of inattention or to recover balance after a disturbance. Sloped kerbs allow cyclists to recover balance while minimising the destabilisation caused by the hard edge. Forgiving shoulders offer additional space to correct course deviations or recover balance.

Although these interventions are promising, the direct relationship between their implementation and fall prevention remains largely unvalidated. Evaluating these interventions and systematically comparing their effectiveness with other interventions

is challenging due to limitations in current evaluation approaches:

- The statistical analysis of bicycle crash data approach is hindered by the underreporting of single bicycle crashes [28], limiting the availability of reliable and representative data on cyclist falls. Moreover, this approach excludes the evaluation of most interventions that have yet to be implemented and requires a prolonged data collection period, often spanning multiple years, before reliably evaluating a new intervention becomes feasible.
- Surrogate safety indicators focus on conflicts involving multiple road users, while crash impact indicators evaluate injury mitigation. Neither is suitable for evaluating interventions designed to prevent falls by improving balance recovery in critical situations in which no other road users are involved — which is the case for most falls [20].
- Indicators used in field or experimental studies — such as perceived safety, workload, and bicycle motions — are indirect measures of fall risk. While the links between these indicators and fall risk are intuitive, their validity for predicting falls has not been established due to insufficient fall data. Naturalistic cycling studies and video observations include fall records, but the number of recorded events is too low for robust validation. Simulating falls in operational field experiments is dangerous, though controlled environments may offer a safer alternative, as demonstrated in studies evaluating fall risk while walking [51].
- Traffic microsimulation, behavioural, and crash avoidance models focus primarily on interactions with other road users and are not yet designed to incorporate the bicycle dynamics and cyclist control related to balance, which is required for accurately simulating cyclist falls. FEM and crash simulation models are limited to evaluating interventions aimed at injury mitigation post-crash and cannot address interventions aimed at preventing falls.

These limitations prevent the proactive and systematic evaluation of potentially valuable fall prevention interventions, such as balance training programs, bicycle designs, and edge-of-road infrastructure.

BICYCLE DYNAMICS AND CYCLIST CONTROL MODELS

The aim of this dissertation is to develop an approach to safely and proactively evaluate cyclist fall prevention interventions that aim to reduce fall risk in critical situations.

A validated model that could simulate single bicycle crash types would be ideal for this purpose, as it allows for proactive, cost-effective, and fast evaluations of a wide range of interventions. However, none of the models discussed earlier are suitable, primarily because they do not incorporate the balancing task and lateral dynamics of the bicycle. While collisions can be simulated, reliable fall simulations remain a challenge.

Bicycle dynamics and cyclist control models offer a promising approach to addressing this gap. Bicycle dynamics and cyclist control models are mathematical representations that simulate how bicycles move and how cyclists interact with them. By understanding the dynamics of bicycle and the control inputs from cyclists related

to balance, these models provide valuable insights into how falls can be prevented. An approach using these models could complement existing methods by enabling the evaluation of cyclist fall prevention interventions aimed at reducing fall risk in critical situations.

Existing bicycle dynamics models, such as the Carvallo-Whipple (C-W) model, represent bicycles as interconnected rigid bodies, capturing essential dynamics while incorporating factors like cyclist mass distribution [67]. These models can also incorporate environmental conditions such as road surface properties or environmental disturbances due to collisions or from other sources. Moreover, the C-W model has been extensively validated [68–71].

Extensions to the C-W model have been developed to accommodate for more details such as wheel shape and tyre characteristics to simulate the tyre-ground interactions, account for cornering or acceleration or include passive rider dynamics to simulate how the cyclist's body interacts with the bicycle [72–80]. Although these extensions allow for more nuanced simulations (and evaluation of more types of interventions), these have not yet been validated.

Existing cyclist control models primarily focus on the balancing task via steering, with experiments suggesting leaning plays a minimal role in balancing control, particularly at low speeds [77, 81]. These models describe the vehicle control skill of the cyclist — in this case focussing on the cycling balancing task. Validation of cyclist control models remains limited, with only two models experimentally validated [81, 82]. Inputs for these models include feedback gains and neuromuscular characteristics, which are more abstract than the inputs for bicycle dynamics models.

When combined, these models can simulate real-world cyclist fall scenarios, including scenarios where no other road users are involved. Additionally, these models could simulate the effects of various interventions, including changes in bicycle design, infrastructure, or cyclist behaviour, on fall risk. For example, they could evaluate how modifications to bicycle geometry, training programs, or forgiving road shoulders affect balance recovery in critical situations. Moreover, a direct safety indicator can be computed from the fall scenario simulation, eliminating the need for indirect safety indicators. As such, these models could address the limitations of existing approaches.

PROBLEM STATEMENTS OF BICYCLE DYNAMICS AND CYCLIST CONTROL MODELS

While bicycle dynamics and cyclist control models hold significant promise for evaluating cyclist fall prevention interventions aimed at reducing fall risk in critical situations and complementing existing approaches, several challenges must be addressed before their full potential can be realised:

- Firstly, a collaborative effort between vehicle dynamics and control researchers and road safety researchers is essential to apply these models effectively. While bicycle dynamics and cyclist control models have existed for decades, these have not yet been applied to evaluate cycling safety interventions. One significant hurdle in this collaboration is the language barrier. Road safety research often employs descriptive language to outline trends, patterns, and outcomes related

to traffic crashes, using terms accessible to policy advisers, bicycle designers, transportation planners, and the public. This descriptive language contrasts with the specialised technical language used in vehicle dynamics and control studies, which delves into the physics, mathematics, and engineering principles of vehicle dynamics. Bridging this communication gap is essential to translate the findings from these models into actionable tools for evaluating cyclist fall prevention interventions.

- Secondly, a significant challenge lies in developing and validating a generally applicable, objective indicator to evaluate and compare cyclist fall prevention interventions. While bicycle dynamics and cyclist control models offer versatility in simulating various scenarios, the lack of a standardised indicator to measure intervention effectiveness across the broad cycling population and diverse situations limits their applicability. It hinders the ability to generalise the effectiveness of safety interventions.

- Thirdly, the validation of these models for actual falls still needs to be addressed. Although they have been validated under standard cycling conditions, providing a degree of confidence, the absence of validation studies involving actual falls raises concerns about their applicability in real-world fall scenarios.

- Fourthly, current models often lack intuitive cyclist characteristics, relying instead on abstract variables like feedback gains. This abstractness limits their practical application to evaluate cyclist-control focused interventions.

GOAL

The goal of this dissertation is to develop an approach to safely and proactively evaluate cyclist fall prevention interventions, particularly those aiming to reduce fall risk in critical situations. This approach aims to evaluate the effectiveness of these interventions before they are implemented using an objective, direct and general indicator. By doing so, it eliminates the need to rely solely on statistical analysis of historic bicycle crash data or indirect safety indicators. The proposed approach is intended to complement existing approaches and contribute to improving cycling safety.

APPROACH

Subsequent chapters of this dissertation describe the efforts undertaken to develop an approach to safely and proactively evaluating cyclist fall prevention interventions. This approach is centred around the use of bicycle dynamics and cyclist models.

In Chapter 1, we begin by explaining and illustrating how these models can simulate commonly reported bicycle crash types, including crash types where no other road users are involved, and which types of interventions can be incorporated into these models.

In Chapter 2, we introduce the Maximum Allowable Handlebar Disturbance (MAHD) as a new quantitative, objective, direct and general indicator for safely and proactively evaluating the performance of a wide range of cyclist fall prevention interventions.

In Chapter 3, the results from a cyclist fall experiment are presented in which participants cycled on a treadmill and were subjected to impulse-like handlebar disturbances that caused both falls and balance recoveries. This experimental dataset is used to identify important predictors for cyclist falls and construct a predictive statistical model to predict the MAHD under various experimental conditions.

In Chapter 4, a cyclist control model is developed that describes the cyclists' steering actions to recover balance after a small disturbance. This model incorporates intuitive human characteristics to improve its applicability in evaluating cyclist control-focused interventions.

Finally, in Chapter 5, the work performed in the previous chapters is combined to develop and validate a bicycle dynamics and cyclist control model that can simulate crash types where the cyclist encounters impulse-like disturbances — such as collisions with other road users or obstacles or falls due to loss of balance. The model's reliability is evaluated by comparing its MAHD prediction to the dataset of the cyclist fall experiments, which included actual falls. The practical application of the model is evaluated by incorporating interventions targeting infrastructure design, bicycle design and cyclist balance control training programs and determining their impact on the MAHD.

REFERENCES

[1] United Nations (2020), *Resolution 74/299: Improving global road safety,* https://documents-dds-ny.un.org/doc/UNDOC/GEN/N20/226/30/PDF/N2022630.pdf?OpenElement, accessed 11 January 2025.

[2] World Health Organization (2020), *Cyclist safety: An information resource for decision-makers and practitioners,* https://iris.who.int/bitstream/handle/10665/336393/9789240013698-eng.pdf, accessed 11 January 2025.

[3] W. Wijnen and H. Stipdonk, *Social costs of road crashes: An international analysis,* Accident Analysis & Prevention **94**, 97 (2016), https://doi.org/10.1016/j.aap.2016.05.005.

[4] S. Polinder, J. Haagsma, M. Panneman, A. Scholten, M. Brugmans, and E. van Beeck, *The economic burden of injury: Health care and productivity costs of injuries in the Netherlands,* Accident Analysis & Prevention **93**, 92 (2016), https://doi.org/10.1016/j.aap.2016.04.003.

[5] W. Wijnen, W. Weijermars, A. Schoeters, W. van den Berghe, R. Bauer, L. Carnis, R. Elvik, and H. Martensen, *An analysis of official road crash cost estimates in European countries,* Safety Science **113**, 318 (2019), https://doi.org/10.1016/j.ssci.2018.12.004.

[6] A. Schoeters, M. Large, M. Koning, L. Carnis, S. Daniels, D. Mignot, R. Urmeew, W. Wijnen, F. Bijleveld, and M. van der Horst, *Economic valuation of preventing fatal and serious road injuries. Results of a Willingness-To-Pay study in four European countries,* Accident Analysis & Prevention **173**, 106705 (2022), https://doi.org/10.1016/j.aap.2022.106705.

[7] W. Weijermars, N. Bos, and H. L. Stipdonk, *Serious road injuries in the Netherlands dissected,* Traffic Injury Prevention **17**, 73 (2016), https://doi.org/10.1080/15389588.2015.1042577.

[8] W. Haddon Jr, *Advances in the epidemiology of injuries as a basis for public policy,* Public health reports **95**, 411 (1980), https://pmc.ncbi.nlm.nih.gov/articles/PMC1422748/pdf/pubhealthrep00127-0003.pdf.

[9] N. Leveson, *A new accident model for engineering safer systems,* Safety Science **42**, 237 (2004), https://doi.org/10.1016/S0925-7535(03)00047-X.

[10] P. Schepers, E. Heinen, R. Methorst, and F. Wegman, *Road safety and bicycle usage impacts of unbundling vehicular and cycle traffic in Dutch urban networks,* European Journal of Transport and Infrastructure Research **13**, 221 (2013), https://doi.org/10.18757/ejtir.2013.13.3.3000.

[11] R. Dubbeldam, C. Baten, J. H. Buurke, and J. S. Rietman, *SOFIE, a bicycle that supports older cyclists?* Accident Analysis & Prevention **105**, 117 (2017), https://doi.org/10.1016/j.aap.2016.09.006.

[12] L. Alizadehsaravi and J. K. Moore, *Bicycle balance assist system reduces roll and steering motion for young and older bicyclists during real-life safety challenges,* PeerJ **11**, e16206 (2023), https://doi.org/10.7717/peerj.16206.

[13] A. M. Pierson, A. K. Shortreed, P. D. van Asten, and A. E. Dressel, *A narrow-track tilting tricycle with variable stability that the rider can control manually,* in *International Design Engineering Technical Conferences and Computers and Information in Engineering Conference*, Vol. 83938 (American Society of Mechanical Engineers, 2020) https://doi.org/10.1115/DETC2020-22635.

[14] C. Engbers, R. Dubbeldam, J. H. Buurke, N. Kamphuis, S. H. H. M. de Hair-Buijssen, F. Westerhuis, D. de Waard, and J. S. Rietman, *A front-and rear-view assistant for older cyclists: Evaluations on technical performance, user experience and behaviour,* International Journal of Human Factors and Ergonomics **5**, 257 (2018), https://doi.org/10.1504/IJHFE.2018.096099.

[15] J. Kovaceva, J. Bärgman, and M. Dozza, *On the importance of driver models for the development and assessment of active safety: A new collision warning system to make overtaking cyclists safer,* Accident Analysis & Prevention **165**, 106513 (2022), https://doi.org/10.1016/j.aap.2021.106513.

[16] C. Hughes, M. Glavin, E. Jones, and P. Denny, *Wide-angle camera technology for automotive applications: A review,* IET Intelligent Transport Systems **3**, 19 (2009), https://doi.org/10.1049/iet-its:20080017.

[17] P. Pitchipoo, D. S. Vincent, N. Rajini, and S. Rajakarunakaran, *COPRAS decision model to optimize blind spot in heavy vehicles: A comparative perspective,* Procedia Engineering **97**, 1049 (2014), https://doi.org/10.1016/j.proeng.2014.12.383.

[18] F. Wegman, F. Zhang, and A. Dijkstra, *How to make more cycling good for road safety?* Accident Analysis & Prevention **44**, 19 (2012), https://doi.org/10.1016/j.aap.2010.11.010.

[19] B. Olsson, *Increased bicycle helmet use in the absence of mandatory bicycle helmet legislation: Prevalence and trends from longitudinal observational studies on the use of bicycle helmets among cyclists in Denmark 2004–2022,* Journal of Safety Research **87**, 54 (2023), https://doi.org/10.1016/j.jsr.2023.09.003.

[20] R. Utriainen, S. O'Hern, and M. Pöllänen, *Review on single-bicycle crashes in the recent scientific literature,* Transport Reviews **43**, 159 (2023), https://doi.org/10.1080/01441647.2022.2055674.

[21] A. Badea-Romero and J. Lenard, *Source of head injury for pedestrians and pedal cyclists: Striking vehicle or road?* Accident Analysis & Prevention **50**, 1140 (2013), https://doi.org/10.1016/j.aap.2012.09.024.

[22] M. Öman, R. Fredriksson, P.-O. Bylund, and U. Björnstig, *Analysis of the mechanism of injury in non-fatal vehicle-to-pedestrian and vehicle-to-bicyclist frontal crashes in Sweden,* International journal of injury control and safety promotion **23**, 405 (2016), https://doi.org/10.1080/17457300.2015.1047869.

[23] S. S. Monfort and B. C. Mueller, *Bicyclist crashes with cars and SUVs: Injury severity and risk factors,* Traffic Injury Prevention , 1 (2023), https://doi.org/10.1080/15389588.2023.2219795.

[24] R. Elvik, *Area-wide urban traffic calming schemes: A meta-analysis of safety effects,* Accident Analysis & Prevention **33**, 327 (2001), https://doi.org/10.1016/S0001-4575(00)00046-4.

[25] A. Hoye, *Recommend or mandate? A systematic review and meta-analysis of the effects of mandatory bicycle helmet legislation,* Accident Analysis & Prevention **120**, 239 (2018), https://doi.org/10.1016/j.aap.2018.08.001.

[26] I. I. Hellman and M. Lindman, *Estimating the crash reducing effect of advanced driver assistance systems (ADAS) for vulnerable road users,* Traffic Safety Research **4**, 000036 (2023), https://doi.org/10.55329/blzz2682.

[27] N. Lubbe, Y. Wu, and H. Jeppsson, *Safe speeds: Fatality and injury risks of pedestrians, cyclists, motorcyclists, and car drivers impacting the front of another passenger car as a function of closing speed and age,* Traffic Safety Research **2**, 000006 (2022), https://doi.org/10.55329/vfma7555.

[28] P. Schepers, N. Agerholm, E. Amoros, R. Benington, T. Bjørnskau, S. Dhondt, B. de Geus, C. Hagemeister, B. P. Y. Loo, and A. Niska, *An international review of the frequency of single-bicycle crashes (SBCs) and their relation to bicycle modal share,* Injury Prevention **21**, e138 (2015), https://doi.org/10.1136/injuryprev-2013-040964.

[29] A. C. Scholten, S. Polinder, M. J. M. Panneman, E. F. van Beeck, and J. A. Haagsma, *Incidence and costs of bicycle-related traumatic brain injuries in the Netherlands,* Accident Analysis & Prevention **81**, 51 (2015), https://doi.org/10.1016/j.aap.2015.04.022.

[30] L. Kjeldgård, M. Ohlin, R. Elrud, H. Stigson, K. Alexanderson, and E. Friberg, *Bicycle crashes and sickness absence — a population-based Swedish register study of all individuals of working ages,* BMC public health **19**, 1 (2019), https://doi.org/10.1186/s12889-019-7284-1.

[31] M. Møller, K. H. Janstrup, and N. Pilegaard, *Improving knowledge of cyclist crashes based on hospital data including crash descriptions from open text fields,* Journal of Safety Research **76**, 36 (2021), https://doi.org/10.1016/j.jsr.2020.11.004.

[32] M. S. Myhrmann, K. H. Janstrup, M. Møller, and S. E. Mabit, *Factors influencing the injury severity of single-bicycle crashes,* Accident Analysis & Prevention **149**, 105875 (2021), https://doi.org/10.1016/j.aap.2020.105875.

[33] J. P. Schepers, E. Fishman, P. den Hertog, K. Klein Wolt, and A. L. Schwab, *The safety of electrically assisted bicycles compared to classic bicycles,* Accident Analysis & Prevention **73**, 174 (2014), https://doi.org/10.1016/j.aap.2014.09.010.

[34] F. Westerhuis, P. N. Velasco, P. Schepers, and D. de Waard, *Do electric bicycles cause an increased injury risk compared to conventional bicycles? The potential impact of data visualisations and corresponding conclusions,* Accident Analysis & Prevention **195**, 107398 (2024), https://doi.org/10.1016/j.aap.2023.107398.

[35] R. Elvik, *Some difficulties in defining populations of "entities" for estimating the expected number of accidents,* Accident Analysis & Prevention **20**, 261 (1988), https://doi.org/10.1016/0001-4575(88)90054-1.

[36] C. Johnsson, A. Laureshyn, and T. de Ceunynck, *In search of surrogate safety indicators for vulnerable road users: A review of surrogate safety indicators,* Transport Reviews **38**, 765 (2018), https://doi.org/10.1080/01441647.2018.1442888.

[37] T. Sayed, M. H. Zaki, and J. Autey, *Automated safety diagnosis of vehicle–bicycle interactions using computer vision analysis,* Safety Science **59**, 163 (2013), https://doi.org/10.1016/j.ssci.2013.05.009.

[38] A. R. A. van der Horst, M. de Goede, S. de Hair-Buijssen, and R. Methorst, *Traffic conflicts on bicycle paths: A systematic observation of behaviour from video,* Accident Analysis & Prevention **62**, 358 (2014), https://doi.org/10.1016/j.aap.2013.04.005.

[39] K. Gildea, D. Hall, C. Mercadal-Baudart, B. Caulfield, and C. Simms, *Computer vision-based assessment of cyclist-tram track interactions for predictive modeling of crossing success,* Journal of Safety Research **87**, 202 (2023), https://doi.org/10.1016/j.jsr.2023.09.017.

[40] Å. Svensson and C. Hydén, *Estimating the severity of safety related behaviour,* Accident Analysis & Prevention **38**, 379 (2006), https://doi.org/10.1016/j.aap.2005.10.009.

[41] N. McNeil, C. M. Monsere, and J. Dill, *Influence of bike lane buffer types on perceived comfort and safety of bicyclists and potential bicyclists,* Transportation Research Record **2520**, 132 (2015), https://doi.org/10.3141/2520-15.

[42] J. Kovaceva, P. Wallgren, and M. Dozza, *On the evaluation of visual nudges to promote safe cycling: Can we encourage lower speeds at intersections?* Traffic Injury Prevention **23**, 428 (2022), https://doi.org/10.1080/15389588.2022.2103120.

[43] D. de Waard, P. Schepers, W. Ormel, and K. Brookhuis, *Mobile phone use while cycling: Incidence and effects on behaviour and safety,* Ergonomics **53**, 30 (2010), https://doi.org/10.1080/00140130903381180.

[44] W. P. Vlakveld, D. Twisk, M. Christoph, M. Boele, R. Sikkema, R. Remy, and A. L. Schwab, *Speed choice and mental workload of elderly cyclists on e-bikes in simple and complex traffic situations: A field experiment,* Accident Analysis & Prevention **74**, 97 (2015), https://doi.org/10.1016/j.aap.2014.10.018.

[45] R. Dubbeldam, C. T. M. Baten, P. T. C. Straathof, J. H. Buurke, and J. S. Rietman, *The different ways to get on and off a bicycle for young and old,* Safety Science **92**, 318 (2017), https://doi.org/10.1016/j.ssci.2016.01.010.

[46] K. Kircher and A. Niska, *Interventions to reduce the speed of cyclists in work zones — cyclists' evaluation in a controlled environment,* Traffic Safety Research **6**, e000047 (2024), https://doi.org/10.55329/ohhx5659.

[47] J. Andersson, C. Patten, H. Wallén Warner, C. Andersérs, C. Ahlström, R. Ceci, and L. Jakobsson, *Bicycling during alcohol intoxication,* Traffic Safety Research **4** (2023), https://doi.org/10.55329/prpa1909.

[48] C. Andersérs, J. Andersson, and H. W. Warner, *The importance of individual characteristics on bicycle performance during alcohol intoxication,* Traffic Safety Research **6**, e000042 (2024), https://doi.org/10.55329/vmgb9648.

[49] A. K. Huemer, L. M. Rosenboom, M. Naujoks, and E. Banach, *Testing cycling infrastructure layout in virtual environments: An examination from a bicycle rider's perspective in simulation and online,* Transportation Research Interdisciplinary Perspectives **14**, 100586 (2022), https://doi.org/10.1016/j.trip.2022.100586.

[50] F. L. Berghoefer and M. Vollrath, *Prefer what you like? Evaluation and preference of cycling infrastructures in a bicycle simulator,* Journal of Safety Research **87**, 157 (2023), https://doi.org/10.1016/j.jsr.2023.09.013.

[51] M. Pijnappels, J. C. E. van der Burg, N. D. Reeves, and J. H. van Dieën, *Identification of elderly fallers by muscle strength measures,* European Journal of Applied Physiology **102**, 585 (2008), https://doi.org/10.1007/s00421-007-0613-6.

[52] A. Niska and J. Wenäll, *Simulated single-bicycle crashes in the VTI crash safety laboratory,* Traffic Injury Prevention **20**, 68 (2019), https://doi.org/10.1080/15389588.2019.1685090.

[53] A. Niska, J. Wenäll, and J. Karlström, *Crash tests to evaluate the design of temporary traffic control devices for increased safety of cyclists at road works,* Accident Analysis & Prevention **166**, 106529 (2022), https://doi.org/10.1016/j.aap.2021.106529.

[54] M. Fahlstedt, P. Halldin, and S. Kleiven, *The protective effect of a helmet in three bicycle accidents — A finite element study,* Accident Analysis & Prevention **91**, 135 (2016), https://doi.org/10.1016/j.aap.2016.02.025.

[55] C. Baker, X. Yu, B. Lovell, R. Tan, S. Patel, and M. Ghajari, *How well do popular bicycle helmets protect from different types of head injury?* Annals of Biomedical Engineering **52**, 3326 (2024), https://doi.org/10.1007/s10439-024-03589-8.

[56] Y. Peng, Y. Chen, J. Yang, D. Otte, and R. Willinger, *A study of pedestrian and bicyclist exposure to head injury in passenger car collisions based on accident data and simulations,* Safety Science **50**, 1749 (2012), https://doi.org/10.1016/j.ssci.2012.03.005.

[57] V. Astarita, V. Giofré, G. Guido, and A. Vitale, *Investigating road safety issues through a microsimulation model,* Procedia-social and Behavioral Sciences **20**, 226 (2011), https://doi.org/10.1016/j.sbspro.2011.08.028.

[58] U. Shahdah, F. Saccomanno, and B. Persaud, *Application of traffic microsimulation for evaluating safety performance of urban signalized intersections,* Transportation Research Part C: Emerging Technologies **60**, 96 (2015), https://doi.org/10.1016/j.trc.2015.06.010.

[59] H. Twaddle, T. Schendzielorz, and O. Fakler, *Bicycles in urban areas: Review of existing methods for modeling behavior,* Transportation Research Record **2434**, 140 (2014), https://doi.org/10.3141/2434-17.

[60] C. M. Schmidt, A. Dabiri, F. Schulte, R. Happee, and J. K. Moore, *Essential bicycle dynamics for microscopic traffic simulation: An example using the social force model,* in *The Evolving Scholar-BMD 2023, 5th Edition* (2023) http://dx.doi.org/10.59490/649d4037c2c818c6824899bd.

[61] N. Rinke, C. Schiermeyer, F. Pascucci, V. Berkhahn, and B. Friedrich, *A multi-layer social force approach to model interactions in shared spaces using collision prediction,* Transportation Research Procedia **25**, 1249 (2017), https://doi.org/10.1016/j.trpro.2017.05.144.

[62] K. Gildea, D. Hall, C. R. Cherry, and C. Simms, *Forward dynamics computational modelling of a cyclist fall with the inclusion of protective response using deep learning-based human pose estimation,* Journal of Biomechanics **163**, 111959 (2024), https://doi.org/10.1016/j.jbiomech.2024.111959.

[63] G. Milne, C. Deck, N. Bourdet, R. P. Carreira, Q. Allinne, A. Gallego, and R. Willinger, *Bicycle helmet modelling and validation under linear and tangential impacts,* International Journal of Crashworthiness **19**, 323 (2014), https://doi.org/10.1080/13588265.2013.859470.

[64] V. Keppner, S. Krumpoch, R. Kob, A. Rappl, C. C. Sieber, E. Freiberger, and H. M. Siebentritt, *Safer cycling in older age (SiFAr): Effects of a multi-component cycle training. a randomized controlled trial,* BMC Geriatrics **23**, 131 (2023), https://doi.org/10.1186/s12877-021-02502-5.

[65] B. Janssen, P. Schepers, H. Farah, and M. Hagenzieker, *Behaviour of cyclists and pedestrians near right angled, sloped and levelled kerb types: Do risks associated to height differences of kerbs weigh up against other factors?* European Journal of Transport and Infrastructure Research **18**, 360 (2018), https://doi.org/10.18757/ejtir.2018.18.4.3254.

[66] F. Westerhuis, A. B. M. Fuermaier, K. A. Brookhuis, and D. de Waard, *Cycling on the edge: The effects of edge lines, slanted kerbstones, shoulder, and edge strips on cycling behaviour of cyclists older than 50 years,* Ergonomics **63**, 769 (2020), https://doi.org/10.1080/00140139.2020.1755058.

[67] J. P. Meijaard, J. M. Papadopoulos, A. Ruina, and A. L. Schwab, *Linearized dynamics equations for the balance and steer of a bicycle: A benchmark and review,* Proceedings of the Royal Society A: Mathematical, Physical and Engineering Sciences **463**, 1955 (2007), https://doi.org/10.1098/rspa.2007.1857.

[68] J. D. G. Kooijman, A. L. Schwab, and J. P. Meijaard, *Experimental validation of a model of an uncontrolled bicycle,* Multibody System Dynamics **19**, 115 (2008), https://doi.org/10.1007/s11044-007-9050-x.

[69] D. Stevens, *The stability and handling characteristics of bicycles*, Bachelor's thesis, The University of New South Wales, School of Mechanical and Manufacturing Engineering, Sydney, Australia (2009), http://www.varg.unsw.edu.au/Assets/link%20pdfs/thesis_stevens.pdf.

[70] J. D. G. Kooijman, J. P. Meijaard, J. M. Papadopoulos, A. Ruina, and A. L. Schwab, *A bicycle can be self-stable without gyroscopic or caster effects,* Science **332**, 339 (2011), https://doi.org/10.1126/science.1201959.

[71] T.-O. Tak, J.-S. Won, and G.-Y. Baek, *Design sensitivity analysis of bicycle stability and experimental validation,* in *Bicycle and Motorcycle Dynamics Conference* (Delft, The Netherlands, 20-22 October 2010) http://www.bicycle.tudelft.nl/ProceedingsBMD2010/papers/tak2010design.pdf.

[72] J. P. Meijaard and A. L. Schwab, *Linearized equations for an extended bicycle model,* in *III European Conference on Computational Mechanics: Solids, Structures and Coupled Problems in Engineering* (Lisbon, Portugal, 5-8 June 2006) http://www.bicycle.tudelft.nl/schwab/Publications/MeijaardSchwab2006.pdf.

[73] K. J. Astrom, R. E. Klein, and A. Lennartsson, *Bicycle dynamics and control: Adapted bicycles for education and research,* IEEE Control Systems Magazine **25**, 26 (2005), https://doi.org/10.1109/MCS.2005.1499389.

[74] D. L. Peterson and M. Hubbard, *General steady turning of a benchmark bicycle model,* in *International Design Engineering Technical Conferences and Computers and Information in Engineering Conference* (San Diego, USA, 30 August - 2 September 2009) https://doi.org/10.1115/DETC2009-86145.

[75] G. Frosali and F. Ricci, *Kinematics of a bicycle with toroidal wheels,* Communications in Applied and Industrial Mathematics **3**, 24 (2012).

[76] A. L. Schwab, J. P. Meijaard, and J. D. G. Kooijman, *Lateral dynamics of a bicycle with a passive rider model: Stability and controllability,* Vehicle System Dynamics **50**, 1209 (2012), https://doi.org/10.1080/00423114.2011.610898.

[77] A. L. Schwab and J. P. Meijaard, *A review on bicycle dynamics and rider control,* Vehicle System Dynamics **51**, 1059 (2013), https://doi.org/10.1080/00423114.2013.793365.

[78] G. Franke, W. Suhr, and F. Rieß, *An advanced model of bicycle dynamics,* European Journal of Physics **11**, 116 (1990), http://bicycle.tudelft.nl/schwab/Bicycle/BicycleHistoryReview/FraSuhRie90.pdf.

[79] A. Lennartsson, *Efficient multibody dynamics*, Ph.D. thesis, KTH Royal Institute of Technology, Stockholm, Sweden (1999), https://www.diva-portal.org/smash/get/diva2:8540/FULLTEXT01.pdf.

[80] P. Basu-Mandal, A. Chatterjee, and J. M. Papadopoulos, *Hands-free circular motions of a benchmark bicycle,* Proceedings of the Royal Society A: Mathematical, Physical and Engineering Sciences **463**, 1983 (2007), https://doi.org/10.1098/rspa.2007.1849.

[81] A. L. Schwab, P. D. L. de Lange, R. Happee, and J. K. Moore, *Rider control identification in bicycling using lateral force perturbation tests,* Proceedings of the Institution of Mechanical Engineers, Part K: Journal of Multi-body Dynamics **227**, 390 (2013), https://doi.org/10.1177/1464419313492317.

[82] J. K. Moore, *Human control of a bicycle*, Ph.D. thesis, University of California, Davis, USA (2012).

1

APPLYING BICYCLE DYNAMICS AND CYCLIST CONTROL MODELS TO CYCLING SAFETY RESEARCH

M.M. Reijne, F.C.T. van der Helm and A.L. Schwab

ABSTRACT

The rise of cycling crashes, especially those related to losing balance, underscores the critical need for identifying and implementing effective fall prevention interventions. Unfortunately, traditional approaches for evaluating cycling safety interventions often fall short of accurately, safely and proactively evaluating the impact of a large number of cyclist fall prevention interventions, particularly those that aim to reduce fall risk in critical situations. As such, policy advisors and designers of infrastructure, bicycles, and training programs cannot make informed decisions about safe designs or the most cost-effective designs to improve cycling safety.

This Chapter is under review at Traffic Safety Research

Bicycle dynamics and cyclist control models offer potential solutions to this problem. These models can simulate bicycle motions and cyclist behaviour and be applied to simulate cyclist falls. However, despite their existence for several decades and their application in fundamental bicycle stability and handling research, these models still need to be applied in cycling safety research.

The goal of our study is to integrate bicycle dynamics and cyclist control models with cycling safety research to safely and proactively evaluate a broader range of cyclist fall prevention interventions. In this chapter, we explain and illustrate these models' potential impact and application. Specifically, we explain the technical language of bicycle dynamics and cyclist control models in a more accessible language, demonstrate which commonly reported bicycle crash types can be simulated with these models and illustrate which types of interventions can be evaluated.

We demonstrated that bicycle dynamics and cyclist control models have the potential to simulate all eight commonly reported crash types considered in this study. These include crash types such as falling due to slipping on a slippery road surface or falling after a collision with an obstacle or another road user. In addition, for these crash types, we illustrated that bicycle dynamics and cyclist control models could evaluate the effectiveness of interventions aimed at bicycle design, cyclist control, and environmental factors like road surface conditions, disturbances and available space to recover balance.

However, it is crucial to note that these models require further development to unlock their full potential. Improvements are needed in developing a more accurate bicycle tyre model and cyclist control models that incorporate intuitive human characteristics and simulate other crucial cycling tasks beyond balancing. It is also essential to validate these models under real-world crash conditions and standardise evaluation methods. This ongoing research and development is essential to ensure these models' effectiveness, reliability, and practical application.

In conclusion, applying bicycle dynamics and cyclist control models to cycling safety offers a valuable addition to existing evaluation methods, allowing for the proactive and safe evaluation of a broader range of interventions. By making the potential application and existing gaps of these models explicit, our study not only creates a deeper understanding of these models but also encourages further development of these models and application of these models to cycling safety research.

1.1. INTRODUCTION

The rise in cyclist fatalities and serious injuries highlights the urgent need for improved cycling safety strategies and interventions [1]. As cycling gains popularity worldwide, prioritising cost-effective safety interventions becomes crucial to reduce the human and economic impact of such crashes [2]. Identifying which interventions improve safety effectively is important for professionals in designing and developing safe infrastructure, bicycles and training programs. In addition, identifying which interventions are most cost-effective is vital for policy advisors to efficiently allocate available resources.

Among the various safety interventions, those preventing cyclist falls are notably promising to be cost-effective, given that many cycling injuries are related to loss of balance resulting in falls [3]. However, the effectiveness of a large number of fall

prevention interventions in reducing fatalities and serious injuries remains unclear. Moreover, the effectiveness can often not be evaluated proactively and safely.

Current evaluation approaches and their limitations

Existing approaches to evaluate cycling safety interventions include statistical analyses of crash data [4–7], surrogate safety indicators determined from video observation [8, 9], field and experimental cycling studies [10–17], crash tests [18–22], and models that simulate traffic scenarios [23–27].

While these approaches have evaluated a large number of interventions, they face significant limitations when applied to evaluate cyclist fall prevention interventions, particularly those aimed at reducing fall risk in critical situations. Examples of such interventions include balance training programs [28], steer-assist systems [29], sloped kerbs [30] or ridable road shoulders [31].

Statistical crash data analyses are hindered by the underreporting of single-bicycle crashes [32], making reliable statistical analyses infeasible. Surrogate safety indicators focus on conflicts between road users, overlooking falls that occur without interactions between road users — despite this accounting for the majority of severe cycling injuries [3]. Field studies and cycling experiments rely on indirect indicators such as perceived safety and bicycle motions, but their connection to fall risk remains unvalidated. Crash experiments and crash simulation models focus on injury mitigation rather than fall prevention, while other existing simulation models — such as traffic microsimulation, behavioural, and crash avoidance models — fail to incorporate the balancing task and lateral bicycle dynamics needed to simulate falls.

These limitations highlight the need for an approach that can proactively and systematically evaluate cyclist fall prevention interventions, particularly those aiming to improve balance recovery in critical situations. Such an approach can complement existing methods, enabling the evaluation of promising interventions that could improve cycling safety.

Proposed approach: bicycle dynamics and cyclist control models

Bicycle dynamics and cyclist control models offer a promising approach to safely and proactively evaluate interventions that aim to reduce fall risk in critical situations. These models are mathematical models designed to simulate the movement of bicycles and the interaction of cyclists with the bicycle [33]. Bicycle dynamics models capture the physics of bicycle motion — including elements such as forces, momentum, and the influence of variables like mass, inertia, and road surface conditions. On the cyclist side, cyclist control models aim to mimic cyclist's actions for key tasks such as balancing, following the intended path, braking and evasive manoeuvres.

However, despite their existence and potential for over a decade, these models have yet to be applied to evaluate cycling safety interventions. One possible reason for this is a need for more understanding by cycling safety researchers of the models' potential in evaluating cyclist fall prevention interventions, possibly due to the technical language used by vehicle dynamics and control researchers. Additionally, vehicle dynamics and control researchers may need to fully grasp the gaps in the models that hinder their practical application in evaluating cyclist fall prevention interventions.

Study objective
The goal of this study is to apply bicycle dynamics and cyclist control models to cycling safety research to safely and proactively evaluate cyclist fall prevention interventions. We achieve this by examining existing bicycle dynamics and control models, addressing the technical language of these models, and illustrating how these models can simulate common crash types reported in scientific literature. Furthermore, we will explore the interventions that can be evaluated using these models.

By improving the understanding and application of these models, we hope to encourage their broader adoption by cycling safety researchers and refinement by bicycle dynamics and cyclist control researchers. Adopting this approach can ultimately result in solid evidence for a broader array of cycling safety interventions. The solid evidence will aid policy advisors in prioritising cost-effective interventions and help professionals design safer bicycles, infrastructure, and training programs.

1.2. BICYCLE DYNAMICS AND CONTROL MODELS

This section briefly overviews existing bicycle dynamics models and cyclist control models. A more elaborate review can be found in Schwab and Meijaard (2013) [33].

1.2.1. BICYCLE DYNAMICS MODELS

The Carvallo-Whipple (C-W) bicycle model can be considered the basic and the simplest model that still accurately captures the bicycle dynamics [34]. This section delves into the C-W bicycle model and its validity. It also discusses significant extensions to the C-W model that incorporate additional complexities, such as acceleration forces and the influence of tyre characteristics, to simulate real-world cycling scenarios more accurately. We end with discussing the input values required to simulate the bicycle's motion.

Carvallo-Whipple bicycle model
The C-W bicycle model models the bicycle as four rigid, laterally symmetric parts. It consists of two wheels nominally placed behind each other and the rear and front frame. A horizontal revolute joint connects the front wheel to the front frame, which allows the front wheel to rotate. The revolute joint can be considered to consist of the axle and bearing. Similarly, the rear wheel is connected by a revolute joint to the rear frame. A vertical or inclined revolute joint connects the front frame and rear frame and allows the handlebars to rotate.

The cyclist, who has the more significant part of the total mass, is actually also an integral part of the C-W bicycle model. The C-W model assumes the cyclist to be rigidly attached to the rear frame. As such, the cyclist's mass distribution is also included in the bicycle dynamics model. In the section on cyclist control models, we will elaborate on whether this assumption is valid.

The model operates under several other key assumptions, including that the road surface is flat and both wheels touch the ground, knife-edge contact between the wheels and ground, and zero longitudinal and lateral slips. As a result of these assumptions, the

C-W model has three degrees of freedom: forward speed, the lean angle and the steering angle.

The motion of the bicycle, defined by these three degrees of freedom, can be described by a set of three linearised equations of motion if we consider normal cycling conditions, with small disturbances about the steady upright and straight-ahead motion. Given an initial configuration, the C-W model can then simulate the bicycle's motion over time through these equations of motion.

Validation

The C-W model has been validated for normal cycling conditions in which the bicycle recovered balance after a small disturbance through comparisons with experimental data [35, 36]. In addition, the model has been validated for several bicycles with different geometries but without a cyclist [37]. Finally, the model has also been validated with a cyclist who stopped pedalling and took off both hands from the handlebar, which is a similar condition to the assumption of the rigid cyclist attached to the rear frame [38]. All these validations combined instil in us confidence that the C-W model can be used to accurately and reliably simulate the motions of the bicycle.

Extensions to the Carvallo-Whipple bicycle model

In the original C-W model, the cyclist is assumed to be rigidly connected to the rear frame of the bicycle, and the arms are not connected to the handlebars. Contrarily, in normal bicycling, a rider's arms are connected to the handlebar, and both steering and upper body motions can be used for control. The C-W model can be extended with passive cyclist dynamics to consider the effects of the cyclist's hands on the handlebars, reflecting the additional damping, stiffness, dynamics, and control inputs the cyclist introduces through this interaction. This extension can be done with and without adding degrees of freedom [39, 40]. The additional degrees of freedom correspond to the relative motion of the cyclist's body to the bicycle frame. However, while this may be a more accurate representation of reality, the C-W model with passive cyclist dynamics still needs to be validated.

Also, the C-W model, in combination with the linear equations, assumes a steady motion with constant velocity and only small divergences about the upright and straight-ahead position. It is possible to add accelerations to the C-W model. For this, the linearised equations of motion need to be modified, depending on how the accelerating forces are applied [41].

When a bicycle moves steadily around a gentle curve, again, simple linearised equations of motions can be used to describe its motion [33]. For these equations, good agreement was found with experimental data [42]. However, if the curve gets tighter, non-linear equations have to be used [39, 43–46].

In the original C-W model, it is assumed there is knife-edge contact between the wheels and the ground, and there are zero longitudinal and lateral slips [34]. To study the effect of finite-width tyres on the dynamic behaviour of the bicycle, the C-W model has been extended with rims with a toroidal shape or with a quadratic approximation instead of knife-edge rims [39, 41, 46, 47]. This addition improved the stability of the bicycle, but the added complexity is not needed to accurately describe the motions of

the bicycle.

Tyre force models can also be incorporated into the C-W model to describe the forces generated by tyres under longitudinal and lateral slips. The effect of finite friction, slipping and skidding can be studied by including these tyre models. By including compliance in the normal direction of the tyre, which reflects the ability of the tyre to deform or flex in response to forces and displacements, one can even study the effect of losing ground contact in the normal direction of the tyre contact. This effect is, for instance, relevant to studying rear wheel lift-off during hard braking. While a range of tyre models has existed for motor vehicles for many years [48], research into accurate and reliable bicycle tyre models has only recently begun [49].

Input values

For practical application of the C-W model, case-specific input values of a bicycle's and cyclist's physical parameters are required to ensure realistic simulations. The original C-W model requires the geometry, mass, mass location and mass distributions for the four rigid bodies. Extensions to the C-W model might require estimates of tyre characteristics, friction, and added stiffness or damping by the cyclist's body.

The real-life parameters required for the basic C-W model can be measured or estimated relatively easily [50, 51]. Measurement setups to measure bicycle tyre characteristics and added stiffness or damping by the cyclist's body have been developed but are not yet extensively used [52–55].

Besides these parameters, an initial state of the bicycle-cyclist configuration is required to start the time simulation. This can be considered the initial conditions or start point of the simulation. For the basic C-W model, these consist of an initial: lean angle, lean rate, steering angle, steer rate, and position and heading on the ground.

1.2.2. CYCLIST CONTROL MODELS

Cyclists can exert forces or torques on the bicycle to influence its motion. These are mainly applied by pedalling, braking, leaning, and steering, with the aim of maintaining balance and the desired trajectory. Cyclist control models describe, via algorithms, the control inputs for the bicycle to control the forward and lateral motions. Usually, these are cyclist-applied forces, but they can also be other physical quantities like steering angle, steer rate, or pedal rate.

Cyclist control models have been developed for the navigating and balancing tasks and have been shown to compare well with observed cyclist data [33, 56]. These existing cyclist control models focus on vehicle control and only focus on operational decisions [57]. Consequently, while they can simulate whether a bicycle and rider can follow a prescribed trajectory and remain upright, they do not account for the tactical-level decisions involved in choosing that trajectory. Even in the more mature field of car driver modelling, current models are limited in their ability to simulate tactical and strategic decisions for tasks such as car-following, lane-keeping, and lane-changing behaviours [58–60]. Although both domains address vehicle control, car driver behaviours cannot be directly translated to cycling due to fundamental differences in vehicle dynamics and human behaviour.

Given these considerations, we have focused our detailed description below on

cyclist control models that simulate the bicycle balancing task. Existing models cannot yet capture the diverse collision avoidance strategies a cyclist might employ.

Steering into the fall
Studies have shown that steering toward an undesired fall is the primary, if not exclusive, mechanism for maintaining and recovering balance on a moving bicycle [36]. This corrective action — steering toward the fall — remains effective across various disturbances that may compromise stability.

The coupling between the bicycle's rear frame and the handlebar assembly enables cyclists to prevent a fall by either direct or indirect steering via upper body leaning. Studies underscore steering as the foremost strategy for balancing a bicycle, a finding supported by theoretical and experimental evidence [36, 40]. While it is possible to balance using upper-body movements to lean the bicycle, which, due to the coupling, will turn the handlebars, for instance, when cycling hands-free, data suggest that such movements play a negligible role in balance when the hands are on the handlebars [61]. LQR optimal control and intuitive control models have also shown that it is doubtful that upper body lean will be used for balancing at low speed [62]. However, optimal control models have shown that upper-body motion can contribute to the navigating task, particularly for manoeuvres such as lane change [63]. Furthermore, it is hypothesised that cyclists move their upper bodies primarily to adjust their heads' position for comfort rather than to steer or balance the bicycle [33]. Therefore, modelling a cyclist as rigidly attached to the bicycle and only able to perform steer actions is a good option for a cyclist model for balancing control.

Validation
Although many cyclist control models have been proposed, unfortunately, only two cyclist control models show a validation of the cyclist control model [56, 64]. The validation was based on experimental data in which a cyclist was lightly laterally disturbed while cycling on a treadmill. As such, the control model can be considered representative of the balancing task while also trying to maintain a constant heading.

Input values
The variables of this validated cyclist control model are more abstract than the parameters of the bicycle dynamics models. Required input includes, for example, feedback gains and the cyclist's neuromuscular characteristics. The input values for the feedback gains have only been determined for one cyclist; as such, the model can only be used to describe the behaviour of that individual, experienced cyclist and cannot be generalised for other cyclists. Control models with more intuitive human characteristics exist for other applications but have not yet been applied to cycling.

1.3. COMMONLY REPORTED CRASH TYPES

Determining the most prevalent cyclist crash types is challenging due to the underreporting of single bicycle crashes in most databases, introducing a bias into the datasets. Furthermore, the variation in the level of detail across studies complicates the categorization of crash types.

To address this variability and pragmatically select crash types, we focused on ten studies identified in Utriainen et al. (2023) [3]'s review of single bicycle crashes — which are mainly falls — in recent scientific literature, supplemented by two additional recent studies — which include collisions as well [65–76]. Following the methodology employed by Utriainen et al. (2023) [3], we identified the most commonly reported crash types based on the three most commonly reported crash types from each of these studies.

Based on this selection criteria and methodology, we identified the following crash types:

1. falls due to slipping on a slippery road surface
2. falls after a collision with an obstacle
3. falls following an evasive manoeuvre
4. falls involving (tram) rails
5. falls resulting from hard braking
6. falling over while cornering
7. falls due to loss of balance
8. falls after a collision with another road user.

1.4. WHICH CRASH TYPES AND INTERVENTIONS CAN BE SIMULATED AND WHICH INTERVENTIONS CAN BE EVALUATED?

In this section, we explore how each commonly reported crash type can be simulated using bicycle dynamics and cyclist control models and which types of interventions can be evaluated. Because certain crash types are similar in how these can be simulated, we have combined collisions with an obstacle and collisions with another road user together and falls following an evasive manoeuvre and following hard braking together.

Falls due to slipping on a slippery road surface

To simulate cyclist fall scenarios involving slippery road surfaces, the C-W model extended with a tyre force model is essential. This combination is necessary to simulate whether bicycle tyres maintain grip under different conditions. When a tyre, particularly the front one, loses lateral grip, the cyclist can no longer recover the balance by steering in the direction of the fall, making a fall almost a certainty.

In addition, simulating fall occurrences in slippery conditions necessitate departing from the upright and straight-ahead initial configuration, as lateral tyre forces are absent in such cases, precluding loss of balance. Even minor deviations from the upright and straight-ahead configurations, such as slight initial steer or lean angles, suffice. Alternatively, a slight disturbance triggering a minor lean or steering angle can serve the purpose to generate lateral tyre forces and simulate if slippage occurs.

These slight deviations accurately reflect real-world scenarios where cyclists continually oscillate around the upright position to maintain balance. While cycling, cyclists routinely experience subtle variations in their lean angle, particularly when negotiating corners or making adjustments to maintain balance. Although invisible to casual observers, these adjustments are indispensable for cyclists to uphold stability and control. Even while riding straight, cyclists may subtly alter their body position to counter external factors like wind or changes in the road surface.

By applying a bicycle tyre model, we can simulate this crash type for various road surfaces — including the same road surface with varying weather conditions — and for different tyres. Such models not only predict fall occurrences but also identify the precise conditions under which tyres lose grip, offering insights into the risk levels of real-world road surfaces under diverse weather conditions. Designers can use these to evaluate the safety of road surface designs or bicycle tyre improvements.

Friction coefficients for different real-world road surfaces have already been determined, yet unfortunately, our understanding of bicycle tyre characteristics remains incomplete. While methods for measuring bicycle tyre characteristics have been developed, a bicycle tyre model has only recently been proposed [49]. Further exploration is needed to enhance our knowledge and develop such a tyre model.

Falls after collision with an obstacle or collision with another road user

Critical events like collisions with obstacles or other road users can be incorporated in the C-W models as externally applied forces or torques affecting steering, leaning or forward speed. If the collision induces a steer or lean in the bicycle or cyclist, it affects the lateral dynamics. Likewise, disturbances that impede forward motion or wheel rotation directly impact forward speed. In collisions where wheel rotation is impeded, there may also be a risk of tyre slippage, necessitating the incorporation of a tyre model as well.

While crash descriptions often provide insights into the nature of the collision, determining its specific effects on lean, steer, or forward speed can be challenging. The characteristics of the force profile — its magnitude, duration, location, and direction — depend on the collision's nature. Unfortunately, real-world force profile data for collisions remain largely unmeasured and are, consequently, unknown.

Collisions vary widely in severity, from minor nuisances to catastrophic events. For severe collisions where balance recovery is impossible, the focus shifts to preventive interventions aimed at avoiding such collisions. These interventions operate at the strategic decision level, involving recognising and anticipating dangerous scenarios, which currently fall outside the scope of existing cyclist control models. However, such control models can be developed.

Balance recovery is often possible in less severe collisions, such as those occurring at lower velocities or shallow angles where the cyclist is not fully impacted. To recover balance, lateral space must be available because the cyclist recovers balance by steering into the direction of the fall. Therefore, simulations of this crash type must consider the lateral space required for balance recovery. Once balance is recovered, the cyclist can manoeuvre back to a safe distance from the side of the road.

For these less severe collisions, interventions can target the post-collision-pre-fall phase as well. Such interventions aim to enable cyclists to recover balance

more efficiently or effectively. Existing bicycle dynamics and cyclist control models can incorporate interventions targeting bicycle design, cyclist balancing control, or environmental factors such as road surface and available space. These interventions are particularly suited for simulation and evaluation with bicycle dynamics and cyclist control models, as existing cyclist control models have already been developed and validated for recovering balance after a disturbance.

Falls following an evasive manoeuvre or falls resulting from hard braking
Bicycle dynamics models, extended with a bicycle tyre model and accelerations, can predict the lean angle and deceleration thresholds at which a tyre may lose grip or contact with the ground during an evasive manoeuvre or hard braking. This information allows the ex-ante evaluation of bicycle and tyre design modifications to improve performance in these critical conditions.

Cyclist control models have yet to be specifically developed and validated for simulating evasive manoeuvres, where directional change is prioritised over balancing, and for braking technique, with control actions related to handlebar grip and foot-on-the-ground placement when braking to come to a complete standstill.

Consequently, existing bicycle dynamics and cyclist control models fail to adequately simulate falls resulting from evasive actions and hard braking crash types. However, such cyclist control models can be developed, potentially via the same methodology as has been used to develop the cyclist control model for balancing. Such models could be applied to evaluate the safest strategies for evasive manoeuvres and hard braking.

Falls involving (tram)rails
The description of this crash type presents some ambiguity. A fall may result from slipping on tram rails or the front wheel getting stuck in the tram rails. Both scenarios lend themselves to modelling through bicycle dynamics and cyclist control models. Slip-induced falls are similar to crashes occurring on slippery road surfaces, as described previously.

Conversely, the front wheel becoming wedged in the tram rails can be represented as an externally applied force acting on the wheel's forward rotation and steering, thereby preventing steering into the fall and balance recovery. A fall is, in this case, inevitable. In this crash, the existing cyclist control models — simulating recovering balance by steering towards the fall — are useless to prevent a fall as the steering is locked. Also, here, the focus shifts to preventive interventions aimed at avoiding the front wheel getting lodged in the tram rails.

Falling over while cornering
The C-W bicycle model is adept at simulating cornering manoeuvres. Linear or non-linear equations must be employed depending on the curve's radius. Existing cyclist control models were not specifically designed for cornering scenarios. Consequently, they prioritise returning the bicycle to an upright, straight-ahead position rather than attempting cornering manoeuvres. As such, while the C-W bicycle model, extended with a bicycle tyre model, facilitates the determination of conditions leading to grip loss during cornering, similar to those of an evasive manoeuvre, evaluating interventions

targeting cyclist control during cornering remains challenging.

Falls due to loss of balance
This crash type presents considerable ambiguity in its description, posing challenges in accurately simulating it. Because of the inherent instability of the bicycle, it is reasonable to assume some disturbance caused the fall. Typical disturbances include sudden wind gusts, irregularities in road surfaces, the presence of debris or obstacles, or abrupt shifts in the weight distribution by the cyclist or their luggage. Given this assumption, we can model these falls as collisions involving obstacles or other road users. However, these falls might also include falls due to veering off the road due to inattentiveness or falls during (dis)mounting. These cannot be simulated with existing bicycle dynamics and cyclist control models.

1.5. DISCUSSION

The goal of this study was to apply bicycle dynamics and cyclist control models with cycling safety research to safely and proactively evaluate cyclist fall prevention interventions. Using accessible language instead of technical jargon, we demonstrated that these models can simulate a broad spectrum of commonly reported bicycle crash types. The study encourages adoption by cycling safety researchers and identifies areas where model developers can improve the practical use of these models in evaluating fall prevention interventions.

Our study showed that bicycle dynamics and cyclist control models have the potential to simulate all eight commonly reported crash types considered in this study. Examples include crash types such as falling due to slipping on a slippery road surface or falling after a collision with another road user. Additionally, our study showed that these models have the potential to ex-ante evaluate the effectiveness of interventions aimed at bicycle and tyre design, cyclist control skills like balancing, and environmental factors like road surface conditions, disturbances and available space.

In particular, existing models can already simulate falls due to balance loss or collisions. They can also already evaluate interventions related to bicycle design, cyclist balance control, disturbances, and spatial constraints. However, it is important to note that present cyclist control models primarily describe the cyclist's ability to recover balance after a disturbance. Consequently, they focus mainly on improving skills to recover balance through interventions like training programs or assistance systems rather than improving skills to avoid disturbances, such as recognising potential dangers. Therefore, these models are currently limited to simulating falls from less severe collisions, such as those occurring at low speeds or at shallow angles, where recovery of balance is feasible.

Added value of our research, strengths and practical application
Our research demonstrates that integrating bicycle dynamics and cyclist control models with cycling safety can significantly broaden the scope of cycling safety interventions that can be evaluated. Compared with traditional statistical analyses of crash data, these models stand out for their ability to evaluate intervention effectiveness safely and proactively. These models offer detailed insights into the interactions between

the cyclist, the bicycle, and their environment, thus providing a more comprehensive understanding than that offered by statistical correlations alone.

Unlike video observation or traffic simulation studies using surrogate safety indicators, these models can simulate bicycle crash scenarios without the involvement of other road users. This ability is particularly relevant as five of the eight most frequently reported crash types are crashes without the involvement of other road users.

In contrast to field or experimental studies, which focus on indirect indicators — such as perceived safety, mental workload, or lean angles — determined mostly in relatively normal cycling situations, bicycle dynamics and cyclist control models can simulate actual falls. This direct relationship with fall scenarios enables a more accurate evaluation of safety interventions, focusing on preventing falls rather than merely reducing their perceived risk or improving comfort.

Furthermore, these models distinguish themselves by simulating the phase before a fall. This distinction allows for the evaluation of interventions aimed at reducing the likelihood of a fall, a phase not covered by crash experiments or simulations, which focuses on mitigating the severity of impacts post-fall.

Incorporating bicycle dynamics and cyclist control models into cycling safety aligns with the principles of the Dutch Safe System approach. It provides a proactive framework to quantify fall risks and identify effective safety interventions related to infrastructure, bicycle design, speed, and cyclist behaviour. These models can offer valuable tools for road safety professionals, such as aiding the design of safer bicycles and infrastructure and helping policy advisors identify the most effective safety interventions to stimulate or implement.

Limitations and recommendations for future research

Despite their potential, further improvements are necessary to maximise the full potential and application of these models. For example, developing a bicycle tyre model would be a crucial extension of the bicycle dynamics model for simulating tyre slippage. This is essential for simulating commonly reported crash types, such as falls due to slipping on a slippery road surface, hard braking, or evasive manoeuvres. Such a tyre model would enable professionals to evaluate which tyre and road surface designs minimise slip and fall risks. Moreover, this can already be determined in the design phase. Developing such a bicycle tyre model can draw inspiration from previously developed car tyre models [48] and the bicycle tyre model proposed by Dell'Orto et al. (2024) [49].

Improvements in cyclist control models are also recommended. Improving existing models that simulate the balancing task by incorporating intuitive human characteristics, such as experience and reaction time, would improve their practical application and would improve the evaluation of cyclist control interventions. These improvements could draw on insights from models of postural balance control [77, 78].

Furthermore, developing cyclist control models that simulate tracking, braking, and evasive manoeuvres — encompassing operational and strategic control levels — would allow for a more comprehensive simulation of various crash types. Such cyclist control models would also increase the types and number of fall prevention interventions that can be evaluated. Potential frameworks for these models could be inspired by existing

bicycle balancing control models [56] and functional driver models that simulate car driver behaviours for various tasks.

Before deploying bicycle dynamics and cyclist control models to evaluate cyclist fall prevention intervention, a critical aspect is validating these models in actual crash conditions. To date, validation efforts have predominantly focused on normal cycling conditions with minor disturbances. Such a validation is challenging. To date, only one experimental study involving disturbances that led to both falls and recoveries has been conducted, and it was specific to walking [79]. This experimental setup could be a valuable reference for designing a similar study for cyclists.

Further steps to fully leverage these models for cycling safety evaluations include collecting real-world data on the forces and torques involved in disturbances and collisions. This data is crucial for improving the simulation accuracy of common crash scenarios, such as collisions and balance loss.

Additionally, it is essential to adopt a standardised approach to evaluating cycling safety interventions using these models. This approach should define a universal performance indicator applicable across various crash types and interventions, complemented by a consistent set of crash types and input values for simulation. Such a standardised framework would facilitate systematic evaluations and comparative analyses of different interventions. In this context, inspiration can be drawn from the EuroNCAP methodology for assessing the safety of new car designs.

Focusing on these key areas can significantly advance the development and application of bicycle dynamics and cyclist control models, thereby making significant progress in cycling safety research and ex-ante intervention evaluation.

1.6. CONCLUSIONS

To conclude, this study establishes the potential of applying bicycle dynamics and cyclist control models to improve cycling safety. These models expand the scope of safety interventions that can be evaluated, even allowing for a safe and proactive evaluation. They are particularly valuable for evaluating cyclist fall prevention interventions aimed at bicycle design, cyclist control, and environmental factors such as road surfaces and available width to recover balance. It can evaluate the effectiveness of these interventions for a wide range of commonly reported crash types, ranging from falls due to slipping on a slippery road surface to falls after collisions with other road users. This approach broadens the scope of the existing intervention evaluation approaches.

Additionally, this study not only advocates for applying these models to cycling safety research but also highlights opportunities for model developers to improve the practical utility of their models. Future research should focus on validating these models under critical conditions, collecting real-world data to improve the accuracy of the simulations of commonly reported crash types, and developing advanced models for bicycle tyres and cyclist control that address critical tasks beyond balance. Furthermore, incorporating intuitive human characteristics and establishing a standardised framework for evaluating cycling safety interventions are essential steps forward.

Through these advancements and interdisciplinary collaboration, we can significantly improve our understanding of effective cycling safety interventions.

This knowledge can then be applied to design safer cycling infrastructure, bicycles, and training methods for cyclists, thereby making a substantial impact on the field of cycling safety.

REFERENCES

[1] United Nations (2020), *Resolution 74/299: Improving global road safety,* https://documents-dds-ny.un.org/doc/UNDOC/GEN/N20/226/30/PDF/N2022630.pdf?OpenElement, accessed 11 January 2025.

[2] World Health Organization (2020), *Cyclist safety: An information resource for decision-makers and practitioners,* https://iris.who.int/bitstream/handle/10665/336393/9789240013698-eng.pdf, accessed 11 January 2025.

[3] R. Utriainen, S. O'Hern, and M. Pöllänen, *Review on single-bicycle crashes in the recent scientific literature,* Transport Reviews **43**, 159 (2023), https://doi.org/10.1080/01441647.2022.2055674.

[4] R. Elvik, *Area-wide urban traffic calming schemes: A meta-analysis of safety effects,* Accident Analysis & Prevention **33**, 327 (2001), https://doi.org/10.1016/S0001-4575(00)00046-4.

[5] A. Hoye, *Recommend or mandate? A systematic review and meta-analysis of the effects of mandatory bicycle helmet legislation,* Accident Analysis & Prevention **120**, 239 (2018), https://doi.org/10.1016/j.aap.2018.08.001.

[6] I. I. Hellman and M. Lindman, *Estimating the crash reducing effect of advanced driver assistance systems (ADAS) for vulnerable road users,* Traffic Safety Research **4**, 000036 (2023), https://doi.org/10.55329/blzz2682.

[7] N. Lubbe, Y. Wu, and H. Jeppsson, *Safe speeds: Fatality and injury risks of pedestrians, cyclists, motorcyclists, and car drivers impacting the front of another passenger car as a function of closing speed and age,* Traffic Safety Research **2**, 000006 (2022), https://doi.org/10.55329/vfma7555.

[8] T. Sayed, M. H. Zaki, and J. Autey, *Automated safety diagnosis of vehicle — bicycle interactions using computer vision analysis,* Safety Science **59**, 163 (2013), https://doi.org/10.1016/j.ssci.2013.05.009.

[9] A. R. A. van der Horst, M. de Goede, S. de Hair-Buijssen, and R. Methorst, *Traffic conflicts on bicycle paths: A systematic observation of behaviour from video,* Accident Analysis & Prevention **62**, 358 (2014), https://doi.org/10.1016/j.aap.2013.04.005.

[10] N. McNeil, C. M. Monsere, and J. Dill, *Influence of bike lane buffer types on perceived comfort and safety of bicyclists and potential bicyclists,* Transportation Research Record **2520**, 132 (2015), https://doi.org/10.3141/2520-15.

[11] J. Kovaceva, P. Wallgren, and M. Dozza, *On the evaluation of visual nudges to promote safe cycling: Can we encourage lower speeds at intersections?* Traffic Injury Prevention **23**, 428 (2022), https://doi.org/10.1080/15389588.2022.2103120.

[12] D. de Waard, P. Schepers, W. Ormel, and K. Brookhuis, *Mobile phone use while cycling: Incidence and effects on behaviour and safety,* Ergonomics **53**, 30 (2010), https://doi.org/10.1080/00140130903381180.

[13] W. P. Vlakveld, D. Twisk, M. Christoph, M. Boele, R. Sikkema, R. Remy, and A. L. Schwab, *Speed choice and mental workload of elderly cyclists on e-bikes in simple and complex traffic situations: A field experiment,* Accident Analysis & Prevention **74**, 97 (2015), https://doi.org/10.1016/j.aap.2014.10.018.

[14] R. Dubbeldam, C. T. M. Baten, P. T. C. Straathof, J. H. Buurke, and J. S. Rietman, *The different ways to get on and off a bicycle for young and old,* Safety Science **92**, 318 (2017), https://doi.org/10.1016/j.ssci.2016.01.010.

[15] J. Andersson, C. Patten, H. Wallén Warner, C. Andersérs, C. Ahlström, R. Ceci, and L. Jakobsson, *Bicycling during alcohol intoxication,* Traffic Safety Research **4** (2023), https://doi.org/10.55329/prpa1909.

[16] K. Kircher and A. Niska, *Interventions to reduce the speed of cyclists in work zones — cyclists' evaluation in a controlled environment,* Traffic Safety Research **6**, e000047 (2024), https://doi.org/10.55329/ohhx5659.

[17] C. Andersérs, J. Andersson, and H. W. Warner, *The importance of individual characteristics on bicycle performance during alcohol intoxication,* Traffic Safety Research **6**, e000042 (2024), https://doi.org/10.55329/vmgb9648.

[18] A. Niska and J. Wenäll, *Simulated single-bicycle crashes in the VTI crash safety laboratory,* Traffic Injury Prevention **20**, 68 (2019), https://doi.org/10.1080/15389588.2019.1685090.

[19] A. Niska, J. Wenäll, and J. Karlström, *Crash tests to evaluate the design of temporary traffic control devices for increased safety of cyclists at road works,* Accident Analysis & Prevention **166**, 106529 (2022), https://doi.org/10.1016/j.aap.2021.106529.

[20] Y. Peng, Y. Chen, J. Yang, D. Otte, and R. Willinger, *A study of pedestrian and bicyclist exposure to head injury in passenger car collisions based on accident data and simulations,* Safety Science **50**, 1749 (2012), https://doi.org/10.1016/j.ssci.2012.03.005.

[21] M. Fahlstedt, P. Halldin, and S. Kleiven, *The protective effect of a helmet in three bicycle accidents – A finite element study,* Accident Analysis & Prevention **91**, 135 (2016), https://doi.org/10.1016/j.aap.2016.02.025.

[22] C. Baker, X. Yu, B. Lovell, R. Tan, S. Patel, and M. Ghajari, *How well do popular bicycle helmets protect from different types of head injury?* Annals of Biomedical Engineering **52**, 3326 (2024), https://doi.org/10.1007/s10439-024-03589-8.

[23] V. Astarita, V. Giofré, G. Guido, and A. Vitale, *Investigating road safety issues through a microsimulation model,* Procedia-social and Behavioral Sciences **20**, 226 (2011), https://doi.org/10.1016/j.sbspro.2011.08.028.

[24] U. Shahdah, F. Saccomanno, and B. Persaud, *Application of traffic microsimulation for evaluating safety performance of urban signalized intersections,* Transportation Research Part C: Emerging Technologies **60**, 96 (2015), https://doi.org/10.1016/j.trc.2015.06.010.

[25] H. Twaddle, T. Schendzielorz, and O. Fakler, *Bicycles in urban areas: Review of existing methods for modeling behavior,* Transportation Research Record **2434**, 140 (2014), https://doi.org/10.3141/2434-17.

[26] C. M. Schmidt, A. Dabiri, F. Schulte, R. Happee, and J. K. Moore, *Essential bicycle dynamics for microscopic traffic simulation: An example using the social force model,* in *The Evolving Scholar-BMD 2023, 5th Edition* (2023) http://dx.doi.org/10.59490/649d4037c2c818c6824899bd.

[27] N. Rinke, C. Schiermeyer, F. Pascucci, V. Berkhahn, and B. Friedrich, *A multi-layer social force approach to model interactions in shared spaces using collision prediction,* Transportation Research Procedia **25**, 1249 (2017), https://doi.org/10.1016/j.trpro.2017.05.144.

[28] V. Keppner, S. Krumpoch, R. Kob, A. Rappl, C. C. Sieber, E. Freiberger, and H. M. Siebentritt, *Safer cycling in older age (SiFAr): Effects of a multi-component cycle training. a randomized controlled trial,* BMC Geriatrics **23**, 131 (2023), https://doi.org/10.1186/s12877-021-02502-5.

[29] L. Alizadehsaravi and J. K. Moore, *Bicycle balance assist system reduces roll and steering motion for young and older bicyclists during real-life safety challenges,* PeerJ **11**, e16206 (2023), https://doi.org/10.7717/peerj.16206.

[30] B. Janssen, P. Schepers, H. Farah, and M. Hagenzieker, *Behaviour of cyclists and pedestrians near right angled, sloped and levelled kerb types: Do risks associated to height differences of kerbs weigh up against other factors?* European Journal of Transport and Infrastructure Research **18**, 360 (2018), https://doi.org/10.18757/ejtir.2018.18.4.3254.

[31] F. Westerhuis, A. B. M. Fuermaier, K. A. Brookhuis, and D. de Waard, *Cycling on the edge: The effects of edge lines, slanted kerbstones, shoulder, and edge strips on cycling behaviour of cyclists older than 50 years,* Ergonomics **63**, 769 (2020), https://doi.org/10.1080/00140139.2020.1755058.

[32] P. Schepers, N. Agerholm, E. Amoros, R. Benington, T. Bjørnskau, S. Dhondt, B. de Geus, C. Hagemeister, B. P. Loo, and A. Niska, *An international review of the frequency of single-bicycle crashes (SBCs) and their relation to bicycle modal share,* Injury Prevention **21**, e138 (2015), https://doi.org/10.1136/injuryprev-2013-040964.

[33] A. L. Schwab and J. P. Meijaard, *A review on bicycle dynamics and rider control,* Vehicle System Dynamics **51**, 1059 (2013), https://doi.org/10.1080/00423114.2013.793365.

[34] J. P. Meijaard, J. M. Papadopoulos, A. Ruina, and A. L. Schwab, *Linearized dynamics equations for the balance and steer of a bicycle: A benchmark and review,* Proceedings of the Royal Society A: Mathematical, Physical and Engineering Sciences **463**, 1955 (2007), https://doi.org/10.1098/rspa.2007.1857.

[35] J. D. G. Kooijman, A. L. Schwab, and J. P. Meijaard, *Experimental validation of a model of an uncontrolled bicycle,* Multibody System Dynamics **19**, 115 (2008), https://doi.org/10.1007/s11044-007-9050-x.

[36] J. D. G. Kooijman, J. P. Meijaard, J. M. Papadopoulos, A. Ruina, and A. L. Schwab, *A bicycle can be self-stable without gyroscopic or caster effects,* Science **332**, 339 (2011), https://doi.org/10.1126/science.1201959.

[37] D. Stevens, *The stability and handling characteristics of bicycles*, Bachelor's thesis, The University of New South Wales, School of Mechanical and Manufacturing Engineering, Sydney, Australia (2009), http://www.varg.unsw.edu.au/Assets/link%20pdfs/thesis_stevens.pdf.

[38] T.-O. Tak, J.-S. Won, and G.-Y. Baek, *Design sensitivity analysis of bicycle stability and experimental validation,* in *Bicycle and Motorcycle Dynamics Conference* (Delft, The Netherlands, 20-22 October 2010) http://www.bicycle.tudelft.nl/ProceedingsBMD2010/papers/tak2010design.pdf.

[39] K. J. Astrom, R. E. Klein, and A. Lennartsson, *Bicycle dynamics and control: Adapted bicycles for education and research,* IEEE Control Systems Magazine **25**, 26 (2005), https://doi.org/10.1109/MCS.2005.1499389.

[40] A. L. Schwab, J. P. Meijaard, and J. D. G. Kooijman, *Lateral dynamics of a bicycle with a passive rider model: Stability and controllability,* Vehicle System Dynamics **50**, 1209 (2012), https://doi.org/10.1080/00423114.2011.610898.

[41] J. P. Meijaard and A. L. Schwab, *Linearized equations for an extended bicycle model,* in *III European Conference on Computational Mechanics: Solids, Structures and Coupled Problems in Engineering* (Lisbon, Portugal, 5-8 June 2006) http://www.bicycle.tudelft.nl/schwab/Publications/MeijaardSchwab2006.pdf.

[42] S. M. Cain and N. C. Perkins, *Comparison of experimental data to a model for bicycle steady-state turning,* Vehicle System Dynamics **50**, 1341 (2012), https://doi.org/10.1080/00423114.2011.650181.

[43] G. Franke, W. Suhr, and F. Rieß, *An advanced model of bicycle dynamics,* European Journal of Physics **11**, 116 (1990), http://bicycle.tudelft.nl/schwab/Bicycle/BicycleHistoryReview/FraSuhRie90.pdf.

[44] A. Lennartsson, *Efficient multibody dynamics*, Ph.D. thesis, KTH Royal Institute of Technology, Stockholm, Sweden (1999), https://www.diva-portal.org/smash/get/diva2:8540/FULLTEXT01.pdf.

[45] P. Basu-Mandal, A. Chatterjee, and J. M. Papadopoulos, *Hands-free circular motions of a benchmark bicycle,* Proceedings of the Royal Society A: Mathematical, Physical and Engineering Sciences **463**, 1983 (2007), https://doi.org/10.1098/rspa.2007.1849.

[46] D. L. Peterson and M. Hubbard, *General steady turning of a benchmark bicycle model,* in *International Design Engineering Technical Conferences and Computers and Information in Engineering Conference* (San Diego, USA, 30 August - 2 September 2009) https://doi.org/10.1115/DETC2009-86145.

[47] G. Frosali and F. Ricci, *Kinematics of a bicycle with toroidal wheels,* Communications in Applied and Industrial Mathematics **3**, 24 (2012).

[48] H. Pacejka, *Tire and vehicle dynamics* (Elsevier, 2005).

[49] G. Dell'Orto, G. Mastinu, R. Happee, and J. K. Moore, *Measurement of the lateral characteristics and identification of the magic formula parameters of city and cargo bicycle tyres,* Vehicle System Dynamics , 1 (2024), https://doi.org/10.1080/00423114.2024.2338143.

[50] J. K. Moore, M. Hubbard, A. L. Schwab, and J. D. G. Kooijman, *Accurate measurement of bicycle parameters,* in *Bicycle and Motorcycle Dynamics Conference* (Delft, The Netherlands, 20-22 October 2010) 20-22 October 2010.

[51] J. K. Moore, M. Hubbard, J. D. G. Kooijman, and A. L. Schwab, *A method for estimating physical properties of a combined bicycle and rider,* in *International Design Engineering Technical Conferences and Computers and Information in Engineering Conference* (San Diego, USA, 30 August - 2 September 2009) https://doi.org/10.1115/DETC2009-86947.

[52] A. Dressel and A. Rahman, *Measuring sideslip and camber characteristics of bicycle tyres,* Vehicle System Dynamics **50**, 1365 (2012), https://doi.org/10.1080/00423114.2011.615408.

[53] G. Dell'Orto, F. M. Ballo, G. Mastinu, and M. Gobbi, *Bicycle tyres — development of a new test-rig to measure mechanical characteristics,* Measurement **202**, 111813 (2022), https://doi.org/10.1016/j.measurement.2022.111813.

[54] G. Dialynas, J. W. de Haan, A. C. Schouten, R. Happee, and A. L. Schwab, *The dynamic response of the bicycle rider's body to vertical, fore-and-aft, and lateral perturbations,* Proceedings of the Institution of Mechanical Engineers, Part D:

Journal of Automobile Engineering **234**, 1944 (2020), https://doi.org/10.1177/0954407019891289.

[55] A. Doria, M. Tognazzo, and V. Cossalter, *The response of the rider's body to roll oscillations of two wheeled vehicles; experimental tests and biomechanical models,* Proceedings of the Institution of Mechanical Engineers, Part D: Journal of Automobile Engineering **227**, 561 (2013), https://doi.org/10.1177/095440701245750.

[56] A. L. Schwab, P. D. L. de Lange, R. Happee, and J. K. Moore, *Rider control identification in bicycling using lateral force perturbation tests,* Proceedings of the Institution of Mechanical Engineers, Part K: Journal of multi-body dynamics **227**, 390 (2013), https://doi.org/10.1177/1464419313492317.

[57] J. A. Michon, *A critical view of driver behavior models: What do we know, what should we do?* in *Human behavior and traffic safety* (Springer, 1985) pp. 485–524, https://doi.org/10.1007/978-1-4613-2173-6_19.

[58] A. Kesting, M. Treiber, and D. Helbing, *Enhanced intelligent driver model to access the impact of driving strategies on traffic capacity,* Philosophical Transactions of the Royal Society A: Mathematical, Physical and Engineering Sciences **368**, 4585 (2010), https://doi.org/10.1098/rsta.2010.0084.

[59] J. Steen, H. J. Damveld, R. Happee, M. M. van Paassen, and M. Mulder, *A review of visual driver models for system identification purposes,* in *2011 IEEE international conference on systems, man, and cybernetics* (Anchorage, USA, 9-12 October 2011, 2011) https://doi.org/10.1109/ICSMC.2011.6083981.

[60] T. Toledo, H. N. Koutsopoulos, and M. E. Ben-Akiva, *Modeling integrated lane-changing behavior,* Transportation Research Record **1857**, 30 (2003), https://doi.org/10.3141/1857-04.

[61] J. D. G. Kooijman, A. L. Schwab, and J. K. Moore, *Some observations on human control of a bicycle,* in *International Design Engineering Technical Conferences and Computers and Information in Engineering Conference* (San Diego, USA, 30 August - 2 September 2009) https://doi.org/10.1115/DETC2009-86959.

[62] A. L. Schwab, J. D. G. Kooijman, and J. P. Meijaard, *Some recent developments in bicycle dynamics and control,* in *4th European Conference on Structural Control* (St. Petersburg, Russia, 8-12 September 2008) http://www.bicycle.tudelft.nl/schwab/Publications/SchwabKooijmanMeijaard2008.pdf.

[63] R. Hess, J. K. Moore, and M. Hubbard, *Modeling the manually controlled bicycle,* IEEE Transactions on Systems, Man, and Cybernetics-Part A: Systems and Humans **42**, 545 (2012), https://doi.org/10.1109/TSMCA.2011.2164244.

[64] J. K. Moore, *Human control of a bicycle*, Ph.D. thesis, University of California, Davis, USA (2012).

[65] B. Algurén and M. Rizzi, *In-depth understanding of single bicycle crashes in Sweden — crash characteristics, injury types and health outcomes differentiated by gender and age-groups,* Journal of Transport & Health **24**, 101320 (2022), https://doi.org/10.1016/j.jth.2021.101320.

[66] R. Utriainen, M. Pöllänen, S. O'Hern, and N. Sihvola, *Single-bicycle crashes in Finland — characteristics and safety recommendations,* Journal of Safety Research **87**, 96 (2023), https://doi.org/10.1016/j.jsr.2023.09.008.

[67] R. Utriainen, *Characteristics of commuters' single-bicycle crashes in insurance data,* Safety **6**, 13 (2020), https://doi.org/10.3390/safety6010013.

[68] M. S. Myhrmann, K. H. Janstrup, M. Møller, and S. E. Mabit, *Factors influencing the injury severity of single-bicycle crashes,* Accident Analysis & Prevention **149**, 105875 (2021), https://doi.org/10.1016/j.aap.2020.105875.

[69] M. Ohlin, B. Algurén, and A. Lie, *Analysis of bicycle crashes in Sweden involving injuries with high risk of health loss,* Traffic Injury Prevention **20**, 613 (2019), https://doi.org/10.1080/15389588.2019.1614567.

[70] P. Hertach, A. Uhr, S. Niemann, and M. Cavegn, *Characteristics of single-vehicle crashes with e-bikes in Switzerland,* Accident Analysis & Prevention **117**, 232 (2018), https://doi.org/10.1016/j.aap.2018.04.021.

[71] A. V. Olesen, T. K. O. Madsen, T. Hels, M. Hosseinpour, and H. S. Lahrmann, *Single-bicycle crashes: An in-depth analysis of self-reported crashes and estimation of attributable hospital cost,* Accident Analysis & Prevention **161**, 106353 (2021), https://doi.org/10.1016/j.aap.2021.106353.

[72] K. Gildea, D. Hall, and C. Simms, *Configurations of underreported cyclist-motorised vehicle and single cyclist collisions: Analysis of a self-reported survey,* Accident Analysis & Prevention **159**, 106264 (2021), https://doi.org/10.1016/j.aap.2021.106264.

[73] B. Beck, M. R. Stevenson, P. Cameron, J. Oxley, S. Newstead, J. Olivier, S. Boufous, and B. J. Gabbe, *Crash characteristics of on-road single-bicycle crashes: An under-recognised problem,* Injury Prevention **25**, 448 (2019), https://doi.org/10.1136/injuryprev-2018-043014.

[74] L. De Rome, S. Boufous, T. Georgeson, T. Senserrick, D. Richardson, and R. Ivers, *Bicycle crashes in different riding environments in the Australian capital territory,* Traffic Injury Prevention **15**, 81 (2014), https://doi.org/10.1080/15389588.2013.781591.

[75] L. B. Meuleners, M. Fraser, M. Johnson, M. Stevenson, G. Rose, and J. Oxley, *Characteristics of the road infrastructure and injurious cyclist crashes resulting in a hospitalisation,* Accident Analysis & Prevention **136**, 105407 (2020), https://doi.org/10.1016/j.aap.2019.105407.

[76] M. J. Boele-Vos, K. van Duijvenvoorde, M. J. A. Doumen, C. W. A. E. Duivenvoorden, W. J. R. Louwerse, and R. J. Davidse, *Crashes involving cyclists aged 50 and over in the Netherlands: An in-depth study,* Accident Analysis & Prevention **105**, 4 (2017), https://doi.org/10.1016/j.aap.2016.07.016.

[77] H. van der Kooij, R. Jacobs, B. Koopman, and H. Grootenboer, *A multisensory integration model of human stance control,* Biological cybernetics **80**, 299 (1999), https://doi.org/10.1007/s004220050527.

[78] H. van der Kooij, R. Jacobs, B. Koopman, and F. van der Helm, *An adaptive model of sensory integration in a dynamic environment,* Biological Cybernetics **84**, 103 (2001), https://doi.org/10.1007/s004220000196.

[79] M. Pijnappels, J. C. E. van der Burg, N. D. Reeves, and J. H. van Dieën, *Identification of elderly fallers by muscle strength measures,* European journal of applied physiology **102**, 585 (2008), https://doi.org/10.1007/s00421-007-0613-6.

2

A Practical Indicator to Safely and Proactively Evaluate Cyclist Fall Prevention Intervention Effectiveness: The Maximum Allowable Handlebar Disturbance

M.M. Reijne, F.C.T. van der Helm and A.L. Schwab

This Chapter is under review at Traffic Safety Research

ABSTRACT

With the rise in cyclist fatalities and serious injuries in high-volume cycling countries, along with the increasing global popularity of cycling, there is an urgent need to improve cycling safety. While most serious cycling injuries are related to loss of balance, resulting in falls, the effectiveness of fall prevention interventions aiming to reduce fall risk in critical situations remains challenging to evaluate. The goal of this study is to safely and proactively evaluate cyclist fall prevention interventions by applying bicycle dynamics and cyclist control models.

Currently, an indicator still needs to be developed for these models that can systematically quantify the effectiveness of a wide range of cyclist fall prevention interventions across various crash types, enabling a comparison to prioritise the most effective interventions. Drawing from system dynamics theory and methodologies used in human gait fall prevention, we introduce in this chapter a novel, general indicator for predicting the effectiveness of cyclist fall prevention interventions: the Maximum Allowable Handlebar Disturbance (MAHD). The MAHD is defined as the upper limit of a clockwise external applied angular impulse to the handlebars about the steering axis, beyond which a cyclist can no longer recover balance. The angular impulse is approximated by a constant external applied torque for 0.3 seconds. It reflects the cyclist's ability to recover balance from a large disturbance. A cyclist fall prevention intervention is considered effective if it increases the MAHD.

The MAHD can systematically evaluate cyclist fall prevention interventions for crash types where cyclists encounter impulse-like disturbances, such as falls following a collision with other road users or an obstacle, and due to loss of balance. Additionally, the MAHD can evaluate interventions related to bicycle design, cyclist control, and environmental factors such as road surface, available lateral width, and other disturbances.

This indicator, combined with bicycle dynamics and cyclist control models, represents a significant advancement in the proactive and safe evaluation of fall prevention interventions, eliminating the need for real-world implementation. The MAHD provides a practical means for systematically evaluating a range of interventions that were previously difficult to evaluate ex-ante. This approach can aid professionals in designing safer bicycles and infrastructure, developing effective training programs, and assisting policy advisors in allocating resources to the most cost-effective interventions.

2.1. INTRODUCTION

The rise in cyclist fatalities and serious injuries, in combination with cycling's growing global popularity, underscores the urgent need for improved cycling safety interventions [1, 2]. It is imperative to prioritise cost-effective safety interventions. In turn, identifying interventions that improve cycling safety efficiently is crucial to enable policy advisors to allocate resources and professionals to design safe bicycles, infrastructure, and educational or training programs.

Among the various possible cycling safety interventions, those aimed at preventing cyclist falls are particularly promising in terms of effectiveness because many cycling

injuries result from balance-related issues leading to falls [3]. However, currently, the effectiveness of many fall prevention interventions cannot be evaluated safely and proactively (i.e. ex-ante), as we will demonstrate by an overview of existing approaches.

Existing approaches for evaluating cycling safety interventions
A variety of approaches have been developed to evaluate cycling safety interventions, including statistical analyses of crash data [4–7], surrogate safety indicators derived from video observations [8, 9], field and experimental studies [10–19], crash tests [20–24] and models that simulate traffic scenarios [25–29].

Statistical analyses of historical crash data are a common approach, enabling the evaluation of interventions such as traffic calming measures [4] or mandatory helmet laws [5] by comparing crash rates before and after implementation. However, this approach relies on representative and accurate crash data, which is compromised by the underreporting of single bicycle crashes [30]. Furthermore, it cannot evaluate interventions that have not yet been implemented, as significant data collection periods are required to establish their effectiveness.

Surrogate safety indicators, such as Time-To-Collision and Post Encroachment Time, focus on near-miss events and evasive manoeuvres. These indicators do not rely on actual crashes but on near-misses, thereby reducing the lengthy data collection periods. This approach has been applied to evaluate interventions like improved signage [8] or wider bicycle paths [9]. However, surrogate safety indicators primarily focus on interactions and conflicts between road users, overlooking the majority of falls that occur without the involvement of other road users [3].

Field and experimental studies often use indirect indicators, such as perceived safety, mental workload, or bicycle motion (e.g., lean angle), to evaluate interventions. Examples of interventions evaluated with this approach include evaluating the effect of lane buffers and traffic calming measures on perceived safety [10], visual nudges on the speed at intersections [11], mobile phone use on cycling workload [12, 13], and dismounting techniques on bicycle stability [14]. Laboratory-based studies have evaluated the effects of infrastructure interventions on cyclist speed using test tracks [16], alcohol intoxication on stability using treadmills [15, 17], and road design on perceived safety with simulators [18, 19]. While these approaches provide valuable insights, the indirect indicators lack validation for predicting falls, as most studies do not include actual fall data or insufficient falls for robust validation.

Crash tests and crash simulation models are primarily used to evaluate injury mitigation measures like helmets, airbags, or vehicle crash zones [22, 23]. These approaches quantify the forces involved in falls or collisions but are not designed to evaluate interventions aimed at preventing falls altogether.

Models that simulate traffic scenarios — including traffic microsimulation, behavioural models, and crash avoidance models — mainly simulate the interactions between road users. Traffic microsimulation models use mathematical equations to simulate road user movements and interactions within a traffic network, allowing the evaluation of infrastructure design and traffic management policies [25, 26]. Behavioural models simulate the decision-making processes of road users in response to potentially critical situations [27, 28], while crash avoidance models often focus on the execution of

physical manoeuvres [29]. However, none of these models yet incorporate the balancing task and lateral dynamics of the bicycle required to simulate cyclist falls. This limitation significantly reduces their applicability to cyclist fall prevention interventions.

This review of existing approaches highlights the need for a safe and proactive approach to evaluate cyclist fall prevention interventions, particularly those aiming to improve balance recovery in critical situations. Such an approach should be able to evaluate interventions such as balance training programs [31], steer-assist systems [32], and forgiving road infrastructure designs [33, 34].

Bicycle dynamics and cyclist control models

Bicycle dynamics and cyclist control models offer a promising approach for safely and proactively evaluating how different interventions targeting bicycle design, cyclist behaviour, and environmental factors could prevent cyclist falls. These models consist of mathematical equations that simulate the movement of the bicycle, based on Newtonian mechanics, and the cyclist-bicycle interaction using system control theories [35]. As such, these models are grounded in physics and engineering principles. The bicycle dynamics models incorporate the physics of bicycle motion, including forces, momentum, and the impact of factors like mass, inertia, and road surface conditions. Cyclist control models simulate essential actions like steering and leaning, which are required for balancing and following desired trajectories.

As described in Chapter 1, combining bicycle dynamics models with cyclist control models can simulate a range of commonly reported bicycle crash types. In addition, these models allow for the incorporation of diverse interventions targeting bicycle design, cyclist control or environmental conditions, including road surface quality, available space, and disturbances. With these models, it is thus possible to simulate a crash type and safely and proactively evaluate whether a proposed intervention changes the outcome of a given crash type.

However, several aspects need improvement to fully realise these models' application to safely and proactively evaluate cycling safety interventions, as established in Chapter 1. One gap we focus on in this chapter is the lack of an indicator to quantify and systematically compare the effectiveness of different interventions. Such an indicator is valuable for identifying and prioritising interventions that maximise cycling safety.

Which crash types and input values to consider?

Simply simulating a scenario and determining whether an intervention prevents a fall does not suffice as an indicator. While there are a limited number of crash types, simulating each type involves selecting specific input values for the parameters within bicycle dynamics and cyclist control models. These parameters include bicycle geometry, cyclist physical attributes, control characteristics, forward speed, initial conditions, external forces, and environmental factors. Additionally, models may incorporate parameters related to tyre properties, road surfaces, cyclist body motions, structural integrity, and external forces acting on the wheels. For each crash type, many combinations of these input values are possible.

The multitude of combinations introduces challenges regarding selecting relevant input value sets per crash type to evaluate intervention effectiveness. Exhaustively

evaluating all possible combinations of input values using bicycle dynamics and cyclist control models to ascertain if an intervention increases the range of combinations for which balance can be recovered, termed the basin of attraction [36], is impractical due to its time-intensive nature. Moreover, this concept of the basin of attraction could be more intuitive. Due to the high dimensionality of the bicycle-cyclist system, it is challenging to interpret why and how exactly the basin of attraction increased. An intervention could expand the basin of attraction and, as a result, be deemed effective. However, due to non-linear interactions, previously safe combinations might become hazardous, a phenomenon not captured by the basin of attraction. Hence, we argue for the need for a more intuitive indicator.

An alternative strategy involves simulating all historic crashes or a representative subset to predict how many historic falls the intervention would prevent. This estimation could then indicate how many future falls might be avoided. However, this approach faces challenges, primarily in obtaining the necessary input values for real-world crashes. Some parameters required for simulation with bicycle dynamics and cyclist control models are neither readily available nor easily measurable, such as the torque or force profile of a collision or disturbance and the friction coefficient of the road surface at the precise location and time of the crash.

A pragmatic solution may involve selecting the most prevalent or critical crash types and defining ranges or average values for the input values based on the broader cycling population, bicycle types, and environmental conditions. This approach is similar to the EuroNCAP approach for rating new car designs' safety. However, a predefined standardised set of crashes and corresponding input values for this purpose has yet to be proposed. Proposing such a set is beyond the scope of this study. For a standardised set to gain acceptance and be used by researchers, it should be discussed and agreed upon by a broad group of experts with authority in the field of cycling safety research.

Indicator to quantify effectiveness

This study focuses on another important component: the performance indicator to evaluate an intervention's effectiveness. Even with a finite pragmatic set of crash scenarios, it is essential to consider indicators beyond the simplistic binary outcome of a fall or balance recovery. Relying solely on this binary outcome may neglect crucial information. We advocate for an indicator quantifying how an intervention influences the boundary between falling and recovering balance.

Such an indicator offers insights into the proximity to a fall or balance recovery within a crash type, facilitating detailed comparisons between different interventions and trend analysis for evaluation. These insights are invaluable for distinguishing between interventions. Ideally, this indicator should possess generality, enabling application across various crash types and input values. This generality ensures systematic comparisons between interventions using a consistent metric, making it possible to distinguish the effectiveness of a broader set of interventions.

While functional driver behaviour models in traffic psychology [37], such as perception models [38], cognitive models [39], or workload models [12, 40], offer potential indicators like maximum workload, integrating them with existing cyclist control models is, for now, not yet feasible. Consequently, a comprehensive indicator

quantifying the threshold for cyclist falls, computable using bicycle dynamics and cyclist control models, has yet to be proposed.

Goal of the study

The goal of this study is to improve the application of bicycle dynamics and cyclist control models to safely and proactively evaluate cyclist fall prevention interventions. To achieve this, we propose a novel general intervention performance indicator — the Maximum Allowable Handlebar Disturbance (MAHD) — which quantifies the boundary between falling and successfully recovering balance.

2.2. THE INTERVENTION PERFORMANCE INDICATOR

In this section, we introduce a general indicator that can be used to evaluate the effectiveness of interventions that aim to improve cycling safety. This indicator can be computed using existing bicycle dynamics or cyclist control models and quantifies the boundary between falling and successfully recovering balance. Numerous options exist for such indicators. In this section, we first elaborate on why we opted for a disturbance-based indicator, after which we introduce and explain the general concept of our novel indicator: the Maximum Allowable Handlebar Disturbance (MAHD). Finally, we outline the methodology for calculating the MAHD and demonstrate its generalisability across different crash types.

2.2.1. RATIONALE FOR CHOOSING A DISTURBANCE-BASED INDICATOR

In principle, any parameter or variable within bicycle dynamics and cyclist control models — or those derived from them — could serve as an indicator of the boundary between falling and successfully recovering balance. For example, to determine the basin of attraction, all system parameters are kept constant, except for the time-dependent parameters, the so-called states of the system. For cycling, these states describe the initial position and orientation of the bicycle. By systematically varying the input values for the initial position and orientation of the bicycle, one can find the boundary for which a given bicycle-cyclist system can no longer recover balance.

We argue in favour of using disturbances as the threshold indicator. Here, disturbances denote external forces or torques acting on the bicycle-cyclist system, particularly those that disrupt balance. In real-world cycling scenarios, such disturbances arise from internal sources, such as cyclist movements relative to the bicycle, like looking over one's shoulder, and external factors, such as wind gusts, uneven road surfaces, or collisions with other road users or obstacles. These disturbances cause changes in the states of the bicycle-cyclist system. The bicycle is especially sensitive to such disturbance because the bicycle is inherently unstable at low to medium forward speeds. Even minor disturbances can result in falls if no corrective action is taken.

In systems dynamics theory, assessing a system's stability — which reflects the robustness against falls — involves evaluating its ability to recover balance from a disturbance. Observational studies in walking have validated this disturbance-based approach, demonstrating its value in predicting the effectiveness of fall prevention interventions [41–47]. These studies observed individuals who underwent training to

improve disturbance rejection indicators alongside a control group that did not. Results consistently showed fewer falls among trained individuals. Although similar evidence for cycling is lacking, we assume similar effects based on the comparable nature of continuous balance control by a human in both activities.

While our novel indicator focuses on the maximum disturbance from which a cyclist can recover balance, a common approach to investigate the stability of a dynamical system is to investigate the system's response to minor disturbances. This approach entails linearising the behaviour and equations governing the system around a steady-state motion or stable point. When linearised, the response to a minor disturbance of the system can be described by the real components of eigenvalues. This value indicates whether and how fast the system returns to its steady-state motion or deviates from it over time.

Given the prevalence of this method, including its application to cycling [48–51], we feel the need to elaborate on why we choose to quantify the maximum disturbance from which a cyclist can recover balance instead of its response to minor disturbances and why this is crucial for reliably predicting the effectiveness of fall prevention interventions.

The linearised stability approach can be applied to evaluate the stability of the bicycle-cyclist system because the lateral dynamics — consisting of the lean and steering angles, crucial for predicting falls — of the uncontrolled system around steady motion can be described by linearised second-order differential equations [48, 49]. Steady motions in cycling are typical in the real world and include upright, straight-ahead cycling or steady-state turning, both while maintaining constant forward speed. These linearised equations have undergone validation and exhibit good agreement with observed real-world bicycle motions [49, 52–54]. Furthermore, several linear cyclist control models have been developed to simulate realistic cyclist behaviour in maintaining bicycle balance [35, 51, 55].

Consequently, the lateral dynamics of the bicycle-cyclist system can be evaluated for steady-state motion and linear cyclist control using the linearised stability approach. This approach facilitates the evaluation of the real components of eigenvalues, enabling the determination of the stability and speed with which lean and steering angles return to the steady motion in response to minor disturbances.

However, certain elements and conditions complicate evaluating whether an intervention effectively prevents falls in real-world scenarios by only considering the lateral dynamics and the response to minor disturbances.

First, for large disturbances, which cause considerable deviations in lean and steering angles from the steady-state motions, the lateral dynamics, as determined by linearised equations, begin to deviate from actual values. The study of Basu-Mandal *et al.*(2007) demonstrated this by comparing linearised equations with a set of non-linear equations, revealing that the behaviour and motions of the bicycle are no longer accurately captured by linearised models [56]. The linearised equations of the bicycle dynamics are largely accurate for lean and steering angles up to 45 degrees.

Secondly, even for minor disturbances, the linearised stability approach has limitations in predicting real-world falls. While linearised equations can describe lateral dynamics (lean and steering angle), the equations governing how the bicycle moves

through the environment — such as its trajectory — are non-linear [48]. As detailed in Chapter 1, accurately simulating commonly reported crashes requires considering environmental conditions, such as the finite lateral space available for recovering balance. Therefore, the linearised stability approach is inadequate for evaluating real-world cyclist fall interventions.

Thirdly, also discussed in Chapter 1, extending the linear bicycle dynamics model with non-linear components is necessary to simulate certain crash types accurately. For example, crash types such as falls due to slipping on a slippery road surface require an extension of the linear original Carvallo-Whipple bicycle model with a tyre model, while crash types related to falls following an evasive manoeuvre necessitate extensions to accommodate accelerations. In such cases, the linearised stability approach can no longer be applied.

Moreover, while yet to be fully understood, cyclists themselves may exhibit non-linear behaviour and react differently to varying disturbance magnitudes. Such task-specificity has been observed in gait [47, 57], and we assume that similar non-linear behaviour may also exist in cycling. For instance, some cyclists may exert greater effort to counteract minor disturbances, appearing more stable when assessed by measures reflecting their ability to recover balance from minor disturbances. Conversely, others may delay their reaction to more minor disturbances and react when deviations in the lean or steering angle pass a certain threshold. Furthermore, individuals may have different limitations in the maximum disturbance they can handle due to factors like limited strength or reaction time, restricting their response capabilities.

Given these instances, the linearised stability approach fails to provide reliable predictions of real-world falls, so another approach is required.

We also feel the need to elaborate on why we chose not to use validated fall prediction indicators to predict falling while walking. The cycles of human gait, which includes walking, cannot be described by linearised equations due to the intermittent dynamics of steps. This means that the linearised stability approach can also not be applied to gait. Instead, gait stability analysis studies often use non-linear equations in combination with indicators such as the maximum Lyapunov exponent or the maximum Floquet multiplier [58].

The maximum Lyapunov exponent has been validated to predict falling while walking. In contrast, the validity of the maximum Floquet multiplier has yet to be established [41, 42]. While these indicators could also be applied to cycling, they again reflect the ability of a system to recover balance after minor disturbances. As discussed above, the fact remains that the response to large disturbances is pivotal, especially near the threshold of falling. As such, these indicators are also not suitable for our purpose.

2.2.2. GENERAL CONCEPT - THE MAXIMUM ALLOWABLE HANDLEBAR DISTURBANCE

As described above, we want to develop an indicator that quantifies the maximum disturbance threshold a cyclist can handle before losing balance and falling. Given the diverse array of potential disturbances that cyclists may encounter — varying in direction, magnitude, position, and cyclist orientation the moment the disturbance is encountered — it is impractical to evaluate each type of disturbance individually.

To improve the practical application, we draw inspiration from the Gait Sensitivity Norm (GSN) developed for evaluating the balance recovery capabilities of passive bipedal robots mimicking human walking dynamics [59]. We aim to adopt a similar approach for evaluating the probability of cyclist falls.

The GSN methodology offers a balanced framework that considers practicality and accuracy in evaluating disturbance rejection capabilities. A key advantage of the GSN is its general applicability to different types of disturbances. The GSN uses a more general approach by considering a set of disturbances, such as floor irregularities or sensor noise, and a set of gait indicators directly related to the robot's failure modes. The norm measures the dynamic response of these indicators to the disturbances, offering insights into how well the robot can recover to its limit cycle (i.e. normal walking) after large disturbances and taking into account its walking environment.

Building upon the principles underlying the GSN, we have adopted a similar conceptual framework to develop a novel indicator tailored to evaluating cyclist falls. This approach allows us to systematically evaluate cyclists' resilience to disturbances, offering a general indicator for evaluating stability across diverse cycling scenarios.

The Maximum Allowable Handlebar Disturbance

We propose the Maximum Allowable Handlebar Disturbance (MAHD) as a novel indicator to evaluate cyclist fall prevention interventions. The MAHD quantifies the upper threshold for an impulse-like external handlebar disturbance beyond which a cyclist can no longer recover balance. It reflects a cyclist's resilience. A cyclist fall prevention intervention is considered effective if it increases the MAHD.

To simulate a consistent impulse-like handlebar disturbance, we define it as a pure clockwise external pulse-input handlebar torque about the steering axis lasting 0.3 seconds. This disturbance is characterized as an angular impulse measured in Newton-meter-seconds (Nms). We propose varying only the torque magnitude, keeping the time constant. Experimental data from Chapter 3 suggests an MAHD range between 7.5 and 17.5 Nms, depending on variables and conditions. While these values cannot yet be directly correlated to real-world disturbances, they provide a useful benchmark for controlled experimental setups.

We argue that such a disturbance and time duration is an appropriate choice for a disturbance because it offers insights into the cyclist's ability to recover from various similar disturbances. Additionally, we argue that setting maximum thresholds for lean and steering angles and lateral available width constitutes an appropriate selection for indicators associated with the different modes of real-world cyclist falls.

Rationale for disturbance choice

We assume that an impulse-like handlebar disturbance reflects the response to other impulse-like disturbances because of the strong dynamic coupling between the lean and the steering angle. Consequently, it is possible to translate a disturbance in lean into an equivalent disturbance in steering and vice versa.

Moreover, the cyclist's response to lean or steer disturbances remains similar mainly because, during cycling, the primary mechanism for regaining balance after a disturbance is steering in the direction of the undesired fall [49]. Although leaning the

upper body relative to the bicycle can induce a steering effect, as observed when cycling without hands, studies have shown that steering is the most effective, strongest, fastest and most precise action for restoring balance following a disturbance, thus establishing it as the dominant control action [50].

Based on this rationale, an impulse-like handlebar disturbance can be regarded as representative and indicative of a cyclist's ability to recover balance from other impulse-like disturbances as well. Indeed, according to the reasoning presented, any impulse-like disturbance capable of destabilizing the bicycle could be selected, as the initiation of a lean would induce a steering effect and vice versa, resulting in a similar response from the cyclist. While the absolute limit may differ for disturbances in different directions or acting on distinct bicycle components, we anticipate consistent relative differences between types of disturbances due to the coupling between the rear frame and front assembly.

Previous research suggests that a rear frame disturbance would have been a sensible choice. These experimental studies, focusing on lightly disturbing the bicycle, have consistently employed impulse-like disturbances to the rear frame. The disturbances include lateral pulls or pushes using a rod attached to the seat post or altering the ground contact point of the rear tyre [51, 60, 61]. Such choices were likely motivated by safety considerations in experimental setups and the desire to avoid interference with steering actions, which, as previously discussed, are crucial for balance recovery.

In contrast to existing studies, we propose a handlebar disturbance, specifically pure handlebar torque. We made this distinct choice for three primarily practical reasons. This decision stems from the necessity to obtain experimental data on actual falls to validate bicycle dynamics and cyclist control models and potential indicators. Therefore, it is imperative that we can apply disturbances safely, accurately, and in a controlled manner in practice.

The first reason for selecting a handlebar disturbance is that the handlebars are the most sensitive part of bicycle balance, requiring minimal torques to induce cyclists to fall. While disturbances to the rear frame seem safer for minor disturbances, handlebar disturbances are safer for inducing falls due to the smaller magnitudes of force required. This smaller magnitude could mitigate risks in the event of potential experimental setup malfunctions.

Secondly, drawing upon insights from a study investigating disturbance mechanisms affecting balance during walking and standing [62], alongside personal experiences from pilot experiments, it seems likely that the impulse-like disturbance forces or torques necessary to induce cyclist falls via pulls on the rear frame are too high to be generated with existing hardware.

Thirdly, in practical scenarios, we can apply a pure torque to the handlebars, which better simulate real-world disturbances compared to lateral pulls or pushes on the seat post or alterations to the ground contact points of the rear tyre. Lateral pulls or pushes inevitably introduce lateral force components, potentially causing lateral displacement of the bicycle, particularly given the considerable forces required to induce a cyclist's fall. Applying a pure torque to the rear frame is not feasible in practice while translating the ground contact points has no equivalent real-world disturbance.

Similarly to the previous experimental studies applying disturbances to the rear

frame, we propose an impulse-like disturbance. For research, ideally, an angular impulse to the handlebar would be preferred, characterised by a sudden step in the bicycle's angular steering rate. Such an impulse is preferred because the cyclist cannot mitigate the effect of the disturbance through actions like stiffening their arms or using them to dampen the disturbance.

Although real-life disturbance profiles are unavailable for direct evaluation, we posit that most real-world disturbances actually exhibit impulse-like characteristics, and therefore an impulse-like characteristics, with finite magnitude and time duration of the disturbance, is more representative. In addition, the practical implementation of such a disturbance in experiments is impossible.

To ensure practical implementation, the disturbance is approximated as a high torque applied for a short duration (0.3 seconds). This approximation effectively surprises the cyclist, preventing anticipatory actions such as stiffening the arms or damping the effect of the disturbance [62]. Thus, while real-world disturbance profiles remain unavailable, the impulse-like handlebar disturbance serves as a realistic and practical experimental alternative.

Theoretically, the bicycle-cyclist system is symmetric, suggesting that the direction of the handlebar disturbance should not matter. However, external factors, such as dexterity or environmental asymmetries like kerbs on one side and traffic on the other side, might influence the response. To provide an exact definition, we define the MAHD using a clockwise disturbance, though further research is needed to investigate directional effects.

Rationale for indicators of real-world cyclist fall modes

Based on an impulse-like handlebar disturbance, we envision three primary fall modes: slipping of the tyres because of a too large lean angle, slipping of the tyres because of a too large steering angle, and cycling off the side of the road.

To recover from a handlebar disturbance, a cyclist must steer in the direction of the fall [49]. This manoeuvre involves both leaning and steering the bicycle. Generally, larger disturbances require larger lean and steering angles to recover balance. However, there is a limit to the lean and steering angles that can be achieved before the tyres lose their ability to maintain the necessary lateral friction with the ground. Beyond these limits, the tyres begin to slip, and the cyclist cannot recover the balance by steering, as the ground contact points of the tyres will no longer return beneath the bicycle-cyclist centre of gravity. The cyclist loses effective control at this point, making a fall almost inevitable.

When a bicycle leans, the lateral tyre force increases proportionally with the lean angle. A critical lean angle exists beyond which the grip is insufficient to transfer lateral forces to the road, causing the tyres to slip. We conservatively assume that once slippage occurs, it cannot be recovered, resulting in a fall. The critical lean angle depends on the vertical and lateral forces and factors such as road surface friction, tyre characteristics, and the bicycle's forward speed. The critical lean angle is small in conditions with limited friction, such as slippery road surfaces. In contrast, large tyre forces might be transferred to the road surface in dry conditions, resulting in a much larger critical lean angle.

Additionally, steering into the fall to correct a disturbance often necessitates a larger steering angle, which induces a high yaw rate. This manoeuvre requires the tyres to

generate large lateral forces. However, given the finite friction between the tyre and the road, producing such large lateral forces may not always be feasible, particularly at higher forward speeds. This limitation can again lead to tyre slip. Again, we conservatively assume that this slippage cannot be recovered by the cyclist, resulting in a fall. The necessary lateral forces depend on the bicycle's forward speed and the turn's radius, with lower speeds generally requiring less lateral forces. The vertical load, road surface friction, and tyre properties further influence the threshold for the maximum steering angle. The exact critical steering angle threshold is dependent on these conditions.

Furthermore, a handlebar disturbance can cause cyclists to deviate laterally from their initial trajectory to recover balance. In real-world settings, the available lateral space is often limited by boundaries, such as where a bike path ends and an unsuitable surface or high kerb begins. When these boundaries prevent the cyclist from steering further into the fall, required to recover balance from the disturbance, the cyclist loses effective control, making a fall almost inevitable.

Therefore, thresholds for the maximum lean and steering angles at which the tyres start to slip and the maximum available lateral width reflect the relevant cyclist fall modes.

2.2.3. CALCULATION OF THE MAXIMUM ALLOWABLE HANDLEBAR DISTURBANCE

The Maximum Allowable Handlebar Disturbance (MAHD) can be determined using either bicycle dynamics and cyclist control models or experimental setups conducted in a safe and controlled environment.

Bicycle dynamics and cyclist control models

As discussed in Chapter 1, bicycle dynamics and cyclist control models offer a means to simulate the response and motion of a bicycle following a disturbance. These models simulate whether a fall occurs following a handlebar disturbance. To conduct simulations, specific input values must be provided for various parameters, including the bicycle's and cyclist's physical characteristics, initial bicycle positioning, initial lean and steering angles, initial lean and steer rates, and initial heading. Additional factors such as tyre characteristics, road surface conditions and external forces can also be incorporated into the simulations (see Chapter 1 for more details).

By applying a small pulse input external clockwise steer torque lasting 0.3 seconds, similar to the force profile of the MAHD, time response simulations can ascertain whether a fall occurs. The assessment of a fall is based on predefined threshold values for the fall indicators, which are the maximum lean angle and steering angles at which the tyres start to slip and the maximum available lateral width. If any of these thresholds are exceeded during the simulation, a fall is deemed to have occurred.

If no falls occur, the magnitude of the steer torque can be incrementally increased until a fall is observed or incrementally lowered if a fall occurs with the initial small steer torque. The minimum angular impulse at which a fall happens for the first time is the MAHD.

Experiments

The MAHD can also be determined through experiments. We would recommend first to perform experiments in a laboratory setting. Although conducting experiments in a laboratory reduces environmental validity, it ensures safety and controlled conditions. This consideration is particularly crucial since inducing actual falls is essential to accurately determine the MAHD.

The necessity for controlled conditions stems from the anticipated variability in human responses, which precludes a clear-cut threshold. Consequently, multiple experiments under consistent conditions are required to establish a reliable threshold. Employing intelligent algorithms, such as the random staircase procedure used in pain threshold studies [63], can minimise the number of required experiments.

The aggregation of these experiments, characterised by binary outcomes (fall or no fall), allows for the reconstruction of the MAHD through statistical techniques such as logistic regression. This approach yields a continuous probability function relative to the disturbance magnitude. To define the MAHD with consistency, a specific probability threshold of falling is selected. We propose a 50% probability threshold for practicality and ease of calculation, though other probabilities can be adopted with relative ease, depending on the research objective. It is important to note that we focus on relative performance by comparing conditions with and without the intervention to determine intervention effectiveness. Thus, the exact value of the probability threshold is less critical. However, standardising this threshold is recommended for comparability across different studies.

Determining the MAHD for a single crash type with specific conditions requires multiple experiments involving the same cyclist under identical conditions. Consequently, measuring the MAHD for all potential scenarios and conditions for an intervention is very time-consuming. Therefore, we suggest that experimental data should be selectively used to validate bicycle dynamics and cyclist control models. Currently, these models lack validation under actual fall conditions, as discussed in Chapter 1. The experiments, in combination with the MAHD, can be used to validate these models. Once validated, these models can reliably simulate a broader array of crash types and conditions, enhancing their applicability in safely and proactively evaluating cyclist fall prevention interventions.

2.2.4. GENERALISABILITY OF THE MAXIMUM ALLOWABLE HANDLEBAR DISTURBANCE

We demonstrate the generalizability of the MAHD across different crash types by examining the eight commonly reported bicycle crash types, as established in Chapter 1. These are:

1. falls due to slipping on a slippery road surface
2. falls after a collision with an obstacle
3. falls following an evasive manoeuvre
4. falls involving (tram) rails

5. falls resulting from hard braking
6. falling over while cornering
7. falls due to loss of balance
8. falls after a collision with another road user

The MAHD directly indicates intervention effectiveness for the three crash types where cyclists specifically encounter a disturbance. These are falls after colliding with an obstacle, falls after colliding with another road user, and falls due to loss of balance. The description of the last type presents some ambiguity; we assume that due to the inherent instability of bicycles, disturbances like riding over a pothole or encountering a wind gust cause a significant proportion of these falls. However, these falls might also result from cyclists riding off the road due to inattentiveness.

For these three crash types, the MAHD can only be used for interventions targeting the phase between post-collision or post-disturbance and pre-fall. The MAHD reflects the probability that a cyclist will recover balance after a disturbance. It cannot be measured for interventions targeting to prevent the collision or disturbance, as the absence of a disturbance renders the MAHD inapplicable. Additionally, interventions aiming to mitigate the impact forces on the cyclist after a fall are outside the scope of the MAHD.

Interventions to reduce the probability of falls due to slipping on slippery road surfaces can also be quantified with the MAHD. Although disturbances are not explicitly mentioned in this crash type, it is likely that if the cyclist can recover balance from larger disturbances in slippery conditions, the probability of falling in these conditions will also be lower. Again, the MAHD can only be applied to interventions aiming to improve the cyclist's resilience once on a slippery road surface rather than interventions aiming to prevent the cyclist from riding over these slippery surfaces.

The MAHD of a bicycle-cyclist combination is likely small for slippery road surfaces and could approach zero, as tyres are likely to slip even at small lean and steering angles. Effective interventions would increase the MAHD, reflecting improved resilience of the cyclist, allowing them to withstand larger disturbances and apply larger lean and steering angles in slippery conditions. Interventions that reduce slipperiness will also result in an increased MAHD.

The effectiveness of interventions targeting this crash type can also be evaluated using the friction coefficient, a more direct indicator of slippery conditions. However, this indicator cannot be generalised to other crash types.

The MAHD is either inapplicable or not a direct indicator of intervention effectiveness for the other four commonly reported crash types. The MAHD cannot be applied to falls involving the front wheel getting stuck in tram rails or falls resulting from hard braking. Steering is prevented for an extended period when the front wheel gets stuck in tram rails. The cyclist loses effective control over balancing, making a fall inevitable.

Hard braking generates high decelerations and forces that can cause cyclists to fly over the handlebars. This fall mode is outside the scope of the MAHD. Similarly, a cyclist must put a foot down when braking hard and coming to a complete standstill.

A fall might occur because the cyclist could not safely do so or did not have time to do so. This fall mode is also outside the scope of the MAHD. An indicator for evaluating interventions for falls due to hard braking might be the maximum deceleration at which a cyclist can safely stop. However, this is not generalisable to many other crash types.

The remaining crash types are falls following evasive manoeuvres and falls while cornering. The MAHD can quantify the effectiveness of interventions targeting these crash types, though it is not a direct indicator. A higher MAHD, indicating a cyclist's ability to withstand higher impulse-like handlebar disturbances, suggests greater resilience during evasive manoeuvres or cornering. This resilience could result from better tyre grip or decreased lateral space to recover balance, reducing the probability of slipping or riding off the road. However, the MAHD does not directly reflect the relationship with evasive manoeuvres or cornering. Indicators such as maximum lateral accelerations, lateral swerving distance, or minimum turn radius might be used, but these are not generalisable to other crash types.

In summary, the MAHD is generalisable to several crash types in which the cyclist encounters a disturbance or slippery road surfaces.

2.3. DISCUSSION

The goal of this study was to improve the application of bicycle dynamics and cyclist control models to safely and proactively evaluate cyclist fall prevention interventions. To achieve this, we proposed a novel general intervention performance indicator — the Maximum Allowable Handlebar Disturbance (MAHD) — which quantifies the boundary between falling and successfully recovering balance. An intervention is effective if it increases the MAHD.

The MAHD draws inspiration from approaches commonly employed in evaluating fall prevention strategies in human gait, particularly the Gait Sensitivity Norm (GSN) [59]. Given that a significant portion of severe cycling injuries stem from falls attributed to loss of balance rather than collisions with other road users, we advocate that comparing cyclist falls to falls during walking, wherein balance is a critical factor, is more apt than analogies drawn from vehicular conflicts.

Defined as the upper limit for handlebar disturbance beyond which a cyclist cannot recover balance, the MAHD quantifies and reflects the cyclist's ability to recover balance in response to disturbances. Moreover, it considers real-time circumstances such as the bicycle he or she is cycling, the road surface and available space.

Specifically, the MAHD is defined as a pure pulse-input handlebar torque lasting 0.3 seconds, with only the magnitude being variable. Such a pulse-input disturbance is approximately similar to impulse-like disturbances in the real world, such as brief front-rear wheel contact between cyclists, riding over a pothole, short contact with a kerb, or a sudden wind gust. As there is one singular response to all these impulse-like disturbances, the MAHD reflects the ability of a cyclist to handle these types of disturbances. We consider such a generalisation valid based on the strong coupling between the bicycle's rear frame and front assembly, which enables the translation of lean disturbances into equivalent steer disturbances and vice versa. Moreover, cyclists exhibit similar responses to various impulse-like balance-threatening disturbances, which is to steer towards the fall [49, 50]. Nonetheless, empirical validation of this

assumption remains necessary.

Strengths

The MAHD presents several strengths compared with existing approaches for evaluating cycling safety interventions. Most importantly, the MAHD can be used with bicycle dynamics and cyclist control models to proactively and safely evaluate and quantify the effectiveness of cyclist fall interventions. As such, it presents a valuable addition to existing approaches and fills a previously existing gap, enabling us to evaluate interventions aiming to reduce fall risk in critical situations.

The MAHD can systematically evaluate cyclist fall prevention interventions targeting crash types in which cyclists encounter impulse-like disturbances. These include commonly reported crash types such as falls after a collision with other road users, falls after a collision with an obstacle, or falls due to loss of balance. For this last crash type, disturbances are likely a contributing factor.

It can also systematically evaluate interventions related to bicycle design, cyclist control, or environmental factors such as road surface, available lateral width, and disturbances. Consequently, the MAHD facilitates systematic comparison of intervention effectiveness across diverse road system components and crash types, thereby serving as a general indicator to evaluate cyclist fall prevention interventions.

Finally, the operational definition of the MAHD lends itself to experimental measurement, thereby facilitating the validation of bicycle dynamics and cyclist control models in predicting the MAHD and the validity of the MAHD in predicting falls. We recommend such experiments as a valuable next step for future research.

Limitations

While we have established that the MAHD can serve as a general intervention performance indicator, it is crucial to recognise that it is not a universal indicator for evaluating all cycling safety interventions.

The MAHD is adequate for evaluating interventions for crash types where the cyclist encounters a disturbance. However, it is inadequate for evaluating interventions targeting falls following an evasive manoeuvre, falls involving (tram)rails, falling over while cornering, and falls resulting from hard braking. The effectiveness of interventions targeting evasive manoeuvre or hard braking resulting from a conflict with another road user can be safely and proactively evaluated using traffic simulation models and surrogate safety indicators. Evaluating interventions for the other single bicycle crash types, where no conflict with other road users occurs, remains challenging.

Although preventing collisions or disturbances might initially seem more effective than increasing cyclists' resilience to these disturbances, it is unrealistic to assume that all collisions and disturbances can be eliminated from the road environment. Furthermore, it might be more effective to slightly improve the MAHD, improving the cyclist's ability to recover balance from a wide range of impulse-like disturbances, than to eliminate a specific type of collision or disturbance.

A more effective strategy would be to eliminate disturbances significantly above the MAHD threshold and improve cyclists' resilience to disturbances close to this threshold. Unfortunately, real-world collision and disturbance force profiles have not

been measured, and their relationship to the MAHD is unknown. Future research should document these profiles so that disturbances can be categorised relative to the MAHD. The MAHD can then serve as a scoring metric to prioritise which types of disturbances and collisions should be eliminated from the road environment.

While it is evident that certain collisions, such as those with a motor vehicle travelling at 50 km/h, are far above the MAHD and impossible to recover from, we believe that many disturbances causing serious injuries are relatively minor and could be recoverable if the cyclist is attentive, knows what to do, and has a safe bicycle.

The MAHD evaluates intervention effectiveness based solely on the cyclist's response to impulse-like disturbances. This presents additional limitations because the risk of a cyclist falling after a disturbance is only part of the broader context needed to evaluate injury risk in real-world conditions. This evaluation also requires considering exposure — how frequently cyclists encounter specific disturbances — and the injury risk once a cyclist falls.

Future studies should integrate exposure and injury risk into the current approach by collecting empirical data on the frequency and severity of crash types and the corresponding input values for bicycle dynamics and cyclist control models. This analysis could help to prioritise crash types and input values, focusing on those most common or leading to severe outcomes. We encourage dialogue among cycling safety researchers to determine if the set of crash scenarios can be standardised. Identifying a subset that captures the most vulnerable, frequent, or severe scenarios could improve intervention practicality. Establishing a consensus on which crash scenarios to evaluate would enable standardised assessments across studies and systematic comparisons of interventions.

Despite these limitations, the MAHD, combined with bicycle dynamics and cyclist control models, allows for the evaluation of many interventions that could not previously be evaluated safely and proactively. The MAHD alone is an extremely valuable indicator for evaluating a wide range of interventions that cannot be assessed safely and proactively with existing approaches. These interventions include changes to bicycle design, cyclist balancing control skills, road surface conditions, disturbances, and available lateral width.

Practical application

The practical implications and applications of our research findings are evident. We aim to develop an approach to evaluate cyclist fall prevention interventions safely, systematically and pragmatically using bicycle dynamics and cyclist control models. The newly proposed intervention performance indicator, the MAHD, is a valuable step in accomplishing this goal.

We demonstrate the practical application of our approach through three qualitative examples targeting the core components of cycling: bicycle design, cyclist control, and infrastructure improvement.

Firstly, modifications to bicycle design, such as adjustments to the bicycle frame by changing the trail or head tube angle, can be integrated into bicycle dynamics models. By simulating the impact of these modifications on the MAHD, we can evaluate their effectiveness. An increase in MAHD resulting from such design changes indicates

improved cyclist resilience and an enhanced ability to recover balance after large disturbances.

Secondly, changes to cyclist control can be evaluated through integration into cyclist control models. This integration allows for the evaluation of how modifications in control strategies affect the cyclist's ability to recover balance from large disturbances.

Lastly, the effectiveness of increasing lateral space for balance recovery can be examined by adjusting the threshold for available lateral width. Through simulation, we can analyse changes in MAHD resulting from the expansion of lateral space. These results provide insight into the potential benefits of infrastructure improvements like a forgiving shoulder on which a bicycle can be ridden or increasing bicycle path width [64].

Existing bicycle dynamics and control models can predict the MAHD for such interventions. For instance, the Carvallo-Whipple bicycle model, combined with the cyclist control model of Schwab et al. (2013) [51], can simulate the cyclist's response to an impulse-like handlebar disturbance, allowing for the calculation of the MAHD for prescribed input values. However, this model still needs to be validated for conditions near falling, and no bicycle tyre model currently exists to simulate the exact lean and steering angle at which tyres start to slip. Future research should focus on validating these models under near-fall conditions and developing a comprehensive bicycle tyre model.

2.4. CONCLUSIONS

In conclusion, this study introduces a novel indicator that can be combined with bicycle dynamics and cyclist control models to safely and proactively evaluate cyclist fall prevention interventions. This novel indicator is the Maximum Allowable Handlebar Disturbance (MAHD), which serves as a quantitative indicator to evaluate the boundary between balance recovery and falling in response to a handlebar disturbance. The MAHD enables systematic evaluation and comparison of the effectiveness of interventions related to bicycle design, cyclist control, and environmental factors. It applies to all crash types where the cyclist encounters an impulse-like disturbance (lasting for a short period).

Despite its strengths, the study also highlights areas for future research. These include validating the MAHD's generalizability to various disturbance types, validating bicycle dynamics and cyclist control models for large disturbances, measuring real-world disturbances' force and torque profiles, and developing a bicycle tyre model.

This study contributes significantly to cycling safety research by filling a critical gap in the proactive evaluation of cyclist fall prevention interventions. It provides a practical indicator for systematically evaluating a range of interventions which could previously not be evaluated. The research supports evidence-based decision-making, aiding professionals in designing safe bicycles, safe infrastructure and training programs and aiding policy advisors in allocating resources to the most effective interventions.

REFERENCES

[1] United Nations (2020), *Resolution 74/299: Improving global road safety*, https://documents-dds-ny.un.org/doc/UNDOC/GEN/N20/226/30/PDF/

N2022630.pdf?OpenElement, accessed 11 January 2025.

[2] World Health Organization (2020), *Cyclist safety: An information resource for decision-makers and practitioners,* https://iris.who.int/bitstream/handle/10665/336393/9789240013698-eng.pdf, accessed 11 January 2025.

[3] R. Utriainen, S. O'Hern, and M. Pöllänen, *Review on single-bicycle crashes in the recent scientific literature,* Transport Reviews **43**, 159 (2023), https://doi.org/10.1080/01441647.2022.2055674.

[4] R. Elvik, *Area-wide urban traffic calming schemes: A meta-analysis of safety effects,* Accident Analysis & Prevention **33**, 327 (2001), https://doi.org/10.1016/S0001-4575(00)00046-4.

[5] A. Hoye, *Recommend or mandate? A systematic review and meta-analysis of the effects of mandatory bicycle helmet legislation,* Accident Analysis & Prevention **120**, 239 (2018), https://doi.org/10.1016/j.aap.2018.08.001.

[6] I. I. Hellman and M. Lindman, *Estimating the crash reducing effect of advanced driver assistance systems (ADAS) for vulnerable road users,* Traffic Safety Research **4**, 000036 (2023), https://doi.org/10.55329/blzz2682.

[7] N. Lubbe, Y. Wu, and H. Jeppsson, *Safe speeds: Fatality and injury risks of pedestrians, cyclists, motorcyclists, and car drivers impacting the front of another passenger car as a function of closing speed and age,* Traffic Safety Research **2**, 000006 (2022), https://doi.org/10.55329/vfma7555.

[8] T. Sayed, M. H. Zaki, and J. Autey, *Automated safety diagnosis of vehicle-bicycle interactions using computer vision analysis,* Safety Science **59**, 163 (2013), https://doi.org/10.1016/j.ssci.2013.05.009.

[9] A. R. A. van der Horst, M. de Goede, S. de Hair-Buijssen, and R. Methorst, *Traffic conflicts on bicycle paths: A systematic observation of behaviour from video,* Accident Analysis & Prevention **62**, 358 (2014), https://doi.org/10.1016/j.aap.2013.04.005.

[10] N. McNeil, C. M. Monsere, and J. Dill, *Influence of bike lane buffer types on perceived comfort and safety of bicyclists and potential bicyclists,* Transportation Research Record **2520**, 132 (2015), https://doi.org/10.3141/2520-15.

[11] J. Kovaceva, P. Wallgren, and M. Dozza, *On the evaluation of visual nudges to promote safe cycling: Can we encourage lower speeds at intersections?* Traffic Injury Prevention **23**, 428 (2022), https://doi.org/10.1080/15389588.2022.2103120.

[12] D. de Waard, P. Schepers, W. Ormel, and K. Brookhuis, *Mobile phone use while cycling: Incidence and effects on behaviour and safety,* Ergonomics **53**, 30 (2010), https://doi.org/10.1080/00140130903381180.

[13] W. P. Vlakveld, D. Twisk, M. Christoph, M. Boele, R. Sikkema, R. Remy, and A. L. Schwab, *Speed choice and mental workload of elderly cyclists on e-bikes in simple and complex traffic situations: A field experiment,* Accident Analysis & Prevention **74**, 97 (2015), https://doi.org/10.1016/j.aap.2014.10.018.

[14] R. Dubbeldam, C. T. M. Baten, P. T. C. Straathof, J. H. Buurke, and J. S. Rietman, *The different ways to get on and off a bicycle for young and old,* Safety Science **92**, 318 (2017), https://doi.org/10.1016/j.ssci.2016.01.010.

[15] J. Andersson, C. Patten, H. Wallén Warner, C. Andersérs, C. Ahlström, R. Ceci, and L. Jakobsson, *Bicycling during alcohol intoxication,* Traffic Safety Research **4** (2023), https://doi.org/10.55329/prpa1909.

[16] K. Kircher and A. Niska, *Interventions to reduce the speed of cyclists in work zones – cyclists' evaluation in a controlled environment,* Traffic Safety Research **6**, e000047 (2024), https://doi.org/10.55329/ohhx5659.

[17] C. Andersérs, J. Andersson, and H. W. Warner, *The importance of individual characteristics on bicycle performance during alcohol intoxication,* Traffic Safety Research **6**, e000042 (2024), https://doi.org/10.55329/vmgb9648.

[18] A. K. Huemer, L. M. Rosenboom, M. Naujoks, and E. Banach, *Testing cycling infrastructure layout in virtual environments: An examination from a bicycle rider's perspective in simulation and online,* Transportation Research Interdisciplinary Perspectives **14**, 100586 (2022), https://doi.org/10.1016/j.trip.2022.100586.

[19] F. L. Berghoefer and M. Vollrath, *Prefer what you like? Evaluation and preference of cycling infrastructures in a bicycle simulator,* Journal of Safety Research **87**, 157 (2023), https://doi.org/10.1016/j.jsr.2023.09.013.

[20] A. Niska and J. Wenäll, *Simulated single-bicycle crashes in the VTI crash safety laboratory,* Traffic Injury Prevention **20**, 68 (2019), https://doi.org/10.1080/15389588.2019.1685090.

[21] A. Niska, J. Wenäll, and J. Karlström, *Crash tests to evaluate the design of temporary traffic control devices for increased safety of cyclists at road works,* Accident Analysis & Prevention **166**, 106529 (2022), https://doi.org/10.1016/j.aap.2021.106529.

[22] Y. Peng, Y. Chen, J. Yang, D. Otte, and R. Willinger, *A study of pedestrian and bicyclist exposure to head injury in passenger car collisions based on accident data and simulations,* Safety Science **50**, 1749 (2012), https://doi.org/10.1016/j.ssci.2012.03.005.

[23] M. Fahlstedt, P. Halldin, and S. Kleiven, *The protective effect of a helmet in three bicycle accidents — a finite element study,* Accident Analysis & Prevention **91**, 135 (2016), https://doi.org/10.1016/j.aap.2016.02.025.

[24] C. Baker, X. Yu, B. Lovell, R. Tan, S. Patel, and M. Ghajari, *How well do popular bicycle helmets protect from different types of head injury?* Annals of Biomedical Engineering **52**, 3326 (2024), https://doi.org/10.1007/s10439-024-03589-8.

[25] V. Astarita, V. Giofré, G. Guido, and A. Vitale, *Investigating road safety issues through a microsimulation model,* Procedia-social and Behavioral Sciences **20**, 226 (2011), https://doi.org/10.1016/j.sbspro.2011.08.028.

[26] U. Shahdah, F. Saccomanno, and B. Persaud, *Application of traffic microsimulation for evaluating safety performance of urban signalized intersections,* Transportation Research Part C: Emerging Technologies **60**, 96 (2015), https://doi.org/10.1016/j.trc.2015.06.010.

[27] H. Twaddle, T. Schendzielorz, and O. Fakler, *Bicycles in urban areas: Review of existing methods for modeling behavior,* Transportation Research Record **2434**, 140 (2014), https://doi.org/10.3141/2434-17.

[28] C. M. Schmidt, A. Dabiri, F. Schulte, R. Happee, and J. K. Moore, *Essential bicycle dynamics for microscopic traffic simulation: An example using the social force model,* in *The Evolving Scholar-BMD 2023, 5th Edition* (2023) http://dx.doi.org/10.59490/649d4037c2c818c6824899bd.

[29] N. Rinke, C. Schiermeyer, F. Pascucci, V. Berkhahn, and B. Friedrich, *A multi-layer social force approach to model interactions in shared spaces using collision prediction,* Transportation Research Procedia **25**, 1249 (2017), https://doi.org/10.1016/j.trpro.2017.05.144.

[30] P. Schepers, N. Agerholm, E. Amoros, R. Benington, T. Bjørnskau, S. Dhondt, B. de Geus, C. Hagemeister, B. P. Y. Loo, and A. Niska, *An international review of the frequency of single-bicycle crashes (SBCs) and their relation to bicycle modal share,* Injury Prevention **21**, e138 (2015), https://doi.org/10.1136/injuryprev-2013-040964.

[31] V. Keppner, S. Krumpoch, R. Kob, A. Rappl, C. C. Sieber, E. Freiberger, and H. M. Siebentritt, *Safer cycling in older age (SiFAr): Effects of a multi-component cycle training. a randomized controlled trial,* BMC Geriatrics **23**, 131 (2023), https://doi.org/10.1186/s12877-021-02502-5.

[32] L. Alizadehsaravi and J. K. Moore, *Bicycle balance assist system reduces roll and steering motion for young and older bicyclists during real-life safety challenges,* PeerJ **11**, e16206 (2023), https://doi.org/10.7717/peerj.16206.

[33] B. Janssen, P. Schepers, H. Farah, and M. Hagenzieker, *Behaviour of cyclists and pedestrians near right angled, sloped and levelled kerb types: Do risks associated to height differences of kerbs weigh up against other factors?* European Journal of Transport and Infrastructure Research **18**, 360 (2018), https://doi.org/10.18757/ejtir.2018.18.4.3254.

[34] F. Westerhuis, A. B. M. Fuermaier, K. A. Brookhuis, and D. de Waard, *Cycling on the edge: The effects of edge lines, slanted kerbstones, shoulder, and edge strips on cycling behaviour of cyclists older than 50 years,* Ergonomics **63**, 769 (2020), https://doi.org/10.1080/00140139.2020.1755058.

[35] A. L. Schwab and J. P. Meijaard, *A review on bicycle dynamics and rider control,* Vehicle Systems Dynamics **51**, 1059 (2013), https://doi.org/10.1080/00423114.2013.793365.

[36] A. L. Schwab and M. Wisse, *Basin of attraction of the simplest walking model,* in *International Design Engineering Technical Conferences and Computers and Information in Engineering Conference* (Pittsburgh, USA, 9-12 September 2001, 2001) https://doi.org/10.1115/DETC2001/VIB-21363.

[37] P. Schepers, M. Hagenzieker, R. Methorst, B. van Wee, and F. Wegman, *A conceptual framework for road safety and mobility applied to cycling safety,* Accident Analysis & Prevention **62**, 331 (2014), https://doi.org/10.1016/j.aap.2013.03.032.

[38] P. Schepers and B. den Brinker, *What do cyclists need to see to avoid single-bicycle crashes?* Ergonomics **54**, 315 (2011), https://doi.org/10.1080/00140139.2011.558633.

[39] J. Theeuwes and H. Godthelp, *Self-explaining roads,* Safety Science **19**, 217 (1995), https://doi.org/10.1016/0925-7535(94)00022-U.

[40] D. de Waard, *The measurement of drivers' mental workload*, Ph.D. thesis, University of Groningen, Groningen, The Netherlands (1996), https://pure.rug.nl/ws/portalfiles/portal/13410300/09_thesis.pdf.

[41] T. E. Lockhart and J. Liu, *Differentiating fall-prone and healthy adults using local dynamic stability,* Ergonomics **51**, 1860 (2008), https://doi.org/10.1080/00140130802567079.

[42] M. J. P. Toebes, M. J. M. Hoozemans, R. Furrer, J. Dekker, and J. H. van Dieën, *Local dynamic stability and variability of gait are associated with fall history in elderly subjects,* Gait & Posture **36**, 527 (2012), https://doi.org/10.1016/j.gaitpost.2012.05.016.

[43] D. Hamacher, N. B. Singh, J. H. van Dieën, M. O. Heller, and W. R. Taylor, *Kinematic measures for assessing gait stability in elderly individuals: A systematic review,* Journal of The Royal Society Interface **8**, 1682 (2011), https://doi.org/10.1098/rsif.2011.0416.

[44] A. Hamed, S. Bohm, F. Mersmann, and A. Arampatzis, *Follow-up efficacy of physical exercise interventions on fall incidence and fall risk in healthy older adults: A systematic review and meta-analysis,* Sports Medicine — Open **4**, 1 (2018), https://doi.org/10.1186/s40798-018-0170-z.

[45] K. M. Sibley, S. M. Thomas, A. A. Veroniki, M. Rodrigues, J. S. Hamid, C. C. Lachance, E. Cogo, P. A. Khan, J. J. Riva, K. Thavorn, *et al., Comparative effectiveness of exercise interventions for preventing falls in older adults: A secondary analysis of a systematic review with network meta-analysis,* Experimental Gerontology **143**, 111151 (2021), https://doi.org/10.1016/j.exger.2020.111151.

[46] A. Mansfield, J. S. Wong, J. Bryce, S. Knorr, and K. K. Patterson, *Does perturbation-based balance training prevent falls? Systematic review and meta-analysis of preliminary randomized controlled trials,* Physical therapy **95**, 700 (2015), https://doi.org/10.2522/ptj.20140090.

[47] M. H. G. Gerards, C. McCrum, A. Mansfield, and K. Meijer, *Perturbation-based balance training for falls reduction among older adults: Current evidence and implications for clinical practice,* Geriatrics & Gerontology International **17**, 2294 (2017), https://doi.org/10.1111/ggi.13082.

[48] J. P. Meijaard, J. M. Papadopoulos, A. Ruina, and A. L. Schwab, *Linearized dynamics equations for the balance and steer of a bicycle: A benchmark and review,* Proceedings of the Royal Society A: Mathematical, Physical and Engineering Sciences **463**, 1955 (2007), https://doi.org/10.1098/rspa.2007.1857.

[49] J. Kooijman, J. P. Meijaard, J. M. Papadopoulos, A. Ruina, and A. L. Schwab, *A bicycle can be self-stable without gyroscopic or caster effects,* Science **332**, 339 (2011), https://doi.org/10.1126/science.1201959.

[50] A. L. Schwab, J. P. Meijaard, and J. D. G. Kooijman, *Lateral dynamics of a bicycle with a passive rider model: Stability and controllability,* Vehicle Systems Dynamics **50**, 1209 (2012), https://doi.org/10.1080/00423114.2011.610898.

[51] A. L. Schwab, P. D. L. de Lange, R. Happee, and J. K. Moore, *Rider control identification in bicycling using lateral force perturbation tests,* Proceedings of the Institution of Mechanical Engineers, Part K: Journal of multi-body dynamics **227**, 390 (2013), https://doi.org/10.1177/1464419313492317.

[52] J. D. G. Kooijman, A. L. Schwab, and J. P. Meijaard, *Experimental validation of a model of an uncontrolled bicycle,* Multibody System Dynamics **19**, 115 (2008), https://doi.org/10.1007/s11044-007-9050-x.

[53] D. Stevens, *The stability and handling characteristics of bicycles*, Bachelor's thesis, The University of New South Wales, School of Mechanical and Manufacturing Engineering, Sydney, Australia (2009), http://www.varg.unsw.edu.au/Assets/link%20pdfs/thesis_stevens.pdf.

[54] T.-O. Tak, J.-S. Won, and G.-Y. Baek, *Design sensitivity analysis of bicycle stability and experimental validation,* in *Bicycle and Motorcycle Dynamics Conference* (Delft, The Netherlands, 20-22 October 2010) http://www.bicycle.tudelft.nl/ProceedingsBMD2010/papers/tak2010design.pdf.

[55] J. K. Moore, *Human control of a bicycle*, Ph.D. thesis, University of California, Davis, USA (2012), https://www.researchgate.net/profile/Jason-Moore-23/publication/232200635_Human_Control_of_a_Bicycle/links/0fcfd5078c76753288000000/Human-Control-of-a-Bicycle.pdf.

[56] P. Basu-Mandal, A. Chatterjee, and J. M. Papadopoulos, *Hands-free circular motions of a benchmark bicycle,* Proceedings of the Royal Society A: Mathematical, Physical and Engineering Sciences **463**, 1983 (2007), https://doi.org/10.1098/rspa.2007.1849.

[57] C. McCrum, T. S. Bhatt, M. H. G. Gerards, K. Karamanidis, M. W. Rogers, S. R. Lord, and Y. Okubo, *Perturbation-based balance training: Principles, mechanisms and implementation in clinical practice,* Frontiers in Sports and Active Living **4**, 1015394 (2022), https://doi.org/10.3389/fspor.2022.1015394.

[58] S. M. Bruijn, O. G. Meijer, P. J. Beek, and J. H. van Dieen, *Assessing the stability of human locomotion: A review of current measures,* Journal of the Royal Society Interface **10**, 20120999 (2013), https://doi.org/10.1098/rsif.2012.0999.

[59] D. G. E. Hobbelen and M. Wisse, *A disturbance rejection measure for limit cycle walkers: The Gait Sensitivity Norm,* IEEE Transactions on Robotics **23**, 1213 (2007), https://doi.org/10.1109/TRO.2007.904908.

[60] V. E. Bulsink, H. Kiewiet, D. van de Belt, G. M. Bonnema, and B. Koopman, *Cycling strategies of young and older cyclists,* Human movement science **46**, 184 (2016), https://doi.org/10.1016/j.humov.2016.01.005.

[61] G. Dialynas, C. Christoforidis, R. Happee, and A. L. Schwab, *Rider control identification in cycling taking into account steering torque feedback and sensory delays,* Vehicle Systems Dynamics **61**, 200 (2023), https://doi.org/10.1080/00423114.2022.2048865.

[62] G. R. Tan, M. Raitor, and S. H. Collins, *Bump'em: An open-source, bump-emulation system for studying human balance and gait,* in *2020 IEEE International Conference on Robotics and Automation (ICRA)* (2020) 1 June - 31 August 2020.

[63] R. J. Doll, J. R. Buitenweg, H. G. E. Meijer, and P. H. Veltink, *Tracking of nociceptive thresholds using adaptive psychophysical methods,* Behavior Research Methods **46**, 55 (2014), https://doi.org/10.3758/s13428-013-0368-4.

[64] P. Schepers, E. Theuwissen, P. N. Velasco, M. N. Niaki, O. van Boggelen, W. Daamen, and M. Hagenzieker, *The relationship between cycle track width and the lateral position of cyclists, and implications for the required cycle track width,* Journal of Safety Research **87**, 38 (2023), https://doi.org/10.1016/j.jsr.2023.07.011.

3

A Model Based on Cyclist Fall Experiments Which Predicts The Maximum Allowable Handlebar Disturbance From Which A Cyclist Can Recover Balance

M.M. Reijne, F.H. van der Meulen, F.C.T. van der Helm and A.L. Schwab

Abstract

Falls are a significant cause of serious injury among cyclists, emphasising the urgency of implementing effective fall prevention interventions. However, evaluating these interventions, especially those aiming to reduce fall risk in critical situations, is challenging. This limits engineers in designing safe infrastructure, bicycles, and road safety professionals to design effective training programs. This study explores the use of bicycle dynamics and cyclist control models to evaluate fall prevention interventions by simulating common fall scenarios and quantifying intervention effectiveness with the Maximum Allowable Handlebar Disturbance (MAHD) as a performance indicator.

This Chapter is under review at Accident Analysis & Prevention.

This indicator quantifies the maximum impulse-like handlebar disturbance from which a cyclist can recover balance, where a higher value indicates a lower risk of falling.

Despite the promise of this approach, it still faces significant hurdles before it can be applied reliably and practically to ex-ante evaluate interventions. Two such hurdles are the need for more validation of these models in critical situations and the abstract nature of existing cyclist control models, which complicates the practical application to evaluate cyclist-control focused interventions.

The goal of this study is to improve the practical application of the bicycle dynamics and cyclist control models. In this study, we conducted experiments involving 24 participants with diverse characteristics for variables such as skill and age. The participants were exposed to controlled impulse-like handlebar disturbances while cycling on a treadmill. The magnitude of the disturbance was varied to cause falls and balance recoveries.

The dataset we obtained, comprising actual cyclist falls, can be used in future research to validate the reliability of bicycle dynamics and cyclist control models in simulating fall scenarios and predicting the MAHD.

In addition, we identified key cyclist control characteristics influencing fall outcomes and the MAHD through Bayesian Model Averaging. Our results highlight the importance of forward speed and the cyclist balancing skill performance, defined as the ability to maintain balance and follow a centreline while cycling undisturbed, as critical characteristics to predict the outcome after a large disturbance. Incorporating these parameters into cyclist control models can substantially improve their practical application, particularly in evaluating interventions targeting cyclist control. We also developed a Bayesian multilevel logistic regression model using the identified key characteristics to predict the MAHD for various cyclist types.

Combined, these results significantly advance the application of bicycle dynamics and cyclist control models for safely and proactively evaluating cyclist fall prevention interventions.

3.1. INTRODUCTION

Falls during cycling are a leading cause of serious injuries among cyclists, accounting for approximately two-thirds of such incidents [1]. This underscores the need for cycling fall prevention interventions [2–12].

The risk of falling during cycling is significant due to the inherent instability of the bicycle-cyclist system, especially in emergency situations where non-linear dynamics are involved. Balance recovery in such situations is complex, requiring considerable skill and effort. Beyond a certain threshold, balance recovery becomes impossible.

Although the stability and mechanisms for maintaining and recovering balance during cycling have been extensively studied [13–16], the evaluation of potential cyclist fall prevention interventions has been limited by methodological limitations.

The evaluation of cycling safety interventions relies on a range of approaches, including the statisticial analysis of crash records [17–20], surrogate safety indicators extracted from video recordings [21, 22], field-based and experimental studies involving cyclists [23–30], crash-testing experiments [31–35], and models that simulate traffic scenarios [36–40].

While these techniques provide important insights, they exhibit substantial limitations when applied to interventions focused on preventing cyclist falls, particularly those aiming to reduce fall risk in critical situations. Notable interventions of this type include balance training programs [41], steer-assist technologies [42], sloped kerbs [43], and ridable road shoulders [44].

Statistical analysis of historic bicycle crash data, the primary evaluation approach for cycling safety interventions [17, 18], falls short in evaluating cyclist fall prevention interventions due to the underreporting of single bicycle crashes [1] — which are primarily falls. Surrogate safety indicators focus on interactions with other road users, overlooking falls in which no other road users were involved — which account for the majority of severe cycling injuries [45]. Studies involving cyclists in controlled or field settings typically evaluate indirect indicators, such as perceived safety, workload or lean or steering angles. However, these indirect indicators lack validation for fall risk. Similarly, crash tests and simulation models aim to mitigate injuries rather than address the prevention of falls. Moreover, existing models that simulate traffic scenarios — including traffic microsimulation, behavioural, and crash avoidance models — do not account for the balance task and lateral dynamics of the bicycle, both of which are essential to accurately simulate falls. While falls constitute the majority of serious cycling injuries, evaluating potential interventions that aim to reduce fall risk in critical situations remains challenging with existing approaches.

Bicycle dynamics and cyclist control models offer a promising novel approach for safely and proactively evaluating cyclist fall prevention interventions, complementing existing approaches. As established in Chapter 1, these models can simulate a wide range of commonly reported crash types and incorporate a variety of interventions related to the bicycle, cyclist, and environment.

In Chapter 2, we proposed a novel performance indicator called the Maximum Allowable Handlebar Disturbance (MAHD) to be used by bicycle dynamics and cyclist control models to ex-ante evaluate fall prevention interventions. The MAHD quantifies the critical boundary between falling and recovering balance, reflecting the cyclist's ability to recover balance from a large disturbance. An effective intervention increases the MAHD. Unlike the binary outcome of a fall or recovery, the MAHD provides a detailed measure of an intervention's effectiveness. It applies to crash types where cyclists encounter impulse-like disturbances, such as falls following a collision or an obstacle or falls due to a loss of balance. It can evaluate interventions targeting the phase between post-collision or post-disturbance and pre-fall — for instance, balance training programs, steer-assist technologies, sloped kerbs, or ridable road shoulders.

While this approach allows for safe and proactive evaluation of cyclist fall prevention interventions, practical application challenges remain. This study addresses two limitations: 1) validating bicycle dynamics and cyclist control models to simulate actual falls and predict the MAHD, and 2) addressing the abstract nature of existing cyclist control models, which have only been calibrated for a single individual cyclist (details in Chapter 1). The first limitation affects the reliability of model predictions, while the second limits the incorporation of interventions targeting cyclist control.

The goal of this study is to improve the practical application of bicycle dynamics and cyclist control models to safely and proactively evaluate cyclist fall prevention

interventions. To accomplish this, we conducted experiments with 24 participants of varying characteristics, exposing them to controlled impulse-like handlebar disturbances resulting in balance recoveries and falls. This is the first experiment to simulate actual cyclist falls in a controlled and safe manner. Using Bayesian Model Averaging and a Bayesian multilevel logistic regression model, we identify key cyclist characteristics predictive of fall outcomes, determine the MAHD for experimental participants, and predict the MAHD for different types of cyclists on one specific bicycle.

The experimental data will be used in Chapter 5 to validate bicycle dynamics and cyclist control models. The identified key cyclist characteristics will be used in Chapter 4 to improve cyclist control models, allowing more cyclist control interventions to be incorporated and evaluated.

This study contributes to widening the scope of potential interventions that can be evaluated safely and proactively, supporting engineers in designing safe infrastructure and bicycles and aiding road safety professionals in developing effective training programs.

3.2. EXPERIMENTAL DATA

In this section, we describe the cyclist experiments. In the experiments, we repeatedly disturbed the handlebars of the bicycle while the participant was cycling on a treadmill. The disturbances resulted in falls and balance recoveries. We varied the magnitude of the disturbance to determine the threshold at which the participant could no longer recover balance. We call this threshold the MAHD.

To identify key cyclist characteristics that influence the probability of falling and the MAHD, we conducted experiments with 24 participants with varying characteristics. We also varied the forward speed to investigate the influence of speed choice on the risk of falling. In addition, we randomly varied the direction of the handlebar disturbance, clockwise or counterclockwise, to leave an element of surprise for the participant. We kept the other parameters as constant as possible to limit a further increase in the number of varying parameters.

Below, we describe the participant characteristics and the experimental setup, including safety precautions, the protocol and the data collection. The experimental data will be used in Section 3.3 to identify key cyclist characteristics that predict the probability of falling and estimate the MAHD for both experimental participants and different types of cyclists.

3.2.1. PARTICIPANTS

The experiments were performed with 24 participants equally divided into two age groups. Twelve participants were between 20 and 35 years of age, and twelve participants were aged 60 years or older. Both the younger and older age group contained seven men and five women. The distribution of heights and weights between the two age groups was approximately similar and can be considered representative of the average Dutch population. A summary of the participant's characteristics is given in Table 3.1. All participants were in good health, had years of cycling experience, and cycled almost weekly.

Table 3.1: Summary of participant characteristics by age group, including number of participants, gender distribution, mean age, height, and weight with standard deviations (S.D.)

group	*#*	*gender*	*age* (y)	*height* (m)	*weight* (kg)
young	12	7 ♂, 5 ♀	28.8 (4.1)	1.82 (0.10)	75.2 (13.4)
old	12	7 ♂, 5 ♀	65.2 (4.9)	1.78 (0.09)	78.0 (11.6)

3.2.2. EXPERIMENTAL SETUP

The experimental setup is shown in Figure 3.1 and consisted of a treadmill, a standard Dutch city bicycle equipped with sensors to measure its forward speed, steer rate and lean rate, a set of four force perturbators connected to the handlebars and controlled in real-time, twelve optoelectronic cameras to capture images and motion, four EMG sensors attached to the upper arms of the cyclist, an intelligent safety harness to catch the cyclist in case of fall, an aluminium frame around the treadmill covered with gymnastic mats and additional safety features.

Treadmill

The treadmill was 2.62 m long and 1.2 m wide, had a maximum speed of 18 km/h, and had an emergency stop button.

Figure 3.1: Overview of the experimental setup, with: 1-treadmill, 2-bicycle, 3-pull force motor (4), 4-pull rope (4), 5-force sensor (4), 6-Speedgoat real-time controller, 7-intelligent harness, 8-soft padding (8), 9-disc wheel cover (2), 10-foot strap (2), 11-mechanical rotation limiter, 12-rear-brake handle, 13-helmet, 14-protective gloves (2), 15-motion capture camera (12), 16-IMU (4), 17-EMG measurement unit (4), 18-folding fence.

Bicycle
All participants rode the same bicycle, a small frame size of the Gazelle Grenoble/Arroyo Elite HMB. They were free to adjust the saddle height and handlebar position to their preference. During the experiment, they were also free to select any of the seven gears. The Gazelle Grenoble/Arroyo Elite HMB is an e-bike. The battery and head unit were removed for the experiment. The participants thus cycled without the assistance of the electric motor.

Disturbances
We aimed to apply a disturbance to the handlebars, which follows the convention of the MAHD, which is described in Chapter 2. To achieve this, we chose to apply disturbances via four motor-controlled ropes. A rope was knotted to each side of the elongated handlebar in the forward and aft direction, as shown in Figure 3.1. With this configuration, a clockwise steer torque could be generated by simultaneously pulling on the rope in the forward direction on the left side of the handlebar and the rope in the aft direction on the right side and vice versa for a counterclockwise disturbance.

The perturbator mechanism was a closed-loop force control rope-driven system that could exert impulsive type of torque profiles on the handlebars in clockwise and counterclockwise directions. Since the controller was based on force inputs rather than torque or angular impulse, we refer to forces throughout the text when discussing the disturbance selection algorithm. However, it is important to note that these forces can be easily translated into an angular impulse, as will be described in Section 3.2.4.

Each motor in the system can generate forces up to 200 N with a 90% rise time of as little as 44 ms, outpacing the human capacity to perceive and react to such forces [46]. For details and build instructions for the perturbator mechanism, the reader is referred to Tan et al. (2020) [46]. The forces were measured by a force sensor (Sciame) placed in series with the rope. The motors were a 260 W Maxon brushless motor (EC-90 Flat, Maxon Group, Switzerland) driven by a motor driver (ECSON 70/10, Maxon Group, Switzerland).

We used a Speedgoat real-time controller running at 1000 Hz to control the tension in the ropes. The ropes were kept at a 5 N pre-tension between disturbances to minimise slack in the ropes. The closed-loop force controller applied corrections based on a proportional term K_p and an integral term K_i. Tuning the feedback gains for each motor resulted in K_p values of 1.5 (-) for motors 1 and 3, 2.00 (-) for motor 2, and 1.75 (-) for motor 4, with a uniform K_i value of 2 (1/s) for all motors. The motors were positioned relative to the cyclist on the treadmill as follows: motor 1, front right; motor 2, front left; motor 3, rear left; and motor 4, rear right.

We have chosen a step-input handlebar torque disturbance with a duration of 0.3 seconds, following the definition of the MAHD introduced in Chapter 2. This torque profile was sufficient to cause an experienced cyclist to fall at motor force levels of 100 N, well below its maximum value. An example of a force profile is shown in Figure 3.2. The disturbance was applied after the operator pushed a button to ensure the disturbance was only applied if the participant was cycling steadily, upright, straight-ahead and in the middle of the treadmill. We measured the states of the bicycle when the disturbance was applied to evaluate whether the cyclist was cycling upright, straight-ahead and in

the middle of the treadmill. An algorithm chose the magnitude and direction of the handlebar disturbance. Details of the algorithm are explained in Section 3.2.3 where the protocol to determine the MAHD is described.

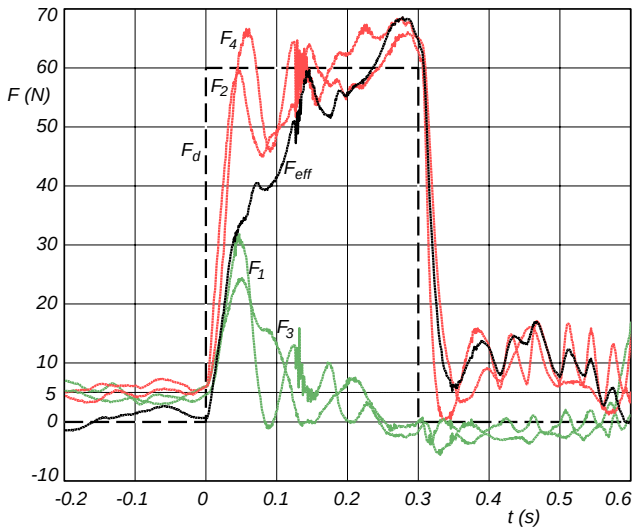

Figure 3.2: Disturbance force profile for a clockwise handlebar disturbance of 60 N for 0.3 seconds, with the desired step-like force profile F_d, denoted by the dashed line. This corresponds to an angular impulse ΔL of 18 Nms. The red lines are the measured clockwise forces on the left and right handlebars F_2 and F_4, whereas the green lines are the counterclockwise forces F_1 and F_3. The ropes generating the disturbance forces were positioned relative to the cyclist on the treadmill as follows: rope 1, front right; rope 2, front left; rope 3, rear left; and rope 4, rear right. The black line is the effective force profile $F_{\text{eff}} = (F_2 + F_4 - F_1 - F_3)/2$. All ropes have a controlled pre-tension of 5 N.

Safety precautions

Because we need to capture actual falls to determine the MAHD, the experimental setup should allow the participants to fall safely without injury. Therefore, we chose the setup where participants were secured by an intelligent harness [47]. This harness is considered intelligent because it uses an innovative mechanical design to decouple vertical and horizontal movements, allowing the cyclist freedom to cycle naturally while providing immediate safety during falls. The system consists of an overhead structure with rails, pulleys, motors and cables, which were attached to the ceiling. This system minimises forces exerted on the user during normal cycling but engages when a fall is detected, ensuring safety and efficiency.

The harness had a finite operating volume that was too small for free cycling. We have, therefore, chosen to cycle on a treadmill. The operating volume of the harness was slightly larger than the area of the treadmill. The dynamics of cycling straight ahead with constant speed is similar for a treadmill compared to cycling outside at constant speed. As a backup, in case the harness would fail, the treadmill was surrounded by soft padding under an angle of 45 degrees. During the experiment, the intelligent harness

caught the participant every time. Each time the intelligent harness came into action, it was classified as a fall. A snapshot of a situation where the harness caught the cyclist is shown in Figure 3.3.

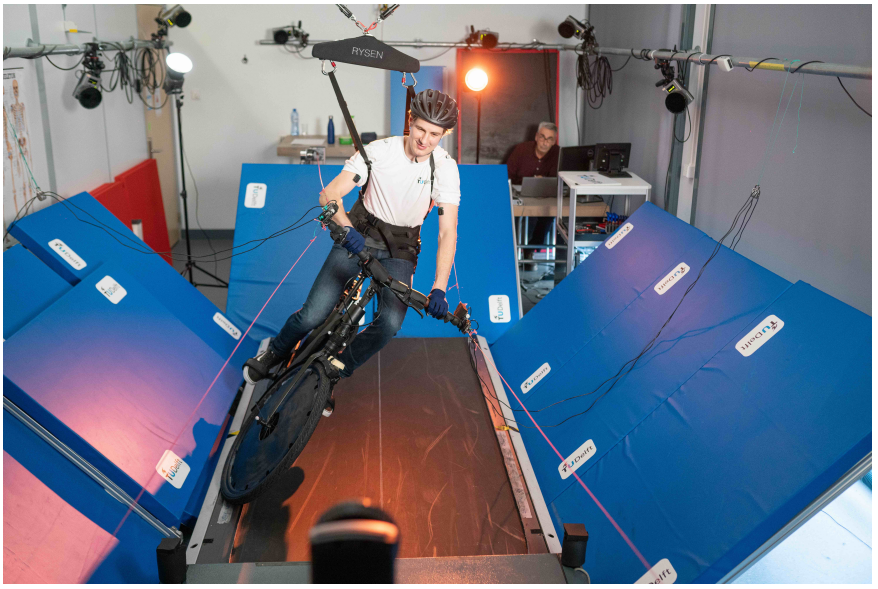

Figure 3.3: A snapshot of a situation where the harness caught the participant.

Modifications were made to the bicycle to ensure the participants' safety further. To prevent the participants' feet from being caught between the spokes, we covered the spokes with a plastic disc and attached the feet of the participant to the pedals with hook-and-loop fasteners. The handlebar and frame were covered with foam where possible to prevent a hard impact in case of a fall. The handlebars were also elongated so that the ropes of the perturbator mechanism were not too close to the participant's body. A mechanical stop prevented the handlebars from turning more than 45 degrees either way. None of the participants ever reached this limit during the experiment. The front brake was removed, and the rear brake lever was placed in the middle of the handlebar to ensure the participants could not brake suddenly, which is dangerous on a treadmill. Additionally, participants had to wear a helmet and gloves.

To prevent high uncontrolled pull forces a fishing line was tied in series with the ropes of the perturbator mechanism. The fishing line broke for loads higher than 129 N. Additional safety precautions were also taken in the software of the controller, such as limiting the maximum current to the motors, to prevent uncontrolled forces.

3.2.3. EXPERIMENTAL PROTOCOL

Participants were informed of the research procedures before they gave informed consent according to the guidelines of the Delft University of Technology human research ethics committee (ethics approval number 1870). All participants participated voluntarily.

Below, we describe the protocols to let the participant gain trust that the harness would catch him or her when falling and learn how to cycle on the treadmill — followed by a description of the protocol used to determine the MAHD per participant.

Protocols to gain trust in the harness and learn how to cycle on the treadmill
The protocol to gain trust in the harness started without the bicycle. The participants were instructed to stand on the treadmill away from the bicycle while wearing the harness, with a spotter beside them. They could first let themselves fall sideways and make a sidestep if they felt the harness would not catch them on time. The spotter would also intervene to catch the participant if he or she thought the participant would fall. This procedure was repeated until the participants indicated they felt safe, usually two to three times. The spotter did not have to intervene a single time. Next, the participants were instructed to sit on a standing-still bicycle, still wearing the harness, and hold on to a fence on the right-hand side, which was also covered in padding and could fold away during the experiments. The participants were then instructed to let go of the fence and let themselves fall to the left. Participants could use their left feet to catch them if they thought they would fall and the harness would not catch them. This was repeated until the participants indicated that they felt safe. Usually, this was three to four times. Finally, the participants were allowed to perform a self-intended fall while cycling without a disturbance. Approximately a third of the participants chose this option. Before a participant could do this, he or she needed to learn to cycle on the treadmill. Often, the participant fell a couple of times while learning to cycle on the treadmill. These falls also gave them experience and trust that the harness would catch them in case of a fall.

Participants needed to learn to cycle on the treadmill because although the dynamics of cycling straight ahead with constant forward speed is the same for cycling on a treadmill compared to cycling outside, the sensorial input, such as optical flow, is different for the cyclist. The participants learned to cycle on the treadmill at moderate speed. Participants could hold on to a fence, covered in padding, on the right-hand side for balance while the treadmill got up to the prescribed speed. Once the participants felt the treadmill had sufficient speed (an operator also communicated the current speed of the treadmill), they could let go of the fence. Another operator would then remotely fold the fence by pulling a rope that would unlock the support of the fence. The foldable fence was also used during the experiments. Participants could hold on to it every time the treadmill was started. The fence was always folded when the steer torque disturbances were applied.

Most participants needed between one to five attempts to adjust to this sensorial difference before they could cycle steadily and straight ahead at the constant prescribed speed of the treadmill. The learning phase was finished if the participant could cycle in a controlled way for several seconds 10 cm from the left and right border of the treadmill and one minute on the centerline of the treadmill. For most participants, this took approximately ten minutes. One participant took almost an hour to complete the learning phase.

Once the participants had learned to cycle on the treadmill, they were given a feel for the handlebar torque disturbances while standing still, holding the handlebars, wearing

the harness, and standing with two feet on the ground. The participant was then given two or three low steer torque disturbances. After this, the experiments started.

Protocol to determine the MAHD

It is highly unlikely that there will be a clear-cut boundary between falling and being able to recover (i.e. the MAHD) for any participant. More likely, due to human variations in response to a disturbance, there is a probability that a participant will fall depending on the magnitude of the disturbance. To determine the MAHD for a participant, we applied several disturbances varying in magnitude so that the participant both fell and recovered balance multiple times. Using a logistic regression model, we can then convert a binary outcome (i.e. fall or recovery) into a probability as a function of the disturbance magnitude.

To illustrate this concept, Figure 3.4 displays the outcomes of a logistic regression analysis applied to the example trial data from Figure 3.5. In the rest of this study, we define the MAHD as the threshold at which there is a 50% probability the cyclist will fall, similar to the definition proposed for the MAHD in Chapter 2. In Section 3.3, we describe the Bayesian multilevel logistic regression model used to determine the MAHD for each participant.

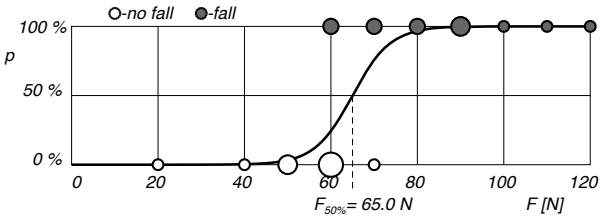

Figure 3.4: Example of a logistic regression model applied to the pull force data from figure 3.5. The white dots mark no fall, the dark dots mark a fall, and the area of the dots corresponds to the number of pulls at that specific force value. The solid line is the logistic regression line for the probability p of falling as a function of the pull force F. The pull force for which there is a 50 % chance of falling is $F_{50\%} = 56.1$ N. This corresponds to an angular impulse of 13 Nms.

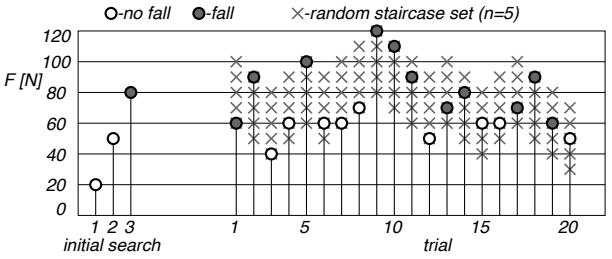

Figure 3.5: Example of the random and adaptive staircase procedure to find the MAHD of the pull force F applied at the handlebar for which a cyclist will not fall. White dots mark no fall, dark dots mark a fall, and grey crosses show potential pull forces from which is chosen at random. The initial search is to locate where the random staircase procedure should start.

To start with a reasonable guess of the MAHD, we performed a simple staircase search procedure, during which the magnitude of the disturbances was increased by a constant step size if the preceding disturbance did not result in a fall. This procedure stopped once the participant fell. The magnitude of the last disturbance was then chosen as the initial estimate of the MAHD for the experiments. These initial disturbances started with torques of 9 Nms and increased with steps of 6 Nms. Most participants fell after two or three disturbances, and only one had already fallen at the first.

The disturbance forces during the experiment were chosen according to a random and adaptive staircase procedure, enabling disturbance forces to be performed above and below the falling threshold and to allow small progression of the threshold [48]. The random staircase procedure works as follows. A set of five equidistant disturbance forces centred around the initial estimate MAHD was defined, from which the upcoming force was randomly selected. All five forces were 10 N apart and were increased or decreased with a fixed step size of 10 N after a balance recovery or fall, respectively. The step size was chosen after several pilot tests and is a trade-off between accuracy and the required time to determine the MAHD. Clockwise and counterclockwise disturbances were presented in a random order. If the random staircase algorithm proposed a zero or negative disturbance force, the outcome was assumed to be no fall, and the operator continued to the next disturbance. An illustration of the simple and random staircase procedure (with twenty disturbances) is given in Figure 3.5.

The participants were told before the experiment started that a handlebar disturbance would be applied and were instructed to brace themselves and try their best to recover balance. After a recovery, participants were to return to the centerline of the treadmill, after which a new disturbance was presented. In case of a fall, participants were caught by an intelligent tethered harness, and the treadmill was stopped with the emergency stop button. The participant was helped upright again and placed back upright in the middle of the treadmill. After this, the treadmill was started again, and once the participant cycled steadily again, a new disturbance was applied.

Each participant started the experiment at a prescribed cycling speed of 12 km/h. A maximum of twenty disturbances were applied to each participant, chosen after several pilot tests. This number is a trade-off between the four hours available per participant, the physical effort it costs participants, and the minimum number of trials required to obtain a robust and reliable estimate of the disturbance threshold. Only one participant stopped after ten disturbances; all others completed all twenty disturbances.

During this set of twenty disturbances, participants could stop or take a break at any time they wished. Several participants took one break of five to ten minutes in a set of twenty disturbances. Several times, there was also a break because of small reparations to the setup. For a small number of disturbances, the operator stopped the treadmill too soon before it was certain the participant would have fallen, or the perturbator mechanism did not apply the disturbance correctly. In this case, the same disturbance was applied again, and data from the previous disturbance was discarded.

After a participant finished a set of twenty disturbances, there was a break in which he or she was given the choice to redo the experiment at another velocity. If the participant agreed to this, it was randomly selected if the velocity was 6 or 18 km/h. After

the participants finished the set of twenty disturbances at this velocity, they were given the choice to redo the experiment at the last remaining velocity.

The three speeds were chosen based on the results of several pilot studies. In pilot studies, participants indicated that 12 km/h was a comfortable speed. Participants further indicated that 6 km/h was the slowest speed at which they could still cycle steadily and straight ahead, and 18 km/h felt like cycling fast (and was also the maximum speed limit of the treadmill). If the participant agreed to perform the experiments at another velocity, the procedure to learn to cycle on the treadmill at that speed and the simple staircase procedure to determine an initial estimate for the MAHD were repeated at that velocity.

Six participants performed the experiments at 12 km/h only, six performed the experiments at 12 and 6 km/h, six participants performed the experiments at 12 and 18 km/h, and six participants performed the experiments at all three velocities. For the set of twenty random disturbances per velocity, each participant fell at least seven times and recovered balance at least eight times, which shows that the random staircase procedure ensured that each participant fell approximately 50% of the time (see also Figure 3.6).

3.2.4. DATA COLLECTION

This study focuses on identifying key cyclist control characteristics that predict falls and the MAHD. In the experiments, we collected several characteristics of cyclists. The cyclist characteristics were divided into task-unrelated characteristics and task-related characteristics. The task-related characteristics are those directly associated with the balancing task and the ability of the cyclist to recover balance from a disturbance. The task-unrelated characteristics are those not directly associated with the balancing task. In addition, we collected disturbance and trial characteristics. Table 3.2 gives a summary of all the variables, and details are provided below. Some variables were measured with the equipment shown in Figure 3.1.

Task-unrelated participant characteristics

The participant's age a and height h were given by the participant prior to the experiment. The participant's mass m was measured using scales just before the experiment started and when he or she was wearing a helmet, gloves, the belt of the intelligent tethered harness, shoes, and clothes. The subscript i denotes the participant's identification number, and a number between 1 and 24 was randomly assigned before the experiment.

Task-related participant characteristics

The cycling skill performance S reflects the ability of the cyclist to maintain balance and follow a centerline while cycling undisturbed. It was determined from position measurement data of nine markers placed on the bicycle, measured by 12 Qualisys cameras and captured at 100 Hz. The position of the bicycle's front wheel ground contact point $(x_{\mathrm{fw}}, y_{\mathrm{fw}}, z_{\mathrm{fw}})$ was reconstructed from the redundant marker position data using rigid body constraints and least square methods. The skill performance S was defined as the standard deviation of y_{fw} during the one-minute cycling on the centerline task, which was the final phase of the learning phase. The skill performance S was determined separately for each of the three forward speeds before the disturbances were applied at

Table 3.2: Independent variables collected and considered for the statistical analysis to identify the key variables predictive of fall outcomes and the MAHD.

symbol	*description*	*unit*
trial characteristics		
v	forward speed	km/h
ϕ_0	lean angle at the moment the disturbance was applied	rad
$\dot{\phi}_0$	lean rate at the moment the disturbance was applied	rad/s
δ_0	steering angle at the moment the disturbance was applied	rad
$\dot{\delta}_0$	steer rate at the moment the disturbance was applied	rad/s
ψ_0	heading at the moment the disturbance was applied	rad
$y_{Q,0}$	lateral position of the ground contact point of the front wheel at the moment the disturbance was applied	mm
disturbance characteristics		
ΔL	angular impulse (magnitude of the applied handlebar disturbance)	Nms
j	identification number of disturbance	-
d	rotational direction of the disturbance, where 0 is a counterclockwise disturbance and 1 a clockwise perturbation	-
y	outcome of disturbance, where 0 is a recovery of balance and 1 is a fall	-
task-unrelated participant characteristics		
a	age	years
m	mass	kg
h	height	m
g	gender, where 0 is female and 1 is male	-
i	identification number of participant	-
task-related participant characteristics		
S	balancing control skill performance	mm
E	balancing control effort	rad^2/s
τ	reaction time of participant to applied disturbance	s

that forward speed.

The steer effort E reflects how much effort the participant put into following the centerline. It was determined by integrating the square of the steer rate $\dot{\delta}$ for the same one-minute period. The steering rate $\dot{\delta}$ was determined from the angular velocity measurements of IMU placed on the front fender, which was a Delsys Trigno EMG sensor. The raw data was collected at 2 kHz and smoothed using a second-order low-pass Butterworth filter with a cut-off frequency of 20 Hz. The steer effort E was also determined separately for each of the three forward speeds before the disturbances were applied at that forward speed.

The cyclist's reaction time τ was determined for each disturbance using the measured EMG signal. A Delsys Trigno Avanti EMG sensor was placed on each bicep and each tricep. The raw data was rectified, normalised and smoothed using a second-order low-pass Butterworth filter with a cut-off frequency of 40 Hz. The reaction time was defined as the time when the EMG signal of one of the four EMG sensors first exceeded

two times the standard deviation of the EMG signal for the second before $t = 0$, where $t = 0$ is the time after the operator clicked the button to apply a disturbance and when one of the four pull force measurements exceeded two times the standard deviation of the force signal 1 second before.

Trial and disturbance characteristics

The forward speed v was set equal to the treadmill's speed when the disturbance was applied. Depending on the experiment's conditions, the speed could be either 6 km/h, 12 km/h or 18 km/h.

The states of the bicycle at the moment the disturbance was applied were also reconstructed from the redundant marker position data and using rigid body constraints and least square methods. The states include the lean angle at the moment the disturbance was applied ϕ_0, the lean rate at the moment the disturbance was applied $\dot{\phi}_0$, the steering angle at the moment the disturbance was applied δ_0, the steer rate at the moment the disturbance was applied $\dot{\delta}_0$, the heading at the moment the disturbance was applied ψ_0, and the lateral position of the ground contact point of the front wheel at the moment the disturbance was applied $y_{Q,0}$.

The disturbance magnitude ΔL, defined as the angular impulse, was determined from measurements of four force sensors (Sciame) placed in series with the ropes. Using the handlebar width d of 0.82 m and assuming the ropes and force were always properly aligned in the horizontal plane, the handlebar disturbance was determined by multiplying the effective force applied by the four ropes F_{eff} by the handlebar width w_h, integrating them for the time the disturbance was applied Δt, which was 0.3 seconds, and correcting for the steer axis tilt λ, which was 21.5°.

$$\Delta L = \frac{F_2 + F_4 - F_1 - F_2}{2} \cos(\lambda) w_h \Delta t \tag{3.1}$$

The load cells were sampled at 1000 Hz. The start of the disturbance, $t = 0$, was defined as the time when one of the four pull force measurements exceeded two times the standard deviation of the force signal 1 second before.

The computer automatically collected the disturbance identification number j once the operator clicked a button to apply a disturbance. The identification number j started from 1 for each participant and continued to increase when the velocity changed. The subscript j denotes the jth disturbance for the participant. The rotational direction d was determined from the measured load cells signal.

The outcome of the disturbance was denoted by y. We followed the convention that $y = 1$ if a cyclist falls and $y = 0$ otherwise. Whether the disturbance resulted in a fall or not, y could, in most situations, be determined manually by the operator. In most of these situations, the participant rode off the treadmill or placed a foot on the ground while cycling at a forward speed above 6 km/h. Before the experiment, we defined a fall as a situation where the steering or leaning angle exceeded ± 45 degrees. However, this did not occur at all during the experiment.

Synchronisation

The Delsys Trigno EMG and Qualisys human motion capture systems were synchronised via the Qualisys Track Manager software. To synchronise the disturbance data, which was collected on the Speedgoat real-time controller, with the bicycle and cyclist

kinematics, logged via the Qualisys Track Manager software, a continuous voltage signal, which was equal to the desired force of the disturbance, was sent from the Speedgoat real-time controller to the Qualisys Track Manager.

Number of observations
A total of 928 observations were collected for the 24 participants. The disturbance direction d was missing for four observations. The reaction time τ was missing for seventeen observations, and for one participant at one forward speed (i.e. twenty observations) the skill performance S was missing.

3.3. STATISTICAL MODELING

In this section, we analyse the collected experimental data. We start with exploratory data analysis. To explore the inclusion of variables in subsequent models, we generate variable importance plots by fitting a random forest, providing initial insights into their relevance. We adopt the Bayesian approach to statistics to facilitate uncertainty quantification and derive a multilevel logistic regression model. For general background on Bayesian multilevel regression modeling we refer to Gelman et al. (2013) [49]. We first use Bayesian Model Averaging to choose relevant variables. These are chosen to be those variables which are in the posterior median model [50, 51]. We then refine the model based on the chosen set of variables by taking the multilevel structure of the data into account. Clearly, such a structure is present in the data since experiments can be grouped by participant. From the obtained multilevel logistic regression model we derive the posterior distribution of $\Delta L_{50\%}$, which we define as the angular impulse for which a participant has chance 50% of falling (i.e. according to our definition of the MAHD).

The dataset, R-scripts and online supplementary are available in the GitHub repository at the following URL: `https://github.com/fmeulen/CyclingFall`.

3.3.1. EXPLORATORY DATA ANALYSIS

The number of experiments for each participant and the velocities they experienced in these experiments vary. This is visualised in Figure 3.6.

To obtain a rough idea of the importance of each of the collected variables for predicting y_{ij} we fit a random forest model using the default settings in the `caret` package [52]. Here, we removed experiments in the data where any of the predictor values were missing. The left part of Figure 3.7 displays the variable importance of each independent variable (scaled from 0 to 100). The figure should be interpreted somewhat loosely, as strongly correlated predictors cannot be distinguished by the method. However, not surprisingly, it clearly reveals that angular impulse ΔL is highly important for predicting the dependent variable y. Other important independent variables are differences among participants (hinting at the importance of inherent skills specific to each participant), forward speed v and disturbance number j. When participant ID i is removed from the dataset as an independent variable and the analysis is redone, we obtain the variable importance shown in the right part of Figure 3.7. This results in higher variable importance for the independent variables: height h, mass m and age a.

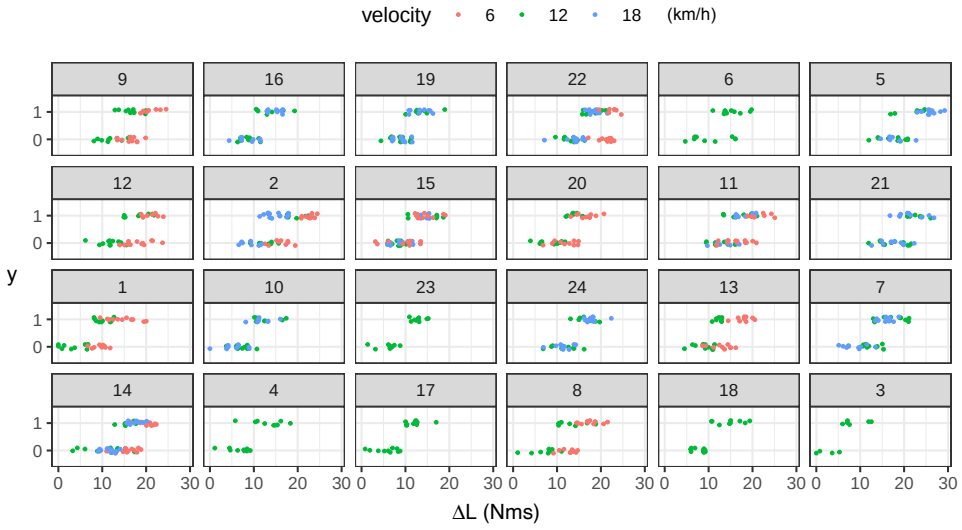

Figure 3.6: Each panel corresponds to a participant, ordered by age. The binary outcome variable "falling" is displayed versus angular momentum (i.e. the magnitude of the disturbance). The colouring of points corresponds to forward speed. This figure shows the substantial influence of angular momentum on the outcome variable.

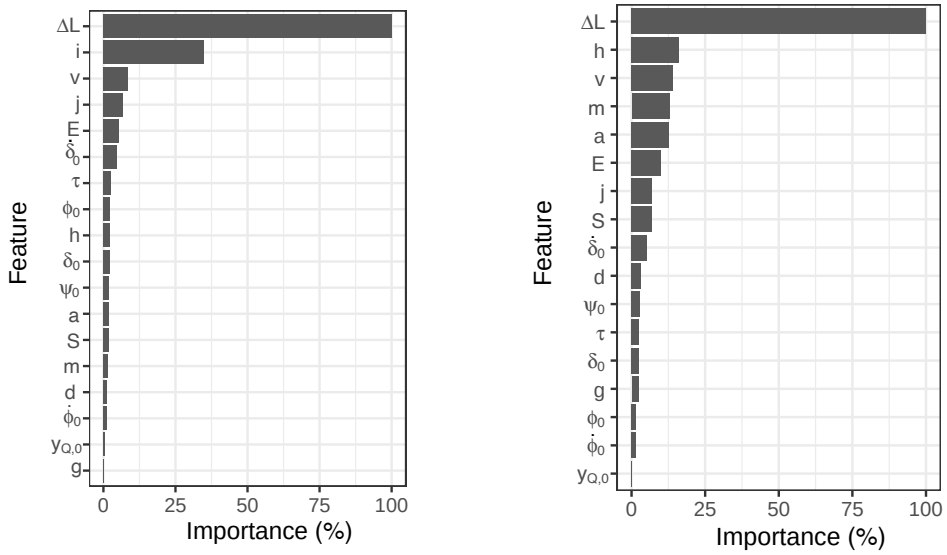

Figure 3.7: Random forest variable importance plots. Left: including participant ID i. Right: excluding participant ID i.

Whereas this exploratory data analysis sheds some light on which inputs determine whether a participant will fall or not, it does not provide an interpretable model. Nor does it provide us with an expression for the disturbance threshold $\Delta L_{50\%}$ (i.e. the MAHD). The latter requires a probabilistic model.

In the following sections, we have centred and scaled all numerical predictors to have average zero and unit standard deviation.

3.3.2. BAYESIAN MODEL AVERAGING

In the logistic regression model, we assume

$$y_{ij} \mid \theta_{ij} \overset{\text{ind}}{\sim} \text{Ber}(\theta_{ij})$$

with $\log(\theta_{ij}/(1-\theta_{ij}))$ being modelled by a linear combination of the available predictors. Suppose the coefficient of the kth predictor in the model is α_k. With p predictors, there are 2^p possible models. In the Bayesian approach, we equip each of these models with a prior probability. If additionally a prior on the coefficients $\alpha_1, \ldots, \alpha_p$ is imposed, the posterior probability of each of the models can be derived. In general, the computations can be intensive, and approximation- or sampling methods may be required. For the logistic regression model this topic is covered in Clyde et al. (2011) [51]. Bayesian Model Averaging (see for instance Hoeting et al. (1999) [53]) encapsulates the idea that there may be multiple models that explain the data and predictions should be aggregated over predictions within all models, weighted by their posterior probabilities. In our setting, however, besides model prediction, we also care about finding those predictors that are relevant, hoping that some predictors are irrelevant (and therefore need not be recorded) for the prediction of the outcome. Barbieri & Berger (2004) [50] advocate the *median probability model*, which is the model that only includes all predictors which have posterior inclusion probability exceeding $1/2$. It is this approach we follow here, using the `R`-package `BAS` [54]. Specific settings (including the prior specification) can be found in the GitHub repository. In the search over models, we impose that angular momentum is always included in the model. Furthermore, we impose that participant ID i is treated as one factor, which is either in- or excluded from the model.

Figure 3.8 shows a heat map of models, ordered along the horizontal axis by their log posterior odds, where a higher value indicates that the model is more strongly supported by the data compared to competing models. Predictors that are coloured black are not in the model. Hence, the model which is a posteriori most likely (having log posterior odds 1.594) does not contain gender g, age a, mass m, height h, skill effort E, reaction time τ, lean rate at the moment the disturbance was applied $\dot{\phi}_0$, steering angle at the moment the disturbance was applied δ_0, heading at the moment the disturbance was applied ψ_0 and the lateral position at the moment the disturbance was applied Q_0. The model which ranks second in terms of posterior probability has log posterior odds 1.438. Compared to the highest-ranked model, it also excludes pull direction d.

In Figure 3.9 we show the posterior inclusion probabilities of all predictors. The median probability model is therefore the model that includes angular impulse ΔL, participant ID i, pull ID j, forward speed v, steer rate at the moment the disturbance was applied $\dot{\delta}_0$, skill performance S, pull direction d and the lean angle at the moment the disturbance was applied ϕ_0.

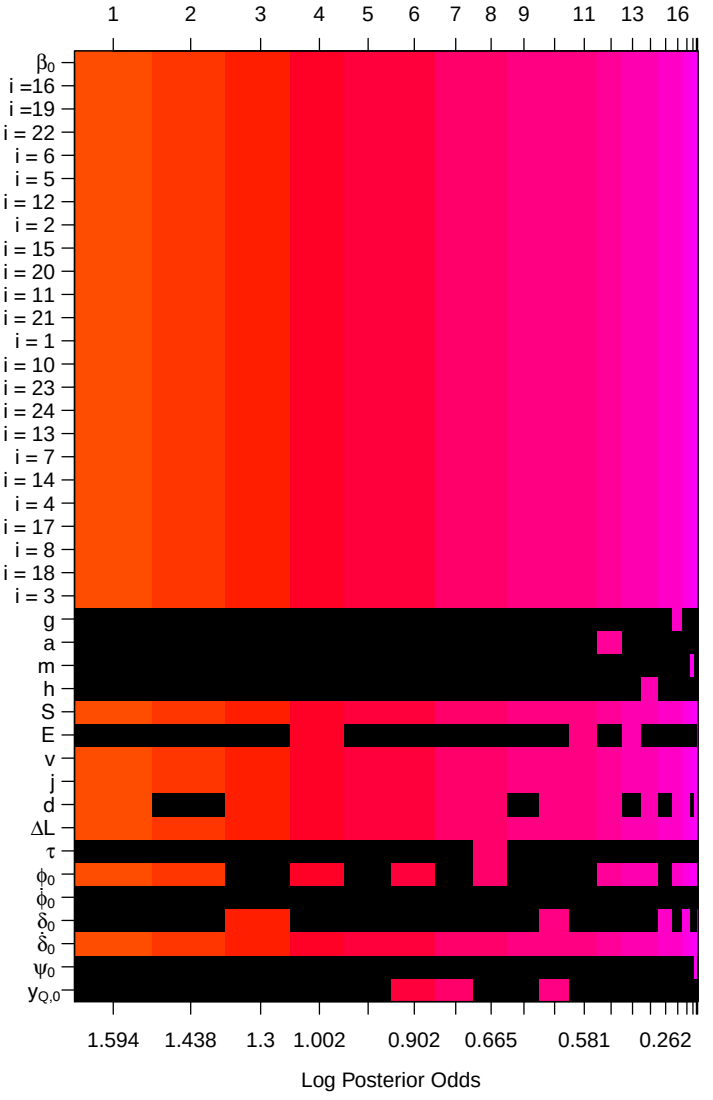

Figure 3.8: Heat map of models, ordered along the horizontal axis by their log posterior odds. Black boxes denote that the variable is not in the model. The participant IDs i are ordered according to age.

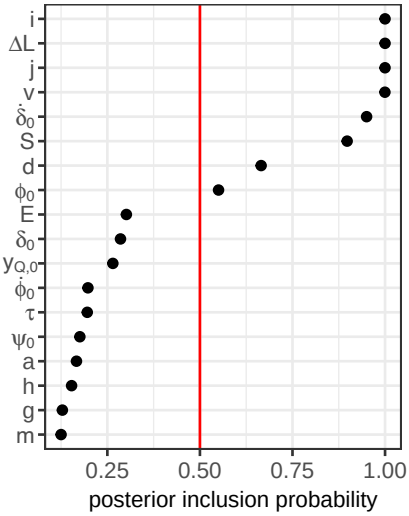

Figure 3.9: Posterior inclusion probabilities. Variables which have a probability exceeding 1/2, indicated by the red vertical line, are in the median probability model.

3.3.3. MULTILEVEL LOGISTIC REGRESSION MODEL

The dataset comprises multiple observations per participant. By using the grouping variable participant β_i we induce a hierarchical (multilevel) structure as one can expect that some participants simply perform better than others.

The very simplest model that takes the grouping structure into account is the following

$$\begin{aligned} y_{ij} \mid \theta_i &\overset{\text{ind}}{\sim} \text{Ber}(\theta_i) \\ \Lambda(\theta_i) &= \beta_i \\ \{\beta_i\} &\sim \text{N}(\bar{\beta}, \sigma^2_{\beta}). \end{aligned} \tag{3.2}$$

Here $\Lambda(x) = \log(x/(1-x))$ and $\text{Ber}(\theta)$ denote the logit-function and Bernoulli-distribution respectively where θ_i denotes the probability of falling for the ith participant. The bottom line specifies the prior distribution of the model parameters. One disadvantage of this model is the data for each participant are analysed separately. A multilevel model rightfully acknowledges that these participants are part of a larger population and share common features: data of one participant may help predict if a similar participant will fall in a particular setting. This pooling (sharing) of information is a key idea in multilevel models. Within the Bayesian viewpoint taken here, this can be accomplished by providing priors on $\bar{\beta}$ and σ^2_{β}.

Another apparent disadvantage of the model specified in Equation 3.2 is that it *only* takes participant variation into account. Potentially better models can be obtained by adding variables. We add the variables that we found to be in the posterior median model of the previous section.

To simplify notation, let

$$\left(x_{ij}^{(1)}, x_{ij}^{(2)}, x_{ij}^{(3)}, x_{ij}^{(4)}, x_{ij}^{(5)}, x_{ij}^{(6)}\right) = \left((\phi_0)_{ij}, 1_{\{d_{ij}=\text{CW}\}}, S_{ij}, (\dot{\delta}_0)_{ij}, \nu_{ij}, j_i\right).$$

Then we propose the following model

$$\begin{aligned} y_{ij} \mid \theta_{ij} &\overset{\text{ind}}{\sim} \text{Ber}(\theta_{ij}) \\ \Lambda(\theta_{ij}) &= \beta_0 + \beta_i + \sum_{k=1}^{6} \alpha_k x_{ij}^{(k)} + \gamma \Delta L_{ij} \\ \{\beta_i\} &\overset{\text{iid}}{\sim} \text{N}(0, \sigma_\beta^2) \\ \beta_0, \{\alpha_k\}, \gamma &\overset{\text{iid}}{\sim} \text{N}(0, \sigma^2) \\ \sigma_\beta &\sim \text{half-t}_3(2.5). \end{aligned} \tag{3.3}$$

Recall that for this model it is assumed that all numerical predictors have been centred and scaled. For the results presented, we took $\sigma = 2$. We comment on sensitivity to this choice in Section 3.3.5.

We used the `brms`-library in the `R`-language [55] to get posterior samples for the model specified in Equation 3.3. For σ_β we used the default half Student-t prior with 3 degrees of freedom and scale parameter equal to 2.5, which is denoted by half-$t_3(2.5)$.

3.3.4. POSTERIOR DISTRIBUTIONS OF VARIABLES AND POSTERIOR PREDICTIVE CHECKS

The posterior distributions of the variables of the fitted model can be summarised by the output from `brms` and are shown in Table 3.3. None of the credible intervals from all the variables contains a zero and the Rhat-values indicate no problems with the underlying Hamiltonian-Monte-Carlo method.

Figures 3.10 and 3.11 display the posterior distributions of the participant effects (i.e. β_i) and coefficients of the independent variables, respectively. Here, β_i can be

Table 3.3: Results for the highest ranked model, defined in Equation 3.3. The table shows the posterior mean estimate, the estimated error, the lower and upper 95% credible interval, the Rhat values, and the bulk and tail ESS.

variable	*coeff.*	*estimate*	*est. error*	*l-95% CI*	*u-95% CI*	*Rhat*	$bulk_{ESS}$	$tail_{ESS}$
Intercept	β_0 (-)	0.47	0.73	-0.97	1.90	1.00	8326	15883
ϕ_0	α_1 (1/rad)	0.42	0.18	0.08	0.77	1.00	40802	41365
d	α_2 (-)	-0.49	0.25	-0.98	-0.01	1.00	46800	43224
S	α_3 (1/mm)	0.71	0.22	0.28	1.14	1.00	31057	39087
$\dot{\delta}_0$	α_4 (s/rad)	-0.49	0.15	-0.79	-0.18	1.00	45573	42651
ν	α_5 (h/km)	1.62	0.18	1.27	1.98	1.00	32852	38786
j	α_6 (-)	-0.77	0.15	-1.07	-0.48	1.00	43014	39719
ΔL	γ (1/Nms)	5.26	0.38	4.55	6.03	1.00	32380	36693
sd(Intercept)	σ_β (-)	3.69	0.63	2.66	5.10	1.00	11420	21438

interpreted as the ability of the ith participant. A lower coefficient indicates a higher ability and better performance (i.e. higher MAHD). The posterior of each β_i seems to be approximately normally distributed and there is more variation in β_i among younger participants than older participants. The posterior distributions of the coefficients of the independent variables also seem to be normally distributed.

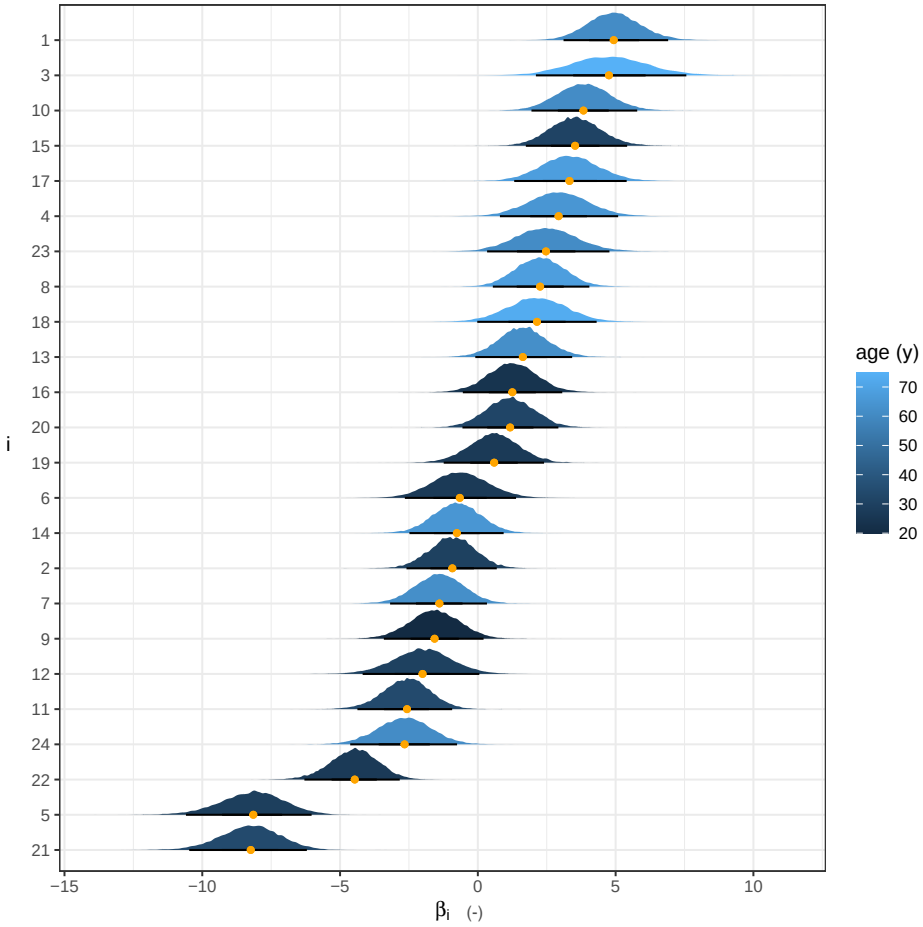

Figure 3.10: Posterior distribution of coefficients β_i, which represent a baseline for each participant's cycling performance based on the highest ranked model, which is described by Equation 3.3. The coefficients are ordered from the lowest to the highest coefficient. The colour indicates the age of the individual participant.

To assess the quality of the model, we performed several posterior predictive checks. For an excellent accessible exposition on this topic we refer to Chapter 10 in Lambert (2018) [56]. Figure 3.12 provides such a check. Here we compare the fraction of falling per total number of disturbances for the observed data and the fraction predicted by the model. The visual check displays reasonable agreement on what is actually observed in the data and data drawn from the predictive distribution.

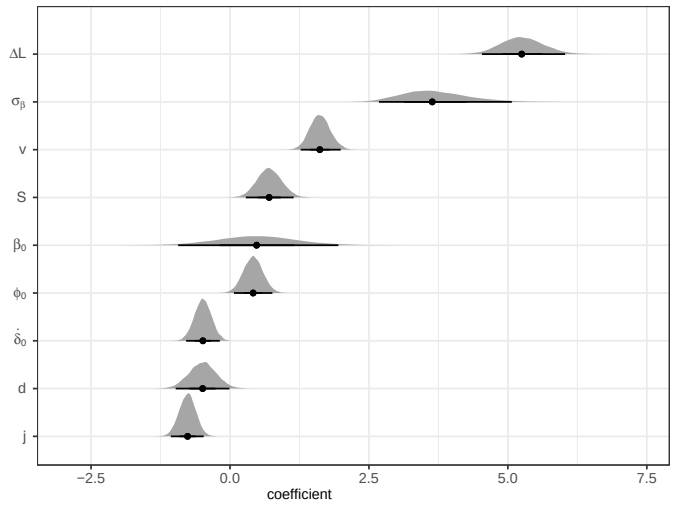

Figure 3.11: Posterior distribution of coefficients for the highest ranked model, which is described by Equation 3.3.

3.3.5. ROBUSTNESS CHECK

As an alternative, the model can also be fitted as a generalised linear model including random effects model using the `lme4`-package in `R` [57]. The results from fitting this model can be found in the online supplementary material available in the GitHub repository. The estimates agree very well with the coefficient estimates obtained within the Bayesian setup. At 5% significance level all included variables are significant. While we have a preference for the Bayesian approach, it is reassuring to see that the frequentist approach gives similar results. We also refitted the Bayesian model in Equation 3.3 with σ equal to 5. The results in the latter case are not much different from those presented. If σ is set to 1 we noticed that the estimates get more shrunken towards zero.

3.3.6. DISTURBANCE THRESHOLD — MAXIMUM ALLOWABLE HANDLEBAR DISTURBANCE

We define the disturbance threshold, the Maximum Allowable Handlebar Disturbance (MAHD), as the angular impulse that induces a 50% chance of falling and use model Equation 3.3 to determine this threshold. Note that the 50% is an arbitrary value, but other thresholds can be derived in a similar manner.

The value of the angular impulse for which the probability of falling equals 50% (i.e. 1/2), denoted by $\Delta L_{50\%}$, is uniquely determined by the relation

$$\beta_0 + \beta_i + \sum_{k=1}^{6} \alpha_k x^{(k)} + \gamma \Delta L_{50\%} = 0$$

from which we derive

$$\Delta L_{50\%}(x^1, \ldots, x^K) = -\frac{\beta_0 + \beta_i + \sum_{k=1}^{6} \alpha_k x^{(k)}}{\gamma} \tag{3.4}$$

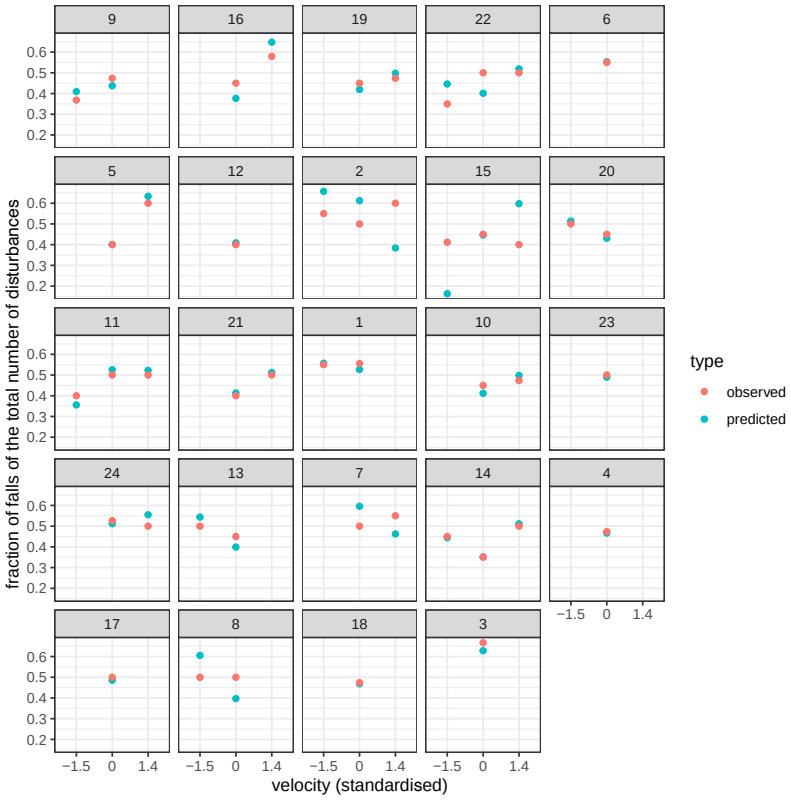

Figure 3.12: Posterior predictive check for the highest ranked model, which is described by Equation 3.3: fraction of falling per total number of disturbances for each participant and each velocity, both observed in the experimental data and as predicted by the highest ranked model.

The posterior distribution of $\Delta L_{50\%}$ is intractable, but can be approximated using Monte-Carlo simulation, as the fitted model provided us with samples from the posterior distribution of $(\beta_0, \{\beta_i\}, \{\alpha_k\}, \gamma)$. Hence, the posterior distribution of $\Delta L_{50\%}$ for participant i can be approximated as follows

1. take a posterior sample $(\beta_i, \beta_0, \{\alpha_k\}, \gamma)$;
2. compute $\Delta L_{50\%}$ according to Equation 3.4;
3. repeat steps (1) and (2) a large number of times.

Here, we see that the Bayesian approach easily allows for uncertainty quantification on $\Delta L_{50\%}(x^1, \ldots, x^K)$. Rather than a simple point estimate, we get its posterior distribution.

In Figure 3.13 we show approximations of the posterior distribution of $\Delta L_{50\%}$ for participants 1, 9, 11 and 12 at multiple forward speeds. These participants have varying ages and skill performances.

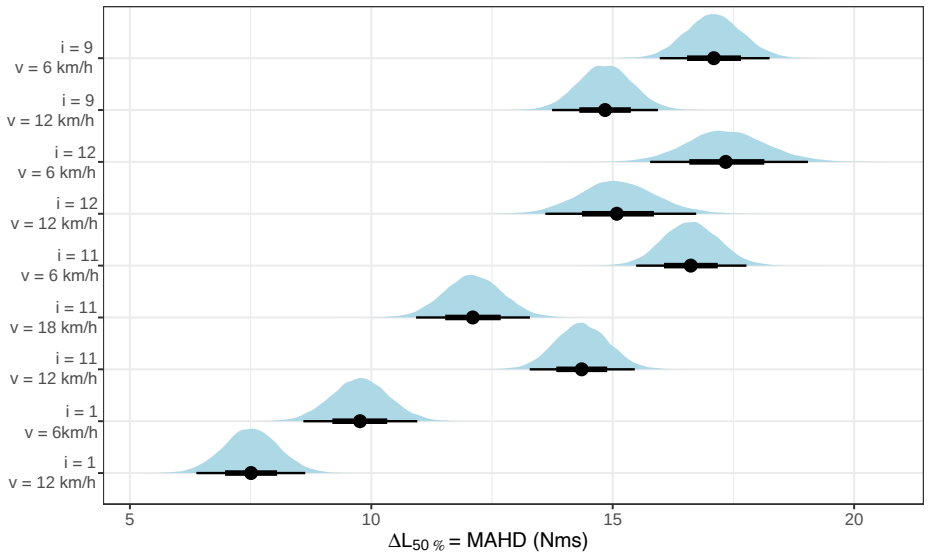

Figure 3.13: Posterior distribution of parameter $\Delta L_{50\%}$, which is equivalent to the MAHD, for participants 1, 9, 11 and 12 at different tested forward speeds v (km/h) indicated in the labels on the vertical axis.

3.3.7. PRACTICAL APPLICATION OF THE MODEL

For a new participant, not part of the experiment, steps (1) and (2), described in the previous section, need a slight adjustment. In this case, we do not have any samples from β_i in step (2). Instead, we first sample σ_β from its posterior and subsequently sample from a Normal distribution with this standard deviation. As a consequence, there is much higher uncertainty on predictions for people who were not among the participants in the experiment.

In Figure 3.14 we show approximations of the posterior distribution of $\Delta L_{50\%}$ for 6 hypothetical new participants, with characteristics as displayed in Table 3.4.

Table 3.4: Characteristics of hypothetical participants. The name is representative of the characteristics of that participant. For example, s40v12 has a skill performance S of 40 mm and cycles at a forward speed v of 12 km/h. A lower skill performance S value indicates a better line-tracking ability. The disturbance number j and disturbance direction d were kept constant and were 1 and CW, respectively.

participant	S (mm)	v (km/h)
s40v12	40	12
s90v12	90	12
s40v6	40	6
s90v6	90	6
s40v18	40	18
s40v25	40	25

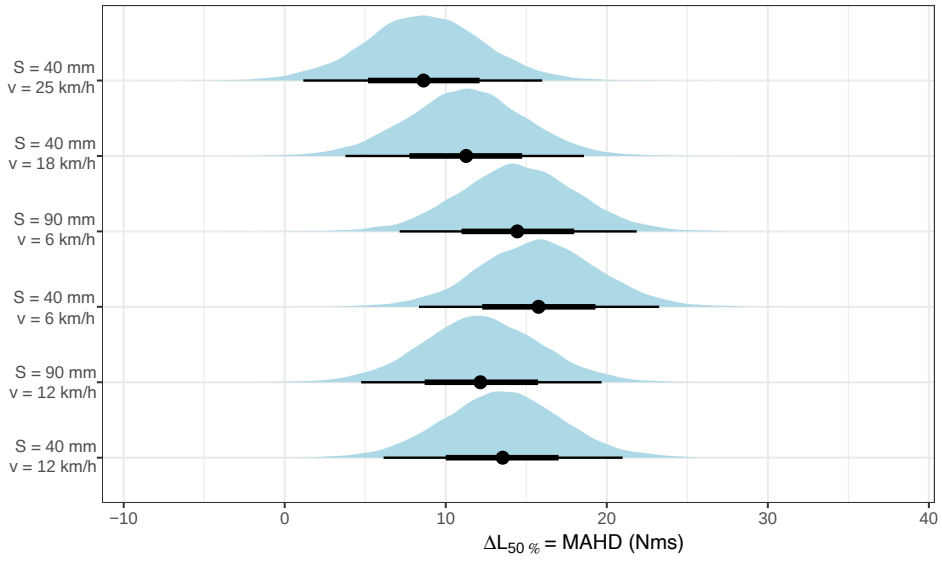

Figure 3.14: Posterior distribution of parameter $\Delta L_{50\%}$, which is equivalent to the MAHD, for 6 hypothetical new participants, with characteristics as displayed in Table 3.4.

3.3.8. DISCUSSION ON THE STATISTICAL ANALYSIS

The problem of model selection has received substantial attention in the statistics literature. There are many approaches to this and conclusions on a "best" model do not necessarily agree among methods. In an early analysis of the data, model choice was based on expected log predictive density (elpd) [58], implemented in the `loo`-package [59]. Here, one can choose between leave-one-out or leave-group-out cross-validation to estimate the elpd. The grouping by participant makes the second option a natural choice but is computationally very intensive. While it is feasible to compare a given set of models, to the best of the author's knowledge the `loo`-package does not provide a methodology to effectively screen through a large set of models. The `BAS`-package does allow for this, though it appears not easy to include the multilevel structure into it. For that reason, we have used the median probability model for variable selection and subsequently fitted the multilevel model in Equation 3.3.

3.4. DISCUSSION

The study's goal was to improve the practical application of bicycle dynamics and cyclist control models for safely and proactively evaluating cyclist fall prevention interventions. This goal arises from recognising that falls are a predominant cause of serious injuries among cyclists, yet evaluating interventions to prevent these falls faces challenges due to methodological constraints of existing approaches.

Our research addresses two significant gaps hindering the practical application of bicycle dynamics and cyclist control models. Firstly, it addresses the lack of

experimental data on actual falls and the maximum disturbance from which a cyclist can successfully recover balance. Such data are essential for validating bicycle dynamics and cyclist control models in fall scenarios, as these models have thus far only been validated for small disturbances during cycling, which did not result in a fall [14, 60–62]. Understanding the critical disturbance boundary between balance recovery and falling is crucial for validating whether these models accurately predict the Maximum Allowable Handlebar Disturbance (MAHD), proposed in Chapter 2 as a general indicator for evaluating the effectiveness of cyclist fall prevention interventions.

Secondly, it addresses the abstract nature of existing cyclist control models, which use parameters such as feedback gains, which, in turn, only have been calibrated for a single cyclist [15]. This abstraction hinders the practical application of cyclist control models, making it challenging to integrate cyclist control interventions within these models. Our ultimate goal is to refine cyclist control models by incorporating more intuitive variables related to cyclist control interventions. However, before achieving this, it is essential to define key variables that influence a cyclist's ability to respond to large disturbances (i.e., the MAHD).

In this study, we conducted experiments with 24 participants with varying characteristics in controlled conditions. The controlled conditions allowed us to simulate both falls and recoveries in response to a large impulse-like handlebar disturbance. Utilising Bayesian Model Averaging and developing a Bayesian multilevel logistic regression model, we identified key cyclist characteristics predictive of the cyclist's ability to respond to large disturbances, determined the MAHD for participants in the experiment, and predicted the MAHD for hypothetical new cyclists.

Cyclist fall experiments

The experiments conducted in this study marked the first instance of simulating actual cyclist falls. We showcased the practicality and safety of our newly developed experimental setup and protocol for simulating cyclist falls and determining the MAHD. While some participants expressed anxiety about falling beforehand, this apprehension dissipated after the initial fall. Remarkably, only one out of the 24 participants dropped out after 10 of the 20 disturbances required to determine the MAHD and no injuries were sustained during the experiments. This dropout rate is notably low compared to similar disturbance-based experiments for falling while standing or walking [63, 64].

Furthermore, within the allocated 4 hours per participant, we successfully determined the MAHD for all remaining 23 participants based on 20 disturbances. For a subset of participants, we even assessed MAHD at multiple forward speeds, with some completing up to 60 disturbances across the three different forward speeds evaluated in this study (6, 12 and 18 km/h).

The sole participant who dropped out, the oldest in our cohort, encountered difficulties adjusting to cycling on the treadmill. With extended training, this participant still completed experiments for ten disturbances but ultimately withdrew due to physical fatigue. This withdrawal underscores the necessity for a certain fitness level to complete all 20 disturbances, though well below the average fitness level of experienced cyclists.

Practical implementation of our experimental setup may be hindered by the need for specialised and potentially costly measurement equipment, including optoelectronic

camera systems, intelligent safety harnesses, and perturbator mechanisms. However, these requirements are comparable to other experimental setups. Additionally, a sufficiently spacious room housing a treadmill with surrounding padding and accommodating operators is necessary, with a minimum of three operators required. Finally, 4 hours are required per participant to determine the MAHD for at least one forward speed.

A notable limitation of our experimental setup is the use of a treadmill in a laboratory setting, which compromises the environmental validity of the experiment. Nonetheless, this choice was made for safety reasons and to ensure controlled conditions and accurate measurements. While we did not explicitly assess the environmental validity, the dynamics of cycling with a constant speed, straight ahead on a treadmill, closely mimic real-world cycling under similar conditions. However, differences in sensory input, such as optical flow, may affect participant experience. Almost all participants needed more than one try to cycle steadily on the treadmill. In addition, several participants perceived a cycling speed of 12 km/h on a treadmill belt as equivalent to 18 km/h on an open road. The potential impact of treadmill cycling on cycling behaviour warrants further investigation.

Participants in the study were briefed in advance about the forthcoming disturbances and instructed to prepare accordingly. It is highly likely that when participants anticipate a disturbance, the observed MAHD is higher than when they are unaware of it. To mitigate predictability, we introduced randomness in the direction and magnitude of handlebar disturbances and the timing of their occurrence. Nonetheless, the results revealed that the disturbance sequence (disturbance ID) significantly influenced the MAHD, with later disturbances tending to increase the MAHD.

Consequently, the found MAHD values may be considered unconservative. Disturbances below the found MAHD thresholds could still pose a fall risk for cyclists in real-world scenarios. Conversely, real-world disturbances already exceeding these MAHD values are highly likely to result in falls, and we recommend eliminating them from the road environment.

Investigating how participants' awareness and heightened focus on impending disturbances influence the MAHD is essential for a comprehensive understanding of the results. Exploring the aspect of unpredictability within the experimental setup, although challenging, is feasible to some extent. With a refined understanding of the safety aspects of the experimental setup, future investigations could disturb participants without prior notification, removing their awareness of impending disturbances. However, it is important to note that this opportunity is limited to the first instance, as subsequent disturbances are likely to be anticipated. Given the necessity for multiple disturbances to determine MAHD accurately, relying on a single disturbance would require a considerably large and labour-intensive sample size and many inter-subject comparisons.

An alternative approach involves introducing a dual task for participants, which could divert their focus from the impending disturbances, resembling real-life conditions where distractions increase the risk of falls [25]. Conducting experiments with a dual task is valuable, considering distraction as a recognised risk factor for cycling crashes. However, caution is warranted in designing and executing such experiments, as

individuals allocate attention and cognitive resources differently between the two tasks, potentially impacting performance and confounding the results of the MAHD.

While these approaches may reduce participants' awareness of upcoming disturbances, they will likely remain more alert and aware than in real-world situations due to the experimental setup and safety harness. Comparisons of cyclist steer actions from naturalistic studies can shed light on these differences. However, one must conclude that complete environmental validation is practically impossible.

Lastly, all participants were experienced cyclists with years of weekly cycling experience. Therefore, the applicability of our experimental approach to inexperienced cyclists is yet uncertain, as they may struggle more with treadmill cycling. Nevertheless, despite the participants' experience, significant variance was already observed among them, which will be discussed further in the subsequent section on key cyclist characteristics predictive of fall outcomes.

The generated dataset can be used to validate bicycle dynamics and cyclist control models to simulate cyclist falls. During the experiments, we collected not only the bicycle's state at the time of the disturbance but also before and after. Bicycle dynamics and cyclist control models can be validated by, for instance, comparing these measured transient responses with the transient responses predicted by the model. Such a validated model in actual fall conditions would eliminate the need for experiments to evaluate the effectiveness of an intervention. This is a valuable addition, as evaluating interventions using models is more cost-effective, safer, faster, efficient, accessible, and versatile.

Experimental measurements of the MAHD

In this study, we also determined the MAHD for participants using a Bayesian multilevel logistic regression model. The MAHD is defined as the angular impulse at which there is a 50% probability that the cyclist will fall. Our results indicate that, for the participants of the experiments, the mean MAHD ranges from approximately 8 to 16 Nms within the forward speed range of 6 to 18 km/h, with an approximate standard deviation of 4 Nms. These values are an initial estimation of the maximum magnitude of a handlebar disturbance a cyclist can withstand. We recommend eliminating real-world disturbances above these values from the road environment to reduce the risk of falling.

At present, we cannot directly relate the found values for the MAHD to real-world disturbances, as force or torque profiles of such disturbances have yet to be systematically collected. We recommend that future research focus on gathering these profiles. These profiles could be collected by equipping bicycles with accelerometers or gyroscopes to collect data during events such as riding over potholes, colliding with kerbs, encountering sudden wind gusts, or collisions with other road users. By measuring the resulting steering rates from these disturbances and cataloguing the data, it would be possible to establish a correlation between real-world disturbances and the MAHD.

The generated dataset cannot only be used to validate bicycle dynamics and cyclist control models in predicting the motions of the bicycle but can also be used to validate these models in predicting the MAHD.

Furthermore, we expanded our Bayesian model to predict the MAHD for

hypothetical new participants, thereby improving its practical application beyond the experimental cohort. The Bayesian model can determine the MAHD for cyclists with varying skills and cycling at different forward speeds.

Key cyclist characteristics predictive of fall outcome
In this study, we identified two key characteristics that influence a cyclist's ability to respond to large disturbances: forward speed v and skill performance S.

The forward speed v, which the cyclist chooses in the real world, is one of the most important cyclist control variables to predict the MAHD (see Figure 3.9). While it was anticipated that the MAHD would correlate with forward speed, our findings revealed a more complex relationship. Unexpectedly, cyclists required a greater disturbance force before falling at lower speeds. This is reflected in the positive posterior mean estimate for velocity in Table 3.3, indicating that higher speeds increase the probability of a fall, as also qualitatively illustrated in Figures 3.13 and 3.14. This result is contrary to expectations based on the increased instability of bicycles at reduced speeds [13]. This counterintuitive outcome can be attributed to the environmental constraint of the finite width of the treadmill. Notably, all falls occurred due to this failure mode, indicating its dominance. As forward speeds increased, participants approached the treadmill's edge more rapidly, requiring a faster response to the disturbance.

The skill performance S reflects how effectively a cyclist can maintain a centred trajectory while cycling undisturbed on a treadmill for one minute at a constant forward speed, following a white centerline. This measure is quantified as the lateral deviation during this undisturbed cycling phase. Our results showed that skill performance S was an important predictor for the MAHD.

Our definition of skill performance S warrants a further explanation. We posit that the ability to cycle undisturbed while maintaining a centred trajectory signifies a cyclist's balancing skill. However, it is important to acknowledge that a cyclist's response to disturbances may differ from their performance under undisturbed conditions. Despite this caveat, a precise definition remains elusive, and we have chosen this pragmatic definition. Our research underscores the predictive validity of our proposed definition. This finding reinforces the notion that our definition effectively captures the cyclist's balancing skill.

Participants may have exerted varying levels of effort in tracking the centerline, potentially influencing skill performance S. While skill effort E was also measured, our analysis revealed its limited value in predicting the MAHD.

Perhaps surprisingly, our study did not uncover a correlation between control effort E and skill performance S (see online supplementary in the GitHub repository). However, studies investigating if the car following task could be improved with continuous effort also found a complex relationship between task performance, effort and workload [65–67]. These findings suggest that cyclists may optimise their performance to what they deem sufficiently effective rather than maximising it.

Our study also found that three cyclist-specific attributes we examined — age, mass, and reaction time — exhibited limited predictive capability (see Figure 3.9). Notably, the lack of predictive power regarding age was unexpected given that older cyclists are overrepresented in cycling injury statistics [68–70]. Despite this, age did not improve the

Bayesian model's ability to predict the MAHD. It is intriguing that, once confronted with a critical situation and a disturbance, older cyclists demonstrate a similar probability of recovering balance as their younger counterparts, suggesting that age is not a significant determinant in this context.

As outlined in Chapter 2, it is crucial to recognise that the MAHD — the maximum handlebar disturbance a cyclist can withstand — represents only one aspect of the likelihood of a fall and subsequent injury. The overrepresentation of older cyclists in injury statistics could be attributed to factors beyond the scope of our study. For instance, older cyclists may be more susceptible to injury due to physical frailty upon falling or encountering potentially hazardous situations more frequently (exposure risk). However, the latter is less likely because older cyclists are known to partly apply compensation strategies such as avoiding darkness or crowdedness by changing their cycling routes or departure times [71].

The absence of a predictive relationship between participant mass and MAHD can be explained by our focus on disturbing the handlebars rather than the rear frame, which includes most of the participant's mass. Moreover, given a specific mass distribution, a handlebar disturbance will cause a lateral shift in the tyres' contact points, after which the bicycle will fall over like an inverted pendulum. In this scenario, only the height of the centre of mass is important, not the mass itself.

Although we considered participant mass and length and allowed for variability in cyclist seating positions on the bicycle, we did not measure the mass distribution across the bicycle. However, we assume that the mass distribution or height of the centre of mass would also not have had predictive value. Its impact in our study is constrained since all participants used the same bicycle and could only adjust saddle height or handlebar position within a narrow range. Even if seating positions could have varied more significantly, exploratory analyses employing bicycle dynamics models have shown that seating position's effect on bicycle stability is marginal, reinforcing our view.

Furthermore, it is important to note that cyclist mass and height are not considered components of cyclist control but are integrated as masses and inertia in bicycle dynamics models. This study aimed to identify cyclist characteristics that could improve cyclist control models. Therefore, while mass and height are characteristics of cyclists, they do not directly contribute to cyclist control.

The Bayesian multilevel logistic regression model developed in this study to predict the MAHD does not include reaction time (τ) as a key variable. However, we cannot conclude that it has limited predictive value. Unfortunately, in about 150 instances, we observed an almost zero reaction time, which is physically implausible. These anomalies were attributed to the noisy and spiky nature of the electromyography (EMG) signal, which degraded the signal-to-noise ratio. Consequently, these observations were omitted from the statistical analysis. The reduction in the dataset size and the noisy and spiky nature of the EMG signal might affect the predictive power of the reaction time. Therefore, we cannot conclude that the reaction time has limited predictive value. Importantly, the noisy EMG signal solely affected the reaction time measurement and did not impact the measurement of other variables.

While our analysis thus identified only two explicit cyclist control characteristics as crucial for predicting the MAHD, the results also demonstrate the importance of

participant ID i in predicting the MAHD. The participant ID i includes all the cyclist-specific characteristics that were not defined and measured explicitly. The importance of this variable in predicting the MAHD suggests the presence of other key cyclist characteristics affecting the MAHD, necessitating further investigation.

An important variable for future research is strategies to recover balance from large disturbances in conditions with limited lateral space. While there is one single response to recover balance from a disturbance, which is to steer in the direction of the fall, it is sometimes important to postpone balance recovery so as not to ride off the side of the road. Cyclists might use different strategies, or prioritisation, to recover balance quickly and not get too close to the side of the road. This prioritisation is not captured by existing cyclist control models, based on experiments in which cyclists were subjected to only small disturbances, as the lateral space in these conditions is often not a constraint.

These unidentified cyclist variables influencing the MAHD may relate to the strategies employed by cyclists to recover balance after a disturbance, an aspect not considered in our study. While steering into the direction of the fall was observed as the primary balance recovery mechanism across all participants, variations in strategies may still arise due to the limited width of the treadmill. The finite width of the treadmill imposes constraints on lateral displacement before a fall occurs. Consequently, cyclists face a trade-off between quickly recovering balance by steering towards the fall direction and staying within the treadmill's lateral width by delaying recovery and steering in the opposite direction. Cyclists may adopt different strategies, prioritising swift balance recovery or staying further from the treadmill belt's side edge. These subtle strategy differences may be discernible by analysing steering reactions captured during cyclist fall experiments. However, studying such patterns and strategies was outside the scope of this study.

Another potential strategy difference lies in how cyclists prepare for disturbances. Participants may stiffen their arm muscles to minimise or resist handlebar disturbances, theoretically facilitating easier balance recovery. Although we attempted to gather information about muscle stiffening and reaction time through EMG signals from the biceps and triceps, data processing challenges posed by signal noise led us to exclude this variable from the cyclist fall experiments and our study's scope.

Finally, our study did not exhaustively consider all cyclist variables that could influence the MAHD. Examples of unexplored variables include dual tasks, distractions, cycling under the influence of alcohol, and more. Moreover, certain cyclist variables we considered might not have been accurately defined or measured. Despite these limitations, the insights from our research into key cyclist variables can already contribute to improving cyclist control models. Notably, such models should incorporate a variable that reflects skill performance S, as defined in our study. This variable is more intuitive and easier to measure than feedback gains, which are currently the input values for the only validated cyclist control model. It is worth noting that forward speed is already included in this model.

Other key variables influencing the MAHD prediction

While our focus was on identifying key cyclist control characteristics that influenced the MAHD prediction, our study also resulted in insights into other key variables. These

include various states of the bicycle at the moment the disturbance was applied and the direction of the disturbance.

While we intended to apply the handlebar disturbance during periods of steady, upright, straight-ahead cycling at the treadmill's centre, small variations persisted for the lateral dynamics of the bicycle. The angles and angular rates for leaning and steering varied approximately within +/- 3 degrees and +/- 1 deg/s (see the online supplementary material in the GitHub repository for the distributions). These small variations in the bicycle lean angle and steering rate when the handlebar disturbance was applied were already important in predicting the MAHD. This observation aligns with expectations, as disturbances applied in the same direction as the cyclist was already steering at that time would naturally amplify the effect of the disturbance and vice versa.

The influence of the disturbance's rotational direction on the MAHD might possibly be related to the participant's dexterity (i.e. their handedness). Unfortunately, we did not determine this cyclist-specific characteristic.

Furthermore, other parameters we held constant throughout our study may also impact the MAHD. As discussed in Chapter 2, variables such as bicycle geometry, lateral available width, and tyre-ground friction are believed to be significant contributors to the MAHD. We advocate for future research to explore these variables systematically to determine their respective impacts on MAHD.

Practical implications

Our study was primarily focused on improving the practical application of bicycle dynamics and cyclist control models for safely and proactively evaluating interventions to prevent cyclist falls without implementing these first. This could yield evidence about the effectiveness of a broader collection of cycling safety interventions. In turn, this can aid engineers and professionals in designing safer infrastructure, bicycles, and training programs and aid policy advisors in deciding which interventions to stimulate. However, several other aspects of our study also bear practical implications and applications.

To begin with, the Bayesian multilevel logistic regression model we developed to predict the MAHD for cyclists with different characteristics can serve as a valuable tool. This model provides insights into which disturbances are safe (i.e., below the MAHD) and which are not, guiding decisions on allowable disturbances in cycling environments. For example, if a cyclist can maintain balance after a perpendicular collision with a car travelling at 30 km/h (i.e., below the MAHD) but not at 50 km/h (i.e., above the MAHD), it is advisable to limit the maximum speed at car-bicycle intersections to 30 km/h. Another scenario involves collisions with kerbs. Different kerb designs — such as high vertical kerbs, low vertical kerbs, or sloped kerbs — generate varying impact forces, potentially resulting in disturbances of different magnitudes. Identifying which designs produce disturbances below the MAHD will inform safer kerb implementations. However, before real-world disturbances can be compared to the MAHD, they must be accurately measured and translated into equivalent handlebar disturbances.

Moreover, our findings underscored considerable variability in fall risk among cyclists, with individual cycling skills emerging as the primary predictor of falls, outweighing factors such as age, mass, length, reaction time, and control effort. This finding suggests that investing in cycling skill training could mitigate fall risks

effectively. This finding holds for all cyclists, not only older cyclists. As demonstrated in our experimental setup, implementing disturbance-based training holds promise for enhancing cyclists' ability to recover balance from significant disturbances, as our results showed that later disturbances tended to increase the MAHD. However, the generalizability of this training to different disturbances and real-world cycling contexts warrants further investigation.

Additionally, our results indicate that providing increased lateral space for balance recovery can lower the probability of falls, advocating for increased emergency lateral space for cyclists. While widening bicycle paths can contribute to this goal [72], alternative solutions such as forgiving kerbs or ridable road shoulders might also be effective.

Fourthly, the experimental platform, combined with the MAHD, can already be used to test the effectiveness of cycling safety interventions before they are implemented. For example, it can be used to test different bicycle designs or the medical fitness needed to cycle safely.

Finally, the Bayesian model, combined with the experimental setup, can be used to screen individual cyclists' fall risk and serve as a disturbance-based training program. The experimental setup can be used to screen individual cyclists for fall risk (i.e. low MAHD). Because age was not an important predictor for the MAHD, older cyclists do not necessarily have a higher fall risk. A screening would allow for the identification of individuals with a high fall risk. Consequently, personalised advice regarding the risks of cycling could be provided. Such advice might consist of potential steps to mitigate these risks. For instance, advice to wear a bicycle helmet, transition to a tricycle, or undergo training to improve cycling balancing skills.

This training could be conducted using our experimental setup, where cyclists are exposed to controlled disturbances to train their reactions. Our setup allows for large disturbances near the threshold, simulating actual cyclist fall scenarios. Research has shown that such disturbance-based training programs can effectively reduce the risk of falls, as demonstrated in studies on fall prevention in the home environment [73]. Our findings further support this potential, as the learning effect observed during our experiments suggests that repeated exposure to disturbances can increase the MAHD, thereby decreasing the likelihood of falls. We recommend that future research investigate the transferability of these skills to real-world cycling and the long-term effects of such training on cyclist safety.

3.5. CONCLUSION

In this research, we conducted experiments involving cyclist falls with 24 participants with varying characteristics. From these experiments, we developed a Bayesian multilevel logistic regression model. This model effectively identifies key cyclist control characteristics that reflect the cyclist's ability to recover balance from large disturbances and can predict the Maximum Allowable Handlebar Disturbance (MAHD), which reflects the maximum disturbance from which a cyclist can recover balance, taking into account bicycle parameters and environmental conditions. Importantly, the predictive capability of the Bayesian model extends not only to our original participants but also to hypothetical new types of cyclists.

The combination of our experimental data and the Bayesian multilevel logistic regression model holds significant promise for future research. This toolset can be used to validate the reliability of existing bicycle dynamics and cyclist control models, simulate fall scenarios, and predict the MAHD for cyclist fall prevention interventions.

In addition, we identified forward speed v and skill performance S, defined as the ability to maintain balance and follow a centreline while cycling undisturbed, as important cyclist control predictors for recovering balance after a large disturbance. Surprisingly, age did not emerge as a predictive variable in our analysis. Incorporating forward speed v and skill performance S into cyclist control models can substantially improve their practical utility, particularly in evaluating interventions targeting cyclist control.

Our findings represent a meaningful step in applying bicycle dynamics and cyclist control models to safely and proactively evaluate cyclist fall prevention interventions. Such an approach could increase the evidence base for interventions that improve cycling safety and support engineers and professionals in designing safe infrastructure, bicycles and training programs to improve cycling safety.

REFERENCES

[1] P. Schepers, N. Agerholm, E. Amoros, R. Benington, T. Bjørnskau, S. Dhondt, B. de Geus, C. Hagemeister, B. P. Y. Loo, and A. Niska, *An international review of the frequency of single-bicycle crashes (SBCs) and their relation to bicycle modal share,* Injury Prevention **21**, e138 (2015), https://doi.org/10.1136/injuryprev-2013-040964.

[2] B. Beck, M. Stevenson, S. Newstead, P. Cameron, R. Judson, E. R. Edwards, A. Bucknill, M. Johnson, and B. Gabbe, *Bicycling crash characteristics: An in-depth crash investigation study,* Accident Analysis & Prevention **96**, 219 (2016), https://doi.org/10.1016/j.aap.2016.08.012.

[3] S. Boufous and J. Olivier, *Recent trends in cyclist fatalities in Australia,* Injury Prevention **22**, 284 (2016), https://doi.org/10.1136/injuryprev-2015-041681.

[4] J. Vanparijs, L. I. Panis, R. Meeusen, and B. de Geus, *Characteristics of bicycle crashes in an adolescent population in Flanders (Belgium),* Accident Analysis & Prevention **97**, 103 (2016), https://doi.org/10.1016/j.aap.2016.08.018.

[5] P. Schepers, H. Stipdonk, R. Methorst, and J. Olivier, *Bicycle fatalities: Trends in crashes with and without motor vehicles in the Netherlands,* Transportation Research Part F: Traffic Psychology and Behaviour **46**, 491 (2017), https://doi.org/10.1016/j.trf.2016.05.007.

[6] S. O'Hern and J. Oxley, *Fatal cyclist crashes in Australia,* Traffic Injury Prevention **19**, S27 (2018), https://doi.org/10.1080/15389588.2018.1497166.

[7] L. Kjeldgård, M. Ohlin, R. Elrud, H. Stigson, K. Alexanderson, and E. Friberg, *Bicycle crashes and sickness absence-a population-based Swedish register study of all*

individuals of working ages, BMC Public Health **19**, 1 (2019), https://doi.org/10.1186/s12889-019-7284-1.

[8] M. Ohlin, B. Algurén, and A. Lie, *Analysis of bicycle crashes in Sweden involving injuries with high risk of health loss,* Traffic Injury Prevention **20**, 613 (2019), https://doi.org/10.1080/15389588.2019.1614567.

[9] L. B. Meuleners, M. Fraser, M. Johnson, M. Stevenson, G. Rose, and J. Oxley, *Characteristics of the road infrastructure and injurious cyclist crashes resulting in a hospitalisation,* Accident Analysis & Prevention **136**, 105407 (2020), https://doi.org/10.1016/j.aap.2019.105407.

[10] M. Hosseinpour, T. K. O. Madsen, A. V. Olesen, and H. Lahrmann, *An in-depth analysis of self-reported cycling injuries in single and multiparty bicycle crashes in Denmark,* Journal of Safety Research **77**, 114 (2021), https://doi.org/10.1016/j.jsr.2021.02.009.

[11] M. Møller, K. H. Janstrup, and N. Pilegaard, *Improving knowledge of cyclist crashes based on hospital data including crash descriptions from open text fields,* Journal of Safety Research **76**, 36 (2021), https://doi.org/10.1016/j.jsr.2020.11.004.

[12] R. Utriainen, S. O'Hern, and M. Pöllänen, *Review on single-bicycle crashes in the recent scientific literature,* Transport Reviews **43**, 159 (2023), https://doi.org/10.1080/01441647.2022.2055674.

[13] J. P. Meijaard, J. M. Papadopoulos, A. Ruina, and A. L. Schwab, *Linearized dynamics equations for the balance and steer of a bicycle: A benchmark and review,* Proceedings of the Royal Society A: Mathematical, Physical and Engineering Sciences **463**, 1955 (2007), https://doi.org/10.1098/rspa.2007.1857.

[14] J. D. G. Kooijman, J. P. Meijaard, J. M. Papadopoulos, A. Ruina, and A. L. Schwab, *A bicycle can be self-stable without gyroscopic or caster effects,* Science **332**, 339 (2011), https://doi.org/10.1126/science.1201959.

[15] A. L. Schwab and J. P. Meijaard, *A review on bicycle dynamics and rider control,* Vehicle System Dynamics **51**, 1059 (2013), https://doi.org/10.1080/00423114.2013.793365.

[16] A. L. Schwab, J. P. Meijaard, and J. D. G. Kooijman, *Lateral dynamics of a bicycle with a passive rider model: Stability and controllability,* Vehicle System Dynamics **50**, 1209 (2012), https://doi.org/10.1080/00423114.2011.610898.

[17] R. Elvik, *Area-wide urban traffic calming schemes: A meta-analysis of safety effects,* Accident Analysis & Prevention **33**, 327 (2001), https://doi.org/10.1016/S0001-4575(00)00046-4.

[18] A. Hoye, *Recommend or mandate? A systematic review and meta-analysis of the effects of mandatory bicycle helmet legislation,* Accident Analysis & Prevention **120**, 239 (2018), https://doi.org/10.1016/j.aap.2018.08.001.

[19] I. I. Hellman and M. Lindman, *Estimating the crash reducing effect of advanced driver assistance systems (ADAS) for vulnerable road users,* Traffic Safety Research **4**, 000036 (2023), https://doi.org/10.55329/blzz2682.

[20] N. Lubbe, Y. Wu, and H. Jeppsson, *Safe speeds: Fatality and injury risks of pedestrians, cyclists, motorcyclists, and car drivers impacting the front of another passenger car as a function of closing speed and age,* Traffic Safety Research **2**, 000006 (2022), https://doi.org/10.55329/vfma7555.

[21] T. Sayed, M. H. Zaki, and J. Autey, *Automated safety diagnosis of vehicle-bicycle interactions using computer vision analysis,* Safety Science **59**, 163 (2013), https://doi.org/10.1016/j.ssci.2013.05.009.

[22] A. R. A. van der Horst, M. de Goede, S. de Hair-Buijssen, and R. Methorst, *Traffic conflicts on bicycle paths: A systematic observation of behaviour from video,* Accident Analysis & Prevention **62**, 358 (2014), https://doi.org/10.1016/j.aap.2013.04.005.

[23] N. McNeil, C. M. Monsere, and J. Dill, *Influence of bike lane buffer types on perceived comfort and safety of bicyclists and potential bicyclists,* Transportation Research Record **2520**, 132 (2015), https://doi.org/10.3141/2520-15.

[24] J. Kovaceva, P. Wallgren, and M. Dozza, *On the evaluation of visual nudges to promote safe cycling: Can we encourage lower speeds at intersections?* Traffic Injury Prevention **23**, 428 (2022), https://doi.org/10.1080/15389588.2022.2103120.

[25] D. de Waard, P. Schepers, W. Ormel, and K. Brookhuis, *Mobile phone use while cycling: Incidence and effects on behaviour and safety,* Ergonomics **53**, 30 (2010), https://doi.org/10.1080/00140130903381180.

[26] W. P. Vlakveld, D. Twisk, M. Christoph, M. Boele, R. Sikkema, R. Remy, and A. L. Schwab, *Speed choice and mental workload of elderly cyclists on e-bikes in simple and complex traffic situations: A field experiment,* Accident Analysis & Prevention **74**, 97 (2015), https://doi.org/10.1016/j.aap.2014.10.018.

[27] R. Dubbeldam, C. T. M. Baten, P. T. C. Straathof, J. H. Buurke, and J. S. Rietman, *The different ways to get on and off a bicycle for young and old,* Safety Science **92**, 318 (2017), https://doi.org/10.1016/j.ssci.2016.01.010.

[28] J. Andersson, C. Patten, H. Wallén Warner, C. Andersérs, C. Ahlström, R. Ceci, and L. Jakobsson, *Bicycling during alcohol intoxication,* Traffic Safety Research **4** (2023), https://doi.org/10.55329/prpa1909.

[29] K. Kircher and A. Niska, *Interventions to reduce the speed of cyclists in work zones — cyclists' evaluation in a controlled environment,* Traffic Safety Research **6**, e000047 (2024), https://doi.org/10.55329/ohhx5659.

[30] C. Andersérs, J. Andersson, and H. W. Warner, *The importance of individual characteristics on bicycle performance during alcohol intoxication,* Traffic Safety Research **6**, e000042 (2024), https://doi.org/10.55329/vmgb9648.

[31] A. Niska and J. Wenäll, *Simulated single-bicycle crashes in the VTI crash safety laboratory,* Traffic Injury Prevention **20**, 68 (2019), https://doi.org/10.1080/15389588.2019.1685090.

[32] A. Niska, J. Wenäll, and J. Karlström, *Crash tests to evaluate the design of temporary traffic control devices for increased safety of cyclists at road works,* Accident Analysis & Prevention **166**, 106529 (2022), https://doi.org/10.1016/j.aap.2021.106529.

[33] Y. Peng, Y. Chen, J. Yang, D. Otte, and R. Willinger, *A study of pedestrian and bicyclist exposure to head injury in passenger car collisions based on accident data and simulations,* Safety Science **50**, 1749 (2012), https://doi.org/10.1016/j.ssci.2012.03.005.

[34] M. Fahlstedt, P. Halldin, and S. Kleiven, *The protective effect of a helmet in three bicycle accidents — A finite element study,* Accident Analysis & Prevention **91**, 135 (2016), https://doi.org/10.1016/j.aap.2016.02.025.

[35] C. Baker, X. Yu, B. Lovell, R. Tan, S. Patel, and M. Ghajari, *How well do popular bicycle helmets protect from different types of head injury?* Annals of Biomedical Engineering **52**, 3326 (2024), https://doi.org/10.1007/s10439-024-03589-8.

[36] V. Astarita, V. Giofré, G. Guido, and A. Vitale, *Investigating road safety issues through a microsimulation model,* Procedia-social and Behavioral Sciences **20**, 226 (2011), https://doi.org/10.1016/j.sbspro.2011.08.028.

[37] U. Shahdah, F. Saccomanno, and B. Persaud, *Application of traffic microsimulation for evaluating safety performance of urban signalized intersections,* Transportation Research Part C: Emerging Technologies **60**, 96 (2015), https://doi.org/10.1016/j.trc.2015.06.010.

[38] H. Twaddle, T. Schendzielorz, and O. Fakler, *Bicycles in urban areas: Review of existing methods for modeling behavior,* Transportation Research Record **2434**, 140 (2014), https://doi.org/10.3141/2434-17.

[39] C. M. Schmidt, A. Dabiri, F. Schulte, R. Happee, and J. K. Moore, *Essential bicycle dynamics for microscopic traffic simulation: An example using the social force model,* in *The Evolving Scholar-BMD 2023, 5th Edition* (2023) http://dx.doi.org/10.59490/649d4037c2c818c6824899bd.

[40] N. Rinke, C. Schiermeyer, F. Pascucci, V. Berkhahn, and B. Friedrich, *A multi-layer social force approach to model interactions in shared spaces using collision prediction,* Transportation Research Procedia **25**, 1249 (2017), https://doi.org/10.1016/j.trpro.2017.05.144.

[41] V. Keppner, S. Krumpoch, R. Kob, A. Rappl, C. C. Sieber, E. Freiberger, and H. M. Siebentritt, *Safer cycling in older age (SiFAr): Effects of a multi-component cycle training. a randomized controlled trial,* BMC Geriatrics **23**, 131 (2023), https://doi.org/10.1186/s12877-021-02502-5.

[42] L. Alizadehsaravi and J. K. Moore, *Bicycle balance assist system reduces roll and steering motion for young and older bicyclists during real-life safety challenges,* PeerJ **11**, e16206 (2023), https://doi.org/10.7717/peerj.16206.

[43] B. Janssen, P. Schepers, H. Farah, and M. Hagenzieker, *Behaviour of cyclists and pedestrians near right angled, sloped and levelled kerb types: Do risks associated to height differences of kerbs weigh up against other factors?* European Journal of Transport and Infrastructure Research **18**, 360 (2018), https://doi.org/10.18757/ejtir.2018.18.4.3254.

[44] F. Westerhuis, A. B. M. Fuermaier, K. A. Brookhuis, and D. de Waard, *Cycling on the edge: The effects of edge lines, slanted kerbstones, shoulder, and edge strips on cycling behaviour of cyclists older than 50 years,* Ergonomics **63**, 769 (2020), https://doi.org/10.1080/00140139.2020.1755058.

[45] R. Utriainen, S. O'Hern, and M. Pöllänen, *Review on single-bicycle crashes in the recent scientific literature,* Transport Reviews **43**, 159 (2023), https://doi.org/10.1080/01441647.2022.2055674.

[46] G. R. Tan, M. Raitor, and S. H. Collins, *Bump'em: An open-source, bump-emulation system for studying human balance and gait,* in *2020 IEEE International Conference on Robotics and Automation (ICRA)* (Paris, France, 1 June - 31 August 2020) https://doi.org/10.1109/ICRA40945.2020.9197105.

[47] M. Plooij, U. Keller, B. Sterke, S. Komi, H. Vallery, and J. Von Zitzewitz, *Design of RYSEN: An intrinsically safe and low-power three-dimensional overground body weight support,* IEEE Robotics and Automation Letters **3**, 2253 (2018), https://doi.org/10.1109/LRA.2018.2812913.

[48] R. J. Doll, J. R. Buitenweg, H. G. E. Meijer, and P. H. Veltink, *Tracking of nociceptive thresholds using adaptive psychophysical methods,* Behavior Research Methods **46**, 55 (2014), https://doi.org/10.3758/s13428-013-0368-4.

[49] A. Gelman, J. Carlin, H. Stern, D. Dunson, A. Vehtari, and D. Rubin, *Bayesian Data Analysis, Third Edition*, Chapman & Hall/CRC Texts in Statistical Science (Taylor & Francis, 2013) https://books.google.nl/books?id=ZXL6AQAAQBAJ.

[50] M. M. Barbieri and J. O. Berger, *Optimal predictive model selection,* The Annals of Statistics **32**, 870 (2004), https://doi.org/10.1214/009053604000000238.

[51] M. A. Clyde, J. Ghosh, and M. L. Littman, *Bayesian adaptive sampling for variable selection and model averaging,* Journal of Computational and Graphical Statistics **20**, 80 (2011), https://doi.org/10.1198/jcgs.2010.09049.

[52] M. Kuhn, *Building predictive models in R using the caret package,* Journal of Statistical Software **28**, 1 (2008), https://doi.org/10.18637/jss.v028.i05.

[53] J. A. Hoeting, D. Madigan, A. E. Raftery, and C. T. Volinsky, *Bayesian model averaging: A tutorial (with comments by M. Clyde, David Draper and E. I. George, and a rejoinder by the authors),* Statistical Science **14**, 382 (1999), https://doi.org/10.1214/ss/1009212519.

[54] M. Clyde, *BAS: Bayesian Variable Selection and Model Averaging using Bayesian Adaptive Sampling* (2022), r package version 1.6.4.

[55] P.-C. Bürkner, *brms: An R package for Bayesian multilevel models using Stan,* Journal of Statistical Software **80**, 1 (2017), https://doi.org/10.18637/jss.v080.i01.

[56] B. Lambert, *A student's guide to Bayesian statistics* (Sage, 2018).

[57] D. Bates, M. Mächler, B. Bolker, and S. Walker, *Fitting linear mixed-effects models using lme4,* Journal of Statistical Software **67**, 1 (2015), https://doi.org/10.18637/jss.v067.i01.

[58] A. Vehtari, A. Gelman, and J. Gabry, *Practical Bayesian model evaluation using leave-one-out cross-validation and WAIC,* Statistics and Computing **27**, 1413 (2017), https://doi.org/10.1007/s11222-016-9696-4.

[59] A. Vehtari, J. Gabry, M. Magnusson, Y. Yao, P.-C. Bürkner, T. Paananen, and A. Gelman, *loo: Efficient leave-one-out cross-validation and WAIC for bayesian models,* (2020), https://mc-stan.org/loo/.

[60] J. D. G. Kooijman, A. L. Schwab, and J. P. Meijaard, *Experimental validation of a model of an uncontrolled bicycle,* Multibody System Dynamics **19**, 115 (2008), https://doi.org/10.1007/s11044-007-9050-x.

[61] D. Stevens, *The stability and handling characteristics of bicycles*, Bachelor's thesis, The University of New South Wales, School of Mechanical and Manufacturing Engineering, Sydney, Australia (2009), http://www.varg.unsw.edu.au/Assets/link%20pdfs/thesis_stevens.pdf.

[62] T.-O. Tak, J.-S. Won, and G.-Y. Baek, *Design sensitivity analysis of bicycle stability and experimental validation,* in *Bicycle and Motorcycle Dynamics Conference* (Delft, The Netherlands, 20-22 October 2010) http://www.bicycle.tudelft.nl/ProceedingsBMD2010/papers/tak2010design.pdf.

[63] M. Pijnappels, J. C. E. van der Burg, N. D. Reeves, and J. H. van Dieën, *Identification of elderly fallers by muscle strength measures,* European Journal of Applied Physiology **102**, 585 (2008), https://doi.org/10.1007/s00421-007-0613-6.

[64] J. R. Crenshaw, K. A. Bernhardt, E. J. Atkinson, S. Khosla, K. R. Kaufman, and S. Amin, *The relationships between compensatory stepping thresholds and measures of gait, standing postural control, strength, and balance confidence in older women,* Gait & Posture **65**, 74 (2018), https://doi.org/10.1016/j.gaitpost.2018.06.117.

[65] D. A. Abbink, M. Mulder, F. C. T. van der Helm, M. Mulder, and E. R. Boer, *Measuring neuromuscular control dynamics during car following with continuous haptic feedback,* IEEE Transactions on Systems, Man, and Cybernetics, Part B (Cybernetics) **41**, 1239 (2011), https://doi.org/10.1109/TSMCB.2011.2120606.

[66] D. A. Abbink, M. Mulder, and E. R. Boer, *Haptic shared control: Smoothly shifting control authority?* Cognition, Technology & Work **14**, 19 (2012), https://doi.org/10.1007/s10111-011-0192-5.

[67] S. M. Petermeijer, D. A. Abbink, M. Mulder, and J. C. F. de Winter, *The effect of haptic support systems on driver performance: A literature survey,* IEEE Transactions on Haptics **8**, 467 (2015), https://doi.org/10.1109/TOH.2015.2437871.

[68] W. Weijermars, N. Bos, and H. L. Stipdonk, *Serious road injuries in the Netherlands dissected,* Traffic Injury Prevention **17**, 73 (2016), https://doi.org/10.1080/15389588.2015.1042577.

[69] M. J. Boele-Vos, K. van Duijvenvoorde, M. J. A. Doumen, C. W. A. E. Duivenvoorden, W. J. R. Louwerse, and R. J. Davidse, *Crashes involving cyclists aged 50 and over in the Netherlands: An in-depth study,* Accident Analysis & Prevention **105**, 4 (2017), https://doi.org/10.1016/j.aap.2016.07.016.

[70] S. Boufous, L. de Rome, T. Senserrick, and R. Ivers, *Risk factors for severe injury in cyclists involved in traffic crashes in Victoria, Australia,* Accident Analysis & Prevention **49**, 404 (2012), https://doi.org/10.1016/j.aap.2012.03.011.

[71] P. Schepers, W. Weijermars, M. Boele, I. Dijkstra, and N. Bos, *Oudere fietsers: Ongevallen met oudere fietsers en factoren die daarbij een rol spelen,* SWOV, Den Haag (2020), https://swov.nl/system/files/publication-downloads/r-2020-22a.pdf.

[72] P. Schepers, E. Theuwissen, P. N. Velasco, M. N. Niaki, O. van Boggelen, W. Daamen, and M. Hagenzieker, *The relationship between cycle track width and the lateral position of cyclists, and implications for the required cycle track width,* Journal of Safety Research **87**, 38 (2023), https://doi.org/10.1016/j.jsr.2023.07.011.

[73] M. H. G. Gerards, C. McCrum, A. Mansfield, and K. Meijer, *Perturbation-based balance training for falls reduction among older adults: Current evidence and implications for clinical practice,* Geriatrics & Gerontology International **17**, 2294 (2017), https://doi.org/10.1111/ggi.13082.

4

A Validated Cyclist Control Model With Human Characteristics For Bicycle Lateral Balance

M.M. Reijne, K.D. Wendel, F.C.T. van der Helm and A.L. Schwab

Abstract

This study presents a novel cyclist control model for bicycle lateral balance that mimics observed motions and cyclist control behaviour in response to small disturbances. The need for such a model arises from the high number of single bicycle crashes related to loss of balance, especially in high-volume cycling countries. Existing models often rely on abstract tuning parameters, complicating their practical application for evaluating cyclist-control focused fall prevention interventions.

Our goal was to develop a cyclist control model for the bicycle balancing task with the perspective of safely and proactively studying what changes to cyclist control can reduce the risk of falling in commonly reported bicycle crash scenarios. The presented cyclist control model is based on human control models for postural balance and includes human characteristics like sensory input, muscular dynamics, and multisensory integration to reconstruct a state estimation. We investigated various logical combinations of these elements, evaluating their effectiveness by comparing

This Chapter is under review at IEEE Transactions on Human-Machine Systems.

the predicted and measured human steering responses to disturbances. The measured steering responses were taken from an existing dataset in which three participants cycled on a treadmill and in a pavilion while exposed to small disturbances that threw them off balance. The Variance Accounted For (VAF) for the steering angle was used as the performance metric for selecting the model with the best predictive performance.

Our findings show that the best-performing model consisted of human sensors with partial state feedback, multisensory integration for bicycle state estimation, human steer torque control and muscular dynamics. In this model, the cyclist controls the bicycle in a realistic manner using only the lean rate and steering angle as sensory inputs, with no delay. Using one set of input values representing a generic cyclist, this model had an average VAF score of 65.6%, with a standard deviation of 25.8%, compared to the experimental data of three participants on a narrow treadmill. The average VAF score was 55.6% with a standard deviation of 27.7% in the pavilion setup. These findings indicate a robust capability in simulating balance recovery during cycling, representative of the reaction of multiple cyclists and for different forward speeds.

The most significant advancement in our model is that it only requires one input value to be calibrated, which is the weight factor on the lean angle in the LQR state weighting matrix. The other input values are easy to measure. The weight factor's independence from forward speed means it requires calibration at only one forward speed, unlike existing models, which require the calibration of multiple input variables for each speed independently. This feature greatly improves the practical application of our cyclist control model.

In conclusion, the model proposed in this study is the first cyclist control model for balancing a bicycle, which has human characteristics and parameters that are intuitive and easy to measure or obtain, except for one parameter. It has been validated with experimental data from multiple cyclists. This model holds potential for future research to safely and proactively evaluate cyclist fall prevention interventions targeting cyclist control, such as disturbance-based training, ultimately contributing to fall prevention in cycling.

4.1. INTRODUCTION

In high-volume cycling countries, loss of balance is the leading cause of serious cycling injuries [1–5]. However, evaluating potential interventions to prevent falls currently faces significant methodological challenges.

Existing approaches are diverse and consist of statistical analyses of historical crash data [6–9], video-based observation of surrogate safety indicators [10, 11], experimental and field studies [12–19], crash tests or models [20–24], and models that simulate traffic scenarios [25–29].

Despite the diversity, these approaches face notable challenges when applied to the evaluation of fall prevention interventions, particularly those aiming to reduce fall risk in critical scenarios. Interventions such as balance training programs [30], steer-assist systems [31], sloped kerbs [32], and ridable road shoulders [33] cannot be adequately evaluated by existing approaches.

Crash data is often incomplete, with single bicycle crashes — which are the majority of cycling crashes — underreported [2]. Surrogate safety indicators are primarily

focused on interactions between road users, neglecting falls that occur without the involvement of other road users, which account for a substantial share of serious injuries among cyclists [5]. Field and experimental studies provide insights into perceived safety, workload and bicycle dynamics, yet these indirect indicators lack the necessary validation to predict fall risk directly. Meanwhile, crash-testing experiments and simulations focus on post-fall impact mitigation rather than fall prevention. Additionally, existing traffic and behavioural simulation models fail to incorporate the balancing task and lateral bicycle dynamics essential to simulate falls.

As a result, while falls constitute the majority of serious cycling injuries, cyclist fall prevention interventions aiming to reduce fall risk in critical situations can currently not be evaluated ex-ante. Bicycle dynamics models, when combined with cyclist control models, offer a promising novel approach to address this gap, as discussed in Chapter 1. Despite the advanced understanding of bicycle lateral dynamics, the cyclist's role in maintaining balance within the bicycle-cyclist system remains relatively poorly understood [34–39]. Consequently, designing and ex-ante-evaluating interventions, such as training programs that aim to improve cycling balancing control, remains a challenge.

Previous studies have already proposed different cyclist control model types [39]. These models can be roughly divided into three different categories: classical state feedback [38, 40–42], nested multi-loop [43, 44], and other controllers, like dynamic inversion and nonlinear control [45] or neural network [46]. Of these models, only the nested multi-loop models have been proven to provide somewhat realistic results when used to model human control behaviour [47].

However, the nested multi-loop cyclist control models proposed by Doyle (1987) [43] and Hess et al. (2012) [44] may not accurately represent cyclist balancing behaviour. These models assume full state feedback and overlook critical human characteristics, such as neural time delays [48] and multisensory integration [49]. Furthermore, as noted by van der Kooij et al. (1999) [50], in an unpredictable environment, precise estimation of body orientation is challenging due to inherent delays in sensory information processing [48]. In addition, for postural balance control, the contributions of the different sensory systems are not equal [50, 51].

Current cyclist control models also need a large number of relatively abstract parameters [52, 53]. This precludes the easy incorporation of cycling safety interventions targeting cyclist control. In addition, many of these variables need to be calibrated, making it further challenging to use existing cyclist models to safely and proactively evaluate cyclist fall prevention interventions because input values are difficult and time-consuming to measure.

The goal of this study is to develop a cyclist control model for the bicycle balance task with the perspective of safely and proactively studying what changes to cyclist control can reduce the risk of falling during cycling. This study presents a nested multi-loop cyclist control model for bicycle balance control with partial state feedback, time delay and multisensory integration. This model is based on intuitive, measurable human characteristics and mimics cyclist control behaviour observed in experiments in which cyclists were exposed to small disturbances while cycling in a treadmill setup and a pavilion setup.

4.2. METHOD

For the cyclist control model, we took human control models for postural balance by van der Kooij et al. (1999) [50] and the work by Schwab et al. (2013) [52] and Dialynas et al. (2022) [53] as a point of departure to identify the important parameters required to model human bicycle balance control.

Ideally, we would have developed the cyclist control model using the findings of Chapter 3, which included experimental data of falls and identified key cyclist control characteristics that influenced the probability of a fall. However, this study was conducted before the completion of the cyclist fall experiments. As a result, we utilised an existing dataset where cyclists only experienced small disturbances without actual falls. In addition, the control variables we investigated were instead inspired by postural balance control models. We will delve further into how the findings of this study about the key cyclist control characteristics relate to the findings of Chapter 3 in the discussion section.

Figure 4.1 shows the cyclist control model for the cycling lateral-balance task as proposed in this study. This was the best-performing model. The model is composed of several blocks, and several options were explored for each block. For instance, different models with varying complexities were explored for the bicycle dynamics. We selected the option that yielded the highest similarity with the filtered experimental data while considering both complexity and computational efficiency. The quality of the fit was determined by the Variance-Accounted-For (VAF) score of the predicted steering angle by the cyclist control model δ_b and the filtered measured steering angle $\hat{\delta}_f$. An overview of the details and predictive performance of all explored model block options can be found in Appendix 4.A.1.

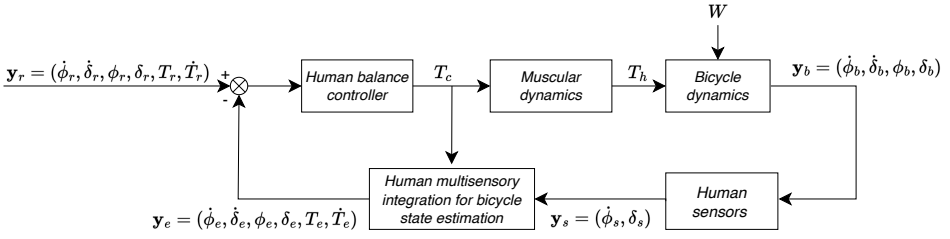

Figure 4.1: Block diagram of the system model for the human lateral balance control of a bicycle. The various blocks are the bicycle dynamics, which describes the motions of the bicycle, human sensors to sense the state of the bicycle, a human multisensory state estimator to reconstruct the full state of the bicycle from the human sensor data together with an internal model. This human balance controller outputs a desired control steer torque which is then applied to the bicycle through a muscular cyclist-arm dynamics block. The variables are the bicycle roll angle ϕ and steering angle δ, the steer torque T and an external disturbance W.

The remaining part of the method section consists of four parts. First, the cyclist control model and the details of the option chosen for each block are presented in Section 4.2.1. Second, the procedure for the parameter input value selection is described in Section 4.2.2. Third, the experimental dataset is described in Section 4.2.3. Fourth, the procedure to evaluate the model's predictive performance is described in Section 4.2.4.

4.2.1. CYCLIST CONTROL MODEL

In the next paragraphs, we describe the separate blocks of the cyclist control model, as shown in Figure 4.1. This section focuses on the option that demonstrated the best predictive performance taking into account complexity and computational efficiency as well. For a comprehensive overview and evaluation of all explored options and their respective predictive performance scores, please refer to Appendix 4.A.1.

BICYCLE DYNAMICS

The bicycle dynamics block contains the submodel that predicts the motions of the bicycle. We explored three different bicycle dynamics models: the Carvallo-Whipple (C-W) bicycle model, the naive bicycle model and the C-W bicycle model with passive rider contribution. We selected the bicycle dynamics model that yielded the highest similarity with the filtered experimental data (see Section 4.2.4), using the VAF as an indicator (see Section 4.2.4) while considering both complexity and computational efficiency. An overview of the VAF scores and details of the other bicycle dynamics models can be found in Appendix 4.A.1. Here, the outcome was to use the C-W bicycle model with passive rider contribution.

The C-W bicycle model consists of four rigid bodies: two wheels, the rear frame, which includes a rigid cyclist attached, and the front frame. The wheels are connected to the rear frame and front frame through revolute joints. The wheels have ideal knife-edge rolling point contacts with the ground. The rear frame and front or steering assembly are connected through a revolute joint, which defines the steering axis. A full description of this simple bicycle model and its history can be found in Meijaard et al. (2007) [35].

The C-W model has three degrees of freedom: the rear frame lean angle ϕ, the steering angle δ, and the forward speed v. The lateral motions, consisting of the lean and steering angle, can be described for small disturbances about the upright steady forward motion with the following linearised equations of motion:

$$\mathbf{M}\ddot{\mathbf{q}} + v\mathbf{C}_1\dot{\mathbf{q}} + [g\mathbf{K}_0 + v^2\mathbf{K}_2]\mathbf{q} = \mathbf{T} \tag{4.1}$$

where the time-varying variables are the lean and the steering angle $\mathbf{q} = (\phi, \delta)^\top$. The torques on the right-hand side, $\mathbf{T} = (T_\phi, T_\delta)^\top$, consist of external disturbance torques like, for instance, wind gusts, which can be a steer or lean torque or a combination of both, and cyclist applied torques, which for bicycle balance control are mainly steer torques. The constant terms ($\mathbf{M}$, $\mathbf{C}_1$, $\mathbf{K}_0$, $\mathbf{K}_2$) are bicycle-cyclist specific and related to the mass, damping and stiffness of the bicycle-cyclist system [35].

In our overall system model, as shown in Figure 4.1, the input to the bicycle dynamics block is only a cyclist-applied steer torque from the muscular dynamics block T_h. We assumed no cyclist applied lean torque for the bicycle balance task. The external disturbance $\mathbf{W}$ in the experiments was a lateral force F on the rear frame, see Section 4.2.3, which mainly results in a lean disturbance torque $T_{d\phi}$ together with a minor steer disturbance torque $T_{d\delta}$.

The torques on the right hand side of equation 4.1 are $\mathbf{T} = (T_\phi, T_\delta)^\top = (T_{d\phi}, T_h + T_{d\delta})^\top$. The output of the bicycle dynamics block is the lean angle and steering angle and their time derivatives combined in the state vector $\mathbf{y}_b = (\dot{\phi}_b, \dot{\delta}_b, \phi_b, \delta_b)^\top$.

The rigid-cyclist bicycle model from above was extended with a passive rider model to account for the passive cyclist contribution of arms and hands to the steering assembly. This extension adds a cyclist's contribution in the steer torque T_δ within the equations of motion presented above. This addition includes terms for inertia I_r, damping c_r, and stiffness k_r. The constant coefficient matrices were adjusted accordingly to $\bar{\mathbf{M}}$, $\bar{\mathbf{C}}_1$, $\bar{\mathbf{K}}_0$, and $\bar{\mathbf{K}}_2$. More details about this adjustment can be found in Appendix 4.A.1.

HUMAN SENSORS

The human sensors block represents the cyclist's ability to sense the bicycle's state. It uses the full state of the bicycle dynamics block as input and generates a selection of that as output with some delay. We explored various combinations of sensory inputs, ranging from full-state feedback to single-state feedback, with and without sensory dynamics, and various delays. Again, we selected the sensory block that yielded the highest similarity with the experimental data while considering both complexity and computational efficiency (see Appendix 4.A.1). The choice here was to use the lean rate and steering angle, $\mathbf{y}_s = (\dot{\phi}_s, \delta_s)^\top$, without sensory dynamics and with zero delay. Zero delay is surprising; we will discuss this in the discussion section.

HUMAN MULTISENSORY INTEGRATION FOR BICYCLE STATE ESTIMATION

The human multisensory integration for bicycle state estimation block reconstructs the full state of the bicycle dynamics from the human sensor data. This human-like state estimator is modelled with a linear Kalman filter, which provides an optimal estimate of the states present in the model, given the sensory channels to which the cyclist has access. The Kalman filter consists of the process noise covariance matrix $\mathbf{Q}_K$ and a measurement noise covariance matrix $\mathbf{R}_K$.

An exploration of different sensory inputs and state estimators showed that the combination with the highest similarity to experimental kinematic data used two sensory inputs, $\mathbf{y}_s = (\dot{\phi}_s, \delta_s)^\top$, and a Kalman filter to estimate the six states required by the controller $\mathbf{y}_e = (\dot{\phi}_e, \dot{\delta}_e, \phi_e, \delta_e, T_e, \dot{T}_e)^\top$.

HUMAN BALANCE CONTROLLER

In this study, we assume that humans optimise their actions when performing specific tasks, such as balancing a bicycle. Consequently, we employ the Linear Quadratic Regulator (LQR) framework, which facilitates the systematic minimisation of a quadratic cost function. Moreover, given that the bicycle-cyclist system's dynamics vary with the forward speed [35], we have implemented gain scheduling to adjust the controller gains based on the forward speed.

The system's control law has the form,

$$\mathbf{T}_c = -\mathbf{K}(\mathbf{y}_e - \mathbf{y}_r), \tag{4.2}$$

where $\mathbf{y}_e$ represents the estimated state vector, $\mathbf{y}_r$ is the references state vector, and $\mathbf{T}_c = (T_c)$ denotes the steer torque. The reference state $\mathbf{y}_r$ is all zeros for the straight-ahead balancing task. The feedback gain matrix $\mathbf{K}$, which is diagonal, simplifies the control problem by treating each state separately. The six feedback gains are determined by

means of the LQR optimal control formulation where the cost function $J = \int (\mathbf{y}_e^\top \mathbf{Q}_{LQR} \mathbf{y}_e + \mathbf{T}_c^\top \mathbf{R}_{LQR} \mathbf{T}_c) \mathrm{d}t$ is minimized. Here $\mathbf{Q}_{LQR}$ is the state weighting matrix, and $\mathbf{R}_{LQR}$ is the control weighting matrix. These matrices are designed to minimise deviations from the desired state and excessive control efforts.

For the matrices $\mathbf{Q}_{LQR}$ and $\mathbf{R}_{LQR}$ we have taken the same approach as used by Bryson & Ho (2018) [54], where we assumed all off-diagonal terms in $\mathbf{Q}_{LQR}$ to be zero and scale the performance index by taking a unit control effort weight. By systematic parameter reduction of the remaining six diagonal terms, we have chosen to place only a weight factor on the lean angle in the state weighting matrix $\mathbf{Q}_{LQR}$, denoted as Q_ϕ. A weight factor on this state, which is the third diagonal term in $\mathbf{Q}_{LQR}$, resulted in the highest resemblance with filtered experimental data at the lowest complexity (see appendix 4.A.1).

MUSCULAR DYNAMICS

In the case of bicycle control, the muscular dynamics submodel describes the relation between the torque command given by the cyclist control model, T_c and the actual steer torque applied through the cyclist's arms on the handlebars, T_h. Such use of a muscular model is widespread in human control models. See, for instance, the overview by Mulder et al. (2007) [55]. Here, we choose to use a second-order low-pass filter where the following transfer function describes the dynamics.

$$H_n(s) = \frac{T_h(s)}{T_c(s)} = \frac{\omega_c^2}{s^2 + 2\zeta\omega_c s + \omega_c^2} \tag{4.3}$$

with a cut-off frequency ω_c and damping coefficient ζ.

The success of adding such a muscular model to human control in cycling was also shown by Schwab et al. (2013) [52]. In our exploration, a model with muscular dynamics yielded the highest similarity with the filtered experimental data (see appendix 4.A.1).

STATE EQUATIONS

For modeling purposes, the closed-loop system equations are written in state-space representation and discretised with a sampling frequency of 200 Hz, which is similar to the sampling rate of the experimental data. The state-space representation is given by

$$\dot{\mathbf{y}}_e = \mathbf{A}\mathbf{y}_e + \mathbf{B}T_c \tag{4.4}$$

$$\mathbf{y}_{e,s} = \mathbf{C}\mathbf{y}_e + \mathbf{D}T_c \tag{4.5}$$

with the state vector $\mathbf{y}_e = (\dot{\phi}_e, \dot{\delta}_e, \phi_e, \delta_e, T_e, \dot{T}_e)^\top$ and output vector $\mathbf{y}_{e,s} = (\dot{\phi}_e, \delta_e)^\top$.

Details of the system matrix **A**, input gain matrix **B**, output matrix **C**, and direct feed-through matrix **D** are given in appendix 4.A.2.

4.2.2. PARAMETER INPUT VALUE SELECTION

The presented model has a total of 95 parameters. Although this number may appear large, most parameters are set to zero or one, simplifying the model's complexity. The remainder of the parameters primarily consist of physical and geometrical values, which

can be relatively easily obtained through measurements or found in existing literature. Only one parameter required fitting on filtered experimental data to ensure accuracy in model predictions.

The linearized equation coefficients of the C-W bicycle model ($\bar{\mathbf{M}}$, $\bar{\mathbf{C}}_1$, $\bar{\mathbf{K}}_0$, and $\bar{\mathbf{K}}_2$) are defined completely by 27 bicycle design parameters [35]. The coefficient matrices of the bicycle-cyclist system ($\bar{\mathbf{M}}$, $\bar{\mathbf{C}}_1$, $\bar{\mathbf{K}}_0$, and $\bar{\mathbf{K}}_2$) were obtained by selecting input values for the 27 bicycle design parameters similar to the experimental conditions described in Section 4.2.3. This ensures that the model accurately simulates the experimental conditions and enables us to evaluate the predictive performance of our cyclist control model.

The muscular dynamics are defined by two parameters: the cut-off frequency ω_c and the damping coefficient ζ. For the muscular dynamics, a cut-off frequency of $\omega_c = 2.17 \cdot 2\pi$ rad/s and damping coefficient of $\zeta = \sqrt{2}$ were used. These parameters, which were not directly derived from the experimental setup used in this study, have been previously validated for predicting cyclist balance in research by Schwab et al. (2013) [52].

The Kalman filter used for state estimation from human sensor data includes two covariance matrices, $\mathbf{Q}_K$ and $\mathbf{R}_K$, comprising 36 and 4 parameters, respectively. Given the absence of specific noise data for cycling, these matrices were initialised as unity matrices — a method successfully applied in similar contexts by van der Kooij et al. (1999) to predict human stance control actions [50]. The input values for the 32 off-diagonal matrix terms are zero, and the input values for the eight diagonal matrix terms are one. This choice assumes equal variance with no covariance across the parameters, a preliminary configuration pending further refinement based on empirical data.

The human balance controller utilises an LQR state weighting matrix $\mathbf{Q}_{LQR}$, with 36 parameters, and a control weighting matrix $\mathbf{R}_{LQR}$, with a single parameter. Following the choices made in the previous section, we set all terms in $\mathbf{Q}_{LQR}$ to zero except for the weight factor on the lean angle ϕ. The control effort weight in $\mathbf{R}_{LQR}$ was set to one.

The LQR weight factor on the lean angle Q_ϕ is the only parameter in the model for which the input value needs to be fitted to the filtered experimental data. We selected the input value for the weight factor on the lean angle Q_ϕ that yielded the highest resemblance to the filtered experimental data. We used the VAF of the steering angle as a performance indicator. An approach similar to the approach used to select the best option for each block of our cyclist control model. Section 4.2.4 gives more details of the fitting procedure.

An overview of the parameter inputs used in this study is provided in Table 4.1. The input value for the lean angle weight factor Q_ϕ is presented in the results section due to its dependence on the fitting process with experimental data.

4.2.3. EXPERIMENTAL DATASET

Moore (2012) [38] performed experiments in which the cyclist was lean-disturbed by pushing or pulling a rod attached at the seat-post of an instrumented bicycle for short periods. Our model's predictive performance and the calibration of the lean angle weight factor Q_ϕ are determined using this experimental dataset. Specifically, we utilised the raw data from the Davis Instrumented Bicycle Experiment [38].[1]

[1]The dataset used in this study is released under the Creative Commons BY 4.0 license and is available without modifications at `https://figshare.com/articles/dataset/Davis_Instrumented_Bicycle_`

Table 4.1: Summary of the parameters of the cyclist model with the assigned input value.

variable	*symbol*	*value*	*unit*
bicycle dynamics with passive cyclist contribution			
mass matrix	$\bar{\mathbf{M}}_0$	$\begin{bmatrix} 131.5085 & 2.6812 \\ 2.6812 & 0.2495 \end{bmatrix}$	$\mathrm{kg\,m^2}$
damping matrix	$\bar{\mathbf{C}}_1$	$\begin{bmatrix} 0 & 42.748 \\ -0.31806 & 1.6022 \end{bmatrix}$	$\mathrm{N\,s}$
stiffness matrices	$\bar{\mathbf{K}}_0$	$\begin{bmatrix} -116.19 & -2.7633 \\ -2.7633 & -0.94874 \end{bmatrix}$	$\mathrm{N\,s^2}$
	$\bar{\mathbf{K}}_2$	$\begin{bmatrix} 0 & 102.02 \\ 0 & 2.5001 \end{bmatrix}$	$\mathrm{N\,s^2/m}$
human multisensory integration for bicycle state estimation			
process noise covariance matrix	$\mathbf{Q}_K$	$\mathbf{I}_{6x6}$	-
measurement noise covariance matrix	$\mathbf{R}_K$	$\mathbf{I}_{2x2}$	-
human balance controller weight factors			
lean angle	Q_ϕ	variable	$1/\mathrm{rad^2}$
control effort	$\mathbf{R}_{LQR}$	$[1]$	$1/(\mathrm{Nm})^2$
muscular dynamics			
cut-off frequency	ω_c	$2.17 \cdot 2\,\pi$	rad/s
damping coefficient	ξ	$\sqrt{2}$	

The experiments were performed at constant forward speeds. The task description was to keep the bicycle upright. The bicycle was driven by an electric motor, keeping the bicycle at the desired constant forward speed. Details of the bicycle design can be found in Moore (2012) [38]. Both knee and upper-body movements were restricted for the experiments to mimic the rigid cyclist modeling assumption. The bicycle was fitted with a sensor set that could measure, among others, the following bicycle states and relevant variables: forward speed $\hat{v}_r$, lean angle $\hat{\phi}_r$, lean rate $\hat{\dot{\phi}}_r$, steering angle $\hat{\delta}_r$, and steering rate $\hat{\dot{\delta}}$. The rod with which the disturbances were applied had a force sensor to measure the disturbance force $\hat{F}_r$.

In preprocessing the experimental data, a crucial step involved distinguishing the cyclist's steer reactions to lean disturbances intended to recover balance from the disturbance, from continuous steer actions to maintain the desired heading and balance. This differentiation is achieved using a Finite-Impulse-Response (FIR) model. The FIR model is particularly suited for this purpose as it effectively isolates specific responses within a signal, devoid of any feedback from previous outputs, thereby clearly demarcating the cyclist's reactions to discrete disturbances. A comprehensive account of the FIR model's application and its efficacy in similar contexts is detailed in Schwab et al. (2013) [52].

`Experiment_Raw_Data/1164632` (accessed on June 16, 2024).

We apply the FIR model across entire runs that encompass multiple instances of disturbances. For a visual demonstration of the effectiveness of the FIR model, Figure 4.3 compares the raw measured steering angle data, indicated by $\hat{\delta}_r$, to the processed signal after applying the FIR model, denoted by $\hat{\delta}_f$.

The dataset had three different participants and two different environments. Experiments were conducted on a narrow horse treadmill and a wide indoor pavilion (see Figure 4.2). These experiments comprised 94 runs at four different speed regimes ranging from 2 to 7 m/s. The cyclists participating in the experiment were all male and of similar age, length and weight.

Figure 4.2: (a) A participant riding the instrumented bicycle on a horse treadmill. (b) A participant riding the instrumented bicycle in the indoor gymnasium. Both figures are adapted from Moore (2012) [38].[2]

Because all participants were of similar build, we used the same cyclist-bicycle specific matrices for the mass, damping and stiffness, as shown in Table 4.1.

However, the external force conversion matrix $\mathbf{H}_{fw}$ — which converts the lateral pulling force F at the seat post to an external lean and steer disturbance torque $\mathbf{W} = \mathbf{H}_{fw}F$ — was not the same for the three participants. For participants A and B,

$$\mathbf{H}_{fw} = \begin{bmatrix} 0.902 \\ 0.011 \end{bmatrix} \text{m},$$

and for participant C,

$$\mathbf{H}_{fw} = \begin{bmatrix} 0.943 \\ 0.011 \end{bmatrix} \text{m}.$$

As can be seen from the entries of the matrices, the lateral disturbance force F mainly causes a lean disturbance torque $T_{d\phi}$ with a minor steer disturbance torque $T_{d\delta}$.

[2]The original figures are released under Creative Commons BY 3.0. Modifications include obstructing recognisable faces for privacy and converting images to grayscale to match document formatting. Accessed on June 16, 2024. License details are available at https://creativecommons.org/licenses/by/3.0/.

4.2.4. PARAMETER IDENTIFICATION AND VALIDATION

In developing our cyclist control model, depicted in Figure 4.1, we used the Variance Accounted For (VAF) as a key metric to guide our selection of the model configurations and the input value for the weight factor on the lean angle Q_ϕ (in Section 4.2.2 we explained why we needed to fit this parameter). A higher VAF score indicates a more accurate model fit.

Specifically, the VAF was determined for the steering angle predicted by the cyclist control model δ_b with the filtered experimental steering angle $\hat{\delta}_f$. We choose the steering angle because a bicycle is balanced by the so-called steer-into-the-fall mechanism [37]. Therefore, the steering angle should represent the cyclist's balance control actions.

The VAF was calculated using the following formula:

$$VAF = \left(1 - \frac{\text{var}(\hat{\delta}_f - \delta_b)}{\text{var}(\hat{\delta}_f)}\right) \cdot 100\% \tag{4.6}$$

where var stands for the variance of the respective signals. This metric quantitatively reflects the proportion of variance in the experimental data that is accounted for by our model predictions, thus providing a robust measure of model performance.

The value chosen for the weight factor Q_ϕ was the one that maximised the VAF. To evaluate the predictive performance of the different options for each block of the cyclist control model, we selected the option that not only provided the highest VAF but also balanced model complexity and computational efficiency.

Because the experimental data was needed to fit a variable and evaluate the predictive performance, we divided the experimental dataset into a train and test set. For the fitting process, we utilised half of the existing experimental dataset from Moore (2012) [38], specifically selecting all runs with an even ID number. This subset was used to fit the weight factor Q_ϕ. The remaining half of the dataset, consisting of runs with an odd ID number, was employed to validate the model's predictive capabilities. The predictive performance was determined by calculating the VAF for this half of the dataset.

To find the optimal value for Q_ϕ, it does not make sense to begin the optimisation with an initial guess for Q_ϕ that does not result in a stable bicycle-cyclist system. Therefore, we first searched for an initial value for Q_ϕ that stabilised the bicycle, after which we further optimised Q_ϕ using the Pattern Search local optimisation method.

The optimisation procedure was run separately for each participant and each run. The final value for Q_ϕ was the median for all runs in each of the two environments, excluding outlier runs where no value could be found for Q_ϕ that stabilised the bicycle (see Table 4.4 in Appendix 4.A.3). This Q_ϕ value for the pavilion and treadmill environment was used to evaluate the model's predictive performance.

4.3. RESULTS

In the results section, we detail the outcomes of two key aspects of our study: 1) the optimisation of the weight factor Q_ϕ and 2) the predictive performance of our proposed model.

4.3.1. OPTIMISED WEIGHT FACTOR ON THE LEAN ANGLE Q_ϕ

The weight factor on the lean angle Q_ϕ is an important component of the state weighting matrix Q_{LQR} in the LQR formulation of our model's cost function. This parameter directly affects the steer torque output, T_c, determined by the human controller block. To identify the optimal input value for Q_ϕ, we conducted a fitting procedure using experimental data from Moore (2012) [38]. The optimal value was selected based on its ability to yield the best fit, determined by calculating the VAF of the steering angle predicted by the cyclist control model δ_b with the filtered measured response steering angle $\hat{\delta}_f$.

The VAF was calculated for an entire run, and a run contained multiple disturbances. An example time series of the predicted steering angle δ_b and the filtered measured human response steering angle $\hat{\delta}_f$ after one lean disturbance is shown in Figure 4.3. This run was performed on the treadmill and with a forward speed of 2.2 m/s. A weight factor Q_ϕ of 4324 1/rad^2 resulted in a maximum VAF score of 85.4 %.

In Figure 4.3, we can see that the predicted steering angle δ_b follows the filtered measured human response steer signal $\hat{\delta}_f$ for the first oscillation and then dampens out. The raw measured human response steering angle $\hat{\delta}_r$ shows additional steer oscillations, which could be steering actions to maintain a forward heading on the treadmill to not run off the treadmill. The cyclist control model does not consider this heading constraint.

The optimised lean angle LQR control weights Q_ϕ for all experimental runs are depicted in Figure 4.4. These weights are plotted as a function of forward speed, participant, and environment, revealing variations both between and within participants. The VAF scores associated with these optimised Q_ϕ are provided in Appendix 4.A.3.

Given the limited dataset, particularly in the treadmill environment, and the observed significant variability, a preliminary linear trendline was assumed. This trendline suggests a negligible dependency of the weights Q_ϕ on forward speed across both environments.

The average lean angle LQR control weight Q_ϕ is slightly higher for the treadmill environment. This is probably because more steer actions are required to maintain a forward heading so as not to run off the treadmill.

The final optimised lean angle LQR control weight Q_ϕ was taken to be the median value of the even runs of all three participants. This is a value of 1926 1/rad^2 for the treadmill and 995 1/rad^2 for the pavilion. These values were selected as the input value for Q_ϕ to determine the predictive performance of our proposed model.

4.3.2. PREDICTIVE PERFORMANCE OF THE MODEL

The predictive performance of our newly proposed cyclist control model was evaluated using odd-numbered runs, the parameter values listed in Table 4.1, and the lean angle LQR weight control factors Q_ϕ identified above. We calculated the VAF score by comparing the predicted steering angle, δ_b, from the cyclist control model to the filtered measured human response, $\hat{\delta}_f$. These results are presented in Table 4.2 and are sorted by forward speed, participant, and environment.

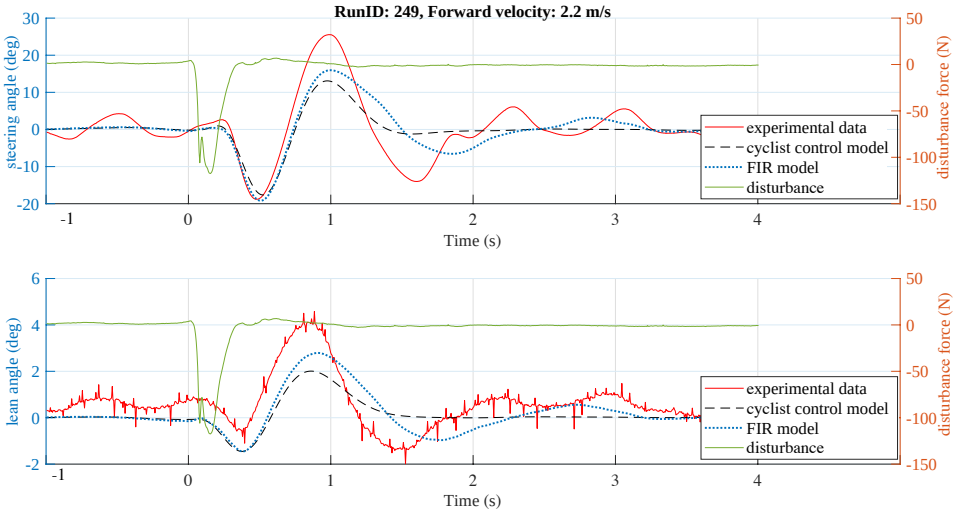

Figure 4.3: Time series example of a single lean disturbance response of the steering angle δ and the lean angle ϕ. The solid lines are the raw measured responses, where red is the steering angle signal and green indicates the lateral force disturbance signal. The dotted lines are the fitted finite impulse responses (FIR), and the dashed lines are the predicted model responses. The time series shows one disturbance out of a series of nine where the bicycle was riding on a treadmill at a constant forward speed of 2.2 m/s. The optimised Q_ϕ resulted in a maximum VAF score for respectively the steer and the lean angle of 85.4 % and 78.8 %.

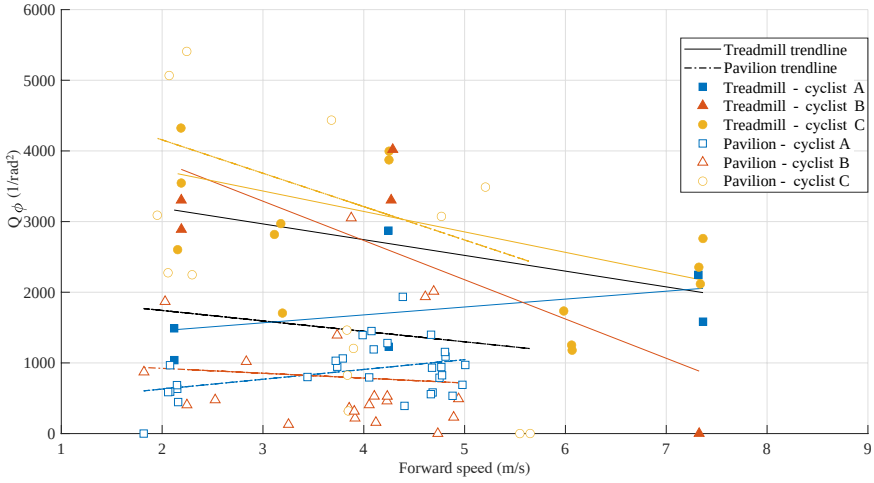

Figure 4.4: Optimised lean angle LQR control weight factors Q_ϕ as a function of the forward speed, for two different environments, the treadmill and the pavilion, and three different participants, together with the linear fitted trend lines for the treadmill and for the pavilion environment.

Table 4.2: Model predictive performance results on the test data, showing the mean *VAF* score for the steering angle in % together with the standard deviation and the number of runs (in brackets). The scores are given per participant, speed, environment, and all runs combined.

database	$v < 3.0$ *m/s*	$3.0 \leq v < 4.0$ *m/s*	$4.0 \leq v < 5.0$ *m/s*	$v \geq 5.0$ *m/s*	*all*
horse treadmill					
participant A	60.8 (0, 1)	N.A. (N.A., 0)	79.3 (0, 1)	80.0 (0, 1)	73.4 (10.9, 3)
participant B	74.8 (0, 1)	N.A. (N.A., 0)	26.3 (0, 1)	0 (0, 1)	33.7 (38.0, 3)
participant C	76.8 (4.7, 2)	66.5 (0, 1)	69.9 (23.3, 2)	85.5 (3.2, 2)	75.9 (12.4, 7)
all 3	72.3 (8.2, 4)	66.5 (0, 1)	61.3 (27.3, 4)	62.8 (6.6, 4)	65.6 (25.8, 13)
pavilion					
participant A	49.5 (15.7, 3)	84.7 (6.0, 5)	73.8 (15.0, 7)	81.0 (0, 1)	73.1 (17.1, 16)
participant B	34.4 (0, 1)	5.3 (7.5, 2)	35.7 (22.1, 5)	N.A. (N.A., 0)	27.9 (22.0, 8)
participant C	63.6 (10.9, 5)	61.4 (32.1, 2)	27.8 (6.2, 2)	0 (0, 1)	49.6 (26.3, 10)
all 3	55.6 (15.2, 9)	61.9 (35.8, 9)	53.6 (26.5, 14)	40.5 (29.0, 2)	55.6 (27.7, 34)

The VAF scores for the treadmill runs were generally higher than those for the pavilion runs, suggesting a more controlled cyclist response is necessary to avoid running off the treadmill.

4.4. DISCUSSION

The goal of this study was to develop a cyclist control model for the bicycle balance task with the perspective of safely and proactively studying what changes to cyclist control, such as training, can reduce the risk of falling during cycling.

Summary of key findings

Our proposed model incorporates human sensors with partial state feedback, multisensory integration for bicycle state estimation, human steer torque control and muscular dynamics. Most of these parameters are either easily measurable for individual cyclists or are generic and can be derived from existing literature. The lone exception among the cyclist control parameters was the LQR control weight for the lean angle, Q_ϕ, which was calibrated using experimental data from Moore (2012) [38].

The model's predictive performance, using this optimised Q_ϕ, was evaluated by comparing the model-predicted steering angle response to measured steering angle responses under two experimental conditions: cycling on a treadmill and cycling in a pavilion. The Variance Accounted For (VAF) was used as the performance indicator. The best-performing model had an average VAF score of 65.6% (standard deviation of 25.8%) for the experimental trials on the treadmill and 55.6% (standard deviation of 27.7%) for the experimental trials in the pavilion.

While these VAF scores may appear relatively low and exhibit considerable variability, the model effectively captures the key characteristics of cyclist control behaviour, particularly in the transient response (see Figure 4.3). Despite using a single generic value for Q_ϕ, the model successfully simulates the primary control features across different participants and varying speeds. This demonstrates its robustness in predicting balance recovery during cycling.

As shown in Table 4.4 in Appendix 4.A.3, the model's predictive performance could be improved by adjusting Q_ϕ for individual cyclists. However, a drawback of this approach

is that the weight factor Q_ϕ is complex and challenging to measure for cyclists who did not participate in the experiment, requiring a repetition of the experiments conducted by Moore (2012) [38].

Regarding the human sensors, our study reveals that cyclists need only two bicycle state variables — lean rate $\dot{\phi}$ and steering angle δ — to reconstruct a full state estimation of the bicycle, both of which exhibit no discernible delay. This finding aligns with the primary balance mechanism where a bicycle is balanced by steering into the fall [37].

Although one might expect a delay, our exploration found that the state estimator cancels out any added delay, leading to instability if a delay is introduced (for details, see appendix 4.A.1). We suspect that the state estimator creates a feed-forward system which cancels the delay, as also suggested by Dialynas et al. (2022) [53].

This study does not delve into the specific sensory system the cyclist employs. However, given the minimal delay, it is likely that the semicircular canals and muscle spindles play a key role. Nonetheless, it is important to note that the human sensory system is redundant, allowing for the possibility of using other sensory systems or a combination thereof. The sensory dynamics, such as explored by van der Kooij et al. (2001) [51], did not improve the predictive value of the cyclist's steer reactions when considering the added complexity. Nonetheless, incorporating these dynamics into cyclist control models could be beneficial for specific interventions, such as those for cyclists with vestibular impairments, allowing for the evaluation of how such conditions influence fall risk.

As previous studies have already validated the Carvallo-Whipple model for simulating the bicycle's response to small disturbances, we have confidence in the accuracy of the bicycle dynamics model. Besides the steering angle prediction, we see a similar predictive performance for the lean angle ϕ. The transient response of the predicted lean angle ϕ, filtered human response lean angle $\hat{\phi}_f$, and raw measured lean angle $\hat{\phi}_r$, shown in Figure 4.3 as well, reveal the quality of the bicycle dynamics model. The bicycle dynamics model predicts the lean angle ϕ with a VAF of 78.8%. Again, the predicted lean angle ϕ is especially accurate for the first oscillation. Note that noise and offset in the raw measured lean angle $\hat{\phi}_r$ is due to the sensor setup, which uses different types of sensors to measure the steer and lean angle respectively [38].

Another notable finding in this study is that the LQR control weight factor Q_ϕ shows only a slight trend with forward velocity, as shown in Figure 4.4. From this, we assume that the cyclist is optimising mainly his or her balance instead of his or her control effort. However, the significant variability observed and the assumption of a linear trendline limit the robustness of this conclusion. Future research should investigate alternative models or approaches to understand this relationship better.

In contrast, the control feedback gains, $\mathbf{K}$, derived from the LQR weight factors, do show a strong forward speed dependency, as can be seen in Figure 4.6 and 4.7 in Appendix 4.A.4. This is expected because the lateral stability of the bicycle strongly depends on forward speed [35]. The primary mechanism of steer-into-the-fall to recover balance from disturbances is observed by the negative values of the feedback gains on the lean angle ϕ and lean rate $\dot{\phi}$ which increase with decreasing forward speed because more steer effort is needed at lower forward speed. The feedback gain on the steering angle δ increases with forward speed, which indicates that the cyclist is stiffening his or

her arms up at higher speeds, whereas the steer damping is slightly decreasing.

Comparison with existing cyclist control models

In comparing our proposed model with existing cyclist control models, we observed several similarities with the models developed by Schwab et al. (2013) and Dialynas et al. (2022) [52, 53], which served as a foundation for our work. Like these models, our approach incorporates the Carvallo-Whipple bicycle model, passive rider dynamics, and muscular dynamics and does not account for sensory delays. However, our model differs by employing partial feedback and integrating human characteristics, in contrast to the full-state feedback used by Schwab et al. (2013) and Dialynas et al. (2022) [52, 53]. Specifically, we demonstrate that only the lean rate and steering angle are necessary as sensory inputs for balancing a bicycle.

Furthermore, our model's predictive performance has been validated across multiple cyclists, whereas Schwab et al. (2013) validated their model with only one cyclist [52]. In contrast, the model by Dialynas et al. (2022) underwent more extensive validation using experimental data from twenty participants in a less controlled environment [53].

The most significant advancement in our model is that it only requires one input value to be calibrated, which is the LQR weight factor on the lean angle Q_ϕ. The other input values are straightforward to measure. Notably, the weight factor's independence from forward speed implies that it requires calibration at only one speed, in contrast to the existing models, which necessitate the calibration of numerous input variables for each speed independently. This feature greatly improves the practical applicability of our cyclist control model.

Limitations

It is important to acknowledge several limitations of our study. First, our model has not yet been fully developed to investigate how changes in cyclist control reduce the risk of falls. The model's predictive performance was tested solely on the experimental data from Moore (2012) [38], which involved a specific set of conditions and three participants. Therefore, the model's performance under different conditions or with other cyclists remains to be determined.

The experimental conditions included knee and upper-body movement restrictions, which may not fully represent real-world cycling scenarios. Additionally, the narrow width of the treadmill compared to conventional cycling paths and the limited sample size may restrict the generalizability of the control strategies derived from the model. Moreover, the participants were exposed to only one type of small disturbance, and no falls were recorded. Control behaviour and bicycle dynamics likely differ in response to larger disturbances approaching the fall threshold. Thus, the model's predictive accuracy in such situations is yet unknown. Future studies should validate the cyclist control model across a broader range of conditions, including different populations and larger disturbances.

Given that the three participants in the current study shared similar backgrounds, it is plausible that the Q_ϕ value might vary for other populations, such as novice or senior cyclists (although our findings in Chapter 3 indicated that age is not a significant predictor of fall risk). Future research should investigate this potential variation to verify

the Q_ϕ's generalizability.

Additionally, the cyclist control model is limited to simulating the cyclist's reactions to recover balance from a disturbance. While the loss of balance is a commonly reported cyclist fall scenario [5], other cycling tasks must also be considered if we wish to simulate a broader range of bicycle crash scenarios. Other crucial tasks related to commonly reported cyclist fall scenarios are, for instance, braking, (dis)mounting or executing an evasive manoeuvre. Also, it focuses on the operational control level of the cyclist to recover balance once a disturbance is encountered. It might, however, be more effective to prevent the disturbance from occurring. This would require a more cognitive cyclist control model, which includes the detection of potential hazards, cognitive decision-making, guidance tasks, and balance tasks. The modular approach of the proposed cyclist control model would allow for expansions to incorporate these other tasks. For instance, a functional two-level driver model like Donges (1978) [56], consisting of guidance and stabilisation level, could be adapted to cyclists and combined with our cyclist control model.

Finally, our approach to model selection could be critiqued as an educated guess regarding the system architecture and its components. However, during the selection process, we also considered a naive bicycle model, sensory dynamics, state feedback with many sensory combinations, delays, predictors on/off, etc. Details of these explorations and their evaluations can be found in Appendix 4.A.1. Including all these variables and combinations in the optimisation process to fit the model to the experimental data proved to be complex and time-consuming and did not result in better results than the educated guess approach. Nevertheless, the model may represent a local optimum because not all possible combinations were explored.

Future research directions

In Chapter 3, we identified skill performance S as a critical characteristic for predicting the maximum disturbance from which a cyclist can recover balance. Skill performance S was defined as the cyclist's ability to maintain balance and follow a centreline under undisturbed conditions. This measure is both easier to obtain and more intuitive than the weight factor Q_ϕ. While the definitions of skill differ between the two studies, we hypothesise that skill performance S could be translated into the weight factor Q_ϕ.

Although this hypothesis may seem counterintuitive, it is essential to recognise that even during undisturbed cycling, cyclists continuously encounter small disturbances, such as pedalling or upper body movements, requiring constant adjustment. Furthermore, our analysis in Chapter 3, which employed Bayesian Model Averaging to identify key variables predicting the likelihood of a fall, suggested that skill performance S significantly predicts a fall outcome.

We recommend that future research explore the potential relationship between skill performance S and the weight factor Q_ϕ. Establishing this link further improves the practical application of the cyclist control model proposed in this study by enabling a more straightforward measurement of input values for individual cyclists.

Additionally, future work should focus on conducting cyclist fall experiments to validate the proposed cyclist control model, particularly in critical scenarios such as falls. Validating the model under these conditions would allow us to integrate it with

bicycle dynamics models to simulate various common crash scenarios. This approach would enable the proactive and safe evaluation of interventions designed to prevent falls, thereby strengthening the evidence base for interventions aimed at improving cycling safety.

Finally, although gain scheduling based on forward speed appears to offer only incremental improvements in predictive performance, a more nuanced approach may still be beneficial. Specifically, gain scheduling tailored to possible different phases following a disturbance could yield more significant results. We hypothesise that the cyclist's response may occur in distinct phases: an initial reflexive reaction to resist the handlebar disturbance, followed by a phase focused on recovering balance by steering toward the direction of the fall, and finally, a phase aimed at returning to straight-ahead cycling. In Figure 4.3, the reflexive reaction may be visible within the first 0.3 seconds post-disturbance, the balance recovery between 0.3 and 1.5 seconds, and the return to straight-ahead cycling thereafter. Further research is recommended to explore the potential of optimising individual gains for different cyclist's reaction phases following the disturbance to improve the model's predictive accuracy of the cyclist's response.

Practical implications

The modular structure of our model facilitates the integration of various control strategies, cyclist assistance systems, or simulations of specific medical conditions, offering practical applications for evaluating interventions aimed at reducing fall risk. For example, the model could be used to assess how medical conditions affecting the vestibular system influence cyclist fall risk, providing a foundation for developing targeted interventions. Moreover, the model's ability to predict a cyclist's response to disturbances can be used to design training programs or electronic cyclist assistance systems that improve cycling safety.

4.5. CONCLUSIONS

In conclusion, the proposed cyclist control model represents a significant step toward developing an approach for safely and proactively evaluating cyclist control interventions aimed at preventing cycling falls. We demonstrated that human balancing of a bicycle in motion, in response to disturbances, can be predicted by a cyclist control model, which has human characteristics and parameters that are intuitive and easy to measure or obtain, except for one parameter. That single parameter is the LQR control weight that minimises the lean angle deviation from the upright position and can be considered to reflect the balancing skill of a cyclist. This parameter was fitted on the experimental data. In this cyclist control model, the lean rate and steering angle provide enough information for the cyclist to control the bicycle in a realistic manner.

Our model for balancing a bicycle includes human characteristics that are more intuitive and easier to measure than existing cyclist control models. It has also been validated with experimental data from multiple cyclists. Road safety professionals and engineers can use the model to design effective training programs or control assistance systems and identify behavioural or physical factors that increase fall risk. While the model has promising prospects for these applications, future research is required to further validate the model's predictive accuracy in near or actual fall scenarios.

REFERENCES

[1] P. Schepers and K. Klein Wolt, *Single-bicycle crash types and characteristics,* Cycling Research International **2**, 119 (2012).

[2] P. Schepers, N. Agerholm, E. Amoros, R. Benington, T. Bjørnskau, S. Dhondt, B. de Geus, C. Hagemeister, B. P. Y. Loo, and A. Niska, *An international review of the frequency of single-bicycle crashes (SBCs) and their relation to bicycle modal share,* Injury Prevention **21**, e138 (2015), https://doi.org/10.1136/injuryprev-2013-040964.

[3] M. J. Boele-Vos, K. van Duijvenvoorde, M. J. A. Doumen, C. W. A. E. Duivenvoorden, W. J. R. Louwerse, and R. J. Davidse, *Crashes involving cyclists aged 50 and over in the Netherlands: An in-depth study,* Accident Analysis & Prevention **105**, 4 (2017), https://doi.org/10.1016/j.aap.2016.07.016.

[4] P. Hertach, A. Uhr, S. Niemann, and M. Cavegn, *Characteristics of single-vehicle crashes with e-bikes in Switzerland,* Accident Analysis & Prevention **117**, 232 (2018), https://doi.org/10.1016/j.aap.2018.04.021.

[5] R. Utriainen, S. O'Hern, and M. Pöllänen, *Review on single-bicycle crashes in the recent scientific literature,* Transport Reviews **43**, 159 (2023), https://doi.org/10.1080/01441647.2022.2055674.

[6] R. Elvik, *Area-wide urban traffic calming schemes: A meta-analysis of safety effects,* Accident Analysis & Prevention **33**, 327 (2001), https://doi.org/10.1016/S0001-4575(00)00046-4.

[7] A. Hoye, *Recommend or mandate? A systematic review and meta-analysis of the effects of mandatory bicycle helmet legislation,* Accident Analysis & Prevention **120**, 239 (2018), https://doi.org/10.1016/j.aap.2018.08.001.

[8] I. I. Hellman and M. Lindman, *Estimating the crash reducing effect of advanced driver assistance systems (ADAS) for vulnerable road users,* Traffic Safety Research **4**, 000036 (2023), https://doi.org/10.55329/blzz2682.

[9] N. Lubbe, Y. Wu, and H. Jeppsson, *Safe speeds: Fatality and injury risks of pedestrians, cyclists, motorcyclists, and car drivers impacting the front of another passenger car as a function of closing speed and age,* Traffic Safety Research **2**, 000006 (2022), https://doi.org/10.55329/vfma7555.

[10] T. Sayed, M. H. Zaki, and J. Autey, *Automated safety diagnosis of vehicle-bicycle interactions using computer vision analysis,* Safety Science **59**, 163 (2013), https://doi.org/10.1016/j.ssci.2013.05.009.

[11] A. R. A. van der Horst, M. de Goede, S. de Hair-Buijssen, and R. Methorst, *Traffic conflicts on bicycle paths: A systematic observation of behaviour from video,* Accident Analysis & Prevention **62**, 358 (2014), https://doi.org/10.1016/j.aap.2013.04.005.

[12] N. McNeil, C. M. Monsere, and J. Dill, *Influence of bike lane buffer types on perceived comfort and safety of bicyclists and potential bicyclists,* Transportation Research Record **2520**, 132 (2015), https://doi.org/10.3141/2520-15.

[13] J. Kovaceva, P. Wallgren, and M. Dozza, *On the evaluation of visual nudges to promote safe cycling: Can we encourage lower speeds at intersections?* Traffic Injury Prevention **23**, 428 (2022), https://doi.org/10.1080/15389588.2022.2103120.

[14] D. de Waard, P. Schepers, W. Ormel, and K. Brookhuis, *Mobile phone use while cycling: Incidence and effects on behaviour and safety,* Ergonomics **53**, 30 (2010), https://doi.org/10.1080/00140130903381180.

[15] W. P. Vlakveld, D. Twisk, M. Christoph, M. Boele, R. Sikkema, R. Remy, and A. L. Schwab, *Speed choice and mental workload of elderly cyclists on e-bikes in simple and complex traffic situations: A field experiment,* Accident Analysis & Prevention **74**, 97 (2015), https://doi.org/10.1016/j.aap.2014.10.018.

[16] R. Dubbeldam, C. T. M. Baten, P. T. C. Straathof, J. H. Buurke, and J. S. Rietman, *The different ways to get on and off a bicycle for young and old,* Safety Science **92**, 318 (2017), https://doi.org/10.1016/j.ssci.2016.01.010.

[17] J. Andersson, C. Patten, H. Wallén Warner, C. Andersérs, C. Ahlström, R. Ceci, and L. Jakobsson, *Bicycling during alcohol intoxication,* Traffic Safety Research **4** (2023), https://doi.org/10.55329/prpa1909.

[18] K. Kircher and A. Niska, *Interventions to reduce the speed of cyclists in work zones — cyclists' evaluation in a controlled environment,* Traffic Safety Research **6**, e000047 (2024), https://doi.org/10.55329/ohhx5659.

[19] C. Andersérs, J. Andersson, and H. W. Warner, *The importance of individual characteristics on bicycle performance during alcohol intoxication,* Traffic Safety Research **6**, e000042 (2024), https://doi.org/10.55329/vmgb9648.

[20] A. Niska and J. Wenäll, *Simulated single-bicycle crashes in the VTI crash safety laboratory,* Traffic Injury Prevention **20**, 68 (2019), https://doi.org/10.1080/15389588.2019.1685090.

[21] A. Niska, J. Wenäll, and J. Karlström, *Crash tests to evaluate the design of temporary traffic control devices for increased safety of cyclists at road works,* Accident Analysis & Prevention **166**, 106529 (2022), https://doi.org/10.1016/j.aap.2021.106529.

[22] Y. Peng, Y. Chen, J. Yang, D. Otte, and R. Willinger, *A study of pedestrian and bicyclist exposure to head injury in passenger car collisions based on accident data and simulations,* Safety Science **50**, 1749 (2012), https://doi.org/10.1016/j.ssci.2012.03.005.

[23] M. Fahlstedt, P. Halldin, and S. Kleiven, *The protective effect of a helmet in three bicycle accidents — a finite element study,* Accident Analysis & Prevention **91**, 135 (2016), https://doi.org/10.1016/j.aap.2016.02.025.

[24] C. Baker, X. Yu, B. Lovell, R. Tan, S. Patel, and M. Ghajari, *How well do popular bicycle helmets protect from different types of head injury?* Annals of Biomedical Engineering **52**, 3326 (2024), https://doi.org/10.1007/s10439-024-03589-8.

[25] V. Astarita, V. Giofré, G. Guido, and A. Vitale, *Investigating road safety issues through a microsimulation model,* Procedia-social and Behavioral Sciences **20**, 226 (2011), https://doi.org/10.1016/j.sbspro.2011.08.028.

[26] U. Shahdah, F. Saccomanno, and B. Persaud, *Application of traffic microsimulation for evaluating safety performance of urban signalized intersections,* Transportation Research Part C: Emerging Technologies **60**, 96 (2015), https://doi.org/10.1016/j.trc.2015.06.010.

[27] H. Twaddle, T. Schendzielorz, and O. Fakler, *Bicycles in urban areas: Review of existing methods for modeling behavior,* Transportation Research Record **2434**, 140 (2014), https://doi.org/10.3141/2434-17.

[28] C. M. Schmidt, A. Dabiri, F. Schulte, R. Happee, and J. K. Moore, *Essential bicycle dynamics for microscopic traffic simulation: An example using the social force model,* in *The Evolving Scholar-BMD 2023, 5th Edition* (2023) http://dx.doi.org/10.59490/649d4037c2c818c6824899bd.

[29] N. Rinke, C. Schiermeyer, F. Pascucci, V. Berkhahn, and B. Friedrich, *A multi-layer social force approach to model interactions in shared spaces using collision prediction,* Transportation Research Procedia **25**, 1249 (2017), https://doi.org/10.1016/j.trpro.2017.05.144.

[30] V. Keppner, S. Krumpoch, R. Kob, A. Rappl, C. C. Sieber, E. Freiberger, and H. M. Siebentritt, *Safer cycling in older age (SiFAr): Effects of a multi-component cycle training. a randomized controlled trial,* BMC Geriatrics **23**, 131 (2023), https://doi.org/10.1186/s12877-021-02502-5.

[31] L. Alizadehsaravi and J. K. Moore, *Bicycle balance assist system reduces roll and steering motion for young and older bicyclists during real-life safety challenges,* PeerJ **11**, e16206 (2023), https://doi.org/10.7717/peerj.16206.

[32] B. Janssen, P. Schepers, H. Farah, and M. Hagenzieker, *Behaviour of cyclists and pedestrians near right angled, sloped and levelled kerb types: Do risks associated to height differences of kerbs weigh up against other factors?* European Journal of Transport and Infrastructure Research **18**, 360 (2018), https://doi.org/10.18757/ejtir.2018.18.4.3254.

[33] F. Westerhuis, A. B. M. Fuermaier, K. A. Brookhuis, and D. de Waard, *Cycling on the edge: The effects of edge lines, slanted kerbstones, shoulder, and edge strips on*

cycling behaviour of cyclists older than 50 years, Ergonomics **63**, 769 (2020), https://doi.org/10.1080/00140139.2020.1755058.

[34] F. J. Whipple, *The stability of the motion of a bicycle,* Quarterly Journal of Pure and Applied Mathematics **30**, 312 (1899).

[35] J. P. Meijaard, J. M. Papadopoulos, A. Ruina, and A. L. Schwab, *Linearized dynamics equations for the balance and steer of a bicycle: A benchmark and review,* Proceedings of the Royal Society A: Mathematical, Physical and Engineering Sciences **463**, 1955 (2007), https://doi.org/10.1098/rspa.2007.1857.

[36] P. Basu-Mandal, A. Chatterjee, and J. M. Papadopoulos, *Hands-free circular motions of a benchmark bicycle,* Proceedings of the Royal Society A: Mathematical, Physical and Engineering Sciences **463**, 1983 (2007), https://doi.org/10.1098/rspa.2007.1849.

[37] J. D. G. Kooijman, J. P. Meijaard, J. M. Papadopoulos, A. Ruina, and A. L. Schwab, *A bicycle can be self-stable without gyroscopic or caster effects,* Science **332**, 339 (2011), https://doi.org/10.1126/science.1201959.

[38] J. K. Moore, *Human Control of a Bicycle,* Ph.D. thesis, University of California at Davis (2012).

[39] A. L. Schwab and J. P. Meijaard, *A review on bicycle dynamics and rider control,* Vehicle System Dynamics **51**, 1059 (2013), https://doi.org/10.1080/00423114.2013.793365.

[40] A. van Lunteren and H. G. Stassen, *Investigations on the bicycle simulator,* Annual report 1969 of the man-machine systems group , 3 (1970).

[41] J. K. Moore, J. D. G. Kooijman, A. L. Schwab, and M. Hubbard, *Rider motion identification during normal bicycling by means of principal component analysis,* Multibody System Dynamics **25**, 225 (2011), https://doi.org/10.1007/s11044-010-9225-8.

[42] P. Wang and J. Yi, *Dynamic stability of a rider-bicycle system: Analysis and experiments,* in *2015 American Control Conference (ACC)* (IEEE, Chicago, USA, 1-3 July 2015) pp. 1161–1166, https://doi.org/10.1109/ACC.2015.7170890.

[43] A. J. R. Doyle, *The skill of bicycle riding*, Ph.D. thesis, University of Sheffield (1987).

[44] R. Hess, J. K. Moore, and M. Hubbard, *Modeling the manually controlled bicycle,* IEEE Transactions on Systems, Man, and Cybernetics-Part A: Systems and Humans **42**, 545 (2012), https://doi.org/10.1109/TSMCA.2011.2164244.

[45] N. H. Getz, *Internal equilibrium control of a bicycle,* in *Proceedings of 1995 34th IEEE Conference on Decision and Control*, Vol. 4 (IEEE, New Orleans, USA, 13-15 December, 1995) pp. 4285–4287, https://doi.org/10.1109/CDC.1995.478913.

[46] M. Cook, *It takes two neurons to ride a bicycle,* Demonstration at NIPS **4** (2004).

[47] D. T. McRuer and H. R. Jex, *A review of quasi-linear pilot models,* IEEE transactions on Human Factors in Electronics , 231 (1967), https://doi.org/10.1109/THFE.1967.234304.

[48] D. Kleinman, *Optimal control of linear systems with time-delay and observation noise,* IEEE Transactions on Automatic Control **14**, 524 (1969), https://doi.org/10.1109/TAC.1969.1099242.

[49] T. Mergner, W. Huber, and W. Becker, *Vestibular-neck interaction and transformation of sensory coordinates,* Journal of Vestibular Research **7**, 347 (1997), https://doi.org/10.3233/VES-1997-7405.

[50] H. van der Kooij, R. Jacobs, B. Koopman, and H. Grootenboer, *A multisensory integration model of human stance control,* Biological Cybernetics **80**, 299 (1999), https://doi.org/10.1007/s004220050527.

[51] H. van der Kooij, R. Jacobs, B. Koopman, and F. van der Helm, *An adaptive model of sensory integration in a dynamic environment,* Biological Cybernetics 103-115 **84** (2001), https://doi.org/10.1007/s004220000196.

[52] A. L. Schwab, P. D. L. de Lange, R. Happee, and J. K. Moore, *Rider control identification in bicycling using lateral force perturbation tests,* Proceedings of the Institution of Mechanical Engineers, Part K: Journal of Multi-body Dynamics **227**, 390 (2013), https://doi.org/10.1177/1464419313492317.

[53] G. Dialynas, C. Christoforidis, R. Happee, and A. L. Schwab, *Rider control identification in cycling taking into account steering torque feedback and sensory delays,* Vehicle System Dynamics , 1 (2022), https://doi.org/10.1080/00423114.2022.2048865.

[54] A. E. Bryson and Y.-C. Ho, *Applied optimal control: Optimization, estimation, and control* (Routledge, 2018).

[55] M. Mulder, D. M. Pool, D. A. Abbink, E. R. Boer, P. M. T. Zaal, F. M. Drop, K. van der El, and M. M. van Paassen, *Manual control cybernetics: State-of-the-art and current trends,* IEEE Transactions on Human-Machine Systems **48**, 468 (2017), https://doi.org/10.1109/THMS.2017.2761342.

[56] E. Donges, *A two-level model of driver steering behavior,* Human Factors **20**, 691 (1978), https://doi.org/10.1177/001872087802000607.

[57] A. L. Schwab, J. P. Meijaard, and J. D. G. Kooijman, *Lateral dynamics of a bicycle with a passive rider model: Stability and controllability,* Vehicle System Dynamics **50**, 1209 (2012), https://doi.org/10.1080/00423114.2011.610898.

[58] A. Doria, M. Tognazzo, G. Cusimano, V. Bulsink, A. Cooke, and B. Koopman, *Identification of the mechanical properties of bicycle tyres for modelling of bicycle dynamics,* Vehicle System Dynamics **51**, 405 (2013), https://doi.org/10.1080/00423114.2012.754048.

[59] R. Hosman, *Pilot's Perception and Control of Aircraft Motions*, Ph.D. thesis, Delft University of Technology (1996).

[60] R. Happee, E. de Vlugt, and A. Schouten, *Posture maintenance of the human upper extremity; identification of intrinsic and reflex based contributions,* SAE International Journal of Passenger Cars: Mechanical Systems (2009).

4.A. APPENDICES

4.A.1. EXPLORATION OF DIFFERENT CYCLIST CONTROL MODELS

The cyclist control model presented in this chapter — from now on called the baseline model — is the one that best predicts the experimental data within the limits of our chosen model structure. This model is a simplified and reduced version of the elaborate model structure we used as a starting point. Due to the large model search space, we arrived at the baseline model based on educated guesses on the form an optimal controller for bicycle balancing might take. Which model options to investigate was based on our experience with the subject matter, intuition and findings during the subsequent simulations. This resulted in the baseline model presented in this chapter.

In this appendix, we substantiate our choices and present several trend studies around the baseline model to show the sensitivity of the different model components and variables. Mathematical descriptions of the different model components are also included.

The elaborate model, shown in Figure 4.5, is based upon the human stance control model presented in van der Kooij et al. (1999) [50], the cyclist control model presented in Schwab et al. (2013) [52] and the work by Dialynas et al. (2022) [53]. Compared to the baseline model, the elaborate model has the following two additional components: sensory dynamics, which are included in the human sensors block, and a predictor. Furthermore, one additional parameter can be optimised: the sensory and torque feedback delay τ.

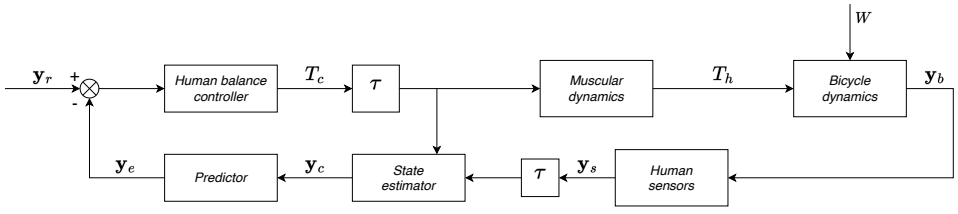

Figure 4.5: Block diagram of the elaborate system model for the human lateral balance control of a bicycle. The various blocks are the bicycle dynamics, including a rigid cyclist and passive cyclist contribution, human sensors with sensory dynamics to sense the state of the bicycle, a human time delay τ, a human multisensory integration to estimate the full state of the bicycle from the sensor data together with an internal model, a human state predictor, the human balance controller which outputs a desired steer torque, which after a delay is then applied to the bicycle through a muscular cyclist-arm dynamics block to the bicycle.

The elaborate model has the following component choices:

1. bicycle dynamics model
2. passive cyclist contribution
3. predictor on/off
4. sensor channels
5. sensory dynamics on/off
6. muscular dynamics on/off

and the following parameters that can be optimised:

1. optimal control LQR weights
2. sensory delay

During the semi-structured exploration approach, we observed that some components and variables had more effect on the predictive capabilities than others. To illustrate the sensitivity of the different components and variables, we performed a trend study of the baseline model. A summary of the different model versions that were analysed and their VAF score is shown in Table 4.3. Note that the order in the table does not indicate the order in which the model structures were investigated.

For our search, we simplified the internal bicycle model, removed the passive rider model, added delay, included sensory dynamics, explored different state feedback combinations, varied the Kalman filter parameters, added a predictor, placed LQR weights on different states, and removed muscular dynamics. Details of each model variant are described directly below.

BICYCLE DYNAMICS

To simulate the bicycle dynamics, we tested three models of different complexity: the Carvallo-Whipple (C-W) linear bicycle model, a simplified model we call the naive bicycle model, and a C-W model including passive cyclist contributions. Each model is described below.

Carvallo-Whipple linear bicycle model

The C-W bicycle model is already described in Section 4.2.1.

For control purposes, expressing the bicycle equations 4.1 in state-space form is convenient. The state-space representation is given by

$$\begin{aligned} \dot{\mathbf{y}}_b &= \mathbf{A}_b\mathbf{y}_b + \mathbf{B}_b\mathbf{f}_b \\ \mathbf{y}_s &= \mathbf{C}_b\mathbf{y}_b + \mathbf{D}_b\mathbf{f}_b \end{aligned} \tag{4.7}$$

with the state vector $\mathbf{y}_b = (\dot{\phi}_b, \dot{\delta}_b, \phi_b, \delta_b)^\top$, input vector $\mathbf{f} = (T_\phi, T_\delta)^\top$ and output vector $\mathbf{y}_s = (\dot{\phi}_s, \delta_s)^\top$.

Table 4.3: Characteristics of system model variants and their mean *VAF* score (in %) on a subset of the data for the treadmill and pavilion environment.

	bicycle model	*passive rider model*	*delay*	*sensory dynamics*	*feedback*	R_K	*predictor*	Q_{LQR} *weight factor*	*neuromuscular dynamics*	*average VAF score treadmill*	*pavilion*
most complete	C-W	x	0.06	x	$\phi, \dot{\phi}, \delta, \dot{\delta}, \psi$	*1	x	$\phi, \dot{\phi}, \delta, \dot{\delta}, T, \dot{T}, \psi$	x	63.0	68.1
baseline	C-W	x	0		$\dot{\phi}, \delta$	1		ϕ	x	67.7	72.2
# 1	*naive*	x	0		$\dot{\phi}, \delta$	1		ϕ	x	53.6	60.9
# 2	C-W		0		$\dot{\phi}, \delta$	1		ϕ	x	0	0
# 3	C-W	x	*0.06*		$\dot{\phi}, \delta$	1		ϕ	x	25.0	25.7
# 4	C-W	x	*0.06*		$\dot{\phi}, \delta$	1	*x*	ϕ	x	39.7	42.3
# 5	C-W	x	0	*x*	$\dot{\phi}, \delta$	1		ϕ	x	57.2	54.6
# 6	C-W	x	0		ϕ	1		ϕ	x	11.1	24.0
# 7	C-W	x	0		$\dot{\phi}$	1		ϕ	x	33.4	43.2
# 8	C-W	x	0		δ	1		ϕ	x	0	0
# 9	C-W	x	0		$\dot{\delta}$	1		ϕ	x	0	0
# 10	C-W	x	0		$\phi, \dot{\phi}$	1		ϕ	x	60.9	65.6
# 11	C-W	x	0		ϕ, δ	1		ϕ	x	5.1	7.4
# 12	C-W	x	0		$\phi, \dot{\delta}$	1		ϕ	x	8.9	4.8
# 13	C-W	x	0		$\dot{\phi}, \dot{\delta}$	1		ϕ	x	20.7	28.9
# 14	C-W	x	0		$\delta, \dot{\delta}$	1		ϕ	x	0	0
# 15	C-W	x	0		$\dot{\phi}, \delta$	0.01		ϕ	x	68.6	72.8
# 16	C-W	x	0		$\dot{\phi}, \delta$	100		ϕ	x	56.1	62.0
# 17	C-W	x	0		$\dot{\phi}, \delta$	1		$\dot{\phi}$	x	56.1	58.0
# 18	C-W	x	0		$\dot{\phi}, \delta$	1		δ	x	33.4	40.4
# 19	C-W	x	0		$\dot{\phi}, \delta$	1		$\dot{\delta}$	x	5.9	13.5
# 20	C-W	x	0		$\dot{\phi}, \delta$	1		T	x	13.7	23.2
# 21	C-W	x	0		$\dot{\phi}, \delta$	1		$\dot{T}$	x	0	7.2
# 22	C-W	x	0		$\dot{\phi}, \delta$	1		ψ	x	51.4	52.9
# 23	C-W	x	0		$\dot{\phi}, \delta$	1		ϕ		0	1.3

The system matrix **A**, input gain matrix **B**, output matrix **C** and direct feed-through matrix **D** are then given by

$$\begin{aligned}
\mathbf{A}_b &= \begin{bmatrix} -\mathbf{M}^{-1}(g\mathbf{K}_0 + v^2\mathbf{K}_2) & -\mathbf{M}^{-1}v\mathbf{C}_1 \\ \mathbf{I} & \mathbf{0} \end{bmatrix} \\
\mathbf{B}_b &= \begin{bmatrix} \mathbf{M}^{-1} \\ \mathbf{0} \end{bmatrix} \\
\mathbf{C}_b &= \begin{bmatrix} 1 & 0 & 0 & 0 \\ 0 & 0 & 0 & 1 \end{bmatrix} \\
\mathbf{D}_b &= \begin{bmatrix} \mathbf{0} \end{bmatrix}
\end{aligned} \tag{4.8}$$

The heading angle of the bicycle can be interesting information for the cyclist to use for the control task. The heading angle rate, $\dot{\psi}$, can be expressed as a function of linear bicycle model states, as in,

$$\dot{\psi} = \frac{v\cos(\lambda)}{w}\delta + \frac{c\cos(\lambda)}{w}\dot{\delta}$$

where v denotes the forward speed, λ represents the head tube angle of the bicycle, and w is the wheelbase [35].

The state-space form is then given by:

$$\begin{bmatrix} \dot{\psi} \end{bmatrix} = \begin{bmatrix} 0 & \frac{v\cos(\lambda)}{w} & 0 & \frac{c\cos(\lambda)}{w} & 0 \end{bmatrix} \begin{bmatrix} \dot{\phi} \\ \dot{\delta} \\ \phi \\ \delta \\ \psi \end{bmatrix} \tag{4.9}$$

Naive bicycle model

The naive bicycle model has the same three degrees of freedom as the C-W bicycle model, but the geometric parameters are very simplified. The model includes the following additional assumptions: the steering axis is straight, the trail is zero, and the wheels are massless. In addition, the model treats the entire system as a single-point mass with steering inertia. The mass, stiffness and damping matrices now only depend on five parameters: total mass m, centre-of-gravity height h, wheelbase w and the rotational inertia of the handlebars I.

Hence, the system matrices $\mathbf{M}_0$, $\mathbf{K}_0$, $\mathbf{K}_2$ and $\mathbf{C}_1$ reduce to the following matrices:

$$\bar{\mathbf{M}}_0 = \begin{bmatrix} mh^2 + I & 0 \\ 0 & I \end{bmatrix}$$

$$\bar{\mathbf{K}}_0 = \begin{bmatrix} -mh & 0 \\ 0 & 0 \end{bmatrix}$$

$$\bar{\mathbf{K}}_2 = \begin{bmatrix} 0 & \frac{mh}{w} \\ 0 & 0 \end{bmatrix}$$

$$\bar{\mathbf{C}}_1 = \begin{bmatrix} 0 & \frac{1}{2}mh \\ 0 & \frac{I}{w} \end{bmatrix}$$

The parameters are based on the bicycle-cyclist parameters of the experiment and round off to $m = 105$ kg, $h = 1$ m, $w = 1$ m, and $I = 0.1$ kgm^2.

Passive cyclist model
The passive cyclist model implemented is inspired by Schwab et al. (2013) [57] and Doria et al. (2013) [58]. Inertia, damping and stiffness are added to the steer equation, resulting in the following C-W type bicycle model:

$$\mathbf{M}\begin{bmatrix} \ddot{\phi} \\ \ddot{\delta} \end{bmatrix} + v\mathbf{C}_1\begin{bmatrix} \dot{\phi} \\ \dot{\delta} \end{bmatrix} + [g\mathbf{K}_0 + v^2\mathbf{K}_2]\begin{bmatrix} \phi \\ \delta \end{bmatrix} = \begin{bmatrix} T_\phi \\ T_\delta - I_r\ddot{\delta} - c_r\dot{\delta} - k_r\delta \end{bmatrix}$$

$$\mathbf{M}, \mathbf{C}_1, \mathbf{K}_0, \mathbf{K}_2 \in \mathbb{R}^{2x2} \quad (4.10)$$

For the free parameters, we used $I_r = 0.32$ kgm^2 as the inertial contribution, $c_r = 0$ Nms/rad as the damping contribution, and $k_r = 10$ Nm/rad as the stiffness contribution of the passive rider holding the handlebars.

SENSORY DYNAMICS

The sensory dynamics are implemented according to van der Kooij et al. (2001) [51], except for the semicircular canals where the parameters by Hosman (1996) [59] are used.

The transfer functions describing the various sensory organs are:

muscle spindle model:

$$\frac{\text{afferent fire rate}}{\text{joint angle}} = \frac{5(s+4)}{s+20} \quad (4.11)$$

Semicircular canals:

$$\frac{\text{afferent fire rate}}{\text{angular acceleration}} = \frac{80s}{1+80s} \cdot \frac{5.73(1+5.92s)}{(1+0.11s)(1+0.005s)} \tag{4.12}$$

Visual model:

$$\frac{\text{afferent fire rate}}{\text{visual cue}} = 1 \tag{4.13}$$

Tactile model:

$$\frac{\text{afferent fire rate}}{\text{force}} = \frac{s+0.01}{s+0.1} \tag{4.14}$$

STATE ESTIMATOR — KALMAN FILTER

State estimation is implemented with a Kalman filter according to van der Kooij et al. (1999) [50]. The free parameter is the measurement noise covariance matrix $\mathbf{R}_k$, which influences the Kalman gain $\mathbf{K}_k$. The Kalman gain is used to balance the weight given to incoming sensory data versus the data predicted by the internal model.

PREDICTOR AND DELAY (τ)

The optimal state estimate $\mathbf{x}_e[k]$, as a function of the optimal state estimate $\hat{\mathbf{x}}[k-\tau_s]$ from a Kalman filter, the (discrete) delay τ_s, and the delayed inputs, can be calculated using:

$$\hat{\mathbf{x}}[k] = \mathbf{A}^{\tau_s}\mathbf{x}[k-\tau_s] + \sum_{n=1}^{\tau_s} \mathbf{A}^{n-1}\mathbf{B}\mathbf{u}[k-n] \tag{4.15}$$

HUMAN BALANCE CONTROLLER

The linear-quadratic regulator (LQR) algorithm is used to find a controller that minimises undesired state deviations. The level of "undesiredness" of certain states are free parameters on the diagonal of the LQR weight matrix $\mathbf{Q}_{LQR}$. The weight factor on the control effort, $\mathbf{R}_{LQR}$, was taken as the unit for scaling purposes.

MUSCULAR DYNAMICS

For the muscular dynamics, we assume a second-order model, which for control purposes is convenient to express here in state-space representation by

$$\begin{aligned} \dot{\mathbf{x}}_h &= \mathbf{A}_h\mathbf{x}_h + \mathbf{B}_h\mathbf{f}_h \\ \mathbf{y}_h &= \mathbf{C}_h\mathbf{x}_h + \mathbf{D}_h\mathbf{f}_h \end{aligned} \tag{4.16}$$

with the state vector $\mathbf{x}_h = (T_h \quad \dot{T}_h)^\top$, input vector $\mathbf{f}_h = (T_c)$ and output vector $\mathbf{y}_h = (T_h)$.

The system matrix $\mathbf{A}_h$, input gain matrix $\mathbf{B}_h$, output matrix $\mathbf{C}_h$ and direct feed-through matrix $\mathbf{D}_h$ are then given in Equation 4.17 with a cut-off frequency $\omega_c = 2.17 \cdot 2\pi$

rad/s and the damping coefficient $\zeta = \sqrt{2}$ from Happee et al. (2009) [60] and Schwab et al. (2013) [52]. These values are also used in this paper.

$$\begin{aligned} \mathbf{A}_h &= \begin{bmatrix} 0 & 1 \\ -\omega_c^2 & -2\zeta\omega_c \end{bmatrix}, \qquad \mathbf{B}_h = \begin{bmatrix} 0 \\ \omega_c^2 \end{bmatrix} \\ \mathbf{C}_h &= \begin{bmatrix} 1 & 0 \end{bmatrix}, \qquad \mathbf{D}_h = \begin{bmatrix} 0 \end{bmatrix} \end{aligned} \tag{4.17}$$

4.A.2. STATE-SPACE MATRICES

This appendix contains the system matrix **A**, input gain matrix **B**, output matrix **C**, and direct feed-through matrix **D** for the cyclist control model described in section 4.2.1. The input system matrix **A** is defined as

$$\mathbf{A} = \begin{bmatrix} \mathbf{A}_{C_1} & \mathbf{A}_{K_1} & \mathbf{A}_M \\ \mathbf{I}_2 & \mathbf{0}_2 & \mathbf{0}_2 \\ \mathbf{0}_2 & \mathbf{0}_2 & \mathbf{A}_T \end{bmatrix}$$

with

$$\mathbf{A}_{C_1} = -\mathbf{M}^{-1} v \mathbf{C}_1$$

$$\mathbf{A}_{K_1} = -\mathbf{M}^{-1}(g\mathbf{K}_0 + v^2\mathbf{K}_2)$$

$$\mathbf{A}_M = \begin{bmatrix} \mathbf{M}^{-1} \cdot \begin{bmatrix} 0 \\ 1 \end{bmatrix} & \begin{matrix} 0 \\ 0 \end{matrix} \end{bmatrix}$$

$$\mathbf{A}_T = \begin{bmatrix} 0 & 1 \\ -\omega^2 & -2\zeta\omega \end{bmatrix}$$

$$\mathbf{I}_2 = \begin{bmatrix} 1 & 0 \\ 0 & 1 \end{bmatrix}$$

$$\mathbf{0}_2 = \begin{bmatrix} 0 & 0 \\ 0 & 0 \end{bmatrix}$$

The input gain matrix **B**, output matrix **C**, and direct feed-through matrix **D** are defined as

$$\mathbf{B} = \begin{bmatrix} 0 & 0 & 0 & 0 & 0 & \omega^2 \end{bmatrix}^T$$

$$\mathbf{C} = \begin{bmatrix} 1 & 0 & 0 & 0 & 0 & 0 \\ 0 & 0 & 0 & 1 & 0 & 0 \end{bmatrix}$$

$$\mathbf{D} = \begin{bmatrix} 0 \\ 0 \end{bmatrix}$$

4.A.3. VAF SCORES FOR THE OPTIMIZED LEAN ANGLE WEIGHT FACTOR Q_ϕ

The optimised lean angle LQR control weights Q_ϕ for all experimental runs were depicted in Figure 4.4. The VAF scores associated with these optimised Q_ϕ are provided in Table 4.4. The table displays the mean VAF scores as a function of forward speed, participant, and environment. The number of runs used to calculate the average VAF score is also indicated between brackets.

Table 4.4: The mean VAF scores (%) for the optimised lean angle LQR control weights Q_ϕ, along with the standard deviation and the number of runs used to calculate the average VAF between brackets. The scores are given per participant, speed, and environment and for all runs combined.

case	*$v < 3.0$ m/s*	*$3.0 \leq v < 4.0$ m/s*	*$4.0 \leq v < 5.0$ m/s*	*$v \geq 5.0$ m/s*	*all*
horse treadmill					
participant A	47.5 (19.4, 2)	N.A. (N.A., 0)	83.6 (1.5, 2)	67.3 (18.6, 2)	66.2 (20.1, 6)
participant B	73.3 (5.1, 2)	N.A. (N.A., 0)	49.9 (20.9, 2)	0 (0, 1)	49.3 (31.8, 5)
participant C	81.3 (6.0, 3)	81.6 (10.8, 3)	93.0 (4.6, 3)	84.5 (6.8, 6)	85.0 (7.8, 15)
all 3	69.4 (17.7, 7)	81.6 (10.8, 3)	78.0 (21.6, 7)	71.3 (29.0, 9)	73.8 (22.0, 26)
pavilion					
participant A	59.1 (10.8, 7)	85.5 (6.7, 5)	82.1 (6.0, 17)	81.0 (0, 1)	77.3 (12.4, 30)
participant B	67.2 (19.5, 5)	51.9 (11.0, 6)	46.9 (26.0, 10)	N.A. (N.A., 0)	53.2 (21.9, 21)
participant C	78.0 (13.2, 5)	63.1 (28.8, 7)	73.0 (27.6, 2)	15.6 (27.0, 3)	60.2 (31.4, 17)
all 3	67.0 (15.7, 17)	65.6 (22.9, 18)	69.3 (23.3, 29)	32.0 (39.4, 4)	65.6 (23.7, 68)

4.A.4. FEEDBACK GAINS OF THE HUMAN BALANCE CONTROLLER

We determined the feedback gains K_ϕ, K_δ, $K_{\dot{\phi}}$, $K_{\dot{\delta}}$, K_T, and $K_{\dot{T}}$ using the optimized roll angle LQR weights Q_ϕ. These gains are illustrated in Figure 4.6 for the treadmill and in Figure 4.7 for the pavilion.

Due to the experimental design, where measurements were taken at discrete speed intervals, the feedback gains derived from Q_ϕ are also discrete. To estimate continuous feedback gains for each participant, we employed the median of the lean angle LQR weights obtained from runs at each speed step.

Defining clear trends was challenging because of the limited number of observations in the treadmill setup and the significant variability inherent in these measurements. Consequently, we established preliminary trend lines — either linear or polynomial — based on our understanding of the dynamics involved and previous experiences. These are subject to future adjustments pending additional empirical validation.

For the construction of a generic cyclist controller, we calculated the median lean angle LQR weight from the even-numbered runs across all participants. This approach revealed noticeable differences between participants; however, the overall trends across the feedback gains were consistent.

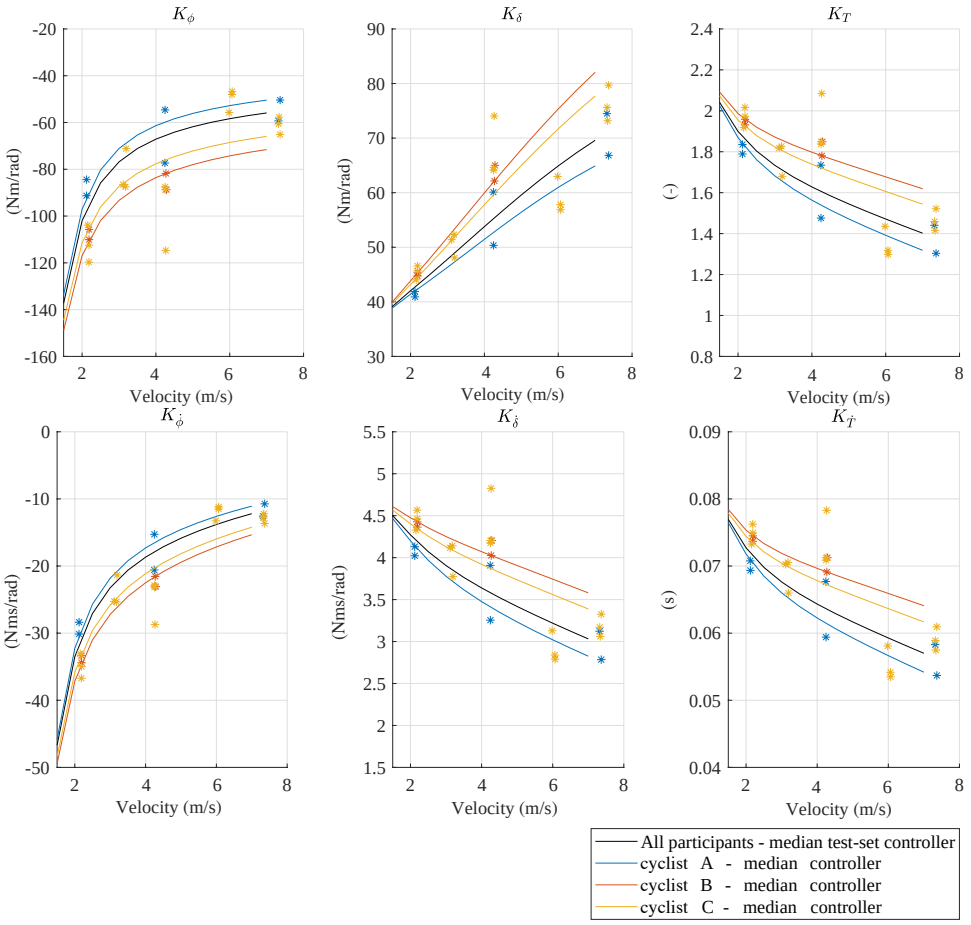

Figure 4.6: The six feedback gains K_ϕ, K_δ, K_T, $K_{\dot{\phi}}$, $K_{\dot{\delta}}$, and $K_{\dot{T}}$ for the optimized weight factor on the lean angle Q_ϕ in the cost function of the LQR controller for all runs performed on the treadmill as function of the forward speed and the participant. Markers are the discrete identified values, whereas solid lines are the trend lines of the median values.

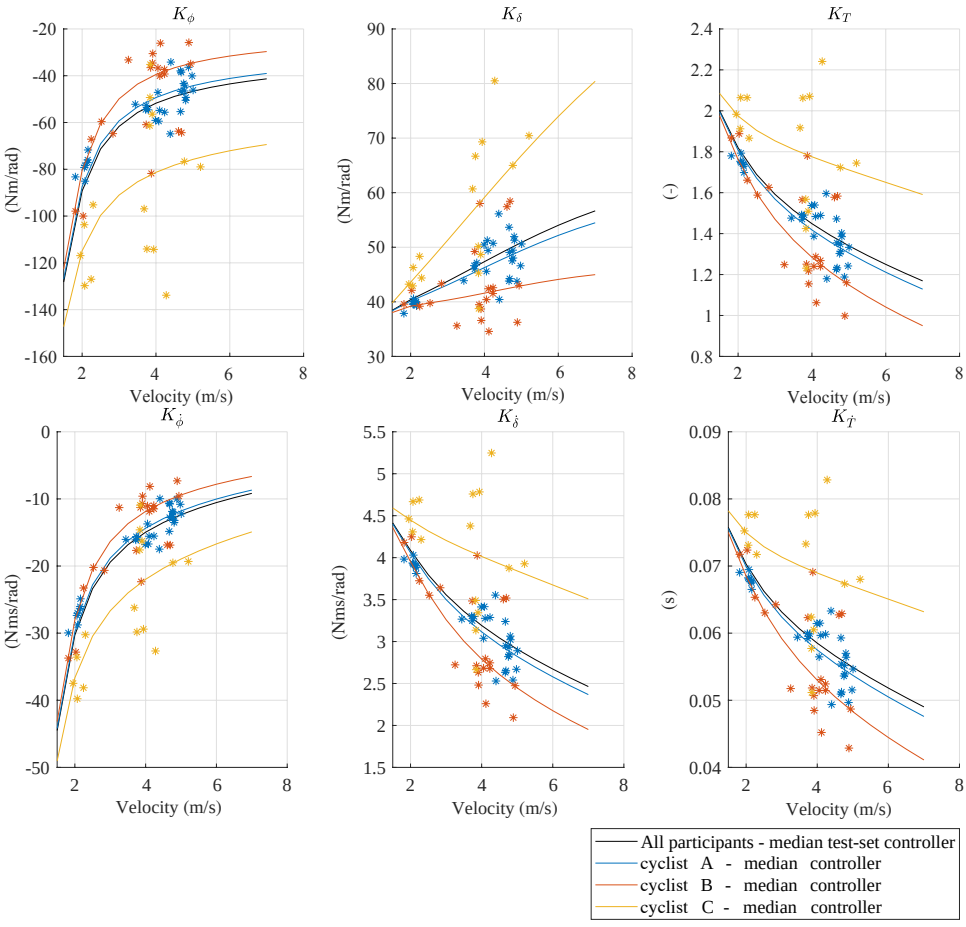

Figure 4.7: The six feedback gains K_ϕ, K_δ, K_T, $K_{\dot{\phi}}$, $K_{\dot{\delta}}$, and $K_{\dot{T}}$ for the optimized weight factor on the lean angle Q_ϕ in the cost function of the LQR controller for all runs performed in the pavilion as function of the forward speed and the participant. Markers are the discrete identified values, whereas solid lines are the trend lines of the median values.

5

A Model to Safely and Proactively Evaluate Cyclist Fall Prevention Interventions

M.M. Reijne, F.C.T. van der Helm and A.L. Schwab

Abstract

Loss of balance is a leading cause of serious injuries among cyclists, yet the safe and proactive evaluation of interventions to prevent such falls remains a challenge. The goal of this study was to develop and validate a practical and reliable approach for the safe and proactive evaluation of such interventions.

This study investigates the application of bicycle dynamics and cyclist control models as a novel approach for evaluating these interventions. These models use Newtonian mechanics and systems control theory to simulate a wide range of typical cyclist fall scenarios. They can incorporate various interventions aimed at improving cyclist control, bicycle design, and infrastructure. The Maximum Allowable Handlebar Disturbance (MAHD) can be combined with these models as a performance indicator to safely and proactively evaluate cyclist fall prevention interventions. The MAHD quantifies the maximum disturbance from which a cyclist can recover balance, where higher MAHD values correspond to a reduced probability of falling. Despite the potential of this approach, it has yet to be widely applied in the context of cyclist fall prevention.

In this study, we not only evaluated the reliability of a candidate bicycle dynamics and cyclist control model but also demonstrated its practical utility. We did this by

This Chapter is under review at IEEE Transactions on Human-Machine Systems.

comparing its MAHD predictions with experimental data where cyclists were subjected to handlebar disturbances that led to both falls and recoveries. Furthermore, we showcased the model's practicality through three illustrative case studies, evaluating interventions targeting cyclist control, bicycle design, and the lateral space available for balance recovery.

Our findings confirm the candidate model's accuracy in predicting MAHD across cyclists of varying skill levels and capturing the critical aspects of cyclist reactions to large disturbances. The model's Root Mean Square Error (RMSE) for MAHD predictions within the speed interval of 6 to 18 km/h was approximately 0.30 Nms for four different cyclists, each with different skill levels. Further analysis of the model's predictive performance revealed high Variance Accounted For (VAF) values for critical bicycle states, such as steering angle and heading, reinforcing the model's reliability. However, certain discrepancies were observed, such as a residual lateral offset of the cyclist relative to the treadmill's centreline, persisting three seconds post-disturbance. This indicates potential areas where the model could be refined for improved accuracy.

These results not only validate the model's reliability but also underscore its potential as a robust and practical approach for safely and proactively evaluating the effectiveness of different cyclist fall prevention interventions. This potential offers valuable insights for designers, engineers, and policy advisors focused on improving cycling safety.

5.1. INTRODUCTION

In countries with high cycling volumes, loss of balance is the leading cause of serious injuries among cyclists [1–5]. Yet, existing approaches to evaluate interventions aimed at preventing such falls face significant methodological challenges. The goal of this study is to develop and validate a practical and reliable approach for the safe and proactive evaluation of cyclist fall prevention interventions.

Several approaches have been developed to evaluate cycling safety interventions. These approaches include crash data analysis [6–9], video-based surrogate safety analyses, which focus on conflict events and near-misses [10, 11], experimental and field studies [12–19], controlled crash experiments [20–24] and models that simulate traffic scenarios [25–29].

While these approaches have been proven valuable in evaluating cycling safety interventions, these approaches face limitations when evaluating cyclist fall prevention interventions, especially those aiming to reduce fall risk in critical situations. Examples of such interventions include training programs for improving balance skills [30], steer-assist systems [31], infrastructure design improvements such as sloped kerbs [32], and ridable road shoulders [33].

Bicycle crash data underreport single bicycle crashes, which are mainly falls [2]. Surrogate safety indicators focus predominantly on interactions with other road users, overlooking falls that occur with the involvement of other road users, which represent the majority of cycling-related injuries [5]. Experimental and field studies often focus on indirect indicators of fall risk, such as perceived safety, workload or lean angles, but the reliability to directly predict fall risk has not yet been completely proven. Meanwhile, crash-testing experiments and simulation models typically focus on post-crash injury mitigation and cannot be applied to evaluate interventions that aim to

prevent falls. Additionally, existing models that simulate traffic scenarios — including traffic, behavioural and crash avoidance models — fail to integrate the balance task and lateral bicycle dynamics necessary to simulate fall scenarios realistically.

In contrast, bicycle dynamics and cyclist control models show potential in safely and proactively evaluating cyclist fall prevention interventions. As established in Chapter 1, these models can simulate a wide range of commonly reported crash types, including falls without the involvement of other road users, and incorporate a variety of interventions related to the bicycle, cyclist, and environment. Despite their potential, these models have yet to be used to evaluate cycling safety interventions. Their reliability and practicality to safely and proactively evaluate cyclist fall prevention interventions have yet to be determined.

The goal of this study is to evaluate the reliability and practicality of an existing candidate bicycle dynamics and cyclist control model. We evaluate the reliability of this model's predictions by comparing them to experimental data where cyclists were subjected to handlebar disturbances that led to both falls and recoveries. Furthermore, we apply this candidate model to safely and proactively evaluate three interventions: one focused on bicycle design, one on bicycle control, and one on infrastructure design.

The findings of this study will contribute to establishing confidence in the use of this approach for reliably and proactively evaluating cyclist fall prevention interventions. As such, this approach will broaden the range of interventions that can be safely and proactively evaluated, supporting engineers in designing safer infrastructure and bicycles and supporting road safety professionals in developing effective training programs.

5.2. METHOD

In this study, we aim to evaluate the reliability and practicality of an existing candidate bicycle dynamics and cyclist control model to evaluate cyclist fall prevention interventions safely and proactively.

The candidate bicycle dynamics model chosen for this purpose is the Carvallo-Whipple bicycle model combined with the cyclist balance control model developed in Chapter 4. We evaluate the reliability of this model's predictions by comparing them with experimental data collected in Chapter 3, where cyclists were subjected to handlebar disturbances that led to both falls and recoveries.

Specifically, we evaluate the model's ability to predict the Maximum Allowable Handlebar Disturbance (MAHD) from which a cyclist can recover balance. This indicator was introduced in Chapter 2 as a practical indicator to safely and proactively evaluate cyclist fall prevention interventions. Additionally, we evaluate the model's predictions regarding several states of the bicycle in response to large disturbances to verify if the model cannot only predict the boundary for which a cyclist can no longer recover balance but can also capture the cyclist's control reaction.

This method section provides an overview and rationale for the chosen candidate bicycle dynamics and cyclist control model in section 5.2.1. Section 5.2.2 outlines the experiments used for comparison with the model's predictions. In Section 5.2.3 we describe the approach we used to evaluate the candidate model's predictions for the MAHD, while Section 5.2.4, explains the approach for evaluating the candidate model's

predictions of the cyclist's response to a large disturbance.

To evaluate the practicality of this candidate model, we apply it to evaluate three different interventions. The methodology and results of this application are presented in Section 5.4.

5.2.1. CANDIDATE BICYCLE DYNAMICS AND CYCLIST CONTROL MODEL

The bicycle dynamics and cyclist control model consists of a bicycle dynamics model, which simulates the motions of the bicycle, and a cyclist control model, which simulates the control actions of the cyclist. For our candidate model that we aim to evaluate, we have chosen the Carvallo-Whipple (C-W) bicycle model to simulate the bicycle dynamics and the cyclist control model for the balancing task developed in Chapter 4 to simulate the cyclist's control actions.

Below, we provide a brief overview. For more details about the C-W bicycle model we used, the reader is referred to Meijaard et al. (2007) [34]. An overview of more accessible language can be found in Chapter 1. For more details about the cyclist control model, the reader is referred to Chapter 4.

Bicycle dynamics model

The C-W model models the bicycle as a system composed of four rigid, laterally symmetric components: two wheels aligned behind each other and the front and rear frames. The front wheel is connected to the front frame via a horizontal revolute joint, enabling it to rotate, while the rear wheel is similarly connected to the rear frame. A vertical or inclined revolute joint links the front and rear frames such that the handlebar and front wheel can rotate with respect to the rear frame.

The cyclist is assumed to be a rigid cyclist where the mass and inertia are added to the rear and front frame. The rigid cyclist assumption assumes the cyclist does not move relative to the bicycle. Although this assumption might seem counterintuitive, theoretical and experimental studies have demonstrated its validity. These studies have shown that steering is the primary mechanism for balancing a bicycle and that upper-body movements have a negligible impact on the balancing task when the cyclist's hands are on the handlebars [35–37].

Several key assumptions underlie the model: the road surface is flat, both wheels maintain in contact with the ground, the wheels have knife-edge contact with the surface, and there is zero longitudinal and lateral slip. As a result, the C-W model has three degrees of freedom: forward speed v, the lean angle of the rear frame ϕ and the steering angle of the front frame with respect to the rear frame δ.

The motion of the bicycle, governed by these three degrees of freedom, can be described by a set of nonlinear equations [38] or by three linearised equations of motion if we consider normal cycling conditions, with small disturbances about the steady upright and straight-ahead motion [34].

We selected the C-W bicycle model because it is the simplest model that still accurately captures bicycle dynamics [34]. The C-W model has been validated for conditions where the bicycle recovers balance after small disturbances [36, 39]. Moreover, the model has been tested and validated for different bicycles [40]. These validations provide confidence that the C-W model is reliable for simulating bicycle

motion.

Furthermore, we have chosen to describe the lateral dynamics of the bicycle, which consists of the lean rate $\dot{\phi}$ and the steering rate $\dot{\delta}$, using the linearised equations of motion, because this approach simplifies the practical application of the C-W model. These linearised equations are generally accurate for lean and steering angles up to 45 degrees [38], which we consider adequate for simulating the experimental conditions and commonly reported crash scenarios. We will revisit this in Section 5.2.3.

In this context, the forward speed v is assumed constant, and the lateral motions are described by the equation:

$$\mathbf{M}\ddot{\mathbf{q}} + v\mathbf{C}_1\dot{\mathbf{q}} + [g\mathbf{K}_0 + v^2\mathbf{K}_2]\mathbf{q} = \mathbf{T} \tag{5.1}$$

where the time-varying variables are the lean and the steering angle (i.e. $\mathbf{q} = (\phi, \delta)^\top$). The torques on the right-hand side, $\mathbf{T} = (T_\phi, T_\delta)^\top$, consist of external disturbance torques such as wind gusts, which can induce a steer or lean torque or a combination thereof, and cyclist-applied torques, which in our chosen cyclist control model only includes a steer torque. The constant terms ($\mathbf{M}$, $\mathbf{C}_1$, $\mathbf{K}_0$, $\mathbf{K}_2$) are specific to the bicycle-cyclist system and account for mass, damping, and stiffness properties.

The rigid-cyclist bicycle model was extended to include a passive rider model to account for the passive contributions of the cyclist's arms and hands to the steering assembly. This extension introduces the cyclist's influence on the steering torque T_δ in the equations of motion. The constant coefficient matrices are adjusted accordingly to $\bar{\mathbf{M}}$, $\bar{\mathbf{C}}_1$, $\bar{\mathbf{K}}_0$, and $\bar{\mathbf{K}}_2$.

Finally, the kinematic equations describing the bicycle's heading angle ψ and the lateral positions of the rear and front wheel ground contact points (y_P,y_Q) can be described by the linear state equations:

$$\dot{\psi} = (v\delta + c\dot{\delta})\cos\lambda / w \tag{5.2}$$

$$\dot{y}_P = v\psi \tag{5.3}$$

$$y_Q = y_p + w\psi - c\delta\cos\lambda \tag{5.4}$$

where w is the wheelbase, c is the trail, and λ is the steer axis tilt of the bicycle [34].

Cyclist control model

For the cyclist control model, we have chosen to use the model developed in Chapter 4, which can simulate the cyclist's reaction to recover balance after a disturbance. This model assumes the cyclist uses steer torque control only to balance the bicycle and optimises the control actions to recover balance. In addition, the model includes human characteristics like partial state feedback, muscular dynamics and multisensory integration to reconstruct an estimate of the full state of the bicycle.

Our choice for this cyclist control model was based on the facts that it includes human characteristics which are relatively more intuitive and easier to measure compared to other existing cyclist control models [41, 42], and that this model has been validated with experimental data of multiple cyclists.

The full state of the bicycle-cyclist system ($\mathbf{y}_e = (\dot{\phi}_e, \dot{\delta}_e, \phi_e, \delta_e, T_e, \dot{T}_e)^\top$) is estimated using a Kalman filter based on two sensor states: the lean rate $\dot{\phi}$ and the steering angle δ. The Kalman filter consists of the process noise covariance matrix $\mathbf{Q}_K$ and a measurement noise covariance matrix $\mathbf{R}_K$.

The bicycle is only controlled by a steering torque, which is determined by a linear feedback system and muscular dynamics. The gains of the feedback system are determined using the LQR approach. The system's control law has the form,

$$\mathbf{T}_c = -\mathbf{K}(\mathbf{y}_e - \mathbf{y}_r), \tag{5.5}$$

where $\mathbf{y}_e$ represents the estimated state vector, $\mathbf{y}_r$ is the references state vector, and $\mathbf{T}_c = (T_c)$ denotes the steer torque. For the straight-ahead balancing task, the reference state $\mathbf{y}_r$ is all zeros. The feedback gain matrix $\mathbf{K}$ is a row vector with the same number of entries as the state vector $\mathbf{y}$. Gain scheduling, to adjust the controller gains based on the forward speed v, is applied to incorporate the dependency of the dynamics of the bicycle on forward speeds.

The six feedback gains are determined using the LQR optimal control formulation where the cost function $J = \int (\mathbf{y}_e^\top \mathbf{Q}_{LQR} \mathbf{y}_e + \mathbf{T}_c^\top \mathbf{R}_{LQR} \mathbf{T}_c) \mathrm{d}t$ is minimized. Here $\mathbf{Q}_{LQR}$ is the state weighting matrix, and $\mathbf{R}_{LQR}$ is the control weighting matrix. These matrices are designed to minimise both deviations from the desired state and control efforts, respectively.

For the cyclist control model developed in Chapter 4, all terms of the matrices $\mathbf{Q}_{LQR}$ are assumed to be zero except for the weight factor on the roll angle in the state weighting matrix, which is the third diagonal term in $\mathbf{Q}_{LQR}$. We define this specific weight factor as Q_ϕ. The corresponding control weight $\mathbf{R}_{LQR}$ was chosen to be one, because of the free scaling of the cost function J.

We made one small modification to the cyclist control model presented in Chapter 4. We extended the state of the bicycle, reconstructed by the state estimator, with the kinematic variables for the heading, ψ, and the lateral displacement of the front wheel contact point, y_Q, and added a non-zero weight factor in the LQR control matrix on this state as well Q_{y_Q}. These states can be determined from the linearised kinematic differential equations, which describe the motion of the contact points (Equations 5.2-5.4).

We added this because the treadmill's limited width becomes a constraint for larger disturbances. As it happened, all falls in the cyclist fall experiments described in Chapter 3 were the result of riding off the side of the treadmill. The limited width of the treadmill was not a constraint for the experiments on which the cyclist control model was validated in Chapter 4, in which the participants were only exposed to small disturbances.

Finally, the torque command from the controller T_c is translated to the torque applied on the handlebars T_h via the muscular dynamics submodel. The torque applied on the handlebars T_h is the control input torque for the bicycle dynamics model. The muscular dynamics submodel consists of a second-order low pass filter, including a cut-off frequency ω_c and damping coefficient ζ, and by the following transfer function:

$$H_n(s) = \frac{T_h(s)}{T_c(s)} = \frac{\omega_c^2}{s^2 + 2\zeta\omega_c s + \omega_c^2} \tag{5.6}$$

5.2.2. EXPERIMENTAL DATA

We aim to compare the candidate model's predictions to the data collected from a series of experiments conducted in Chapter 3. These experiments were designed to simulate cyclist falls and recoveries due to a large handlebar disturbance. We have chosen this dataset as these were the first experiments to simulate actual cyclist falls in a safe and controlled environment.

The experiments were conducted on a treadmill, and the participants cycled on a standard Dutch city bicycle equipped with various sensors (see Figure 3.1). The setup included a perturbator system for applying controlled impulse-like disturbances to the handlebars, which resulted in either falls or recoveries. This perturbator system consisted of four ropes attached to the handlebars of the bicycle. Two ropes were attached in the front direction and two in the aft direction. The tension in the ropes could be controlled with a motor using force sensors aligned in series with the ropes as feedback. We regulated the motors to apply step-input handlebar disturbances of 0.3 seconds.

Many precautions were taken to ensure the experiment's safety, including having participants wear an intelligent safety harness that freezes when a fall is detected, wearing bicycle helmets, and surrounding the treadmill with padding.

A total of 24 participants participated in the experiments, divided equally into two age groups: 12 participants aged 20-35 years and 12 participants aged 60 years or older. Both groups were balanced for gender and had similar distributions of height and weight, representative of the average Dutch population. All participants were experienced cyclists, in good health, and cycled regularly.

Participants were first acclimated to the experimental setup by learning to cycle on the treadmill and gaining trust in the safety harness. Once comfortable, they were subjected to a series of 20 controlled handlebar disturbances while cycling at three different speeds. The three speeds were 6 km/h, 12 km/h, and 18 km/h. The disturbance was always applied when the cyclist was cycling in the middle of the treadmill straight ahead and upright. The disturbances varied in magnitude and direction, with a random and adaptive staircase procedure employed to determine the threshold at which participants could no longer recover balance. This protocol ensured all participants fell approximately on average for 10 of the 20 trials. The experiments generated a total of 928 trials, where each disturbance was categorised as a separate trial.

An optoelectronic measurement system collected signals just before and after each disturbance for the position of nine markers on the bicycle, from which the bicycle's states can be reconstructed. The magnitude of the disturbance, quantified as an angular impulse, could be reconstructed from the force sensors.

In addition, a parameter called skill performance S was collected for each participant. This parameter reflects the ability of the cyclist to maintain balance and follow a centreline while cycling undisturbed. It was determined separately for each of the three forward speeds and defined as the standard deviation of the lateral position of

the front wheel ground contact point y_Q during one minute of cycling, during which the cyclist was instructed to follow the centreline of the treadmill. The skill performance S was determined in the final learning phase, just before the disturbances were applied. The lateral position of the front wheel ground contact point y_Q was reconstructed from position measurement data of nine markers placed on the bicycle using rigid body constraints and least square methods.

Note that other parameters, such as mass, age and reaction time, were also collected. However, via Bayesian Model Averaging, the predictive performance of these parameters for the MAHD was found to be limited. For more details, the reader is referred to Chapter 3.

5.2.3. APPROACH TO EVALUATE THE MAXIMUM ALLOWABLE HANDLEBAR DISTURBANCE PREDICTION OF CANDIDATE MODEL

Unfortunately, the MAHD predictions of the candidate bicycle dynamics and cyclist control model could not be directly compared to those of the experiments. The predictions could not be compared directly because the candidate model requires an input value for the weight factor, which minimises lean angle deviations Q_ϕ — as part of the LQR controller. However, this weight factor Q_ϕ was not directly measured for the participants who took part in the experiments.

The weight factor Q_ϕ reflects a cyclist's balancing skill. In our experiments in Chapter 3, we defined and measured each participant's skill performance metric S. This variable reflected how well a cyclist could track a centerline while cycling undisturbed (see section 5.2.2). While the definitions of skill vary between the two studies, we hypothesise that skill performance S can be translated into the weight factor Q_ϕ, and therefore in the feedback gains $\mathbf{K}$.

While this may appear counterintuitive, it is important to recognise that even during undisturbed cycling, cyclists are continually subjected to small disturbances, such as those arising from pedalling, upper body movements or small bumps on the road, to which they must respond. Furthermore, our analysis in Chapter 3, which used Bayesian Model Averaging to identify key variables predicting the probability of a fall, suggested that skill performance S is an important predictor of this outcome.

Given that the MAHD varied with forward speed for each cyclist, but Q_ϕ was shown to be independent of forward speed (see results in Chapter 4), we conducted a test in this study to evaluate if Q_ϕ can be translated to skill performance S. For this test, Q_ϕ was calibrated by matching it to the MAHD predictions of the Bayesian model for a given cyclist with a specific skill performance S over a forward speed range of 6 to 18 km/h. The quality of the fit was optimised using the root-mean-square-error (RMSE) of the MAHD.

In this study, RMSE was used as a metric both to evaluate the correspondence between Q_ϕ and S and to evaluate whether the bicycle dynamics and cyclist control models can reliably predict the MAHD trend for cyclists with different skill levels S across a range of forward speeds v.

MAHD values derived from experimental data

Due to the nature of human-subject experiments, there was often no clear-cut boundary

per participant in the disturbance threshold between falling and being able to recover balance. We have chosen to use the Bayesian multilevel logistic regression model, developed in Chapter 3, to translate the binary experimental outcomes of falls and recoveries into a continuous function that describes the probability of a cyclist falling given the magnitude of the handlebar disturbance. We have chosen for the MAHD the disturbance magnitude for which the cyclist has a 50 % chance of falling, following the definition for the MAHD proposed in Chapter 2.

The independent variables of the Bayesian model include the participant identification number i, the disturbance identification number j, forward speed v, the steering rate at the moment the disturbance was applied $\dot{\delta}_0$, a skill performance indicator S, the rotational direction of the disturbance d and the lean angle at the moment the disturbance was applied ϕ_0.

The MAHD and its confidence interval can be determined for a cyclist using the following equation:

$$\Delta L_{50\%}(x^1,\ldots,x^K) = -\frac{\beta_0 + \beta_i + \sum_{k=1}^{6} \alpha_k x^{(k)}}{\gamma} \tag{5.7}$$

Here, the variable $\Delta L_{50\%}$ is the value of the angular impulse for which the probability of falling equals 50% and represents the MAHD. The variables β_0 and β_i represent the individual variations within the group of participants who participated in the experiments and can be interpreted as the ability of the ith participant. The vector x contains the predictors of the model, defined as $x = (\phi_0, 1_{\{d=\text{CW}\}}, S, \dot{\delta}_0, v, j)^T$. The vector α includes the coefficients of the predictors, and the scalar γ is the coefficient related to the angular momentum of the disturbance ΔL.

The posterior distribution of the MAHD can be approximated using Monte Carlo simulation, as the fitted model presented in Chapter 3 includes the posterior distribution of $(\beta_0, \sigma_\beta, \alpha_k, \gamma)$, where σ_β is the standard deviation of the participant-specific random effects β_i. The posterior distribution of the MAHD for cyclist i can then be approximated as follows:

1. take a posterior sample $(\sigma_\beta, \beta_0, \{\alpha_k\}, \gamma)$;
2. sample β_i from a Normal distribution with σ_β;
3. compute the MAHD according to Equation 5.7 with $\beta = \beta_i$;
4. repeat steps (1) to (3) a large number of times.

The participant identification number i is unavailable for cyclists who did not participate in the experiments. This limitation can be overcome by sampling from distributions of the participants who did participate in the experiment, which is done in step 2.

For this study, we defined four cyclists, each representing different skill levels: elite skilled cyclist, advanced skilled cyclist, intermediate skilled cyclist, and basic skilled cyclist. We define a basic-skilled cyclist as one with the highest standard deviation of the lateral position of the ground contact point of the front wheel while cycling and instructed to follow a centerline S, indicating the lowest balance skill. The skill

performances S of these four hypothetical different types of cyclists were chosen to evenly span the skill performance S range observed among the 24 participants of the cyclist fall experiments conducted in Chapter 3. The characteristics of the four 'standard' cyclists are summarised in Table 5.1.

Table 5.1: Characteristics of the four cyclist types. The name is representative of the characteristics of that participant. A lower skill performance S value indicates a better line-tracking ability.

cyclist type	S (mm)
elite skilled cyclist	40
advanced skilled cyclist	60
intermediate skilled cyclist	80
basic skilled cyclist	100

Additionally, we assumed that the cyclist was riding upright and straight ahead at the moment of the disturbance ($\phi_0 = \dot{\delta}_0$=0). It was also assumed that this was the cyclist's initial encounter with this specific type of handlebar disturbance (j=1), characterised by a clockwise rotation of the handlebars (ΔLCW=1).

The MAHD was calculated for these conditions and for the 6-18 km/h speed range, consistent with the velocities tested in the experimental trials, using a step size of 0.01 km/h.

MAHD predictions by the candidate model

To predict the MAHD using the candidate bicycle dynamics and cyclist control model, we performed a transient analysis. A step-input steer torque disturbance lasting 0.3 seconds was applied, with an initial guess for the torque magnitude. The choice of a 0.3-second step-input steer torque disturbance was defined in Chapter 2 as the 'standard' disturbance type for determining the MAHD.

The transient analysis lasted for a further 3 seconds after the disturbance was applied. During this period, we determined the maximum lean angle ϕ, steering angle δ, and lateral displacement of the front wheel contact point with respect to the centre of the treadmill y_Q. The duration of 3 seconds was chosen because, from experience, almost all falls happen within 3 seconds of a disturbance. Otherwise, the cyclist has enough time to respond adequately and recover balance. Longer durations are possible but require slightly more computational time.

During the transient analysis, the bicycle's lean angle ϕ, steering angle δ, and lateral displacement of the front wheel contact point y_Q were used to identify instances of falls. As established in Chapter 2, three primary cyclist fall modes exist. These are slipping of the tyres because of a too-large lean angle, slipping of the tyres because of a too-large steering angle, and cycling off the side of the road.

As established in Chapter 1, a bicycle tyre model is required to describe and calculate the forces generated by the tyres under lateral slip and determine slippage occurrences. Unfortunately, such a validated model does not yet exist. While extensive research has been conducted on car tyre models [43], the technology of measuring the lateral characteristics of bicycle tyres is still at its very beginning [44].

Consequently, a comprehensive model that accurately describes the transition

from static to dynamic friction during tyre-road interactions does not yet exist. This knowledge gap prevents us from precisely determining the boundary at which a bicycle tyre begins to slip, a crucial factor in determining whether two of the three cyclist fall modes occur.

However, for non-slippery conditions, such as in the cyclist fall experiments conducted in Chapter 3, we posit that we can bypass the complexities of tyre modeling. Here, we suggest using an estimated threshold for lean and steering angles beyond which slip likely occurs. This approach draws from Nadal's L/V ratio principle, a railway engineering concept that predicts derailment risks on curves [45]. The L/V ratio, which measures the lateral force on a wheel (L) relative to its vertical load (V), is a proxy for the frictional forces at play, offering a practical measure of lateral stability.

Applying the L/V ratio to cycling, we propose a critical lean angle of 45 degrees, where the lateral force equals the vertical load (L/V ratio = 1) as the threshold at which slip is likely. This angle provides a practical reference point for predicting loss of control.

Similarly, we propose a critical steering angle of 45 degrees because friction limits the lateral force at the front contact point that can be generated. This limits the lateral force that can be generated and the cornering motions that can be performed.

To summarise, we defined falls as simulations where cyclists exceeded a prescribed maximum lateral displacement, steering angle, or lean angle threshold. The maximum lean and steering angle threshold was set at 45 degrees. The value for the lateral displacement was set at 0.6 m, both to the left and right. This value was chosen as it is half the width of the treadmill as used in the cyclist fall experiments from Chapter 3, and the disturbances were only applied when the participant was cycling in the middle of the treadmill in a straight ahead and upright position.

To take the treadmill's limited width into account in the transient analysis, the state of the bicycle was extended with the kinematic variables for the heading, ψ and the lateral displacement of the front wheel contact point y_Q. These states can be determined from the linearised kinematic differential equations, which describe the motion of the contact points (Equations 5.2-5.4).

Because the model is linear, we could directly calculate the MAHD following the initial guess. The maximum allowable magnitudes for lateral displacement, steering angle and lean angle were computed using linear interpolation, with the MAHD being the lowest of these three magnitudes. It is important to note that the model is deterministic, providing a clear-cut boundary for the MAHD value between falling and not falling.

The parameters used in this study for the candidate bicycle dynamics and cyclist control model are provided in Table 5.2. The coefficient matrices of the C-W bicycle model, including passive rider contribution, were chosen to match the experimental conditions in Chapter 3. These conditions were the basis for the data used to fit the statistical model.

The parameter values for the covariance matrices of the Kalman filter ($\mathbf{Q}_K$ and $\mathbf{R}_K$), the cut-off frequency ω_c, and the damping coefficient ζ were set to similar values as used in Chapter 4. The control effort weight, $\mathbf{R}_{LQR}$, was also set to unity.

For the weight factors $\mathbf{Q}_{LQR}$, all terms were set to zero except for the weight factors on the lean angle Q_ϕ and on the lateral displacement of the front wheel contact point with

Table 5.2: Summary of the parameters of the rider model with the assigned value.

variable	*symbol*	*value*	*unit*
bicycle dynamics with passive cyclist contribution			
mass matrix	$\bar{\mathbf{M}}_0$	$\begin{bmatrix} 81.6996 & 2.0722 \\ 2.0722 & 0.5092 \end{bmatrix}$	$\mathrm{kg\,m^2}$
damping matrix	$\bar{\mathbf{C}}_1$	$\begin{bmatrix} 0 & 28.8118 \\ -0.4799 & 1.5636 \end{bmatrix}$	$\mathrm{N\,s}$
stiffness matrices	$\bar{\mathbf{K}}_0$	$\begin{bmatrix} -81.4674 & -2.2622 \\ -2.2622 & -0.8291 \end{bmatrix}$	$\mathrm{N\,s^2}$
	$\bar{\mathbf{K}}_2$	$\begin{bmatrix} 0 & 69.1375 \\ 0 & 2.0392 \end{bmatrix}$	$\mathrm{N\,s^2/m}$
gravity	g	9.81	$\mathrm{m/s^2}$
wheelbase	w	1.108	m
trail	c	0.08	m
head angle	λ	90°-68.5°	degrees
forward speed	v	variable	m/s
human multisensory integration for bicycle state estimation			
process noise covariance matrix	$\mathbf{Q}_K$	$\mathbf{I}_{6x6}$	-
measurement noise covariance matrix	$\mathbf{R}_K$	$\mathbf{I}_{2x2}$	-
human balance controller weight factors			
lean angle	Q_ϕ	variable	$\mathrm{1/rad^2}$
contact point front wheel	Q_{y_Q}	variable	$\mathrm{1/m^2}$
control effort	$\mathbf{R}_{LQR}$	$[1]$	$\mathrm{1/(Nm)^2}$
muscular dynamics			
cut-off frequency	ω_c	$2.17 \cdot 2\,\pi$	rad/s
damping coefficient	ξ	$\sqrt{2}$	-

respect to the centre line of treadmill Q_{y_Q}. These are the third and seventh entries on the diagonal, respectively. Because the ratio between the two weight factors is unknown, we assumed an equal weight between them. Consequently, the same value was used for the two weighting factors.

The weight factor Q_ϕ was calibrated by matching it to the MAHD predictions of the Bayesian model for a given cyclist with a specific skill performance S over a forward speed range of 6 to 18 km/h. The quality of the fit was optimised using the root-mean-square-error (RMSE) of the MAHD. The weight factor was determined separately for the four distinct cyclists as defined for the Bayesian model (see Table 5.1).

5.2.4. APPROACH TO EVALUATE PREDICTIONS OF CANDIDATE MODEL FOR CYCLIST RESPONSE TO A LARGE DISTURBANCE

This study also aims to evaluate whether the candidate model can predict the cyclist's response to a large disturbance. For this purpose, we compare in the time domain the steering angle δ, lean angle ϕ, the lateral position of the front wheel ground contact point

with respect to the centre line of the treadmill y_Q and the heading angle of the bicycle ψ, from the model prediction with the measured data from the cyclist fall experiments for two trials.

The participant's reaction to a disturbance was determined from position measurement data of nine markers placed on the bicycle, measured by 12 Qualisys cameras and captured at 100 Hz. The steering angle, lean angle, heading and the bicycle's front wheel lateral ground contact point were reconstructed from the redundant marker position data using rigid body constraints and least square methods.

To evaluate the predictive performance of our candidate model, we calculated the Variance Accounted For (VAF), which measures the proportion of variance in the measured signal that the model predicts. We calculated the VAF for the steering angle δ using the following equation:

$$VAF = \left(1 - \frac{\text{var}(\hat{\delta}_f - \delta)}{\text{var}(\hat{\delta}_f)}\right) \cdot 100\% \tag{5.8}$$

where var stands for the variance of the respective signals, $\hat{\delta}_f$ is the filtered measured steering angle and δ_f is the steering angle predicted by the candidate model. A higher VAF indicates a better fit and predictive performance.

Data for these variables were collected for every participant and every disturbance in the cyclist fall experiments performed in Chapter 3. A complete evaluation of all trials was outside the scope of this study. We have selected only to compare the model's prediction to three trials. While not constituting a definitive proof, the above observations offer valuable insights and instil confidence in the mechanical model's ability to predict the MAHD, suggesting that it aptly captures the underlying mechanisms governing motion and control strategies. We will revisit this in the discussion section.

To evaluate the candidate model's prediction of the cyclist's response to a large disturbance, we chose experimental trials of two participants with a skill performance close to the skill performance of a basic skilled cyclist. For one participant, we analysed two trials at a forward speed of 12 km/h, while for the other, we selected a trial at 6 km/h. Two trials were chosen where the applied disturbance was just below the MAHD to ensure the participant recovered balance. The cyclist control model is based on the strategy that the cyclist recovers balance by steering in the direction of the fall. We suspect that for disturbances exceeding the MAHD, where there is a high probability of falling, the cyclist may employ a different strategy, such as bracing for impact or dismounting. The cyclist control model does not capture these alternative strategies. To demonstrate this, we included another trial at 12 km/h, of the same participant, where the disturbance resulted in a fall. Additionally, we focused on lower forward speeds and disturbances just below the threshold because we anticipated larger steering angles in these conditions, posing a potentially greater challenge for the (linear) bicycle dynamics model in making accurate predictions.

The magnitude of the step-input torque disturbance lasting 0.3 seconds was set similarly to the disturbance magnitude applied in the experimental trial. The forward

speed v was set similarly to the experimental trial's. The transient analysis lasted 3 seconds from the beginning of the disturbance. We set the weight factor Q_ϕ equal to that of the basic-skilled cyclist, as determined via the fine-tuning process described above. All other variables were kept similar, as shown in Table 5.2, similar to the experimental conditions.

5.3. RESULTS

This section presents the results of our evaluation of the candidate model. We first evaluate the reliability of the candidate model in predicting the MAHD and then evaluate the model's prediction for the cyclist's reaction to a large disturbance.

Evaluation of the MAHD prediction of the candidate model

Figure 5.1 shows the final results of the calibrating process of the Q_ϕ-factor for the advanced skilled cyclist with a skill performance S of 60 mm. The results show a forward speed range of 0 to 24 km/h. The Bayesian model's MAHD prediction is shown in the graph as well. The solid black line represents the mean MAHD value for which there is a 50% chance of falling, while the grey band specify the 64% confidence levels of this prediction. The bicycle dynamics and cyclist control model's MAHD prediction consists of three lines, each representing the different fall modes.

Among these fall modes, the one with the lowest maximum disturbance before a fall at a given forward speed is considered the most critical and is defined as the MAHD. According to the bicycle dynamics and cyclist control model, at speeds below 6 km/h, the slipping of the tyres because of a too-large steering angle is the most critical fall mode, while for higher speeds, riding off the side of the bicycle path is the most critical fall mode.

It is important to note that in the experiments performed for speeds between 6 and 18 km/h, all falls were attributed to participants riding off the side of the treadmill. The comparison of the bicycle dynamics and cyclist control model and its associated fall modes, as shown in Figure 5.1 for the advanced skilled cyclist, is similar to the other three cyclist types with different skill performances.

The MAHD predictions for the advanced skilled cyclist align closely with the MAHD predictions of the Bayesian model in the forward speed range of 6 to 18 km/h, which was the speed interval at which the experiments were conducted. In this forward speed interval, the Root Mean Square Error (RMSE) between the experimental results (i.e. Bayesian model) and the bicycle dynamics and cyclist control model is 0.3 Nms. At forward speeds below 6 km/h, which is outside the experimental conditions, we qualitatively observe in Figure 5.1 a nonlinear response and deviations in the MAHD predictions. This deviation might be attributed to the candidate's model change in fall mode from riding off the side of the treadmill to falling due to slipping of the tyres because of a too-large steering angle.

In Figure 5.2, we compare the candidate model's final MAHD predictions and those of the Bayesian model for the four different skilled cyclists. Table 5.3 showcases the final and optimized weight factors Q_ϕ for the four differently skilled cyclists, alongside the RMSE.

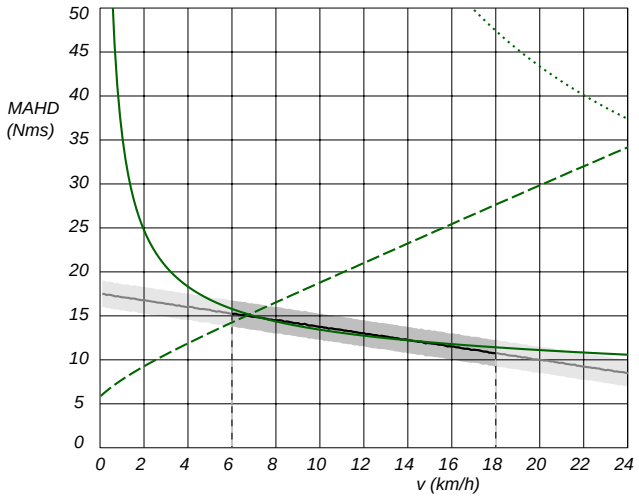

Figure 5.1: The MAHD predictions of the Bayesian model (black line) and the candidate model (green lines) for the advanced skilled cyclist (S = 60 mm) in a forward speed range of 0 to 24 km/h. The MAHD predictions of the Bayesian model include the mean MAHD value for a 50% chance of falling (solid black line) together with the 64% confidence interval (grey band). The green lines represent the MAHD of the different fall modes of the candidate model. The solid green line is for which the maximum lateral displacement of the front wheel from the centre line of the treadmill is exceeded, the dashed line is for slipping of the tyres because of a too-large steering angle, and the dotted line is for a too-large lean angle. The minimum value of these three is the true MAHD prediction for the candidate model. Note that the experimental data for the statistical model were obtained only within a forward speed range of 6 to 18 km/h (dashed vertical lines). The values outside this range are extrapolations from the statistical model.

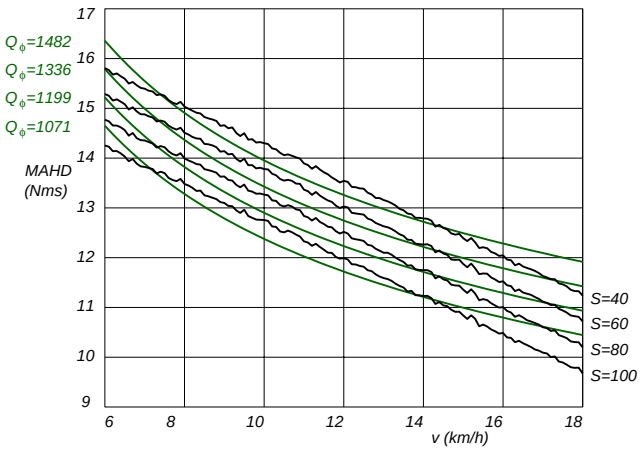

Figure 5.2: A comparison between the MAHD predictions of the candidate model, the green lines, and those of the Bayesian model for the four differently skilled cyclists, black lines.

Table 5.3: The calibrated LQR weight factors Q_ϕ of the candidate model for the four differently skilled cyclists with their skill level S, LQR weight factor Q_ϕ and the root mean square error (RMSE) of the MAHD.

cyclist type	S (mm)	Q_ϕ (1/rad^2)	*RMSE* (Nms)
elite skilled cyclist	40	1482	0.30
advanced skilled cyclist	60	1336	0.30
intermediate skilled cyclist	80	1199	0.31
basic skilled cyclist	100	1071	0.32

Evaluation of the cyclist's response predictions of the candidate model

Figure 5.3 compares the predicted steering angle δ, lean angle ϕ, heading ψ and lateral position of the front wheel contact point with respect to the centre line of treadmill y_Q by the candidate model for a basic skilled cyclist with the observed measured data from participant 17. The trial was at 12 km/h with an impulse-like handlebar disturbance of 9.8 Nms, which is close to the MAHD of the basic skilled cyclist at that speed (see Figure 5.2). Figure 5.4 shows the same comparison but with measured data of a trial of Participant 1 at 6 km/h with a disturbance of 12.3 Nms.

A qualitative observation shows that the number of steering actions taken to recover balance after a disturbance is similar (i.e., 3). At 12 km/h, as shown in Figure 5.3, the absolute minimum and maximum steering angles during the 3-second response to the handlebar disturbance deviate by 22% and 10%, respectively. At 6 km/h, these angles are 32% and 8%, respectively.

The VAF for the steering angle response was 90% at 12 km/h and 82% at 6 km/h. Similar observations were made for the lean angle ϕ and the heading ψ. The lateral position of the front wheel contact point with respect to the centre of the treadmill

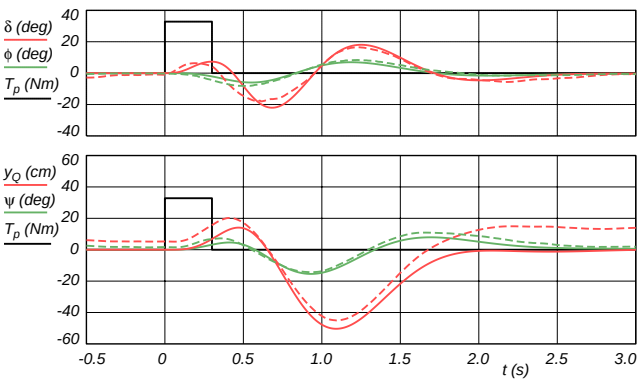

Figure 5.3: Transient response after a handlebar disturbance at $t = 0$ of applied steer torque $T_p = 32.8$ Nm lasting 0.3 seconds, simulated for 3 seconds. The solid lines are the simulated data, whereas the dotted lines are from measured data. Shown are the steering angle δ, the rear frame lean angle ϕ, The lateral position of the front wheel contact point with respect to the centre line of treadmill y_Q, and the heading angle of the bicycle ψ. The bicycle was driven at 12 km/h by Participant 17, and the disturbance was pull 13, which had a constant steer torque of 32.8 Nm for 0.3 seconds, which resulted in no fall. The optimal control weight factor for the simulation model was $Q_\phi = 1071$, which corresponds to a basic skilled cyclist, see Table 5.3.

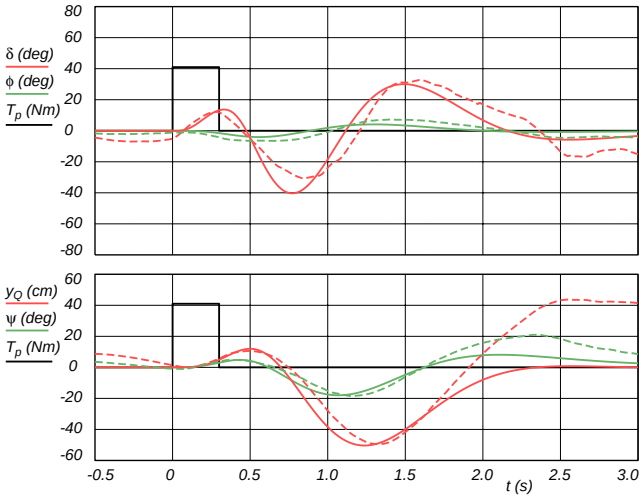

Figure 5.4: Transient response after a handlebar disturbance at $t = 0$ of applied steer torque $T_p = 41$ Nm lasting 0.3 seconds, simulated for 3 seconds. The solid lines are the simulated data, whereas the dotted lines are from measured data. Shown are the steering angle δ, the rear frame lean angle ϕ, the lateral position of the front wheel contact point with respect to the centre line of treadmill y_Q, and the heading angle of the bicycle ψ. The bicycle was driven at 6 km/h by Participant 1, and the disturbance was pull 9, which was a constant steer torque of 41 Nm for 0.3 seconds, which resulted in no fall. The optimal control weight factor for the simulation model was $Q_\phi = 1071$, which corresponds to a basic skilled cyclist, see Table 5.3.

y_Q did show an offset after approximately 2 seconds at both velocities. Although the heading angle ψ returned to zero, indicating the participant recovered balance and returned to straight-ahead cycling, the lateral position had not yet returned to the centre of the treadmill within three seconds after the disturbance. This offset implies that the participant prioritizes recovering balance and returning to straight-ahead cycling above the lateral position.

Figure 5.5 shows the same comparison but with measured data of a trial of Participant 17 at 12 km/h with a disturbance that resulted in a fall. In this case, the steering responses predicted by the model immediately following the disturbance aligns well with the experimental data. However, deviations in steering behaviour are observed when the participant approaches the edge of the treadmill (at -60 cm and around 0.8 seconds). A notable divergence between the model and the experimental data occurs once the cyclist moves off the treadmill. In the experimental data, both the lean angle and steering angle increase significantly, indicating a fall where the cyclist is caught by the safety harness. The model does not account for the finite width of the treadmill and assumes the cyclist can still return to the middle by steering into the fall and recover balance.

5.4. PRACTICAL APPLICATION

To illustrate the practical application of our candidate model and novel approach, we evaluate three types of interventions: 1) a steer-assist system designed to help cyclists

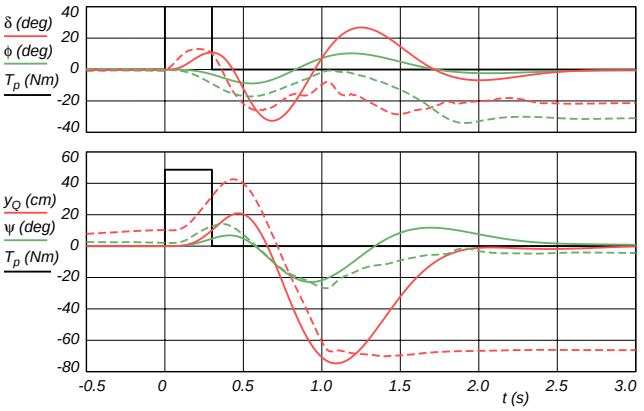

Figure 5.5: Transient response after a handlebar disturbance at $t = 0$ of applied steer torque $T_p = 49.2$ Nm lasting 0.3 seconds, simulated for 3 seconds. The solid lines are the simulated data, whereas the dotted lines are from measured data. Shown are the steering angle δ, the rear frame lean angle ϕ, the lateral position of the front wheel contact point with respect to the centre line of treadmill y_Q, and the heading angle of the bicycle ψ. The bicycle was driven at 12 km/h by Participant 17, and the disturbance was pull 19, which was a constant steer torque of 49.2 Nm for 0.3 seconds, which resulted in a fall where the cyclist rode off the side of the treadmill ($y_Q <$ -60 cm). The optimal control weight factor for the simulation model was $Q_\phi = 1071$, which corresponds to a basic skilled cyclist, see Table 5.3.

recover balance, 2) a 5 degrees increase and decrease of the head tube angle of the bicycle, and 3) a 10% increase and decrease of the lateral width available to recover balance (i.e. 6 cm). The first intervention represents a cyclist fall prevention intervention targeting cyclist control, the second targets bicycle design and the third targets the infrastructure.

The steer-assist system, an active control system designed to help cyclists recover balance, was implemented based on the intuitive controller proposed by Schwab et al. [46]. This controller uses the fundamental principle of bicycle balance: steering into the undesired lean. This steering into the undesired lean is done by a linear feedback controller on the lean rate, which outputs steer torque. To increase stability, some damping on the steering angle is added. The steer-assist control law then takes the form:

$$T_\delta = -C_v(v_{max} - v)\dot{\phi} - C_d\dot{\delta} \qquad \text{for } v < v_{max}, \tag{5.9}$$

$$T_\delta = 0 \qquad \text{for } v \geq v_{max}, \tag{5.10}$$

where v_{max} is a forward speed where the bicycle becomes self-stable, usually above 18 km/h.

We use a technique called gain scheduling, which means adjusting the controller's parameters based on the forward speed. This adjustment is necessary because the bicycle's (in)stability changes significantly with speed. Specifically, the control parameters were set as $v_{max} = 7$ m/s, $C_v = 12$ Ns^2, and $C_d = 8$ Nms. These values were selected by trial and error so that the bicycle is self-stable in a forward speed range between 6 and 25 km/h. This example serves as an illustrative example. An even better

controller can be designed with appropriate analyses and structured processes.

The head tube angle is a term commonly used by bicycle manufacturers and is the angle between the steering axis and the horizontal plane when the bicycle is upright. It is related to the steer axis tilt λ, which is measured relative to the vertical plane and positive when the steering axis is tipped backwards through the relationship $90° - \lambda$. A steer axis tilt λ of 0 degrees, or a head tube angle of 90 degrees, would position the front fork straight down, perpendicular to the ground. In practice, the head tube angle is typically less than 90 degrees, usually ranging between 70 and 75 degrees.

The change in steer axis tilt λ was incorporated into the bicycle dynamics model by changing this geometry variable with plus and minus five degrees. This change affects the mass, damping, and stiffness matrices of the Carvallo-Whipple bicycle model. The head tube angle was chosen more or less arbitrarily, although there is some empirical evidence that the head angle significantly changes the dynamics and control of the bicycle. Similarly, a designer could change the trail, wheelbase, seating position or any other bicycle geometric variable. These bicycle geometry changes would also affect the MAHD.

To incorporate the additional lateral space, we adjusted the threshold for maximum lateral displacement of 0.6 m with plus or minus 0.06 m. This threshold is related to the fall mode cycling off the side of the road.

We evaluated the effectiveness of the three interventions by calculating the MAHD, using a similar procedure as described above, and comparing the values of the MAHD across the forward speed range to those of the benchmark case, which was the bicycle parameters listed in Table 5.2 and the basic skilled cyclist parameters listed in Table 5.3. These parameters correspond to the MAHD predictions for the basic skilled cyclist (S=100 mm) shown in Figure 5.2. The results of this comparison are shown in Figure 5.6.

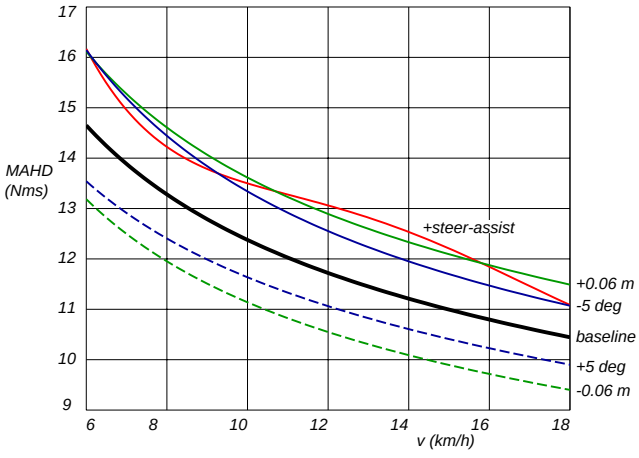

Figure 5.6: The effect of design changes on the MAHD from the candidate model for a basic skilled cyclist (Q_1 = 1071). The thick black line is the baseline MAHD, the red line is for the addition of a steer-assist system, the blue lines are for a change in the bicycle head angle of -/+ 5 degrees, and the green lines are for a 10% change in the bicycle path width (+/- 0.06 m).

These illustrative examples show that a steer-assist system, a 5-degree decrease in head angle, and a 6 cm increase in lateral width to recover balance can increase the MAHD in approximately the same way. In this case, these relatively small changes in the parameters approximately increased the MAHD threshold of the basic skilled cyclist to that of an advanced skilled cyclist in the original scenario.

5.5. DISCUSSION

The goal of the study is to develop and validate a practical and reliable approach for the safe and proactive evaluation of cyclist fall prevention interventions. Bicycle dynamics and cyclist control models might be potential approaches, but their reliability and practicality still need to be determined. In this study, we evaluated these aspects for a candidate model.

We evaluated the reliability of the candidate model by comparing its predictions to data from experiments in which cyclists were subjected to handlebar disturbances that led to both falls and recoveries. Specifically, we evaluated the model's ability to predict the Maximum Allowable Handlebar Disturbance (MAHD) from which a cyclist can recover, a key indicator for safely and proactively evaluating fall prevention interventions.

To predict the MAHD, we first established optimal values for the control weight factor on the lean angle Q_ϕ, as this parameter was unknown for the participants of the experiments. A calibration process was employed, translating the measured skill performance S into the weight factor Q_ϕ, reflecting each cyclist's skill. This calibration was achieved by matching Q_ϕ to the MAHD predictions of the Bayesian model based on the experimental data across a forward speed range of 6 to 18 km/h.

The results, summarised in Table 5.3, reveal a strong linear relationship between the skill performance S and the weight factor Q_ϕ, with a high coefficient of determination (R^2 = 0.9991). The RMSE of the model's MAHD predictions across the speed interval was approximately 0.30 Nms for all four differently skilled cyclists, indicating reliable predictions given that the MAHD values ranged between 10 and 16 Nms.

Further evaluation of the model's predictive performance showed high Variance Accounted For (VAF) values for key bicycle states. However, some discrepancies, such as a residual lateral offset of the cyclist with respect to the treadmill's centreline three seconds after the disturbance, suggest potential areas for refinement.

We also evaluated the candidate model's practicality by incorporating various fall prevention interventions and determining their impact on the MAHD. The model successfully evaluated these changes, showing that specific adjustments in bicycle parameters, cyclist control, and infrastructure can significantly improve cyclists' ability to recover balance, reducing the probability of a fall.

Strengths

Key findings are that the MAHD predictions of the proposed candidate model align with experimental data, to which we applied a Bayesian multilevel logistic regression model to determine the MAHD. Moreover, the predicted cyclist behaviour following a disturbance closely resembles observed behaviour (see Figures 5.3 and 5.4), with comparable numbers of steering actions and maximum state magnitudes. Furthermore,

our calibration process revealed a linear relationship between cyclist skill performance S and control model weight factor Q_ϕ. Future weight factor determination can be simplified by measuring the one-minute undisturbed tracking capability to determine S and then translating it to Q_ϕ.

This study's findings instil confidence in the reliability and practicality of the candidate model for safely and proactively evaluating interventions aimed at preventing cyclist falls by addressing cyclist control, bicycle design, or environmental conditions related to disturbances or available space for balance recovery.

This approach complements existing approaches to evaluate cycling safety interventions. Specifically, it addresses the limitations of existing approaches to evaluate cyclist fall prevention interventions that aim to reduce fall risk in critical situations.

Limitations

While the proposed approach and evaluation of the candidate model offer a valuable contribution to preventing future cyclist falls, several limitations impact the reliability of MAHD predictions, the general applicability of the model, and the scope of interventions that can be evaluated.

Calibrating the optimal weight factor Q_ϕ based on experimental data introduces some uncertainty in the model's predictive capability. However, this calibration step was necessary to establish suitable input values for the weight factor Q_ϕ, required for the cyclist control model. To still evaluate the model's accuracy, we evaluated the MAHD trend relative to forward speed. This comparison demonstrates that the bicycle dynamics and cyclist control model effectively captures the observed trend.

We would recommend creating a new experimental dataset and repeat the comparison, this time by directly translating the skill performance S of participants with the optimal weight factor Q_ϕ using the linear trend observed between S and Q_ϕ for the four differently skilled cyclists (see Table 5.3). This approach could provide more robust insights into the model's predictive reliability.

In addition, the reliability of predictions is contingent upon the specific conditions analysed in the experiments. These conditions encompass a forward speed range of 6 to 18 km/h, involvement of 24 experienced cyclists, a single bicycle type, a specific disturbance type (albeit with varied magnitudes), uniform road surfaces, and consistent treadmill width. Extrapolation beyond these parameters may yield reliable outcomes for some variables while introducing uncertainty for others, as discussed in the following paragraphs.

In Figure 5.1, the candidate model's predictions of the MAHD begin to diverge from those of the Bayesian model at forward speeds below 6 km/h. Within this lower speed range, the primary fall mode is characterised by large steering angles that lead to front wheel slippage and subsequent cyclist falls. This low-speed instability is consistent with existing research. For instance, studies have shown that bicycles become more unstable as velocities decrease [34]. The Bayesian model, however, may not yet adequately reflect this behaviour. It was calibrated using experimental data primarily collected at speeds ranging from 6 to 18 km/h, where the bicycle-cyclist system exhibits relatively stable and consistent behaviour, thus supporting the expectation of an almost linear relationship

within this speed regime.

In the experimental data, the 24 participants, although varying in age and skill performance, were all experienced cyclists. Consequently, the observed range in skill performance S may only partially represent novice cyclists. Conducting similar experiments with novice participants could provide additional insights into the skill performance range among cyclists. Safety concerns precluded the inclusion of inexperienced cyclists in these initial fall experiments used to validate our bicycle dynamics and cyclist control model. Now that the safety of the experimental setup has been proven, inexperienced cyclists can be included in future experiments.

Additionally, as shown in Figure 5.2, while the RMSE demonstrates that our candidate model reliably predicts the MAHD, the model's predictions display nonlinear behaviour in contrast to the linear trend observed in the experimental data. We suspect this discrepancy arises because the experimental trials were conducted at only three forward speeds, limiting the Bayesian model's ability to capture potential nonlinear trends. To confirm the presence of a nonlinear trend, we recommend repeating the experiments at additional forward speeds.

Furthermore, participants were forewarned about the disturbances, and given that these disturbances were repeated to measure the MAHD, participants had the opportunity to learn from previous trials. This preparatory element challenges the environmental validity of the experimental setup because cyclists in the real world are not likely to encounter the same disturbance many times in a row such that they can learn from it. As a result, the MAHD values recorded in our study likely represent an optimistic upper threshold, which might be lower under real-world conditions. In addition, using a treadmill for cycling likely further lowers the environmental validity of the setup, although the differences have yet to be determined.

Additionally, the experiments did not vary other key variables, such as the width available to recover balance (i.e. the treadmill width) and the type of bicycle used. However, the proposed bicycle dynamics and cyclist control model should reliably predict MAHDs across different bicycle types and path widths. This assertion is supported by the validation of the linearised equations of motion in the Carvallo-Whipple model across various bicycle configurations as demonstrated in several studies [34, 36, 39, 40, 47].

The experiments were conducted under consistent road surface conditions, specifically non-slippery surfaces. While this controlled environment allowed for reliable predictions of cyclist behaviour, it limits the generalizability of the findings to more variable real-world conditions, such as slippery surfaces, which are frequently implicated in cycling crashes [5]. A detailed bicycle tyre model that accurately captures the transition from static to dynamic friction during tyre-ground interactions has yet to be developed. Consequently, we employed a simplified approach, estimating the maximum steering and lean angles at which tyre slippage might occur under non-slippery conditions. Although this study has demonstrated the reliability of this approach in predicting the MAHD and cyclist responses to disturbances, its applicability to slippery conditions remains uncertain.

In the controlled, non-slippery environment of our experiments, the critical fall mode observed was cycling off the side of the treadmill rather than tyre slippage.

As a result, we cannot conclusively determine whether the thresholds of 45 degrees for maximum lean and steering angles are applicable in these conditions. However, based on the experimental data (see Figure 5.4), it is evident that participants could recover balance at steering angles exceeding 35 degrees, suggesting that the threshold for steering angle should be set above this value. The data also show that lean angles were significantly smaller, reducing the likelihood of falls due to excessive lean. This observation is consistent with the candidate model's predictions of different fall modes, as illustrated in Figure 5.1.

We recommend that future research focus on developing a robust bicycle tyre model capable of accurately capturing these friction transitions. Alternatively, experiments should be repeated at lower forward speeds to verify whether slipping due to excessive steering angles occurs within this lower speed range.

The analysis of the reliability of existing bicycle dynamics and cyclist control models to predict cyclist responses to large disturbances is based on just two trials. While the VAF scores indicate a reliable prediction for the cyclist's reaction, we see some differences with the experimental data shown in Figures 5.3 and 5.4. Although the participants returned to straight-line cycling after two seconds, they did not realign to their original position on the treadmill's centerline. Instead, they maintained a lateral offset. Current cyclist control models do not capture such variations in recovery strategies and lateral positions and assume a return to the initial central position without lateral deviations. Differences in responses across trials may be due to varied balance recovery strategies, different priorities in avoiding the treadmill edge, or residual effects from the perturbator mechanism, such as tension in the ropes. While kinematic data are available for all trials, a detailed evaluation of these data to identify distinct balance recovery strategies was beyond this study's scope. Although we are confident in the cyclist control model's ability to capture the primary reactions to balance recovery, we recommend that future research delves deeper into these data to uncover subtle differences and evaluate the effectiveness of various cyclist strategies.

Practical application

In the previous section, we illustrated how the proposed linear bicycle dynamics and cyclist control model can be used to safely and proactively evaluate the effectiveness of cyclist fall prevention interventions targeting cyclist control, bicycle design and available space to recover balance. Initial results suggest that these interventions could significantly increase the MAHD for cyclists, effectively improving the performance of a novel cyclist to that of an experienced one without requiring additional skill training.

These illustrative examples underscore the potential of such fall prevention strategies. By quantifying the MAHD, we can systematically evaluate and compare the potential effectiveness of these interventions. Ultimately, these results provide engineers and professionals designing infrastructure, bicycles, and training programs with a robust approach to safely and proactively evaluate the safety of their designs. In addition, the approach can provide policy advisors with a robust basis for making informed decisions regarding the most cost-effective interventions and allocation of resources dedicated to cycling safety.

5.6. CONCLUSIONS

This study contributes to cycling safety research by developing a novel approach, relying on bicycle dynamics and cyclist control models, to safely and proactively evaluate cyclist fall prevention interventions.

Our research evaluated the reliability and practicality of a candidate bicycle dynamics and cyclist control model by comparing its predictions with experimental data from cyclist fall scenarios. The findings confirm the model's accuracy in predicting the MAHD across cyclists of varying skill levels and capturing the main characteristics of the cyclist's response to a large disturbance.

This approach facilitates the safe and proactive evaluation of interventions to improve cyclist control, bicycle design, and the available space for balance recovery. Preliminary results demonstrate that such interventions can improve a cyclist's ability to recover balance and decrease the probability of falls. Utilising this approach to compare such interventions systematically lays a robust groundwork for designers and professionals to evaluate the safety of their bicycles, infrastructure, or training designs. In addition, it supports policy advisors in making informed decisions regarding the most cost-effective interventions and allocation of resources dedicated to cycling safety.

Future research should expand the model's capabilities to include a more comprehensive array of cycling conditions, such as slippery conditions, and undergo further validation with more experimental data. Such research will help further establish the model's reliability and broaden its applicability across diverse cycling scenarios.

REFERENCES

[1] P. Schepers and K. Klein Wolt, *Single-bicycle crash types and characteristics,* Cycling Research International **2**, 119 (2012).

[2] P. Schepers, N. Agerholm, E. Amoros, R. Benington, T. Bjørnskau, S. Dhondt, B. de Geus, C. Hagemeister, B. P. Y. Loo, and A. Niska, *An international review of the frequency of single-bicycle crashes (SBCs) and their relation to bicycle modal share,* Injury Prevention **21**, e138 (2015), https://doi.org/10.1136/injuryprev-2013-040964.

[3] M. J. Boele-Vos, K. van Duijvenvoorde, M. J. A. Doumen, C. W. A. E. Duivenvoorden, W. J. R. Louwerse, and R. J. Davidse, *Crashes involving cyclists aged 50 and over in the Netherlands: An in-depth study,* Accident Analysis & Prevention **105**, 4 (2017), https://doi.org/10.1016/j.aap.2016.07.016.

[4] P. Hertach, A. Uhr, S. Niemann, and M. Cavegn, *Characteristics of single-vehicle crashes with e-bikes in Switzerland,* Accident Analysis & Prevention **117**, 232 (2018), https://doi.org/10.1016/j.aap.2018.04.021.

[5] R. Utriainen, S. O'Hern, and M. Pöllänen, *Review on single-bicycle crashes in the recent scientific literature,* Transport Reviews **43**, 159 (2023), https://doi.org/10.1080/01441647.2022.2055674.

[6] R. Elvik, *Area-wide urban traffic calming schemes: A meta-analysis of safety effects,* Accident Analysis & Prevention **33**, 327 (2001), https://doi.org/10.1016/S0001-4575(00)00046-4.

[7] A. Hoye, *Recommend or mandate? A systematic review and meta-analysis of the effects of mandatory bicycle helmet legislation,* Accident Analysis & Prevention **120**, 239 (2018), https://doi.org/10.1016/j.aap.2018.08.001.

[8] I. I. Hellman and M. Lindman, *Estimating the crash reducing effect of advanced driver assistance systems (ADAS) for vulnerable road users,* Traffic Safety Research **4**, 000036 (2023), https://doi.org/10.55329/blzz2682.

[9] N. Lubbe, Y. Wu, and H. Jeppsson, *Safe speeds: Fatality and injury risks of pedestrians, cyclists, motorcyclists, and car drivers impacting the front of another passenger car as a function of closing speed and age,* Traffic Safety Research **2**, 000006 (2022), https://doi.org/10.55329/vfma7555.

[10] T. Sayed, M. H. Zaki, and J. Autey, *Automated safety diagnosis of vehicle-bicycle interactions using computer vision analysis,* Safety Science **59**, 163 (2013), https://doi.org/10.1016/j.ssci.2013.05.009.

[11] A. R. A. van der Horst, M. de Goede, S. de Hair-Buijssen, and R. Methorst, *Traffic conflicts on bicycle paths: A systematic observation of behaviour from video,* Accident Analysis & Prevention **62**, 358 (2014), https://doi.org/10.1016/j.aap.2013.04.005.

[12] N. McNeil, C. M. Monsere, and J. Dill, *Influence of bike lane buffer types on perceived comfort and safety of bicyclists and potential bicyclists,* Transportation Research Record **2520**, 132 (2015), https://doi.org/10.3141/2520-15.

[13] J. Kovaceva, P. Wallgren, and M. Dozza, *On the evaluation of visual nudges to promote safe cycling: Can we encourage lower speeds at intersections?* Traffic Injury Prevention **23**, 428 (2022), https://doi.org/10.1080/15389588.2022.2103120.

[14] D. de Waard, P. Schepers, W. Ormel, and K. Brookhuis, *Mobile phone use while cycling: Incidence and effects on behaviour and safety,* Ergonomics **53**, 30 (2010), https://doi.org/10.1080/00140130903381180.

[15] W. P. Vlakveld, D. Twisk, M. Christoph, M. Boele, R. Sikkema, R. Remy, and A. L. Schwab, *Speed choice and mental workload of elderly cyclists on e-bikes in simple and complex traffic situations: A field experiment,* Accident Analysis & Prevention **74**, 97 (2015), https://doi.org/10.1016/j.aap.2014.10.018.

[16] R. Dubbeldam, C. T. M. Baten, P. T. C. Straathof, J. H. Buurke, and J. S. Rietman, *The different ways to get on and off a bicycle for young and old,* Safety Science **92**, 318 (2017), https://doi.org/10.1016/j.ssci.2016.01.010.

[17] J. Andersson, C. Patten, H. Wallén Warner, C. Andersérs, C. Ahlström, R. Ceci, and L. Jakobsson, *Bicycling during alcohol intoxication,* Traffic Safety Research **4** (2023), https://doi.org/10.55329/prpa1909.

[18] K. Kircher and A. Niska, *Interventions to reduce the speed of cyclists in work zones — cyclists' evaluation in a controlled environment,* Traffic Safety Research **6**, e000047 (2024), https://doi.org/10.55329/ohhx5659.

[19] C. Andersérs, J. Andersson, and H. W. Warner, *The importance of individual characteristics on bicycle performance during alcohol intoxication,* Traffic Safety Research **6**, e000042 (2024), https://doi.org/10.55329/vmgb9648.

[20] A. Niska and J. Wenäll, *Simulated single-bicycle crashes in the VTI crash safety laboratory,* Traffic Injury Prevention **20**, 68 (2019), https://doi.org/10.1080/15389588.2019.1685090.

[21] A. Niska, J. Wenäll, and J. Karlström, *Crash tests to evaluate the design of temporary traffic control devices for increased safety of cyclists at road works,* Accident Analysis & Prevention **166**, 106529 (2022), https://doi.org/10.1016/j.aap.2021.106529.

[22] Y. Peng, Y. Chen, J. Yang, D. Otte, and R. Willinger, *A study of pedestrian and bicyclist exposure to head injury in passenger car collisions based on accident data and simulations,* Safety Science **50**, 1749 (2012), https://doi.org/10.1016/j.ssci.2012.03.005.

[23] M. Fahlstedt, P. Halldin, and S. Kleiven, *The protective effect of a helmet in three bicycle accidents — a finite element study,* Accident Analysis & Prevention **91**, 135 (2016), https://doi.org/10.1016/j.aap.2016.02.025.

[24] C. Baker, X. Yu, B. Lovell, R. Tan, S. Patel, and M. Ghajari, *How well do popular bicycle helmets protect from different types of head injury?* Annals of Biomedical Engineering **52**, 3326 (2024), https://doi.org/10.1007/s10439-024-03589-8.

[25] V. Astarita, V. Giofré, G. Guido, and A. Vitale, *Investigating road safety issues through a microsimulation model,* Procedia-social and Behavioral Sciences **20**, 226 (2011), https://doi.org/10.1016/j.sbspro.2011.08.028.

[26] U. Shahdah, F. Saccomanno, and B. Persaud, *Application of traffic microsimulation for evaluating safety performance of urban signalized intersections,* Transportation Research Part C: Emerging Technologies **60**, 96 (2015), https://doi.org/10.1016/j.trc.2015.06.010.

[27] H. Twaddle, T. Schendzielorz, and O. Fakler, *Bicycles in urban areas: Review of existing methods for modeling behavior,* Transportation Research Record **2434**, 140 (2014), https://doi.org/10.3141/2434-17.

[28] C. M. Schmidt, A. Dabiri, F. Schulte, R. Happee, and J. K. Moore, *Essential bicycle dynamics for microscopic traffic simulation: An example using the social force model,* in *The Evolving Scholar-BMD 2023, 5th Edition* (2023) http://dx.doi.org/10.59490/649d4037c2c818c6824899bd.

[29] N. Rinke, C. Schiermeyer, F. Pascucci, V. Berkhahn, and B. Friedrich, *A multi-layer social force approach to model interactions in shared spaces using collision prediction,* Transportation Research Procedia **25**, 1249 (2017), https://doi.org/10.1016/j.trpro.2017.05.144.

[30] V. Keppner, S. Krumpoch, R. Kob, A. Rappl, C. C. Sieber, E. Freiberger, and H. M. Siebentritt, *Safer cycling in older age (SiFAr): Effects of a multi-component cycle training. a randomized controlled trial,* BMC Geriatrics **23**, 131 (2023), https://doi.org/10.1186/s12877-021-02502-5.

[31] L. Alizadehsaravi and J. K. Moore, *Bicycle balance assist system reduces roll and steering motion for young and older bicyclists during real-life safety challenges,* PeerJ **11**, e16206 (2023), https://doi.org/10.7717/peerj.16206.

[32] B. Janssen, P. Schepers, H. Farah, and M. Hagenzieker, *Behaviour of cyclists and pedestrians near right angled, sloped and levelled kerb types: Do risks associated to height differences of kerbs weigh up against other factors?* European Journal of Transport and Infrastructure Research **18**, 360 (2018), https://doi.org/10.18757/ejtir.2018.18.4.3254.

[33] F. Westerhuis, A. B. M. Fuermaier, K. A. Brookhuis, and D. de Waard, *Cycling on the edge: The effects of edge lines, slanted kerbstones, shoulder, and edge strips on cycling behaviour of cyclists older than 50 years,* Ergonomics **63**, 769 (2020), https://doi.org/10.1080/00140139.2020.1755058.

[34] J. P. Meijaard, J. M. Papadopoulos, A. Ruina, and A. L. Schwab, *Linearized dynamics equations for the balance and steer of a bicycle: A benchmark and review,* Proceedings of the Royal Society A: Mathematical, Physical and Engineering Sciences **463**, 1955 (2007), https://doi.org/10.1098/rspa.2007.1857.

[35] J. D. G. Kooijman, A. L. Schwab, and J. K. Moore, *Some observations on human control of a bicycle,* in *International Design Engineering Technical Conferences and Computers and Information in Engineering Conference* (San Diego, USA, 30 August - 2 September 2009) https://doi.org/10.1115/DETC2009-86959.

[36] J. D. G. Kooijman, J. P. Meijaard, J. M. Papadopoulos, A. Ruina, and A. L. Schwab, *A bicycle can be self-stable without gyroscopic or caster effects,* Science **332**, 339 (2011), https://doi.org/10.1126/science.1201959.

[37] A. L. Schwab, J. P. Meijaard, and J. D. G. Kooijman, *Lateral dynamics of a bicycle with a passive rider model: Stability and controllability,* Vehicle System Dynamics **50**, 1209 (2012), https://doi.org/10.1080/00423114.2011.610898.

[38] P. Basu-Mandal, A. Chatterjee, and J. M. Papadopoulos, *Hands-free circular motions of a benchmark bicycle,* Proceedings of the Royal Society A: Mathematical, Physical and Engineering Sciences **463**, 1983 (2007), https://doi.org/10.1098/rspa.2007.1849.

[39] J. D. G. Kooijman, A. L. Schwab, and J. P. Meijaard, *Experimental validation of a model of an uncontrolled bicycle,* Multibody System Dynamics **19**, 115 (2008), https://doi.org/10.1007/s11044-007-9050-x.

[40] D. Stevens, *The stability and handling characteristics of bicycles*, Bachelor's thesis, The University of New South Wales, School of Mechanical and Manufacturing Engineering, Sydney, Australia (2009), http://www.varg.unsw.edu.au/Assets/link%20pdfs/thesis_stevens.pdf.

[41] A. L. Schwab, P. D. L. de Lange, R. Happee, and J. K. Moore, *Rider control identification in bicycling using lateral force perturbation tests,* Proceedings of the Institution of Mechanical Engineers, Part K: Journal of multi-body dynamics **227**, 390 (2013), https://doi.org/10.1177/1464419313492317.

[42] G. Dialynas, C. Christoforidis, R. Happee, and A. L. Schwab, *Rider control identification in cycling taking into account steering torque feedback and sensory delays,* Vehicle System Dynamics **61**, 200 (2023), https://doi.org/10.1080/00423114.2022.2048865.

[43] H. Pacejka, *Tire and vehicle dynamics*, 3rd ed. (Elsevier, 2012).

[44] G. Dell'Orto, F. M. Ballo, and G. Mastinu, *Experimental methods to measure the lateral characteristics of bicycle tyres — a review,* Vehicle System Dynamics **61**, 2738 (2023), https://doi.org/10.1080/00423114.2022.2144388.

[45] B. Marquis and R. Greif, *Application of Nadal limit for the prediction of wheel climb derailment,* in *ASME/IEEE Joint Rail Conference*, Vol. 54594 (Pueblo, USA, 16-18 March, 2011) pp. 273–280, https://doi.org/10.1115/JRC2011-56064.

[46] A. L. Schwab, J. D. G. Kooijman, and J. P. Meijaard, *Some recent developments in bicycle dynamics and control,* in *4th European Conference on Structural Control* (St. Petersburg, Russia, 8-12 September 2008) http://www.bicycle.tudelft.nl/schwab/Publications/SchwabKooijmanMeijaard2008.pdf.

[47] T.-O. Tak, J.-S. Won, and G.-Y. Baek, *Design sensitivity analysis of bicycle stability and experimental validation,* in *Bicycle and Motorcycle Dynamics Conference* (Delft, The Netherlands, 20-22 October 2010) http://www.bicycle.tudelft.nl/ProceedingsBMD2010/papers/tak2010design.pdf.

6

Conclusions and Discussion

The goal of this dissertation was to develop an approach to safely and proactively evaluate cyclist fall prevention interventions. Because falls during cycling are one of the leading causes of serious injuries among cyclists, such an approach could contribute to identifying effective interventions and preventing future falls.

Previous studies have evaluated cycling safety interventions through a variety of approaches. Commonly employed approaches include the statistical analysis of crash statistics [1–4], video-based evaluations of surrogate safety indicators of near-miss incidents [5, 6], controlled field studies or experimental setups [7–14], crash tests or crash simulation models [15–19] and models that simulate traffic scenarios [20–24].

Although these approaches have contributed significantly to understanding and improving cycling safety, they fall short when applied to interventions targeting cyclist fall prevention, especially those aiming to reduce fall risk in critical situations. Such interventions, including balance training programs [25], steer-assist technologies [26], sloped kerbs [27], and ridable road shoulders [28] can currently not be safely and proactively evaluated.

Existing approaches face several limitations in this context. Crash data analyses are limited by the underreporting of single bicycle crashes, which are mainly falls [29]. Surrogate safety indicators focus primarily on traffic conflicts and cannot be applied to single bicycle crashes in which no other road users were involved — even though these represent a majority of serious cycling crashes [30]. Experimental and field studies typically use indirect measures of fall risks — such as perceived safety or workload — to quantify safety; however, their predictive validity to quantify direct fall risk has not yet been proven. Crash tests and simulations focus on injury mitigation rather than the prevention of falls. Moreover, existing models that simulate traffic scenarios — such as traffic microsimulation models, behavioural models or crash avoidance models — lack the ability to incorporate the balance task and lateral dynamics of the bicycle, which are critical for simulating cyclist falls.

This dissertation evaluated whether bicycle dynamics and cyclist control models can be employed reliably and practically to safely and proactively evaluate cyclist

fall prevention interventions, particularly those aiming to reduce fall risk in critical scenarios. These models can potentially simulate a wide range of crash scenarios and incorporate diverse interventions. If successful, this approach could facilitate the safe and proactive evaluation of cycling safety interventions rapidly and cost-effectively. Such an approach would improve the design process for bicycles, infrastructure, and training programs by enabling safety evaluations during the design phase. Additionally, this approach could contribute to more efficient resource allocation by systematically comparing a broader range of interventions, ensuring investments are directed towards the most effective cycling safety interventions.

However, several challenges currently limit the full potential and application of these models. There needs to be more communication between vehicle dynamics and control researchers and road safety experts to adapt the models for simulating real-world cyclist fall scenarios and evaluating cyclist fall prevention interventions. Additionally, the lack of a general, objective and direct indicator for evaluating fall prevention interventions poses a challenge for systematic comparisons between different types of interventions. Moreover, the validation of these models against actual fall scenarios remains unresolved. Finally, existing cyclist control models must adequately incorporate intuitive cyclist characteristics, which is crucial for incorporating interventions targeting cyclist control.

This dissertation has addressed these challenges. Below, we present the conclusions of our research, followed by a detailed discussion of the extent to which the research objectives have been met and the broader implications of our findings.

6.1. CONCLUSIONS

In this section, we present a summary of the key conclusions, derived from the research conducted throughout the dissertation. After each conclusion we refer to the relevant chapter, facilitating easy reference for interested readers seeking more in-depth details about the specific research underpinning each conclusion.

1. It is concluded that bicycle dynamics and cyclist control models can simulate all eight commonly reported crash types considered in this dissertation. These crash types include falls due to slipping on a slippery road surface, falls after a collision with an obstacle, falls following an evasive manoeuvre, falls involving (tram) rails, falls resulting from hard braking, falling over while cornering, falls due to loss of balance and falls after a collision with another road user. However, it is crucial to note that these models require further development to unlock their full potential. [Chapter 1]

2. It is concluded that bicycle dynamics and cyclist control models can incorporate and evaluate interventions aimed at bicycle design, cyclist control, and environmental factors like road surface conditions, disturbances and available space to recover balance. [Chapter 1]

3. It is concluded that the newly introduced Maximum Allowable Handlebar Disturbance (MAHD) is the first practical, generalisable indicator for safely and proactively evaluating the effectiveness of cyclist fall prevention interventions

prior to their implementation and for all crash types where the cyclist encounters an impulse-like disturbance. The MAHD quantifies the maximum impulse-like disturbance from which a cyclist is able to recover balance. This indicator directly reflects the probability a cyclist will fall in response to such a disturbance. [Chapter 2]

4. It is concluded that cyclist falls, induced by a handlebar disturbance, can be safely simulated in a laboratory setting where the cyclist cycles on a treadmill, surrounded by padding, and wearing a (intelligent) safety harness. This setup, in combination with the randomised staircase protocol, is a practical approach to experimentally measure the MAHD. [Chapter 3]

5. It is concluded that a Bayesian multilevel logistic regression model can successfully determine the MAHD for a participant based on twenty disturbances, of which the magnitude was selected using a randomised staircase protocol. It can also reliably predict the MAHD for hypothetical participants, provided their characteristics fall within the boundaries of the experimental conditions. [Chapter 3]

6. It is concluded that all falls in the experiments — which simulate falls on a non-slippery finite 1.2 m wide treadmill due to an impulse-like handlebar disturbance — can be characterised as riding off the side of a narrow bicycle path. [Chapter 3]

7. It is concluded that for the variables varied in the cyclist fall experiments, the important predictors for the MAHD — and, consequently, for cyclist fall risk due to an impulse-like handlebar disturbance — are:

   a. forward speed v
   b. skill performance S — defined as the ability to follow a centreline while cycling undisturbed
   c. the lean angle at the moment the handlebar disturbance was applied ϕ_0
   d. the steer rate at the moment the handlebar disturbance was applied $\dot{\delta}_0$
   e. the direction of the handlebar disturbance d
   f. how often the cyclist encountered the disturbance j. [Chapter 3]

8. Counter-intuitively, it is concluded that as forward speed v decreases, the MAHD increases. [Chapter 3]

9. It is concluded that age is not an important predictor of the MAHD. Consequently, age does not significantly influence the probability that a cyclist will fall when encountering an impulse-like handlebar disturbance. [Chapter 3]

10. It is concluded that the steering actions of a cyclist to recover balance after an impulse-like handlebar disturbance can be predicted for a large range of forward speeds v by a bicycle-cyclist control model with only one parameter that needs to be experimentally measured: the optimal control weight that minimises the deviation of the lean angle $Q_{LQR,\phi}$. All other input values for this cyclist control model are physical parameters which can be easily measured. [Chapter 4]

11. It is concluded that the Carvallo-Whipple bicycle model with linear equations of motion [31], in combination with the newly developed cyclist control model, is able to reliably predict the MAHD for forward speeds v ranging from 6 to 18 km/h and for cyclists with varying skill performances S. This predictive capability is comparable to that of the Bayesian multilevel logistic regression model. [Chapter 5]

12. It is concluded that the approach developed in this study is capable of safely and proactively evaluating cyclist fall prevention interventions targeting cyclist balancing control, bicycle design, and environmental factors such as the available width to recover balance or the magnitude of external impulse-like disturbances. [Chapter 5]

13. It is concluded that choosing an appropriate bicycle design — not only the bicycle type and frame size, but also small variations in the geometry of the bicycle like the head tube angle — can improve a cyclist's ability to recover balance from an impulse-like handlebar disturbance. This could improve the MAHD threshold for a basic skilled cyclist to that of an advanced skilled cyclist. [Chapter 5]

14. Additionally, it is concluded that the implementation of a cyclist assistance system, which supports the cyclist in recovering balance, can further increase the MAHD threshold and reduce the probability of a fall after an impulse-like disturbance. [Chapter 5]

6.2. DISCUSSION

In this section we delve into the extent to which the goal of the dissertation has been achieved. The goal was to develop an approach to safely and proactively evaluate cyclist fall prevention interventions. Recommendations for future research are given as well.

6.2.1. ON BICYCLE CRASH TYPES THAT CAN BE SIMULATED WITH BICYCLE DYNAMICS AND CYCLIST CONTROL MODELS (CONCLUSION 1)

Bicycle dynamics and cyclist control models hold significant potential for simulating the eight bicycle crash types commonly reported by road safety experts and considered in this dissertation. These crash types are falls due to slipping on a slippery road surface, falls after a collision with an obstacle, falls following an evasive manoeuvre, falls involving (tram) rails, falls resulting from hard braking, falling over while cornering, falls due to loss of balance and falls after a collision with another road user.

In Chapter 5, we demonstrated that crash types involving short, impulse-like disturbances — such as collisions with an obstacle or another road user and falls due to loss of balance — can already be simulated with existing bicycle dynamics and cyclist control models. The Carvallo-Whipple bicycle model, combined with a cyclist control model that incorporates human sensory feedback, multisensory integration for bicycle state estimation, human steer torque control, and muscular dynamics, has proven effective in these simulations. Moreover, the lateral dynamics of the bicycle, consisting of the lean and steering angles, can be reliably predicted using linearised equations of motion around the upright steady forward motion, further improving the practical

application of this model. This model accounted for 82% to 90% of the variance in steering angle prediction compared to experimentally observed cyclist reactions, as indicated by the Variance Accounted For (VAF) score.

While these results were based on only two trials, the high predictive accuracy suggests the model's reliability in simulating a cyclist's reaction to large disturbances. Additionally, although the experiments focused on impulse-like handlebar disturbances, we hypothesise that the model's reliability can be generalised to other impulse-like disturbances, such as collisions with a kerb or another road user. This hypothesis will be further explored when discussing conclusion 3.

Thus, existing bicycle dynamics and cyclist control models can already reliably simulate crash types such as collisions with obstacles or other road users and falls due to loss of balance.

However, further improvements or validations of the models are necessary to simulate the remaining commonly reported crash types. For example, simulating falls due to slipping on a slippery road surface requires the development of a comprehensive bicycle tyre model. This model, an extension of the Carvallo-Whipple bicycle model, is essential to accurately describe and calculate the forces generated by the tyres under lateral slip and determine whether the tyres maintain grip. While extensive car tyre models exist, research into accurate and reliable bicycle tyre models has only recently begun [32].

> *Recommendations for future research — bicycle tyre model*
> We recommend that future research prioritise developing a detailed bicycle tyre model because slipping is a commonly reported fall cause [30]. Inspiration for the methodology to develop such a tyre model could be drawn from analogous studies in automotive or motorcycle tyre modeling [33]. A validated bicycle tyre model can provide valuable insights into the interactions between bicycle tyres and various road surfaces. These insights can improve our understanding of how falls due to slipping can be prevented effectively and how the design of bicycle tyres or road surfaces can be improved.

Such a tyre model would not only be valuable for simulating falls due to extremely low friction conditions but also for simulating crash types in non-slippery conditions requiring high lateral tyre forces. Even in non-slippery conditions, tyres can slip if lateral forces exceed the friction limit, such as during sharp cornering, evasive manoeuvres, or when recovering balance after a disturbance. This is something that can happen in any of the crash types. Again, a bicycle tyre model is essential to determine tyre forces, the friction limit, and the specific lean and steering angles at which slippage and a fall occur.

The Carvallo-Whipple bicycle model is adept at simulating cornering manoeuvres, but depending on the curve's radius, non-linear equations must be employed. In addition, the model needs to be extended to account for the accelerations during an evasive manoeuvre or hard braking. While such extensions have been proposed, they have yet to be validated.

A more significant constraint in simulating these crash types — falls following an evasive manoeuvre, falls resulting from hard braking, and falling over while cornering — is the current lack of cyclist control models that simulate these specific tasks or manoeuvres. The only validated cyclist control model to date simulates the balancing task and how the cyclist reacts to disturbances.

> *Recommendations for future research — cyclist control models for other tasks*
> We recommend developing cyclist control models that simulate the cyclist's evasive and braking actions. The approach described in this dissertation can serve as a foundation and inspiration for developing and validating these models.

Even more advanced cyclist control models are required to simulate falls where the bicycle's front wheel becomes lodged in tram rails. We will address this in the next section, focusing on conclusion 2.

Finally, while this dissertation has demonstrated that bicycle dynamics and cyclist control models can simulate a wide range of crash types commonly reported by road safety experts, we have also identified that the current descriptions of some crash types could be more specific. For example, "loss of balance" and "interactions with tram rails" can refer to multiple scenarios. Interactions with tram rails could involve a wheel becoming lodged or slipping, each requiring different models for accurate simulation. Moreover, the lack of standardised definitions across studies hinders systematic comparison of results.

> *Recommendations for future research — standardisation of crash type descriptions*
> We recommend fostering a collaborative dialogue between experts in bicycle dynamics, cyclist control, and cycling safety. Establishing standardised, clear definitions of crash types is crucial. Such standardisation would not only facilitate accurate simulation of crash scenarios but also facilitate systematic comparison of studies, which improves the dissemination of research findings.
>
> Involving researchers in bicycle dynamics and cyclist control in this dialogue will also clarify which input values are essential for accurate simulation of real-world crashes. For instance, it may become evident that collecting information on the bicycle type and the whole bicycle geometry is crucial. Similarly, it may become apparent that collecting the cyclist's skill performance level or the force or torque profiles of the disturbances encountered before a crash, though challenging to collect, could significantly improve the accuracy of the simulation.

Furthermore, while standardising crash types may reduce the variability in how they are defined, a significant degree of variation will still exist within each crash type. For example, falls due to slipping on a slippery road surface can occur under a wide range of conditions involving different types of cyclists, bicycles, speeds, and road types. This leads to an almost infinite number of possible simulations, making it impractical to evaluate the effectiveness of interventions for all these possible combinations.

> *Recommendations for future research — standardised set of crash types to evaluate intervention effectiveness*
> We recommend cyclist safety researchers to establish a standardised, finite set of crash types. In addition, relevant variables for infrastructure, bicycle type, cyclist characteristics, speed, and disturbance type should be clearly defined for each crash type. This approach would create a manageable number of simulation scenarios and a guide on safely and proactively evaluating intervention effectiveness. Such an approach would ensure systematic comparisons of intervention effectiveness, aiding in the identification of the most effective cycling safety interventions. This approach is inspired by the EuroNCAP model, which rates the safety of new car designs based on a standardised set of crash scenarios, thereby driving improvements in automotive safety.

6.2.2. ON THE INTERVENTIONS THAT CAN BE INCORPORATED IN BICYCLE DYNAMICS AND CYCLIST CONTROL MODELS (CONCLUSION 2)

Besides simulating commonly reported crash types, bicycle dynamics and cyclist control models offer the potential for safely and proactively evaluating interventions related to bicycle design, cyclist control skills such as balancing, and environmental factors like road surface conditions, disturbances, and available space to recover balance.

The geometry of a bicycle design — including not just the type of bicycle but also details such as wheelbase, trail, and head tube angle — can be integrated into the Carvallo-Whipple bicycle dynamics models. Additionally, the seating position and corresponding mass distribution of a cyclist can also be incorporated into the Carvallo-Whipple model. If a bicycle tyre model is developed, tyre design characteristics could also be included.

In existing cyclist control models, such as the one developed in Chapter 4, the skill level of the cyclist in balancing, particularly in recovering from a disturbance, can be incorporated. The cyclist's choice of forward speed is another factor that can be included in these models. Both are key cyclist characteristics that help to predict the probability of a fall after a disturbance.

However, as discussed earlier, the only validated cyclist control model currently available simulates only the balancing task, precisely the cyclist's reaction to a disturbance. No models yet exist to simulate other tasks, such as braking or executing an evasive manoeuvre. As a result, interventions aimed at improving a cyclist's control in these areas cannot yet be evaluated. Developing cyclist control models for these tasks

is essential, as highlighted earlier in the recommendations for future research on cyclist control models for other tasks.

A further limitation of the existing cyclist control model is that it only simulates the cyclist's control actions in response to impulse-like disturbances, not to those disturbances that occur over a prolonged period. For example, when a front wheel becomes lodged in tram rails — a commonly reported crash type — the current model would attempt to recover balance by steering in the direction of the fall, which is very hard in this instance. In reality, cyclists may apply different strategies to prevent a fall, such as dismounting. For interventions targeting these specific disturbances and crash types, improving a cyclist's balancing control may be less effective than improving their danger recognition, anticipation, and trajectory selection.

Unfortunately, existing cyclist control models do not incorporate interventions to prevent critical situations — such as a wheel getting lodged in tram rails or a cyclist ending up beside the road — from occurring in the first place. Examples of such interventions include improving the visibility of tram rails or applying ribbed markings to warn cyclists when they are too close to the edge of the road. These models only describe control actions, not the tactical or strategic decision-making processes that precede them.

Recommendations for future research: cyclist behavioural models

Future models could benefit from incorporating insights from cognitive and traffic psychology to simulate the decision-making process in the pre-critical situation phase. Incorporating these insights would allow for a better understanding of how cyclists make strategic and tactical choices that could prevent critical situations and falls from occurring.

Additionally, injury simulation software such as Madymo can be used for the post-fall phase, as outlined by Gildea et al. (2021) [34]. This software offers robust methodologies for analysing the aftermath of falls, including potential injuries sustained.

By broadening the scope of cyclist control models to include these elements, we can evaluate a wider range of potential cycling safety interventions, covering all phases of a crash — from ten seconds before the crash to the impact that causes injury.

Environmental interventions can also be incorporated into bicycle dynamics and cyclist control models. Similar to tyre design interventions, road surface characteristics could also be incorporated if a bicycle tyre model is developed. Current models can incorporate the available width for recovering balance and disturbances throwing the cyclist off balance. While realistic values for available width can be easily measured for existing cycling infrastructure, accurately incorporating disturbances is more challenging due to the lack of data on disturbances' real-world force or torque profiles.

Collecting such data, though challenging, is invaluable for accurately simulating these crash types and identifying disturbances that exceed the threshold for maintaining

balance. In simpler terms, it helps determine which disturbances are likely to cause a fall and which are relatively safe, guiding us on which disturbances to prioritise and eliminate. We will address this further in the next section, focusing on conclusion 3.

Recommendations for future research — collecting real-world force and torque profiles of disturbances
We recommend collecting real-world force and torque profiles of disturbances through either naturalistic studies or controlled experiments. These profiles can likely be identified by equipping bicycles with accelerometers or gyroscopes. Data could then be collected for events such as riding over a pothole, colliding with a kerb, experiencing a sudden wind gust, or collisions with another cyclist.

Preferably, the sensors are attached to the fork or handlebars. By measuring the resulting steering rate from these disturbances and cataloguing them, one can quickly establish a correlation with real-world disturbances and the force profile of the handlebar disturbance used in this dissertation to determine the MAHD. We will address the MAHD further in the next section, focusing on conclusion 3.

Establishing these correlations also allows for evaluating real-world disturbances, distinguishing those with minimal impact or low probability of causing a fall (i.e., far below the MAHD) from those that pose a significant danger (i.e., far above the MAHD). Consequently, efforts to identify and prevent the latter types of disturbances can be prioritised, aiding in the effective allocation of cycling safety resources. This risk-based approach aligns with the Dutch government's Strategic Plan for Traffic Safety (Strategisch Plan Verkeersveiligheid, SPV).

6.2.3. ON THE MAXIMUM ALLOWABLE HANDLEBAR DISTURBANCE (CONCLUSION 3)

The Maximum Allowable Handlebar Disturbance (MAHD) concept draws inspiration from indicators commonly used in the evaluation of fall prevention strategies in human gait, particularly the Gait Sensitivity Norm (GSN) [35]. Given that a significant portion of severe cycling injuries result from falls due to loss of balance rather than collisions with other road users, we argue that comparing cyclist falls to falls during walking, where balance plays a critical role, is more appropriate than drawing analogies from vehicular conflicts.

The fundamental principle of the MAHD is a disturbance throwing the cyclist and bicycle off balance, prompting the cyclist to react in order to recover balance. As a function of the disturbance, this reaction provides insights into the probability of successful balance recovery and, conversely, the probability of falling. The MAHD is defined as the upper limit of a clockwise external applied angular impulse to the handlebars about the steering axis, beyond which a cyclist can no longer recover balance. The angular impulse is approximated by a constant external applied torque

for 0.3 seconds. The MAHD quantifies and reflects the cyclist's ability to recover balance in response to disturbances. An intervention is effective if it increases the MAHD.

The MAHD is an intuitive indicator because it establishes a direct relationship between the indicator and the potential outcome (i.e., a fall), making it easily understandable and interpretable in the context of cycling safety. Moreover, the MAHD is generalisable. It can be determined for individual cyclists, bicycles, and environmental conditions. As such, it has the potential to systematically evaluate different interventions targeting either the cyclist, the bicycle, or the environment. The MAHD can also quantify the effectiveness of interventions for various crash types where cyclists encounter impulse-like disturbances. These include commonly reported crash types such as falls after a collision with another road user or an obstacle and falls due to loss of balance. For the latter crash type, while ambiguous, disturbances are also likely a contributing factor to a fall in many cases.

In theory, the MAHD could also be used to evaluate interventions targeting falls due to slipping on a slippery road surface. In such cases, the MAHD would likely be very low in the benchmark scenario before the intervention is incorporated and simulated, as the tyres would quickly lose friction. One could rerun the simulation with a potential safety intervention, like changing the road surface, and if this intervention increases the MAHD, it can be considered effective. However, other indicators focusing on the interaction between the tyres and road surface might be more practical and effective for this specific crash type to safely and proactively predict the effectiveness of cyclist fall prevention interventions.

Unlike the binary outcome of a fall or recovery, which can also be used as a performance indicator to evaluate cycling safety interventions, the MAHD provides a nuanced measure of an intervention's effectiveness. Relying solely on a binary outcome may obscure crucial information. The extent to which the MAHD is increased indicates the effectiveness of interventions, allowing for detailed comparisons and the identification of the most effective interventions.

Three considerations guided the decision to use handlebar disturbances in this dissertation. First, we believe that applying a pure torque to the handlebars closely simulates real-world disturbances, unlike lateral pulls or ground contact alterations, which introduce lateral forces or displace the tyres' ground contact point — scenarios less likely to occur in the real world. Note that this is a hypothesis, and the magnitude and force or torque profiles of real-world disturbances, such as riding over potholes or wind gusts, are yet unknown. This is why we recommend future research to collect real-world force and torque profiles of disturbances (see the previous recommendation for future research).

Second, the handlebars are highly sensitive to balance, requiring minimal force to induce falls, making them a safer option for controlled experiments. While interventions can be evaluated using bicycle dynamics and cyclist control models, a few experiments were at least required to validate the bicycle dynamics and cyclist control models in predicting cyclist falls. Third, existing hardware cannot generate the high forces to induce falls through rear frame disturbances. For more details about these latter two considerations, the reader is referred to Chapter 1 and Chapter 3.

Theoretically, any impulse-like disturbance that throws the bicycle and cyclist off

balance (i.e. causing a lean or steering disturbance) could be used, as the choice is arbitrary and primarily serves as a metric. Although the type and magnitude of the maximum allowable disturbance from which a cyclist can recover balance may vary in that case compared to the MAHD, we hypothesise that the overall trend will remain consistent because the bicycle lean and steering are coupled. The cyclist essentially has only one effective response to an impulse-like disturbance that throws the cyclist or bicycle off balance, and that is to steer into the direction of the fall [36]. This response is indifferent to whether the disturbance is applied to the bicycle's front assembly, the rear frame of the bicycle or the cyclist. Consequently, we hypothesise that the impulse-like handlebar disturbance can be generalisable to other impulse-like disturbances. However, empirical validation of this hypothesis is required.

Recommendations for future research — boundaries for other disturbances
We recommend that future research repeat the experiments performed in Chapter 3 using a different impulse-like disturbance. For instance, a lateral push or pull on the seat-post [37, 38] or lateral shifting of the rear wheel ground contact point [39]. Such experiments could validate our hypothesis about the generalisability of the impulse-like handlebar disturbance to other impulse-like disturbances.

A different perturbator mechanism would need to be developed for this purpose, as the Bump'em system used in the experiments performed in the study of Chapter 3 is likely not capable of generating an impulse-like disturbance large enough to cause a fall [40]. The handlebars are the most sensitive part of the bicycle, requiring the lowest forces to induce a fall. However, inducing falls due to an impulse-like handlebar disturbance already pushed the limits of the forces the hardware could generate.

While we propose the MAHD as a general indicator, it must be noted that it is less versatile than the traditional approach, using statistical analysis applied to historical bicycle crash data. This limitation arises because the MAHD focuses explicitly on the balancing task, excluding critical tasks such as braking, (dis)mounting, navigating, and collision avoidance from its scope. While the exclusive focus on balancing remains valuable, as evidenced by traditional bicycle crash analysis studies that consistently identify loss of balance as the primary cause of cycling injuries [30], there is a need to recognise the importance of an intervention effectiveness indicator that can safely and proactively evaluate a broader range of crash types and cycling tasks as well.

Recommendations for future research — developing other indicators
In the discussion above, it was highlighted that the MAHD could not evaluate interventions targeting three other crucial cycling tasks: collision avoidance, braking, and (dis)mounting. Collision avoidance and braking are two commonly reported crash types [30]. Mounting or dismounting a bicycle represents another consistently highlighted crash type in bicycle crash studies [41, 42], although less prevalent for serious cycling injuries

than the crash types mentioned in Utriainen et al. (2023) [30].

This dissertation did not investigate indicators that would best predict the effectiveness of interventions targeting these crucial tasks and crash types. Nevertheless, we can contemplate potential indicators and draw inspiration from various sources.

For collision avoidance, surrogate safety measures, which quantify conflicts and near-misses, offer a valuable source of inspiration for a suitable indicator. Assessing the effectiveness of interventions aimed at improving braking performance could involve considering the maximum deceleration at which a cyclist can come to a standstill and safely place a foot on the ground. Regarding (dis)mounting, indicators may be found in the research on postural balance or gait stability, such as forces exerted on or accelerations of body parts such as the feet, ankle, or knee joint.

Most importantly, the MAHD can be determined in an experimental setting or through bicycle dynamics and cyclist control models. Therefore, it offers a safe and proactive approach to evaluate and quantify the performance of fall prevention interventions, thereby eliminating the need for real-world implementation before effectiveness has been validated.

6.2.4. ON THE PRACTICALITY OF THE EXPERIMENTAL SETUP TO MEASURE THE MAXIMUM ALLOWABLE HANDLEBAR DISTURBANCE (CONCLUSION 4)

While we have established in the previous section that the MAHD is an intuitive indicator for safely and proactively evaluating the effectiveness of cyclist fall prevention interventions, the MAHD must also be safely and practically measurable in at least a laboratory setting. This measurement is critical to validate the bicycle dynamics and cyclist control models.

The experiments conducted in Chapter 3 are the first experimental simulation of actual cyclist falls, demonstrating the practicality and safety of our novel experimental setup and protocol. A total of 928 disturbances were applied to 24 participants with diverse characteristics, including variables such as skill and age. Half of the participants were between 20 and 35 years old, while the other half were 60 years or older. Approximately half of the disturbances resulted in a fall. Initial apprehensions regarding falls dissipated after participants experienced their first simulated fall. Most importantly, no participant got injured despite this large number of simulated falls, demonstrating the safety of the experimental setup.

This setup could be used to determine the MAHD in a practical manner. Given the varied human response, there is no sharp boundary between falling and recovering balance. Therefore, multiple repetitions with disturbances near the threshold are required to reliably estimate the probability of falling per participant. Using a randomised staircase procedure and a Bayesian multilevel logistic regression model, which we will discuss in more detail in the next section, we found that 20 disturbances were sufficient to predict the MAHD reliably.

Four-hour sessions were allocated for each participant. This time duration was sufficient to determine the MAHD, based on 20 disturbances, for 23 of the 24 participants for at least one forward speed (12 km/h). For twelve of the 24 participants, we also determined the MAHD within this session for another forward speed, either 6 km/h or 18 km/h. We will elaborate on the importance of determining the MAHD at different forward speeds in the section addressing conclusions 7 and 8. For six of the 24 participants, the MAHD was determined at all three forward speeds (6, 12, and 18 km/h) within these four-hour sessions. These participants simulated approximately 30 falls within four hours. These findings demonstrate the feasibility and practicality of our experimental setup to determine the MAHD.

Only one of the 24 participants dropped out after experiencing 10 of the required 20 disturbances to determine the MAHD due to physical fatigue. This dropout rate is considerably lower than that reported in related experiments involving disturbances during standing or walking tasks [43, 44].

The participant who withdrew was the oldest in our cohort and faced challenges adjusting to cycling on a treadmill. Although the dynamics of cycling on a treadmill are similar to real-world cycling, differences in sensory inputs, such as optical flow, required a brief learning phase for most participants. With extended training, the oldest participant could still complete the protocol for ten disturbances but then withdrew due to physical fatigue. This case demonstrates the need for a baseline level of fitness to withstand all 20 disturbances — yet this requirement seems to remain well below average fitness levels.

There is considerable potential to further streamline the MAHD determination process and reduce the time required to measure the MAHD. The experimental dataset collected in Chapter 3 can be used to validate the MAHD predictions of bicycle dynamics and cyclist control models. Instead of relying solely on experimental procedures, the MAHD could then be predicted with these models (as demonstrated in Chapter 5). This modeling approach is more cost-effective and allows for more precise control over variables, facilitating rapid testing of various interventions across numerous scenarios.

The final experimental setup required specialised equipment, such as a human motion capture system, a perturbation device (Bump'em), and a 200 Hz real-time controller, all synchronised on a single time base. While this reduces the practicality of the setup, many universities have access to such equipment or can develop similar systems. Moreover, our method of measuring MAHD through cyclist fall experiments is still faster, more cost-effective, and ethically preferable compared to long-term data collection through intervention implementation and ex-post evaluation, where the cyclist may face additional risks if the interventions do not improve safety.

A limitation of our experimental design was the use of a treadmill in a controlled laboratory setting. This choice, while beneficial for safety and ensuring controlled conditions for accurate measurements, which we prioritised as this was the first experiment to simulate actual cyclist falls, may compromise the environmental validity of our findings. Although we did not directly determine environmental validity, the dynamics of cycling at a constant speed and straight trajectory on a treadmill are dynamically equivalent to cycling on the open road under similar conditions. However, discrepancies in sensory inputs, such as optical flow, could significantly alter

participants' experiences. Notably, most participants required multiple attempts to maintain steady cycling on the treadmill, indicating an adjustment period. Typically, this adjustment period was less than five minutes. Additionally, most participants perceived a cycling speed of 12 km/h on the treadmill as comparable to 18 km/h on an open road, suggesting a perceptual difference in speed that warrants further exploration of the treadmill's impact on cycling behaviour.

> *Recommendations for future research — environmental validity of the treadmill setup*
> We recommend that future studies examine the differences between treadmill cycling and outdoor cycling. These differences can be studied and quantified through a comparative analysis of steering actions in both scenarios. While the precise measurement of steering actions applied by cyclists may pose challenges, their correlation with bicycle dynamics may offer a more practical alternative. Parameters such as steering and lean rates, angles, and forward speed can be quantified using cheap and simple devices like an Inertial Measurement Unit (IMU). However, the application of a human motion capture system yields greater accuracy. Despite the inherent differences in sensory input between the two conditions, a consistent alignment of steering actions or measured bicycle dynamics suggests that the treadmill can be representative of real-life cycling actions.
>
> Initial comparisons should focus on free, undisturbed cycling without specific instructions, followed by assessments under varied conditions such as heightened attentiveness, the addition of secondary tasks, or navigating or cycling over potholes. This multifaceted approach ensures a comprehensive understanding of the implications of different instructions on cycling behaviour within the two conditions.

Before the experiment, participants were informed about the forthcoming disturbances and instructed to prepare accordingly. This prior knowledge likely influenced the outcomes, particularly the measurement of the MAHD. It is likely that the anticipation of disturbances causes an increase in observed MAHD compared to scenarios where participants are unaware of impending disturbances. In an effort to reduce the predictability of these events, we incorporated randomness into the direction and magnitude of the handlebar disturbances, as well as the timing of their occurrence.

Therefore, the MAHD values obtained may be viewed as conservative estimates. Disturbances that fall below these thresholds still present a risk of falling for cyclists in real-world conditions. Conversely, disturbances that exceed these MAHD values are highly likely to cause falls.

> *Recommendations for future research — disturbing cyclists who are unaware or distracted*
> Investigating the impact of participants' awareness and heightened focus on impending disturbances is essential for a comprehensive

understanding of the MAHD. While challenging, exploring unawareness or distractions within the experimental setup is partially achievable. Our increased understanding of the safety aspects of the experimental setup would allow future studies to introduce handlebar disturbances without prior notification to participants, thus eliminating their awareness of these disturbances. However, it is critical to recognise that the element of surprise can only be utilised during the initial disturbance; participants are likely to anticipate subsequent disturbances. Given the need for multiple disturbances to accurately determine MAHD, relying solely on a single disturbance would necessitate a considerably large sample size and extensive inter-subject comparisons, which may not be feasible in practice.

An alternative method could involve introducing a dual task for participants to divert their focus away from impending disturbances, thereby simulating real-world conditions where distractions may increase the risk of falls. This approach is supported by existing literature, which identifies distraction as a significant risk factor for cycling crashes, for instance, the use of mobile phones [9].

Conducting experiments that incorporate a dual task is valuable, as it provides insights into how individuals allocate attention and manage cognitive resources across multiple tasks, which may affect their performance. However, the differences in the allocation of attention and cognitive resources could confound the results if participants prioritise differently between the tasks.

Even with dual tasks or without explaining to participants prior to the experiment that they will be exposed to disturbances, it is likely that participants will remain more alert and aware of disturbances than they would be in real-world conditions due to the controlled experimental environment and the use of safety harnesses. Comparing cyclist steering actions from naturalistic studies could illuminate these discrepancies. Nonetheless, achieving complete environmental validation in such experimental settings is practically unattainable.

If further investigation confirms that the treadmill's configuration and the participant's awareness significantly affect cyclist behaviour compared with outdoor cycling, it becomes imperative to explore alternative experimental setups for measuring the MAHD.

Recommendations for future research — alternative experimental setups
Two noteworthy alternative experimental setups are a bicycle simulator and a setup employing a mobile crane to support the cyclist's harness. While each of these setups presents certain advantages over our current cyclist fall experiment setup, it also comes with unique challenges.

A bicycle simulator offers a method to measure MAHD similar

to our cyclist fall experiment by applying a handlebar disturbance to simulate potential falls. One notable advantage of the bicycle simulator over our treadmill setup is the likelihood of lower impact forces exerted on the participant during a fall, given the static nature of the simulator. This reduction in physical demand on the participant may enhance participation rates. The increased safety may allow for applying disturbances without warning the participants beforehand. Because of the static nature of the simulator, it might also be more accessible to apply different types of disturbances.

However, it is crucial to acknowledge that the behavioural validity of bicycle simulators is subject to more considerable debate compared to our existing experimental setup. Ongoing efforts within the research community to improve bicycle simulators and validate cycling behaviour suggest the potential availability of a validated bicycle simulator in the near future [45].

The measurement of the MAHD during free cycling can be done using a mobile crane to support the cyclist's harness. This configuration offers improved environmental validity compared to treadmill or bicycle simulator setups, as it replicates real-life cycling sensory inputs such as optical flow. However, ensuring the cyclist's safety presents a more significant challenge. The mobile crane must closely track the cyclist to prevent constraining the cyclist's movements while maintaining tension on the harness to prevent falls. Also, applying sudden and impulsive handlebar disturbances over a larger area on a moving bicycle is inherently more challenging than on a treadmill, which has a much smaller operating volume.

Still, it might be interesting to pursue developing such a setup, as the mobile crane setup addresses a limitation of both treadmill and bicycle simulator setups. Treadmills are designed for linear movement and lack the capacity to simulate cornering, a crucial aspect of cycling dynamics. Similarly, static bicycle simulators are ill-suited for replicating cornering scenarios. Although most bicycle crashes occur during straight-line cycling, falls during cornering or falls following an evasive manoeuvre are two of the eight commonly reported crash types considered in this study. In instances where evaluating cycling safety interventions targeting cornering is essential, the mobile crane setup becomes a viable alternative.

Overall, the most practical approach, at present, for experimentally measuring the MAHD is through the treadmill experimental setup outlined in this dissertation. While ongoing research is focused on the development of bicycle simulators, it is crucial to emphasise that the behavioural validity for simulators is, at the moment, more questionable compared to the behavioural validity of the treadmill setup. The potential superiority of simulators in the future is contingent upon establishing and confirming their behavioural validity. If proven, simulators could emerge as a more viable option. Simulators offer a versatile platform

for investigating cycling safety interventions, specifically those targeting critical situations such as collisions or conflicts. This broader functionality allows for the comparison of various interventions.

We advocate for a cautious approach before venturing into the design of an outdoor setup with a mobile crane. We propose prioritising an in-depth investigation into the behavioural validity of the treadmill setup. However, it is important to acknowledge that if the primary focus is on interventions related to cornering, an outdoor setup becomes indispensable as it is the only configuration likely to yield representative results in such scenarios.

6.2.5. ON THE BAYESIAN MODEL (CONCLUSION 5)

In Chapter 3, we introduced a Bayesian multilevel logistic regression model — hereafter referred to as the Bayesian model — which predicts the MAHD from the experimental data. A logistic regression model is required due to the varied human response. Due to this varied response, there is often no clear-cut boundary for the disturbance threshold from which a cyclist can recover balance. Instead, there is a probability that a participant will fall, depending on the disturbance's magnitude.

To determine the MAHD for each participant, we applied twenty disturbances varying in magnitude. A random and adaptive staircase procedure was used to introduce small variations in disturbance magnitude around the threshold and to allow a small progression of the threshold. This approach ensured that the participant could not predict the magnitude of the disturbance and that the magnitude of the disturbances remained close to the threshold.

We then applied the Bayesian model to convert the binary outcome (fall or recovery) into a probability function of the disturbance magnitude. The Bayesian approach was chosen to facilitate uncertainty quantification and to derive a multilevel logistic regression model, reflecting the multilevel structure inherent in the data, with experiments grouped by participant. From this model, we determined the MAHD, defined as the disturbance magnitude (i.e., angular impulse) at which the cyclist had a 50% probability of falling.

For the 24 participants, we found MAHD values to range between 6 and 18 Nms. Unfortunately, we cannot yet relate these values directly to real-world scenarios because of the lack of force or torque profiles of real-world disturbances. This is why we previously recommended future research to collect such force or torque profiles. Additionally, we found that the MAHD values were influenced by factors such as forward speed and skill performance level, which will be further discussed when discussing conclusions 7 and 8.

Our confidence in the Bayesian model's reliability and accuracy is based on the posterior predictive checks we performed and the uncertainty quantifications, as detailed in Chapter 3. The model's fit was examined by comparing observed data to data generated from the posterior distribution, demonstrating its ability to capture patterns in the experimental data. Bayesian models naturally provide uncertainty estimates through posterior distributions. Additionally, an alternative approach — fitting a statistical model as a generalised linear model, including a random effects model

— yielded similar outcomes regarding the model's coefficient estimates. Combined, this provides us with enough confidence to state that the predictions of the statistical model can be considered reliable and accurate.

However, our conclusions about the model's effectiveness, accuracy, and reliability are specific to the cyclists, bicycles, and environmental conditions included in our experimental setup. The scope of the cyclist experiments described in Chapter 3 does not encompass the entire cyclist population or all potential fall scenarios due to practical limitations in testing diverse conditions and extremes. The experimental conditions were controlled, involving 24 experienced cyclists, a single bicycle type, a specific type of disturbance (with variable magnitudes), uniform road surfaces, and a constant lateral width within a forward speed range of 6 to 18 km/h.

Extrapolation beyond these defined boundaries may provide reliable predictions for certain variables but introduces uncertainties for others. Researchers utilising these models should be mindful of these limitations when applying our findings beyond the experimental scope.

> *Recommendations for future research — expanding the boundaries of the experimental conditions*
> Considering the finite scope of our initial experiments, there is significant potential to broaden the experimental boundaries by largely reusing the same setup. Initial efforts should focus on expanding the variety of bicycle types and cyclist demographics. Once the model is validated under these expanded conditions, a further extension to include a broader range of environmental variables — such as a treadmill with a wider belt or different road surface — would also be valuable. By progressively broadening the experimental scope, we can improve the predictive power and utility of the Bayesian model.

The Bayesian model developed in this dissertation, combined with the experimental setup and the MAHD, can also be used to safely and proactively evaluate cyclist fall prevention interventions. This experimental approach offers several advantages over the bicycle dynamics and cyclist control model because it relies on direct observations and fewer assumptions.

While we evaluated the reliability of the MAHD predictions for a bicycle dynamics and cyclist control model in Chapter 5 and found it reliable within experimental conditions, such models require validation each time they are applied beyond those conditions. Until bicycle dynamics and cyclist control models are fully validated, the experimental approach can already have some valuable practical applications.

The experimental approach can, for instance, be used to screen individual cyclists for fall risk, evaluate medical fitness to cycle or evaluate the influence of medicines or other substances on fall risk. By identifying individuals with a high risk of falling, targeted interventions can be implemented. Screening allows for more personalised advice regarding the risks of cycling and suggests potential steps to mitigate these risks. Such steps might include wearing a bicycle helmet, transitioning to a tricycle, or undergoing training to improve cycling balance skills.

Our experimental setup also has the potential to serve as a training platform designed to improve the cyclist's balancing skills and reduce the probability of falling. Evidence suggests such disturbance-based training programs effectively reduce fall risk for falls occurring in and about the house [46]. The potential effectiveness of disturbance-based training is also supported by our observed learning effect during the experiments and the fact that repeated exposure to disturbances reduces the MAHD (see conclusion 7 that how often the cyclist encountered the disturbance was an important predictor of the MAHD).

However, conducting experiments, developing prototypes of new interventions, and, if necessary, adjusting the experimental setup to incorporate these interventions is both costly and time-consuming. In contrast, bicycle dynamics and cyclist control models can more easily incorporate a wide range of interventions and simulate various crash scenarios. They offer a faster and more cost-effective means of evaluating the potential effectiveness of interventions. Therefore, we recommend conducting experiments to validate bicycle dynamics and cyclist control models, which can then be used to evaluate cyclist fall prevention measures safely, proactively, fast, and cost-effectively.

6.2.6. ON THE CRITICAL FALL MODE IN THE PERTURBED CYCLIST EXPERIMENTS (CONCLUSION 6)

In Chapter 2, we defined three primary fall modes for cyclist falls. These are slipping of the tyres due to a too-large lean angle, slipping of the tyres due to a too-large steering angle, and cycling off the side of the road. Among these fall modes, the one with the lowest maximum disturbance before a fall occurs is considered the most critical and is defined as the MAHD.

Our experimental conditions consisted of cycling at speeds ranging from 6 to 18 km/h on a non-slippery 1.2 m wide treadmill belt while exposed to impulse-like handlebar disturbances. For these conditions, the most critical fall mode was riding off the side of the treadmill. All observed falls were due to this particular fall mode.

This finding is similar to the MAHD predictions of the bicycle dynamics and cyclist control model in Chapter 5 when simulating the experimental conditions — as depicted in Figure 5.1. Extrapolating the MAHD predictions of the bicycle dynamics and cyclist control model slightly beyond the experimental range, we observed that below 6 km/h, the critical fall mode transitions to slipping due to a too-large steering angle. This low-speed instability is consistent with existing research, which indicates that bicycles become more unstable as velocities decrease [31].

However, caution is warranted regarding these findings, as we used a simplified method to estimate the maximum steering and lean angles at which tyre slippage might occur under non-slippery conditions. Since slipping was never observed in our experiments, the reliability of this simplified approach remains to be determined. As recommended earlier, developing a detailed bicycle tyre model is crucial for generating reliable predictions in scenarios where tyre slippage could become the critical fall mode. Slipping due to an excessive lean angle appears unlikely under non-slippery conditions, as this would only occur with disturbances significantly higher than those required to induce the other two fall modes.

Recommendations for future research — redo experiments at lower forward speeds
We recommend conducting future experiments at lower forward speeds to confirm the transition of the critical fall mode from cycling off the side of the treadmill to slipping due to an excessive steering angle.

6.2.7. ON VARIABLES INFLUENCING THE MAXIMUM ALLOWABLE HANDLEBAR DISTURBANCE (CONCLUSIONS 7-9)

In this dissertation, we identified from the parameters that were varied in the cyclist fall experiments, which were important predictors for the MAHD. These variables were forward speed v, skill performance S, the lean angle at the moment of the handlebar disturbance ϕ_0, the steer rate at the moment of the handlebar disturbance $\dot{\delta}_0$, the direction of the handlebar disturbance d, and how often the cyclist encountered the disturbance j. These variables were identified as necessary using Bayesian Model Averaging. Below, we discuss these variables in more detail, along with those that showed limited predictive value. Additionally, we explore some variables that were not varied in the experiments but are hypothesised to influence the MAHD based on the predictions of the bicycle dynamics and cyclist control model developed in Chapter 5.

On forward speed
Previous research has established that bicycle stability is dependent on forward speed v, decreasing linearly as forward speed reduces [31]. This relationship was further validated through experimental studies [36, 47]. Our Bayesian Model Averaging analysis, detailed in Chapter 3, confirms these findings by identifying forward speed as an important predictor of the MAHD. However, contrary to initial expectations, an inverse relationship was observed where the MAHD increases as forward speed decreases (conclusion 8).

This counterintuitive result could be attributed to our experimental setup's limited lateral space available for balance recovery. Participants fell by riding off the sides of the treadmill (conclusion 6). Despite reduced stability at lower speeds — we observed increased effort to keep cycling straight ahead at lower forward speeds — participants had more time to respond to disturbances. As a result, they could manage larger disturbances before riding off the side of the treadmill. This finding implies that lower cycling speeds are safer on narrow bicycle paths. In addition, higher forward speeds may increase cognitive demands, potentially raising the likelihood of encountering disturbances or critical situations and, by extension, increasing fall risk due to increased exposure to such events.

However, there may be an optimal forward speed. The experiments did not explore speeds below 6 km/h. The Bayesian model's MAHD predictions do not extend to these lower speeds and a nonlinear interaction likely exists between forward speed and cyclist fall risk. Stability decreases linearly with reduced speed [31]. At speeds below 6 km/h, our bicycle dynamics and cyclist control model predicts a decrease in MAHD due to a transition in fall mode. Instead of cycling off the side of the treadmill, slipping due to a too-large steering angle becomes the critical fall mode — as depicted in Figure 5.1.

This hypothesis is further supported by crash analysis studies indicating elevated risks at both very low and high speeds [30, 48].

> *Recommendations for future research — determine the optimal forward speed for cycling safety*
> We recommend repeating the experiments performed in Chapter 3 at speeds below 6 km/h to investigate further the nonlinear relationship between forward speed and cyclist fall risk. Such studies could validate our hypothesis that there is an optimal forward speed and determine critical low and high forward speed thresholds that significantly influence safety.
>
> Although validating the hypothesis and refining the bicycle dynamics and cyclist control models at these lower speeds would be scientifically valuable, it is important to acknowledge that cycling at speeds as low as 6 km/h may not be practical in real-world scenarios, as it could significantly increase travel time.

On important cyclist control characteristics
Previous research on cyclist control has established, through theoretical models, that cyclist control is crucial for bicycle stability [37]. However, as discussed in Chapter 1, variables related to cyclist balance control skills, such as feedback gains and muscular characteristics, remain abstract. Additionally, input values for these variables have been determined in limited contexts, often involving a single cyclist and lacking scenarios with actual falls. Consequently, which specific balance control skill variables influenced the MAHD remained unclear.

The experiments presented in Chapter 3 were conducted to identify and specify the key cyclist balance control characteristics essential for accurately predicting the MAHD. Our research focused on four variables: balancing control skill performance S, control effort E, reaction time τ, and age a.

Using Bayesian Model Averaging, our analysis identified balancing skill performance S as a significant predictor of the MAHD. Specifically, this performance metric is defined as the lateral deviation of the front wheel's ground contact point during a minute-long ride at a constant speed, reflecting the cyclist's balancing skill.

It is important to consider that this definition of skill performance S, determined when cycling undisturbed, may not fully capture a cyclist's response to large disturbances. Nevertheless, the results demonstrated that skill performance S, as defined in our study, is an important predictor of the MAHD and, therefore, of the maximum disturbance from which a cyclist can recover balance and the probability of a fall.

The fall risk of participants in our experimental dataset was predicted using the Bayesian model and the participant's skill performance S. If this finding can be generalised to real-world falls, it could significantly simplify the process of screening an individual cyclist's fall risk. Instead of conducting extensive fall experiments, which involve 20 disturbances and approximately 10 simulated falls, the fall risk could be determined by measuring skill performance S. This measurement would only require the cyclist to follow a centreline for one minute while cycling without any disturbances.

Furthermore, the process of measuring skill performance S could be carried out with a much simpler setup, eliminating the need for both the perturbator system and the safety harness. It might even be feasible to perform the measurement outside the laboratory setting — such as in a hall or on a stretch of road — allowing the cyclist to avoid the need to adapt to cycling on a treadmill. The reduced complexity of the measurement protocol and equipment would make it much more practical to screen an individual cyclist's fall and scaling up of this approach.

> *Recommendations for future research — predictive validity of skill performance outside laboratory setting*
> We recommend that future research tests whether skill performance S is also predictive of real-world falls. This can be achieved by measuring the skill performance S of a large cohort of cyclists, then retrospectively or prospectively recording real-world falls within this group, and analysing whether there is a significant relationship between the two.

In addition to skill performance S, Bayesian Model Averaging also highlighted the significance of participant-specific characteristics, as indicated by participant ID (i), in predicting the MAHD. This identifier accounts for undefined and unmeasured cyclist-specific characteristics, implying that other crucial cyclist-related factors influencing MAHD remain unexplored. Although this variable's specificity to the participants in our study limits its generalisability, its significance suggests the need for further research to identify and quantify these individual characteristics. Therefore, while this variable is acknowledged in our findings, its exclusion from the conclusion is based on the current inability to generalise these participant-specific characteristics to broader cyclists who did not participate in the experiments.

A potential candidate for further exploration might be the variations in strategies to anticipate and react to disturbances.

> *Recommendations for future research — exploring different strategies to recover balance*
> We recommend future research to explore in more detail different strategies to recover balance after a large disturbance, taking into account limited lateral space to recover balance.
>
> Previous research has demonstrated that steering in the direction of the fall is the primary balance recovery mechanism [36]. However, the constrained width of the treadmill used in our experiments might influence the range of observable strategies. Cyclists may prioritise differently between quickly recovering balance and delaying this recovery to remain within the confines of the road. The prioritisation is a trade-off in strategic choices. Our study did not investigate the nuanced differences in this kind of strategy selection. However, this could be derived in the future from a more detailed analysis of steering responses collected during the experiments.
>
> Additionally, preparatory strategies for disturbances may also vary.

For example, some cyclists might stiffen their arm muscles to resist the handlebar disturbances. Our attempts to analyse such behaviours through electromyography (EMG) were hindered by signal noise, leading to the exclusion of these data from our analysis.

On the disturbance identification number
The disturbance identification number j was also identified through Bayesian Model Averaging to have predictive value for the MAHD, suggesting that prior experience with disturbances can improve a cyclist's resilience and reduce cyclist fall risk. However, encountering the same large disturbance repeatedly in a short period is unlikely in real-world scenarios. Therefore, the disturbance identification number in simulations for naive cyclists should ideally be set to 1.

Furthermore, this result suggests that training cyclists to respond effectively to large disturbances could significantly reduce their fall risk. This finding is particularly promising for cyclists who have a high fall risk, as targeted training could improve their ability to recover from such disturbances. As previously discussed, our experimental setup could potentially also serve as a safe training platform to improve cyclists' skills in recovering from large impulse-like disturbances.

Recommendations for future research — long-term effects and transferability of training
Future studies should explore the long-term effects of disturbance training on cyclist safety and evaluate the transferability of these skills to real-world cycling conditions. Once these aspects are understood, further research is necessary to determine the optimal frequency and intensity of disturbance exposure during training to maximise resilience and minimise fall risk. Inspiration for such research can be drawn from studies on the transferability of perturbation-based training in reducing fall risk while walking or in a domestic environment among older adults.

On the direction of the disturbance
Surprisingly, the direction of disturbance d also had predictive value, potentially indicating a link to the cyclists' dexterity or habitual cycling on the right side of the road, where the road verge is typically closer. The cyclist's dexterity was not recorded for the participants in the experiments, while all participants were used to cycling on the right-hand side of the road.

On the orientation of the bicycle at the time of the disturbance
The bicycle-cyclist system is an inherently unstable system at low to medium forward speeds [36]. While the upright, straight-ahead cycling position is stable, any minor deviations without corrective reaction will result in a fall. The MAHD is influenced by the orientation of the cyclist's lean angle and steering rate at the time the disturbance is applied (ϕ_0, $\hat{\delta}_0$). For example, if a cyclist leans slightly to the left but steers to the right, a disturbance that further rotates the handlebars to the right can exacerbate the imbalance. Conversely, if the cyclist is leaning and steering to the left, a disturbance that

rotates the handlebars to the right may mitigate the imbalance.

The MAHD shows a high sensitivity to these small deviations from the upright and straight cycling position, as evidenced by the findings discussed in Chapter 3. Although the intention was to apply the handlebar disturbance during steady, upright, straight-ahead cycling at the treadmill's centre, slight variations in the lateral dynamics of the bicycle were still observed. These included variations in the angles and angular rates of leaning and steering, which typically ranged within ± 3 degrees and ± 1 deg/s, respectively. These minor variations at the moment of handlebar disturbance were already important to accurately predict the MAHD.

On variables varied in the cyclist fall experiments that have limited predicted value
In the experiments detailed in Chapter 3, age and control effort E were also investigated for their importance in predicting the MAHD via the Bayesian Model Averaging. Surprisingly, age did not improve the model's ability to predict the MAHD (conclusion 9), despite the higher incidence of cycling injuries among older cyclists as reported in previous studies [49–51].

This finding suggests that, in critical situations, the likelihood of balance recovery among older cyclists is similar to that of younger cyclists, indicating that age may not be a critical factor in this specific crash phase. Moreover, this finding suggest that not all older cyclists have an increased fall risk. Through screening, as described above, the cyclist's who do have an increased risk of falling when encountering a large impulse-like disturbance can be identified. Their falls risk can potentially be reduced by disturbance-based training.

The higher incidence of serious cycling injuries among older cyclists might be explained by their physical frailty, which increases the probability of sustaining a serious injury when falling or that they end up more often in critical situations. However, this is unlikely, as older cyclists are known to apply compensation strategies.

Similarly, the control effort E showed limited value in predicting the MAHD, and there was no observed correlation between skill performance S and control effort E. While it may seem counterintuitive there is no correlation, there are several possible explanations for this. First, good balancing performance might not necessarily require more effort. For instance, skilled individuals might perform well with minimal effort because they have mastered efficient techniques. Second, cyclists may also optimise energy efficiency rather than maximising performance. A cyclist might maintain a steady level of performance that is good enough without overexerting themselves, especially if they are balancing other concerns like stamina or safety. This could also explain why performance is predictive of outcomes like MAHD, while effort is not. Related research on the car following task also suggests such a complex interplay between task performance, effort, and workload [52–54].

Although our study initially aimed to include participants' reaction time τ to disturbances, the measurements proved unreliable (see Chapter 3 for details). Consequently, no definitive conclusions could be drawn about its predictive value.

Recommendations for future research — improve measurement of reaction time
We recommend future research to repeat the experiments from Chapter 3 with improved protocols and equipment for accurately measuring reaction time, potentially incorporating better electromyography (EMG) sensors or advanced data processing techniques. Including separate tests to measure reaction time in a controlled environment may also be valuable.

On variables that were not varied in the experiments but shown by bicycle dynamics and cyclist control models to influence the MAHD
One variable not varied in the experiments was the lateral width available to recover balance. Previous studies in the field of bicycle dynamics and cyclist control did not explicitly explore the influence of lateral space on cyclist fall risk. Theoretical research typically focussed on balance recovery without specific spatial constraints [31], and previous experiments, which did utilise a narrow treadmill, only required minimal lateral movements for balance recovery as the applied disturbances were very low [37].

In Chapter 5, we demonstrated — using a bicycle dynamics and cyclist control model — that increasing lateral recovery space linearly increased the MAHD for changes of 10% around a lateral width of 60 cm. This finding supports implementing infrastructure designs that incorporate wider bicycle paths or adjacent evasive zones, such as rideable shoulders or forgiving kerbs, to improve. These interventions could significantly decrease fall risks and collisions by providing cyclists more room to manoeuvre, as confirmed by crash analysis studies [55, 56].

Moreover, although the 60 cm lateral space on our treadmill might seem limited, it is, in fact, conservative compared to real-world applications. The Dutch design manual for cycle traffic suggests a minimum of 150 cm for standalone bidirectional cycle tracks, assuming a 25 cm buffer for each cyclist from the path edge and oncoming traffic [56]. This standard indicates that our experimental and simulation parameters in Chapters 3 and 5 are likely conservative when compared to typical cycling environments (although cyclists usually do not cycle at the centre of the bicycle path as they were instructed during the experiments).

Additionally, we did not vary the bicycle type. In previous research in the field of bicycle dynamics, the stability of a bicycle has been shown to be significantly influenced by its geometry [31, 36, 57]. Given the thorough validation of these bicycle dynamics models, this dissertation intentionally did not vary the bicycle geometry in the experiments described in Chapter 3. Instead, the focus was placed on exploring the characteristics of cyclists that influence their balance control skills.

All participants used the same bicycle for the experimental setup, with adjustments permitted only for saddle height and handlebar position. These adjustments influenced the seating position and, along with participants' varied physical attributes — specifically height and mass — altered the inertia of the bicycle-cyclist system. Although we did not measure the exact cyclist inertia, we did record the height and mass of the participants. Interestingly, our findings in Chapter 3 demonstrated that these factors appeared to have limited predictive value for the MAHD. This highlights the advantage

of using Bayesian Model Averaging in our analysis, which helps to determine which variables contribute to predictive accuracy and which do not.

In Chapter 5, we explored another bicycle geometry variable, the head tube angle. Note that the bicycle geometry, including cyclist inertia, can be described by 25 parameters [31]. We demonstrated that small changes (i.e. 10%) in the head tube angle had a significant impact on the MAHD; see Figure 5.6 and the section on conclusion 13.

6.2.8. ON THE NEWLY DEVELOPED CYCLIST CONTROL MODEL (CONCLUSION 10)

The newly developed cyclist control model, described in Chapter 4, was the first cyclist control model for balancing that includes human characteristics that are more intuitive and easier to measure. Our model only requires one input value to be calibrated, which is the LQR control weight for the lean angle Q_ϕ. This parameter is independent of forward speed. In contrast, existing models necessitate the calibration of numerous input variables for each forward speed. We also demonstrated that this model can reliably predict the steer reactions in response to small disturbances of three cyclists in two environments (i.e. in a treadmill setup and an indoor pavilion setup). These features set our model apart from existing cyclist control models, making it a more practical tool for predicting the MAHD and evaluating potential cyclist fall prevention interventions.

However, a limitation of this model is that its selection and predictive performance were based on experimental data that only contains observations of small disturbances that did not cause a fall. As a result, it remained uncertain whether the model's predictive performance can be extended to situations involving large disturbances, which may provoke different reactions from cyclists.

This difference in reaction became apparent in Chapter 5, where we compared the predictions of the cyclist control model to the experimental data collected in Chapter 3. This dataset included observations of cyclists reacting to large disturbances. We needed to extend the cyclist control model with an optimal control weight on the heading Q_ψ to account for the large lateral displacement required to recover balance from a large disturbance and the finite width of the treadmill used in the experiments. Otherwise, the model predicted that the cyclist would cycle off the side of the treadmill even for small disturbances as the cyclist would not correct for his or her heading. With the added control weight for the heading Q_ψ, the cyclist control model seems capable of predicting the steering actions of a cyclist recovering from a large disturbance (see Figures 5.3 and 5.4).

It is important to note that the cyclist control model can only predict the steering actions for disturbances below the MAHD. Once a cyclist falls, they are likely to adopt different strategies, such as bracing for impact or dismounting the bicycle, even before the actual fall occurs. The current model does not capture these behaviours.

The results presented in Chapter 5 indicate that, when combined with the Carvallo-Whipple bicycle model, our cyclist control model can predict the MAHD comparable to that of the Bayesian model based on experimental data. These results will be discussed further in the following section.

Recommendations for future research — develop cyclist control model using cyclist fall experiments dataset
We would recommend future research to redo the process of the development of the cyclist control model described in Chapter 4 but with the data collected in the experiments described in Chapter 3 which does contain large disturbances and falls. However, it is important to note that only the trials where the cyclist successfully recovers balance should be considered. This is because the cyclist's response will differ significantly in instances where they begin to fall.

In Chapter 5, we calibrated the weight factor for the lean angle, Q_ϕ, against the skill performance S measured for the experiment participants. The results revealed an almost linear relationship between these two variables (see Table 5.3). If such a relationship is generalisable, the weight factor Q_ϕ could be determined in a simplified manner by having cyclists follow a centreline for one minute without any disturbances rather than calibrating it for multiple repetitions of conditions in which the cyclists are disturbed. This would reduce the complexity of the measurement protocol and the required equipment, further improving the practicality of our cyclist control model for simulating the steering reactions of different cyclists.

Recommendations for future research — generalisability of the linear relationship between S and Q_ϕ
To investigate the generalisability of the linear relationship between skill performance S and the weight factor Q_ϕ, future research should replicate the experiments from Chapter 3 with a new cohort of cyclists. The new data and MAHD values should then be compared to the MAHD predictions made by the bicycle dynamics and cyclist control model, using the linear relationship for Q_ϕ and S found in Table 5.3 to determine the input value for Q_ϕ. Such validation could simplify the determination of Q_ϕ for different cyclists.

6.2.9. ON THE RELIABILITY AND ACCURACY OF THE PROPOSED BICYCLE DYNAMICS AND CYCLIST MODEL IN PREDICTING THE MAXIMUM ALLOWABLE HANDLEBAR DISTURBANCE (CONCLUSION 11)

In Chapter 5, we evaluated the reliability of a candidate bicycle dynamics and cyclist control model to predict the MAHD. This candidate model incorporates the linear Carvallo-Whipple bicycle model, the cyclist control model developed in Chapter 4, and predefined thresholds for lean angle, steering angle, and lateral displacement of the front wheel's ground contact point as cyclist fall indicators.

We evaluated the reliability of the candidate model by comparing its predictions to data from the experiments in Chapter 3, where cyclists were subjected to impulse-like handlebar disturbances in non-slippery conditions and on a 1.2 m wide treadmill belt. These disturbances led to both falls and recoveries. Specifically, we compared the MAHD predictions from our model with those derived from the Bayesian model — developed in

Chapter 3 based on the experimental data — across four cyclists with varying skill levels at forward speeds ranging from 6 to 18 km/h. Additionally, we qualitatively compared the bicycle dynamics and cyclist control model's predictions for the steering reactions against the steering responses measured in the experiments for a basic skilled cyclist (i.e. lowest skill performance S) and a disturbance just below the MAHD threshold.

The findings indicate a strong alignment between the MAHD predictions from our proposed model and those derived from a Bayesian model, as evidenced by RMSE values in Table 5.3. Moreover, the model accurately mirrored observed cyclist behaviour post-disturbance in terms of steering actions and transient dynamics (see Figures 5.3 and 5.4). Overall, these results showed that this model can reliably and practically predict the MAHD for a cyclist encountering an impulse-like handlebar disturbance in non-slippery conditions on a finite-width bicycle path.

However, it is important to acknowledge certain limitations regarding the reliability of the MAHD predictions. The calibration of the optimal weight factor Q_ϕ based on experimental data introduces uncertainty in the model's predictive capabilities. The model was calibrated to fit this data rather than independently predicting outcomes as the optimal weight factor Q_ϕ was unknown for the experiment participants. This calibration was essential for establishing appropriate input values for the cyclist control model. To evaluate the accuracy of the model's MAHD predictions, we fitted Q_ϕ for four types of cyclists with different skill levels and then compared the resulting MAHD trends across the forward speed range. Our findings confirmed that the model effectively captures the observed MAHD trends across the forward speed range of 6 to 18 km/h and for all four cyclist types.

Moreover, the calibration process results revealed an almost linear relationship between these two variables (see Table 5.3). To further investigate the reliability of the MAHD predictions, we recommend replicating the experiments of Chapter 3 with a new cohort of cyclists (also see our recommendations for future research about the linear relationship between S and Q_ϕ previously). Such experiments would further substantiate the candidate model's accuracy and reliability in predicting the MAHD.

Of course, the reliability of the model's predictions is contingent on the specific conditions of the experiments. Detailed discussions of these experimental boundaries have been addressed previously when discussing the practicality of the experimental setup (conclusion 4) and will not be reiterated here.

Additionally, we evaluated the model's ability to predict cyclist steering reactions to large disturbances by comparing the model's predictions to experimental measurements. Although alignment in steering reactions was evident in two selected trials, it is important to note that some additional trials that were explored showed inconsistent responses. The differences observed across trials may stem from varied balance recovery strategies, different priorities in avoiding the treadmill edge, or residual effects from the perturbation mechanism.

6.2.10. ON POSSIBLE POTENTIAL INTERESTING CYCLIST FALL PREVENTION INTERVENTIONS THAT CAN BE EXPLORED (CONCLUSIONS 12-14)

In Chapter 5, we evaluated the practicality of a candidate bicycle dynamics and cyclist control model to safely and proactively evaluate cyclist fall prevention interventions.

Specifically, the practicality was evaluated by incorporating interventions targeting cyclist control, bicycle design and infrastructure in the candidate model and analysing their impact on the MAHD.

Our findings demonstrated that the candidate model can successfully incorporate these interventions and evaluate their impact on the MAHD. This suggests that this candidate bicycle dynamics and cyclist control model, in combination with the MAHD, can be used to safely and proactively evaluate cyclist fall prevention interventions. Such a tool could assist designers in developing safer bicycle paths, bicycles and cycling training programs. It could also assist policy advisors in setting guidelines for safe designs and allocating resources to the most effective interventions.

Below, we discuss several promising potential interventions to explore further.

Recommendations for future research — promising interventions
On interventions targeting infrastructure design
Our findings in Chapter 5 suggest that increasing lateral width for balance recovery significantly increases the MAHD. We recommend future research to investigate the feasibility of designing ridable road shoulders or easily navigable kerbs that provide additional lateral space for cyclists in emergencies to recover balance.

Although sloped kerbs are recommended in the Dutch guidelines for a 'forgiving bicycle path design', the specifics of these designs, such as the appropriate slope angle and the radius of the bevel, still need to be validated. Our approach can determine the optimal kerb design by evaluating which shapes and angles reduce cyclist fall risk.

We propose using experiments to collect data on the interaction between bicycles and kerbs by measuring the force profiles from these interactions. With the knowledge of these force profiles, we can employ simulations using bicycle dynamics and cyclist control models to evaluate different kerb designs safely and proactively. This approach offers a cost-effective, safe, and scientifically rigorous method to identify the safest kerb configuration.

By pursuing these recommendations, future research can build on our preliminary findings to improve cyclist safety through better infrastructure and design practices.

On interventions targeting cyclist balancing control
Given the significant individual variation in balance control, as discussed in Chapter 3, it is crucial to examine interventions aimed at improving the cyclists' ability to recover balance following large disturbances.

Traditional training methods primarily rely on expert opinions. With our proposed approach, these methods can now be systematically evaluated using the MAHD and the approaches outlined in our research.

However, identifying effective types of interventions for cyclist balance remains challenging. The current cyclist control models still need to incorporate variables like the effects of alcohol or medication. Future research should focus on experimenting with and refining the model to

include these variables.

In Chapter 5, we investigated the potential of a balance assistance control system — the steer-assist bicycle. Our experiments confirmed that such systems could improve the MAHD, thus improving cyclists' resilience to disturbances. However, selecting the control algorithm carefully is crucial, as some algorithms we tested actually decreased the MAHD. Our approach provides a robust framework to design and select algorithms that optimise safety and effectiveness for such balance assistance systems.

On interventions targeting bicycle design

In Chapter 5, we demonstrated that minor modifications to the head tube angle significantly increased the MAHD. The head tube angle is the angle between the front fork and the ground when the bicycle is standing upright. Empirical evidence also suggests significant effects from other geometric factors such as trail and wheelbase. These findings underscore the potential for improving cycling safety through relatively minor modifications to bicycle design.

The approach presented in Chapter 5 provides a cost-effective, safe, and efficient method for bicycle designers to evaluate various design choices during the development phase, particularly with regard to their safety implications. These insights could eventually not only lead to the design of safer bicycles, but also to the creation of a decision aid for consumers, enabling them to prioritise safety when purchasing a new bicycle. This, in turn, could stimulate manufacturers to focus on safety in their designs, much like the EuroNCAP score has driven improvements in car safety.

The approach we developed is not confined to bicycles alone. With minor adaptations, it can be applied to safely and proactively evaluate the safety of emerging light electric vehicles, such as electric scooters and mopeds. Currently, the lack of reliable and comprehensive crash data for these vehicles poses significant challenges for policy advisors tasked with developing evidence-based and proportionate regulations. The approaches outlined in this dissertation could provide policy advisors with crucial insights into the fall risks associated with these new vehicle types, enabling the implementation of proactive safety measures and proportional regulation rather than relying on post-crash statistics.

6.2.11. ON THE IMPACT OF THE DISSERTATION'S RESEARCH

The goal of this dissertation was to develop an approach that can safely and proactively evaluate the effectiveness of a wide range of cyclist fall prevention interventions before their implementation.

To conclude, we developed a novel approach using a bicycle dynamics and cyclist control model. This model can simulate crash types where the cyclist encounters an impulse-like disturbance — such as collisions with other road users or obstacles or falls

due to loss of balance. The model is capable of incorporating interventions related to cyclist balancing control, bicycle design, and lateral width. In addition, we introduced the Maximum Allowable Handlebar Disturbance (MAHD) as a novel performance indicator to safely and proactively evaluate cyclist fall prevention interventions. The reliability and accuracy of our novel approach are supported by comparisons between the model's predictions of the MAHD and cyclist steering reactions in response to large disturbances and the observations from cyclist fall experiments.

However, our model has certain limitations. It cannot yet simulate crash scenarios involving hard braking, evasive manoeuvres, (tram) rails or slippery conditions, nor does it simulate cognitive decision-making crucial to evaluate interventions targeting the phase leading up to a potentially dangerous situation. These limitations suggest areas for future extension to improve the model's applicability and extend its use to a broader range of scenarios and interventions.

Unlike previous methods that rely on retrospective statistical analyses of crash data or traffic microsimulation models focusing on conflicts between road users, our proactive approach stands out by safely and proactively evaluating potential interventions for preventing single-bicycle crashes before these are implemented. While often overlooked, single bicycle crashes account for a significant proportion of serious injuries among cyclists. Therefore, our novel approach represents an advancement in cycling safety, offering guidance for infrastructure, bicycle and training program designers, as well as for policy advisors on how to best allocate available resources.

While we believe we made a valuable contribution to the scientific field of cycling safety, we can only really make an impact if designers and policy advisors adopt our research findings. Effectively communicating our research findings to designers and policy advisors, who may not have a technical background, is therefore crucial for adopting our approach. Some strategies to bridge this gap might be to provide an accessible summary or policy brief of our work policy-relevant language, engage stakeholders who can act as intermediaries or organise workshops (or start working as designers or policy advisors ourselves).

REFERENCES

[1] R. Elvik, *Area-wide urban traffic calming schemes: A meta-analysis of safety effects,* Accident Analysis & Prevention **33**, 327 (2001), https://doi.org/10.1016/S0001-4575(00)00046-4.

[2] A. Hoye, *Recommend or mandate? A systematic review and meta-analysis of the effects of mandatory bicycle helmet legislation,* Accident Analysis & Prevention **120**, 239 (2018), https://doi.org/10.1016/j.aap.2018.08.001.

[3] I. I. Hellman and M. Lindman, *Estimating the crash reducing effect of advanced driver assistance systems (ADAS) for vulnerable road users,* Traffic Safety Research **4**, 000036 (2023), https://doi.org/10.55329/blzz2682.

[4] N. Lubbe, Y. Wu, and H. Jeppsson, *Safe speeds: Fatality and injury risks of pedestrians, cyclists, motorcyclists, and car drivers impacting the front of another*

passenger car as a function of closing speed and age, Traffic Safety Research **2**, 000006 (2022), https://doi.org/10.55329/vfma7555.

[5] T. Sayed, M. H. Zaki, and J. Autey, *Automated safety diagnosis of vehicle-bicycle interactions using computer vision analysis,* Safety Science **59**, 163 (2013), https://doi.org/10.1016/j.ssci.2013.05.009.

[6] A. R. A. van der Horst, M. de Goede, S. de Hair-Buijssen, and R. Methorst, *Traffic conflicts on bicycle paths: A systematic observation of behaviour from video,* Accident Analysis & Prevention **62**, 358 (2014), https://doi.org/10.1016/j.aap.2013.04.005.

[7] N. McNeil, C. M. Monsere, and J. Dill, *Influence of bike lane buffer types on perceived comfort and safety of bicyclists and potential bicyclists,* Transportation Research Record **2520**, 132 (2015), https://doi.org/10.3141/2520-15.

[8] J. Kovaceva, P. Wallgren, and M. Dozza, *On the evaluation of visual nudges to promote safe cycling: Can we encourage lower speeds at intersections?* Traffic Injury Prevention **23**, 428 (2022), https://doi.org/10.1080/15389588.2022.2103120.

[9] D. de Waard, P. Schepers, W. Ormel, and K. Brookhuis, *Mobile phone use while cycling: Incidence and effects on behaviour and safety,* Ergonomics **53**, 30 (2010), https://doi.org/10.1080/00140130903381180.

[10] W. P. Vlakveld, D. Twisk, M. Christoph, M. Boele, R. Sikkema, R. Remy, and A. L. Schwab, *Speed choice and mental workload of elderly cyclists on e-bikes in simple and complex traffic situations: A field experiment,* Accident Analysis & Prevention **74**, 97 (2015), https://doi.org/10.1016/j.aap.2014.10.018.

[11] R. Dubbeldam, C. T. M. Baten, P. T. C. Straathof, J. H. Buurke, and J. S. Rietman, *The different ways to get on and off a bicycle for young and old,* Safety Science **92**, 318 (2017), https://doi.org/10.1016/j.ssci.2016.01.010.

[12] J. Andersson, C. Patten, H. Wallén Warner, C. Andersérs, C. Ahlström, R. Ceci, and L. Jakobsson, *Bicycling during alcohol intoxication,* Traffic Safety Research **4** (2023), https://doi.org/10.55329/prpa1909.

[13] K. Kircher and A. Niska, *Interventions to reduce the speed of cyclists in work zones — cyclists' evaluation in a controlled environment,* Traffic Safety Research **6**, e000047 (2024), https://doi.org/10.55329/ohhx5659.

[14] C. Andersérs, J. Andersson, and H. W. Warner, *The importance of individual characteristics on bicycle performance during alcohol intoxication,* Traffic Safety Research **6**, e000042 (2024), https://doi.org/10.55329/vmgb9648.

[15] A. Niska and J. Wenäll, *Simulated single-bicycle crashes in the VTI crash safety laboratory,* Traffic Injury Prevention **20**, 68 (2019), https://doi.org/10.1080/15389588.2019.1685090.

[16] A. Niska, J. Wenäll, and J. Karlström, *Crash tests to evaluate the design of temporary traffic control devices for increased safety of cyclists at road works,* Accident Analysis & Prevention **166**, 106529 (2022), https://doi.org/10.1016/j.aap.2021.106529.

[17] Y. Peng, Y. Chen, J. Yang, D. Otte, and R. Willinger, *A study of pedestrian and bicyclist exposure to head injury in passenger car collisions based on accident data and simulations,* Safety Science **50**, 1749 (2012), https://doi.org/10.1016/j.ssci.2012.03.005.

[18] M. Fahlstedt, P. Halldin, and S. Kleiven, *The protective effect of a helmet in three bicycle accidents — a finite element study,* Accident Analysis & Prevention **91**, 135 (2016), https://doi.org/10.1016/j.aap.2016.02.025.

[19] C. Baker, X. Yu, B. Lovell, R. Tan, S. Patel, and M. Ghajari, *How well do popular bicycle helmets protect from different types of head injury?* Annals of Biomedical Engineering **52**, 3326 (2024), https://doi.org/10.1007/s10439-024-03589-8.

[20] V. Astarita, V. Giofré, G. Guido, and A. Vitale, *Investigating road safety issues through a microsimulation model,* Procedia-social and Behavioral Sciences **20**, 226 (2011), https://doi.org/10.1016/j.sbspro.2011.08.028.

[21] U. Shahdah, F. Saccomanno, and B. Persaud, *Application of traffic microsimulation for evaluating safety performance of urban signalized intersections,* Transportation Research Part C: Emerging Technologies **60**, 96 (2015), https://doi.org/10.1016/j.trc.2015.06.010.

[22] H. Twaddle, T. Schendzielorz, and O. Fakler, *Bicycles in urban areas: Review of existing methods for modeling behavior,* Transportation Research Record **2434**, 140 (2014), https://doi.org/10.3141/2434-17.

[23] C. M. Schmidt, A. Dabiri, F. Schulte, R. Happee, and J. K. Moore, *Essential bicycle dynamics for microscopic traffic simulation: An example using the social force model,* in *The Evolving Scholar-BMD 2023, 5th Edition* (2023) http://dx.doi.org/10.59490/649d4037c2c818c6824899bd.

[24] N. Rinke, C. Schiermeyer, F. Pascucci, V. Berkhahn, and B. Friedrich, *A multi-layer social force approach to model interactions in shared spaces using collision prediction,* Transportation Research Procedia **25**, 1249 (2017), https://doi.org/10.1016/j.trpro.2017.05.144.

[25] V. Keppner, S. Krumpoch, R. Kob, A. Rappl, C. C. Sieber, E. Freiberger, and H. M. Siebentritt, *Safer cycling in older age (SiFAr): Effects of a multi-component cycle training. a randomized controlled trial,* BMC Geriatrics **23**, 131 (2023), https://doi.org/10.1186/s12877-021-02502-5.

[26] L. Alizadehsaravi and J. K. Moore, *Bicycle balance assist system reduces roll and steering motion for young and older bicyclists during real-life safety challenges,* PeerJ **11**, e16206 (2023), https://doi.org/10.7717/peerj.16206.

[27] B. Janssen, P. Schepers, H. Farah, and M. Hagenzieker, *Behaviour of cyclists and pedestrians near right angled, sloped and levelled kerb types: Do risks associated to height differences of kerbs weigh up against other factors?* European Journal of Transport and Infrastructure Research **18**, 360 (2018), https://doi.org/10.18757/ejtir.2018.18.4.3254.

[28] F. Westerhuis, A. B. M. Fuermaier, K. A. Brookhuis, and D. de Waard, *Cycling on the edge: The effects of edge lines, slanted kerbstones, shoulder, and edge strips on cycling behaviour of cyclists older than 50 years,* Ergonomics **63**, 769 (2020), https://doi.org/10.1080/00140139.2020.1755058.

[29] P. Schepers, N. Agerholm, E. Amoros, R. Benington, T. Bjørnskau, S. Dhondt, B. de Geus, C. Hagemeister, B. P. Y. Loo, and A. Niska, *An international review of the frequency of single-bicycle crashes (SBCs) and their relation to bicycle modal share,* Injury Prevention **21**, e138 (2015), https://doi.org/10.1136/injuryprev-2013-040964.

[30] R. Utriainen, S. O'Hern, and M. Pöllänen, *Review on single-bicycle crashes in the recent scientific literature,* Transport Reviews **43**, 159 (2023), https://doi.org/10.1080/01441647.2022.2055674.

[31] J. P. Meijaard, J. M. Papadopoulos, A. Ruina, and A. L. Schwab, *Linearized dynamics equations for the balance and steer of a bicycle: A benchmark and review,* Proceedings of the Royal Society A: Mathematical, Physical and Engineering Sciences **463**, 1955 (2007), https://doi.org/10.1098/rspa.2007.1857.

[32] G. Dell'Orto, G. Mastinu, R. Happee, and J. K. Moore, *Measurement of the lateral characteristics and identification of the Magic Formula parameters of city and cargo bicycle tyres,* Vehicle System Dynamics , 1 (2024), https://doi.org/10.1080/00423114.2024.2338143.

[33] H. Pacejka, *Tire and vehicle dynamics* (Elsevier, 2005).

[34] K. Gildea, D. Hall, and C. Simms, *Configurations of underreported cyclist-motorised vehicle and single cyclist collisions: Analysis of a self-reported survey,* Accident Analysis & Prevention **159**, 106264 (2021), https://doi.org/10.1016/j.aap.2021.106264.

[35] D. G. E. Hobbelen and M. Wisse, *A disturbance rejection measure for limit cycle walkers: The Gait Sensitivity Norm,* IEEE Transactions on Robotics **23**, 1213 (2007), https://doi.org/10.1109/TRO.2007.904908.

[36] J. D. G. Kooijman, J. P. Meijaard, J. M. Papadopoulos, A. Ruina, and A. L. Schwab, *A bicycle can be self-stable without gyroscopic or caster effects,* Science **332**, 339 (2011), https://doi.org/10.1126/science.1201959.

[37] A. L. Schwab, P. D. L. De Lange, R. Happee, and J. K. Moore, *Rider control identification in bicycling using lateral force perturbation tests,* Proceedings of the Institution of Mechanical Engineers, Part K: Journal of Multi-body Dynamics **227**, 390 (2013), https://doi.org/10.1177/1464419313492317.

[38] G. Dialynas, C. Christoforidis, R. Happee, and A. L. Schwab, *Rider control identification in cycling taking into account steering torque feedback and sensory delays,* Vehicle System Dynamics **61**, 200 (2023), https://doi.org/10.1080/00423114.2022.2048865.

[39] V. E. Bulsink, H. Kiewiet, D. van de Belt, G. M. Bonnema, and B. Koopman, *Cycling strategies of young and older cyclists,* Human Movement Science **46**, 184 (2016), https://doi.org/10.1016/j.humov.2016.01.005.

[40] G. R. Tan, M. Raitor, and S. H. Collins, *Bump'em: An open-source, bump-emulation system for studying human balance and gait,* in *2020 IEEE International Conference on Robotics and Automation (ICRA)* (Paris, France, 1 June - 31 August 2020) https://doi.org/10.1109/ICRA40945.2020.9197105.

[41] P. Schepers and K. Klein Wolt, *Single-bicycle crash types and characteristics,* Cycling Research International **2**, 119 (2012).

[42] B. Algurén and M. Rizzi, *In-depth understanding of single bicycle crashes in Sweden - crash characteristics, injury types and health outcomes differentiated by gender and age-groups,* Journal of Transport & Health **24**, 101320 (2022), https://doi.org/10.1016/j.jth.2021.101320.

[43] M. Pijnappels, J. C. E. van der Burg, N. D. Reeves, and J. H. van Dieën, *Identification of elderly fallers by muscle strength measures,* European journal of Applied Physiology **102**, 585 (2008), https://doi.org/10.1007/s00421-007-0613-6.

[44] J. R. Crenshaw, K. A. Bernhardt, E. J. Atkinson, S. Khosla, K. R. Kaufman, and S. Amin, *The relationships between compensatory stepping thresholds and measures of gait, standing postural control, strength, and balance confidence in older women,* Gait & Posture **65**, 74 (2018), https://doi.org/10.1016/j.gaitpost.2018.06.117.

[45] B. Sporrel, A. Stuiver, and D. De Waard, *On the use of bicycle simulators, Proceedings of the Human Factors and Ergonomics Society Europe,* https://www.hfes-europe.org/wp-content/uploads/2023/05/Sporrel2023.pdf.

[46] M. H. G. Gerards, C. McCrum, A. Mansfield, and K. Meijer, *Perturbation-based balance training for falls reduction among older adults: Current evidence and implications for clinical practice,* Geriatrics & Gerontology International **17**, 2294 (2017), https://doi.org/10.1111/ggi.13082.

[47] J. D. G. Kooijman, A. L. Schwab, and J. P. Meijaard, *Experimental validation of a model of an uncontrolled bicycle,* Multibody System Dynamics **19**, 115 (2008), https://doi.org/10.1007/s11044-007-9050-x.

[48] I. Krul, H. Valkenberg, S. Asscherman, C. Stam, and K. Klein Wolt, *Fietsongevallen en snor-/bromfietsongevallen in Nederland,* (2022), https://www.veiligheid.nl/sites/default/files/2022-06/Rapportage%20%28Snor-%20en%20brom%29fietsongevallen%20in%20Nederland.pdf, accessed 11 January 2025.

[49] W. Weijermars, N. Bos, and H. L. Stipdonk, *Serious road injuries in the Netherlands dissected,* Traffic Injury Prevention **17**, 73 (2016), https://doi.org/10.1080/15389588.2015.1042577.

[50] M. J. Boele-Vos, K. Van Duijvenvoorde, M. J. A. Doumen, C. W. A. E. Duivenvoorden, W. J. R. Louwerse, and R. J. Davidse, *Crashes involving cyclists aged 50 and over in the Netherlands: An in-depth study,* Accident Analysis & Prevention **105**, 4 (2017), https://doi.org/10.1016/j.aap.2016.07.016.

[51] S. Boufous, L. de Rome, T. Senserrick, and R. Ivers, *Risk factors for severe injury in cyclists involved in traffic crashes in Victoria, Australia,* Accident Analysis & Prevention **49**, 404 (2012), https://doi.org/10.1016/j.aap.2012.03.011.

[52] D. A. Abbink, M. Mulder, and E. R. Boer, *Haptic shared control: Smoothly shifting control authority?* Cognition, Technology & Work **14**, 19 (2012), https://doi.org/10.1007/s10111-011-0192-5.

[53] S. M. Petermeijer, D. A. Abbink, M. Mulder, and J. C. F. de Winter, *The effect of haptic support systems on driver performance: A literature survey,* IEEE transactions on Haptics **8**, 467 (2015), https://doi.org/10.1109/TOH.2015.2437871.

[54] D. A. Abbink, M. Mulder, F. C. T. van der Helm, M. Mulder, and E. R. Boer, *Measuring neuromuscular control dynamics during car following with continuous haptic feedback,* IEEE Transactions on Systems, Man, and Cybernetics, Part B (Cybernetics) **41**, 1239 (2011), https://doi.org/10.1109/TSMCB.2011.2120606.

[55] T. Hoogendoorn, *The contribution of infrastructure characteristics to bicycle crashes without motor vehicles: A quantitative approach using a case-control design*, Master's thesis, Delft University of Technology, Delft, The Netherlands (2017), http://resolver.tudelft.nl/uuid:dcb70ccc-227a-4dcd-9a3a-b99e45080289.

[56] P. Schepers, E. Theuwissen, P. N. Velasco, M. N. Niaki, O. van Boggelen, W. Daamen, and M. Hagenzieker, *The relationship between cycle track width and the lateral position of cyclists, and implications for the required cycle track width,* Journal of Safety Research **87**, 38 (2023), https://doi.org/10.1016/j.jsr.2023.07.011.

[57] D. Stevens, *The stability and handling characteristics of bicycles*, Bachelor's thesis, The University of New South Wales, School of Mechanical and Manufacturing Engineering, Sydney, Australia (2009), http://www.varg.unsw.edu.au/Assets/link%20pdfs/thesis_stevens.pdf.

DANKWOORD

Er wordt wel eens gezegd dat wielrennen een individuele teamsport is. Eén wielrenner kan maar winnen, bijvoorbeeld de Tour de France of een wereldtitel. Maar om te winnen is de steun van zijn of haar team onmisbaar. Teamgenoten motiveren, rijden op kop, brengen bidons, of geven zelfs hun wiel als dat nodig is. Een promotietraject eigenlijk precies zo. Hoewel ik straks misschien een titel krijg, is dit proefschrift tot stand gekomen dankzij de steun van heel veel mensen. Aan hen draag ik dit dankwoord op.

In mijn nieuwe baan heb ik geleerd dat je bij het schrijven moet beginnen met het belangrijkste, dus ik wil beginnen met Minke, mijn ouders, mijn zus en mijn schoonfamilie. Zij zijn de basis waarop dit proefschrift is gebouwd. Minke, jij bent de meest bijzondere vrouw die ik ken. Jij inspireert me elke dag, als persoon en als onderzoeker. Je steun en de mooie herinneringen die we samen creëren geven mij enorm veel kracht, zelfvertrouwen en energie. Bij mijn ouders en zus kan ik altijd terecht. Jullie staan altijd achter me, wat ik ook doe. Dat geeft mij veel zelfvertrouwen. Ik weet dat jullie ook trots op me zouden zijn zonder dit proefschrift, maar ik vind het heel speciaal om deze mijlpaal met jullie te delen. Ook mijn schoonfamilie wil ik bedanken. Jullie maken dat ik me altijd welkom en gesteund voel. Ik hoop dat jullie mijn eindeloze fietsverhalen toch een beetje interessant vonden. En zonder Julia was de voorkant van mijn proefschrift niet zo mooi.

Dit proefschrift was er niet geweest zonder Arend Schwab. Als fietsgek had ik me geen betere begeleider kunnen wensen. Arend, ik wil je bedanken voor al je inhoudelijke (fiets)kennis en voor de waardevolle lessen over samenwerking en levensinstelling. Ik heb hier veel goede en fijne herinneringen aan. Daarnaast waren onze werkreizen naar Australië en Japan niet alleen leerzaam, maar ook onvergetelijk dankzij de (fiets)tochten die we hebben gemaakt. Ook al je steun en kansen die je bood om aan sport gerelateerde projecten te werken was een droom die uitkwam, met als hoogtepunt het ontwerpen van de baanfiets voor de Nederlandse ploeg op de Olympische Spelen van Tokio.

Frans, jouw begeleiding heeft ervoor gezorgd dat ik echt trots ben op dit proefschrift. Jij was de drijvende kracht achter het fietsvalexperiment – het eerste ter wereld! – en je zorgde voor de rode draad die door het hele proefschrift loopt. Dankzij jou bouwen de hoofdstukken logisch op elkaar voort. Ik ben je enorm dankbaar voor je scherpte, je enthousiasme en je betrokkenheid.

Daarnaast wil ik ook Frank en Koen bedanken. Frank, jouw hulp bij het ontwikkelen van het statistisch model en je bijdrage aan hoofdstuk 3 hebben het onderzoek naar een hoger niveau getild. Koen, jouw werk aan het fietsermodel in hoofdstuk 4 was onmisbaar.

Joost, Vincent, Naomi, Thijs en Damian, ook jullie wil ik bedanken. Joost, jouw vriendschap betekent veel voor me en je bent minstens zo gek op fietsen als ik. Onze fietstochten en gesprekken waren niet alleen ontspannend maar ook inspirerend voor mijn onderzoek. Vincent, Thijs en Damian, onze vriendschap begon al tijdens

Luchtvaart- en Ruimtevaarttechniek, en het voelt alsof mijn PhD-reis daar begon. Joost en Vincent, ik ben heel blij dat jullie mijn paranimfen willen zijn. Naomi en Joost, bij jullie kan ik helemaal mijzelf zijn. Onze etentjes, vakanties en oudjaarsavonden zorgden voor de perfecte ontspanning in drukke tijden. Dank jullie wel voor al die fijne momenten die mijn mentale batterij weer oplaadde en energie gaven om gemotiveerd door te gaan met mijn onderzoek.

A special time during my PhD was my visit to Australia at CARRS-Q. Divera, I want to thank you for this opportunity and for your guidance, together with Sébastien, during my stay. This experience broadened my perspective, and I learned so much about surrogate safety measures and ideas for proactive evaluation methods. Additionally, I want to thank Libby, Olaf, Narelle, Oscar, and Javier for the amazing time there. I hope to go on many more cycling trips with Libby and Olaf in the future and to talk with them about cycling again. I would also love to come back and visit Brisbane again someday!

Mijn tijd op de TU Delft werd vooral bijzonder door mijn collegas. Eline, Peter, Frederique, Peter, Bart, Marit en Martijn, jullie maakten het dagelijks leven op kantoor niet alleen leuker maar ook een stuk gezelliger. Dank voor alle humor, steun en fijne gesprekken. Hierdoor ging de tijd snel en hield ik energie om door te gaan.

Voor het fietsvalexperiment was de hulp van Shannon, Jan, Heike, Judith, Zasha en natuurlijk alle proefpersonen onmisbaar. Zonder jullie was dit onderzoek simpelweg niet mogelijk geweest. Heel veel dank daarvoor. Ik ben heel trots op dit resultaat en vind het fietsvalexperiment het leukste hoofdstuk van mijn proefschrift.

Ik wil graag mijn dank uitspreken aan Gazelle, Bosch en SWOV voor hun cruciale bijdragen aan mijn promotieonderzoek. Gazelle en Bosch hebben met hun betrokkenheid gezorgd voor geloofwaardigheid binnen de industrie, terwijl SWOV met haar expertise op het gebied van (wetenschappelijk) fietsveiligheidsonderzoek een stevige wetenschappelijke basis bood. Deze samenwerking opende deuren en creëerde mogelijkheden die essentieel waren voor het succes en de kwaliteit van dit onderzoek. Specifiek wil ik Maarten van Gazelle, Oliver van Bosch en Marjolein van SWOV bedanken voor hun persoonlijke inzet en betrokkenheid.

Tot slot wil ik mijn directe collegas bij het ministerie van Infrastructuur en Waterstaat bedanken. Door de inzichten die ik daar heb opgedaan, heeft mijn proefschrift een meer praktische en toepassingsgerichte richting gekregen. Kate, Robert, Michelle, Herman, Bart, Devon, Geertje, Liselotte, Boas, Martijn en Sara: jullie hebben bijgedragen aan de verbinding tussen wetenschap en praktijk. Heel veel dank daarvoor. Daarnaast is het fantastisch om na een individuele teamsport met jullie in een echt team te werken!

CURRICULUM VITÆ

Marco Michiel REIJNE

21-09-1987 Born in Reimerswaal, The Netherlands.

EDUCATION

2006–2010 B.Sc. in Architecture
Delft University of Technology

2010–2013 B.Sc. in Aerospace Engineering
Delft University of Technology

2013–2016 M.Sc. in Aerospace Engineering
Delft University of Technology

2018–2025 Ph.D. Biomechanics
Delft University of Technology
Thesis: Modeling and Evaluation of Cyclist Fall Prevention Interventions: A Proactive Cycling Safety Approach
Promotor: Prof. dr. F.C.T. van der Helm
Copromotor: dr. A.L. Schwab

AWARDS

2016 Cum Laude M.Sc. degree

2016 1st place International Sports Engineering Association Student Competition for M.Sc. thesis

EXPERIENCE

2022–2024 Policy advisor in road safety
Ministry of Infrastructure and Watermanagement

2024–2025 Senior policy advisor in road safety
Ministry of Infrastructure and Watermanagement

LIST OF PUBLICATIONS

1. **M.M. Reijne**, F.C.T. van der Helm & A.L. Schwab, *Applying bicycle dynamics and cyclist control models to cycling safety research*, Traffic Safety Research, 2025, under review.

2. **M.M. Reijne**, F.C.T. van der Helm & A.L. Schwab, *A practical indicator to safely and proactively evaluate cyclist fall prevention intervention effectiveness: the Maximum Allowable Handlebar Disturbance*, Traffic Safety Research, 2025, under review.

3. **M.M. Reijne**, F.H. van der Meulen, F.C.T. van der Helm & A.L. Schwab, *A model based on cyclist fall experiments which predicts the maximum allowable handlebar disturbance from which a cyclist can recover balance*, Accident Analysis & Prevention, 2025, under review.

4. **M.M. Reijne**, K.D. Wendel, F.C.T. van der Helm & A.L. Schwab, *A validated cyclist control model with human characteristics for bicycle lateral balance*, IEEE Transactions on Human-Machine Systems, 2025, under review.

5. **M.M. Reijne**, F.C.T. van der Helm & A.L. Schwab, *A model to safely and proactively evaluate cyclist fall prevention interventions*, IEEE Transactions on Human-Machine Systems, 2025, under review.


TU Delft
Delft
University of
Technology